

MCR-73-97  
NAS-12182

CR-134154

Volume II

Cryogenic  
Design

October 1973

**Final Report  
Acquisition/  
Expulsion System  
for Earth Orbital  
Propulsion System  
Study**

(NASA-CR-134154) ACQUISITION/EXPULSION  
SYSTEM FOR EARTH ORBITAL PROPULSION  
SYSTEM STUDY. VOLUME 2: CRYOGENIC  
DESIGN Final Report (Martin Marietta  
Corp.) 307 p HC \$17.50

N74-12526

CSSL 22B

G3/31

Unclas  
23518

**MARTIN MARIETTA**

MCR-73-97  
NAS9-12182

Volume II

Cryogenic  
Design

October 1973

**FINAL REPORT  
ACQUISITION/EXPULSION  
ORBITAL PROPULSION  
SYSTEM STUDY**

Approved



Howard L. Payne  
Program Manager

G. Robert Page  
Technical Director  
Cryogenic Systems Phase

Prepared for

National Aeronautics and Space Administration  
Lyndon B. Johnson Space Center  
Houston, Texas

Prepared by

MARTIN MARIETTA CORPORATION  
DENVER DIVISION  
Denver, Colorado 80201

## FOREWORD

---

This document is submitted to the National Aeronautics and Space Administration, Johnson Space Center by Martin Marietta Corporation Denver Division, as part of the final report for Contract NAS9-12182, *Acquisition/Expulsion System for Earth Orbital Propulsion systems*. The final report consists of five volumes as follows:

- Volume I - Summary Report;
- Volume II - Cryogenic Design;
- Volume III - Cryogenic Test;
- Volume IV - Flight Test Article;
- Volume V - Earth Storable Design.

This work was administered under the technical direction of Mr. Larry Rhodes, NASA-JSC Technical Monitor. Mr. Howard L. Paynter, Chief of the Thermodynamics and Fluid Mechanics Section, Propulsion Department, was the Martin Marietta Program Manager.

The following Martin Marietta personnel made significant contribution to the Phase A Cryogenic Design effort:

K. C. Lunden, A. J. Villars, Jr. and T. Richard Barksdale	Fluid Mechanics and Capillary System Design Analysis
R. N. Eberhardt and W. L. Karlin	Thermal and Thermodynamic Analysis
Preston E. Uney	Screen Structural Analysis
E. Robert Wilson	Detail Design

CONTENTS

---

	<u>Page</u>
SUMMARY . . . . .	x
I. INTRODUCTION . . . . .	I-1
A. Background and Objectives . . . . .	I-1
B. Guidelines and Approach . . . . .	I-2
	thru
	I-4
II. CRYOGENIC PROPELLANT ACQUISITION/EXPULSION SYSTEMS . . . . .	II-1
A. Candidate Systems . . . . .	II-1
B. Technical Areas Affecting System Design . . . . .	II-15
C. Results and Conclusions . . . . .	II-109
	thru
	II-111
III. INTEGRATED OMS/RCS DESIGN . . . . .	III-1
A. Mission Requirements and Design Criteria . . . . .	III-1
B. Preliminary Design Analysis . . . . .	III-8
C. Detailed Design . . . . .	III-33
D. Results and Conclusions . . . . .	III-57
IV. DEDICATED OMS . . . . .	IV-1
A. Design Requirements and Criteria . . . . .	IV-1
B. Design Analysis . . . . .	IV-8
C. Detailed Design . . . . .	IV-28
D. Results and Conclusions . . . . .	IV-30
V. SPACE TUG POINT-DESIGN . . . . .	V-1
A. Mission and Spacecraft Criteria . . . . .	V-1
B. NASA Baseline Propellant Storage and Feed Systems Description . . . . .	V-13
C. Martin Marietta Propellant Storage and Feed System . . . . .	V-18
D. Detailed Design . . . . .	V-55
E. Comparison of NASA Baseline and Martin Marietta Storage and Feed System . . . . .	V-69
F. Conclusions . . . . .	V-73
	and
	V-74

VI.	DEVELOPMENT PLAN . . . . .	VI-1
A.	Objectives, Guidelines and Approach . . . . .	VI-2
B.	DSL Tank and Feedline Development Requirements . . . . .	VI-4
C.	Prototype System Development . . . . .	VI-7
D.	DSL Tank and Feedline Costs . . . . .	VI-14
E.	Development Program Schedule . . . . .	VI-15
VII.	CONCLUSIONS AND RECOMMENDATIONS . . . . .	VII-1
VIII.	REFERENCES . . . . .	VIII-1 thru VIII-4

Figure

---

I-1	Program Schedule . . . . .	I-3
II-1	Basic DSL Concept . . . . .	II-3
II-2	Channel/Liner System . . . . .	II-6
II-3	Trap/Liner System . . . . .	II-8
II-4	ESL Dual-Feedline Design . . . . .	II-10
II-5	ESL Single-Feedline Design . . . . .	II-10
II-6	Weeping Tank Concept . . . . .	II-12
II-7	Screen Liner for Cryogenic Feedlines . . . . .	II-14
II-8	Screen Liner for Tank/Feedline System . . . . .	II-14
II-9	Screen Breakdown with DSL . . . . .	II-16
II-10	Hydrostatic Head with DSL . . . . .	II-19
II-11	Hydrostatic Head with Weeping Tank Concept . . . . .	II-19
II-12	Maximum LH <sub>2</sub> Hydrostatic Head vs Acceleration Level . . . . .	II-21
II-13	Maximum LO <sub>2</sub> Hydrostatic Head vs Acceleration Level . . . . .	II-22
II-14	The effect of Temperature on Pressure Retention Capability in Hydrogen . . . . .	II-24
II-15	The Effect of Temperature on Pressure Retention Capability in Oxygen . . . . .	II-25
II-16	Differential Pressure vs Approach Velocity for LH <sub>2</sub> at 19°K (34.2°R), Huyck Feltmetal Materials . . . . .	II-28
II-17	Differential Pressure vs Approach Velocity for LH <sub>2</sub> at 19°K (34.2°R), Bendix "Poroplate" Materials . . . . .	II-29
II-18	Theoretical Single Dry Screen Pressure Drop . . . . .	II-31
II-19	Feedline Schematic . . . . .	II-32
II-20	Outflow Capability of a Spherical Dual Screen Liner with LO <sub>2</sub> . . . . .	II-36
II-21	Outflow Capability of a Spherical Dual Screen Liner in LH <sub>2</sub> . . . . .	II-37
II-22	Outflow Capability of a Spherical Weeping Tank with LO <sub>2</sub> . . . . .	II-38

II-23	Outflow Capability of a Spherical Weeping Tank with LH <sub>2</sub> . . . . .	II-39
II-24	Outflow Capability of a Spherical Channel System with LO <sub>2</sub> , Liquid Annulus = 2.54 cm . . . . .	II-40
II-25	Outflow Capability of a Spherical Channel System in Oxygen, Liquid Annulus = 3.18 cm (1½ in.) . . . . .	II-41
II-26	LO <sub>2</sub> OMS Feedline Start Transient Model Design . . . . .	II-44
II-27	OMS LO <sub>2</sub> Tank Feedline Pressure Transients . . . . .	II-45
II-28	OMS LO <sub>2</sub> Tank Feedline Flow Velocity Transients . . . . .	II-46
II-29	OMS LO <sub>2</sub> Tank Pressure Differential across 25.4-cm (10-in.) 200x1400 Fine Mesh Screen Trap . . . . .	II-47
II-30	Maximum Wicking Length for Liquid Hydrogen as a Function of Heat Flux . . . . .	II-50
II-31	Maximum Wicking Length for Liquid Oxygen as a Function of Heat Flux . . . . .	II-51
II-32	Dryout Limit for LH <sub>2</sub> with 200x1400 Screen on Plate . . . . .	II-52
II-33	Dryout Limit for LO <sub>2</sub> with 200x1400 Screen on Plate . . . . .	II-53
II-34	Transient Movement of Vapor-Liquid Interface on a 200x1400 Screen Wick . . . . .	II-55
II-35	DSL Tank Pressure History . . . . .	II-58
II-36	Tank Pressure Illustrating DSL Vent System . . . . .	II-61
II-37	DSL Vent System Performance Characteristics . . . . .	II-63
II-38	Effect of Gas Annulus Gap on Vent Rate . . . . .	II-65
II-39	Pressure Rise Rate in Spherical Hydrogen Tank, BP = 6.9 N/cm <sup>2</sup> (10 psi) . . . . .	II-68
II-40	Pressure Rise Rate in Spherical Hydrogen Tank, BP = 0.69 N/cm <sup>2</sup> (1.0 psia) . . . . .	II-69
II-41	Pressure Rise Rate in Cylindrical Hydrogen Tank, BP = 6.9 N/cm <sup>2</sup> (10 psia) . . . . .	II-70
II-42	Collapse Time for Spherical Vapor Bubble in Subcooled Liquid (Prisnyakov) . . . . .	II-74
II-43	Spot Cooling Geometry . . . . .	II-76
II-44	Simplified Analysis . . . . .	II-76
II-45	Predicted Thermal Performance of Weeping Tank . . . . .	II-78
II-46	Effect of Wall Thickness on Weeping Tank Thermal Performance . . . . .	II-79
II-47	Pleated Screen Sphere . . . . .	II-82
II-48	Octosphere Capillary Screen Structure . . . . .	II-83
II-49	Structural Weight Estimate for 2.44 m (8 ft) Diameter Octosphere . . . . .	II-85
II-50	Structural Weight Estimate for 3.05-m (10-ft) Diameter Octosphere . . . . .	II-86
II-51	Structural Weight Estimate for a 3.05-m (10-ft) diameter, 4.88-m (16-ft) Long Cylindrical Tank with Octospherical Domes . . . . .	II-87
II-52	Screen Radius or Short Span at Critical Stress . . . . .	II-90

II-53	Pressed-Type Penetration Design . . . . .	II-95
II-54	Riveted and Screwed Type Penetration Designs . . . . .	II-95
II-55	Comparison of Outflow Capability of One-Tank and Two-Tank Systems for Liquid Hydrogen . . . . .	II-98
II-56	Comparison of Outflow Capability of One-Tank and Two-Tank Systems for Liquid Oxygen . . . . .	II-99
II-57	Parallel-Sequenced Drain Concept, Two-Tank System . . . . .	II-100
II-58	Series/Start Tank Concept, Two-Tank System . . . . .	II-101
II-59	Series/Common Drain Concept, Two Tank System . . . . .	II-102
III-1	Ideal Expulsion Efficiency of Screen Systems in a 3.8-m (12.5-ft) Diameter Spherical LH <sub>2</sub> Tank . . . . .	III-11
III-2	Ideal Expulsion Efficiency of Screen Systems in a 2.58-m (8.5-ft) Diameter Spherical LO <sub>2</sub> Tank . . . . .	III-12
III-3	Relationship of Actual to Ideal Expulsion Efficiency for Two Outflow Capability Comparison Criteria . . . . .	III-16
III-4	LH <sub>2</sub> Outflow Rate Capability Comparison for Screen Systems Using the 1.01 Criterion . . . . .	III-17
III-5	LH <sub>2</sub> Outflow Rate Capability Comparison for Screen System Using the 1.01 Criterion . . . . .	III-18
III-6	LO <sub>2</sub> Outflow Rate Capability Comparison for Screen Systems Using the 1.01 Criterion . . . . .	III-19
III-7	LO <sub>2</sub> Outflow Rate Capability Comparison for Screen Systems Using the 1.10 Criterion . . . . .	III-20
III-8	LH <sub>2</sub> Outflow Rate Capability Comparison with Varying Amounts of Propellant Remaining in Tank . . . . .	III-21
III-9	LH <sub>2</sub> Outflow Rate Capability Comparison for Varying Channel Depths . . . . .	III-23
III-10	LO <sub>2</sub> Outflow Rate Capability Comparison for Varying Channel Depths . . . . .	III-24
III-11	Tank in Offloaded Condition . . . . .	III-27
III-12	LH <sub>2</sub> Outflow Rate Capability Comparison between Single- and Double-Layer Screen . . . . .	III-35
III-13	LO <sub>2</sub> Outflow Rate Capability Comparison between Single- and Double-Layer Screen . . . . .	III-36
III-14	LH <sub>2</sub> Outflow Rate Capability Comparison for Positive and Negative Accelerations . . . . .	III-37
III-15	LO <sub>2</sub> Outflow Rate Capability Comparison for Positive and Negative Accelerations . . . . .	III-38
III-16	Detail Design for LH <sub>2</sub> Acquisition/Expulsion System Capillary Liner Assembly . . . . .	III-41
III-17	LH <sub>2</sub> Acquisition/Expulsion System and Tank Assembly Details . . . . .	III-47
III-18	LO <sub>2</sub> Acquisition/Expulsion System and Tank Assembly Details . . . . .	III-49
III-19	Capillary Feedline Configuration . . . . .	III-53

IV-1	OMS Maneuver Requirements for Easterly Launch . . . . .	IV-4
IV-2	OMS Maneuver Requirements for Polar Mission . . . . .	IV-5
IV-3	OMS Maneuver Requirements for Resupply Mission . . . . .	IV-6
IV-4	Radius of Polysphere with Volume Equal to Reference Sphere having a Radius Equal to 1.000 . . . . .	IV-9
IV-5	Volume of Polysphere with Radius Equal to Reference Sphere Radius . . . . .	IV-11
IV-6	Surface Area of Polysphere Compared to Reference Sphere having a Surface Area Equal to 1.000 . . . . .	IV-12
IV-7	Illustration of Aspect Ratio . . . . .	IV-13
IV-8	Device Hardware Weight Comparisons . . . . .	IV-15
IV-9	Residual Propellant Weight Comparisons . . . . .	IV-17
IV-10	Relationship of Flow Rate Capability to Device Hardware Weight . . . . .	IV-18
IV-11	Relationship of Flow Rate Capability to Residual Weight . . . . .	IV-19
IV-12	Total System Weight Comparisons . . . . .	IV-21
IV-13	Outflow Rate Capability for Selected Design . . . . .	IV-22
IV-14	Dedicated OMS LO <sub>2</sub> Tank Pressure History . . . . .	IV-24
IV-15	Trap Installed in High-Pressure OMS LO <sub>2</sub> Tank . . . . .	IV-27
IV-16	Truncated Channel System for a Cylindrical Tank . . . . .	IV-29
V-1	NASA Baseline MPS Schematic . . . . .	V-14
V-2	NASA Baseline APS Schematic . . . . .	V-17
V-3	Hydrostatic Head Retention Capability of Multiple Layers of 200x1400 Dutch Twill Screen in Liquid Hydrogen . . . . .	V-20
V-4	Hydrostatic Head Retention Capability of Multiple Layers of 200x1400 Dutch Twill Screen in Liquid Oxygen . . . . .	V-21
V-5	Refillable Trap Schematic . . . . .	V-27
V-6	Hydrostatic Head Retention Capability of Selected Screens in Liquid Hydrogen . . . . .	V-29
V-7	Hydrostatic Head Retention Capability of Selected Screens in Liquid Oxygen . . . . .	V-30
V-8	Illustration of Stable and Unstable Region . . . . .	V-31
V-9	Weight Tradeoff Matrix for LH <sub>2</sub> Channel Designs . . . . .	V-35
V-10	Channel Configurations for Application with and without a Full Tank Screen Liner . . . . .	V-38
V-11	Cross-Section of Wicking Channel . . . . .	V-39
V-12	Space Tug LH <sub>2</sub> Tank Pressure History for Martin Marietta Design . . . . .	V-43
V-13	Space Tug LO <sub>2</sub> Tank Pressure History for Martin Marietta Design . . . . .	V-44
V-14	LH <sub>2</sub> MPS Capillary Feedline Design Requirements for Space Tug MPS . . . . .	V-48
V-15	Required Layers of Screen versus Feedline Length for LH <sub>2</sub> MPS Feedline . . . . .	V-50
V-16	LO <sub>2</sub> Capillary Feedline Design Requirements for Space Tug MPS . . . . .	V-51

V-17	LH <sub>2</sub> Capillary Feedline Required Layers of Screen . . . . .	V-53
V-18	LH <sub>2</sub> Trap System for Space Tug . . . . .	V-57
V-19	LO <sub>2</sub> Trap System for Space Tug . . . . .	V-59
V-20	LH <sub>2</sub> and LO <sub>2</sub> Channel Systems for Space Tug . . . . .	V-63
V-21	Supporting Rib Design for LH <sub>2</sub> Screen Liner . . . . .	V-65
VI-1	Development Program for Full-Scale Cryogenic Acquisition/ Expulsion System . . . . .	VI-5
VI-2	DSL Tank and Feedline Development Status . . . . .	VI-15

Table

---

II-1	Effect of Bubble Point on Venting . . . . .	II-67
II-2	Complexity Comparison . . . . .	II-104
II-3	Weight and Performance Comparison . . . . .	II-104
II-4	Technology Cost/Risk Comparison . . . . .	II-104
II-5	Foraminous Materials Rating Matrix . . . . .	II-108
III-1	Summary of Design Missions . . . . .	III-3
III-2	Seven-Day Polar Mission Timeline . . . . .	III-4
III-3	Space Station Resupply Mission Timeline . . . . .	III-4
III-4	Easterly Launch Mission Timeline . . . . .	III-5
III-5	Integrated OMS/RCS Baseline Design Parameters . . . . .	III-6
III-6	Acceleration Environment . . . . .	III-7
III-7	Pressurization and Venting Analysis Results . . . . .	III-26
III-8	Integrated OMS/RCS Feedline Summary . . . . .	III-32
III-9	Shuttle Mission Initial Propellant Usage . . . . .	III-39
III-10	Acquisition/Expulsion System - Dimension Summary . . . . .	III-44
III-11	Propellant Storage System Dry Mass for Integrated OMS . . . . .	III-45
III-12	Acquisition/Expulsion System - Performance Characteristics . . . . .	III-46
III-13	Integrated OMS/RCS Capillary Feedline Detailed Design Data . . . . .	III-56
IV-1	Earth Storable OMS Candidate Propellant Performance . . . . .	IV-2
IV-2	OMS Mission Requirements . . . . .	IV-3
IV-3	Propellant Tankage Requirements for OMS Propellant Acquisition System . . . . .	IV-3
IV-4	Propellant Flow Rate Ranges for an OMS Propulsion Module . . . . .	IV-7
V-1	$\Delta V$ Budget for Equatorial Synchronous Orbit . . . . .	V-4
V-2	Space Tug Timeline . . . . .	V-7
V-3	MPS Operating Characteristics and Requirements . . . . .	V-8
V-4	APS Operating Characteristics and Requirements . . . . .	V-9
V-5	Space Tug Weight Summary . . . . .	V-10
V-6	Summary of Space Tug Accelerations . . . . .	V-11
V-7	Space Tug Thermal Characteristics . . . . .	V-12
V-8	LO <sub>2</sub> and LH <sub>2</sub> Requirements for Trap Design . . . . .	V-25

V-9	Propellant Trap Settling Safety Factors . . . . .	V-26
V-10	Propellant Trap Design Safety Factors . . . . .	V-31
V-11	Results of Pressurization and Venting Simulation . . . . .	V-45
V-12	Propellant Settling Distance During MPS Start Transient . . . . .	V-47
V-13	Space Tug MPS Capillary Feedline Design Requirements . . . . .	V-49
V-14	Space Tug APS Capillary Feedline Design Requirements . . . . .	V-54
V-15	Estimated Boiloff for a Martin Marietta Screen Liner Feedline . . . . .	V-55
V-16	Weight Comparison of LO <sub>2</sub> and LH <sub>2</sub> Trap Designs . . . . .	V-56
V-17	Channel Spacing Design Options and Criteria . . . . .	V-62
V-18	Weight Comparison of LO <sub>2</sub> Trap and Liner Designs . . . . .	V-65
V-19	Weight Comparison of LH <sub>2</sub> Trap and Liner Designs . . . . .	V-66
V-20	Weights of LH <sub>2</sub> and LO <sub>2</sub> Channel/Liner Designs . . . . .	V-66
V-21	Space Tug Capillary Feedline Weights . . . . .	V-68
V-22	Comparison of NASA Baseline and Martin Marietta System Weights (without Liners) . . . . .	V-72
V-23	Comparison of NASA Baseline and Martin Marietta System Weights (with Liners) . . . . .	V-72
VI-1	DSL Tank Development Summary . . . . .	VI-8
VI-2	DSL Feedline Development Summary . . . . .	VI-10
VI-3	Fabrication Development Summary . . . . .	VI-11
VI-4	DSL Tank and Feedline Development Program Costs . . . . .	VI-14

## SUMMARY

---

A comprehensive cryogenic design effort was conducted under this phase of the contract. Design methods and techniques for designing cryogenic acquisition/expulsion systems were developed and verified through ground tests.

Detailed designs were made for three Earth orbital propulsion systems: (1) the Space Shuttle (integrated) OMS/RCS, (2) the Space Shuttle (dedicated) OMS (LO<sub>2</sub>), and (3) the Space Tug. The preferred designs from the integrated OMS/RCS were used as the basis for the flight test article design in Phase C. A plan was prepared that outlines the steps, cost, and schedule required to complete the development of the prototype DSL tank and feedline (LH<sub>2</sub> and LO<sub>2</sub>) systems.

Ground testing of a subscale model using LH<sub>2</sub> verified the expulsion characteristics of the preferred DSL designs. Because of the 1-g thermal stratification of LH<sub>2</sub>, the liquid-free vapor venting of the DSL concept could not be completely verified.

The passive cryogenic DSL tank/feedline design has great potential application for space missions in the near future. The design should be validated in a test flight that will provide an extended period (7 to 14 days) of low-g performance at an early date.

## I. INTRODUCTION

Results of the design effort conducted during the cryogenic system phase (Phase A) of the program are presented in this volume. In this phase, preferred passive acquisition/expulsion concepts were designed and recommended for subcritical storage of cryogenics used in the Space Shuttle Orbiter and the Space Tug propulsion systems. The design effort was complemented by the experimental program presented in Volume III.

### A. BACKGROUND AND OBJECTIVES

The design effort was considered to be an extension of work begun under Contract NAS9-10480, a general study that evaluated a wide range of probable subcritical cryogenic storage applications including a design for a low-crossrange Shuttle Orbiter. The parametric and point design results (Ref I-1), show the dual-screen-liner (DSL) concept was extremely attractive for service in both the Orbiter LO<sub>2</sub> and LH<sub>2</sub> storage tanks. The unique feature of the DSL concept (Ref I-2), compared to other proposed acquisition/expulsion concepts, is that it passively controls the entire bulk propellant during long storage. It is the only passive concept that provides the following performance when incorporated in the storage tank and feedline.

- 1) Pressure-relief of the storage system by venting vapor, as required;
- 2) Gas-free liquid expulsion on demand;
- 3) Near-continuous control of the bulk propellant.

Because reliability and weight are key considerations for reusable vehicles such as the Space Shuttle and Space Tug, the attractiveness of the passive DSL screen device is evident. Its pressure-relief technique compares favorably on a thermodynamic basis with other methods such as the liquid venting technique (Ref I-1 and I-3), while allowing either intermittent or continuous venting of vapor. Based on these earlier results, the DSL concept was selected as the baseline for this study. It was modified to satisfy the representative mission/system criteria compiled during the study and listed in Reference I-4.

Martin Marietta conducted the program under direction of the NASA-Johnson Space Center (JSC) as part of NASA's Advanced Technology Program to provide propulsion systems for future manned Earth orbiting vehicles (circa late 1970s and early 1980s). Specific objectives of the cryogenic study phase (Phase A) were to:

- 1) provide detailed cryogenic designs for the Space Shuttle (integrated) OMS/RCS, the Space Shuttle (dedicated) OMS (LO<sub>2</sub>) and the Space Tug;
- 2) verify the designs with subscale ground tests;
- 3) provide a development plan, emphasizing schedules and costs, for the Space Shuttle OMS/RCS integrated systems;
- 4) provide the design for the orbital flight test article to be used for the Phase C effort.

#### B. GUIDELINES AND APPROACH

Contract NAS9-10480 was limited to the cryogen tank only and did not include detailed analyses of the total system integration and performance requirements. These considerations were included in the acquisition/expulsion system analysis and design tasks of program Phase A. The system boundaries, as defined here, began with the pressurant inlet to the propellant tanks and ended at the interface provided by the turbopump assembly (TPA) in the feedline. Design flexibility, i.e., efficient and reliable operation over the range of Shuttle Orbiter and Space Tug missions, was to be emphasized.

The primary operational requirements for propellant acquisition/expulsion system were to: (1) supply gas-free liquid to the TPA on demand; and (2) provide pressure relief of the storage system, as required, by venting liquid-free vapor. Because the Shuttle Orbiter and Space Tug are reusable vehicles (100 missions over 10 years), it was also desirable to make the acquisition/expulsion device be reusable and inspectable with minimum maintenance.

The program was conducted in four separate tasks over a 23-month period, as shown in Fig. I-1. During Task 1, the design criteria and mission duty cycles were compiled for the Shuttle Orbiter (integrated) OMS/RCS, the Shuttle Orbiter (dedicated) OMS (LO<sub>2</sub>), and the Space Tug.



The design criteria were obtained from the most current information available from both NASA-and DOD-funded studies. The criteria and guidelines from Task I (Ref I-4) were used in the design task. (Task II). Under Task II, design analyses and trade studies were performed that resulted in selecting and recommending preferred designs for the three Earth-orbiting vehicles. During Task II, critical technical areas affecting the designs were also evaluated with an eye to establishing recommended design guidelines and approaches while identifying preferred analytical tools. These results are presented in Chapter II of this volume. The results of Task II, and the designs for the integrated OMS/RCS, dedicated OMS (LO<sub>2</sub>), and the Space Tug, are presented separately in Chapters III, IV, and V, respectively. The preferred integrated OMS/RCS design was also selected as the baseline system (see Volume IV) for the orbital flight test article.

The technical approach in this program placed a strong emphasis on ground testing. During the 18 months of testing under Task III, the design methods and analytical models (see Chapter II) were verified experimentally. The ground test plan outlined in Reference I-5 was submitted and approved by NASA in October, 1971. The plan included testing of the 63-cm(25-in.) diameter model to demonstrate vapor-free liquid outflow and liquid-free vapor venting using LH<sub>2</sub> as the test liquid. The plan included low-g tests to be conducted in the KC-135 aircraft. This phase of the program also benefitted by results obtained from two IR&D experimental programs which were conducted concurrently with Phase A. The two programs were: (1) the development and testing of a 6.1-m (20-ft) long cryogenic feedline model using LN<sub>2</sub> as the test liquid; and (2) the fabrication and inspection of the 178-cm (70-in.) diameter screen tank. Results of the Task III effort, including the IR&D programs, are shown in Volume III.

The DSL development plan, Task IV, is presented separately in Chapter VI. This plan outlines the steps necessary to carry the cryogenic systems from an engineering conceptual design to a completely developed prototype system.

Conclusions and recommendations from the Phase A effort are presented in Chapter VII.

## II. CRYOGENIC PROPELLANT ACQUISITION/EXPULSION DEVICES

This chapter presents the basis for the design effort conducted under Phase A. Candidate systems are described, which use passive methods for controlling cryogenic propellants under the operational environments of the Shuttle Orbiter and Space Tug. From these candidates, systems can be selected for more detailed analyses and trade studies to yield the preferred design for a specific vehicle. In addition, this chapter presents design information basic to the analyses and efforts presented in Chapter III through V. The majority of this design information was generated under this program. The information is categorized into the four technical areas that affect the design of cryogenic acquisition devices, as follows:

- 1) Fluid mechanics;
- 2) Thermal and thermodynamic considerations;
- 3) Structural considerations;
- 4) Configuration and size considerations.

### A. CANDIDATE SYSTEMS

The systems evaluated for cryogenic propellant acquisition/expulsion systems were based on the Martin Marietta dual-screen-liner (DSL) capillary concept. The systems are varied from this basic design, as required, to meet the specific mission requirements. The DSL is a complete capillary screen liner within the storage tank that passively controls the bulk propellant during low-g periods.

Capillary systems are designed to provide stability and control of the fluid to assure single-phase fluid withdrawal for vapor venting and liquid expulsions during low-g operation. Stability criteria are available for selecting pore size and type of foraminous material to be used in capillary devices (Ref II-1 and II-2). Whether the capillary system is a small trap or includes a complete liner, the screen device assures the desired liquid/vapor interface stability and bulk liquid control for any vehicle

maneuvers. Technical areas affecting the design of capillary systems, such as pressure retention capability of the screen, are discussed later in this chapter.

The DSL has been analyzed extensively by Martin Marietta under company-funded and contractual programs and compares favorably to the thermodynamic liquid vent method at required operating pressures (Ref II-3). The DSL tends to be simpler (no valves), while weighing less and providing a better system response for intermittent venting. A discussion of the basic DSL concept and variations of the concept is presented in the following paragraphs.

1. Dual-Screen Liner (DSL) System

The basic dual-screen liner (DSL) system is illustrated in Figure II-1. Two complete Dutch-twill metal cloth liners are positioned within the tank to (1) enclose all of the propellant during low-g storage; (2) provide a liquid trap that will supply gas-free liquid on demand; and (3) provide a controlled vapor region to permit liquid-free gas venting as required for achieving tank pressure control during long low-g coast periods.

The outer screen liner isolates the propellant from the tank wall during low-g storage periods. The region between the liner and tank wall provides a controlled volume from which vapor can be vented overboard to control tank pressure. The annular region between the two screens provides a preferential path for gas-free liquid to flow to the tank outlet on demand. Liquid in this annulus is displaced during expulsions by liquid from the central bulk region. Passive communication screens allow pressurization of the bulk propellant region by introducing pressurant in the outer annulus.

While vaporization of liquid at the surface of the outer liner tends to thermally isolate the bulk propellant, it also raises the pressure in the outer gas annulus. If the pressure is not relieved by venting, gas will break through the communication screen and enter the bulk region. This occurs when the pressure difference between the vapor region and the bulk liquid exceeds the bubble point (BP) of the screen.

During high-g operation, the liner will protrude some distance above the gravity-dominated liquid position and liquid will be in the annular region formed by the liner and tank wall. Sufficient ullage volume is provided in the central portion of the

tank so liquid can be positioned within the liner when the high-g condition is removed. This liquid repositioning can be accomplished in at least two ways: (1) self-pressurization, and (2) external pressurization. Heat leaking into the system will vaporize liquid near the tank wall. The resulting increase in pressure will force liquid into the lower pressure central region until all liquid is enclosed by the screen liner. A quicker method of emptying this region is to introduce pressurization gas into the outer annulus, thus, forcing the liquid into the central region.

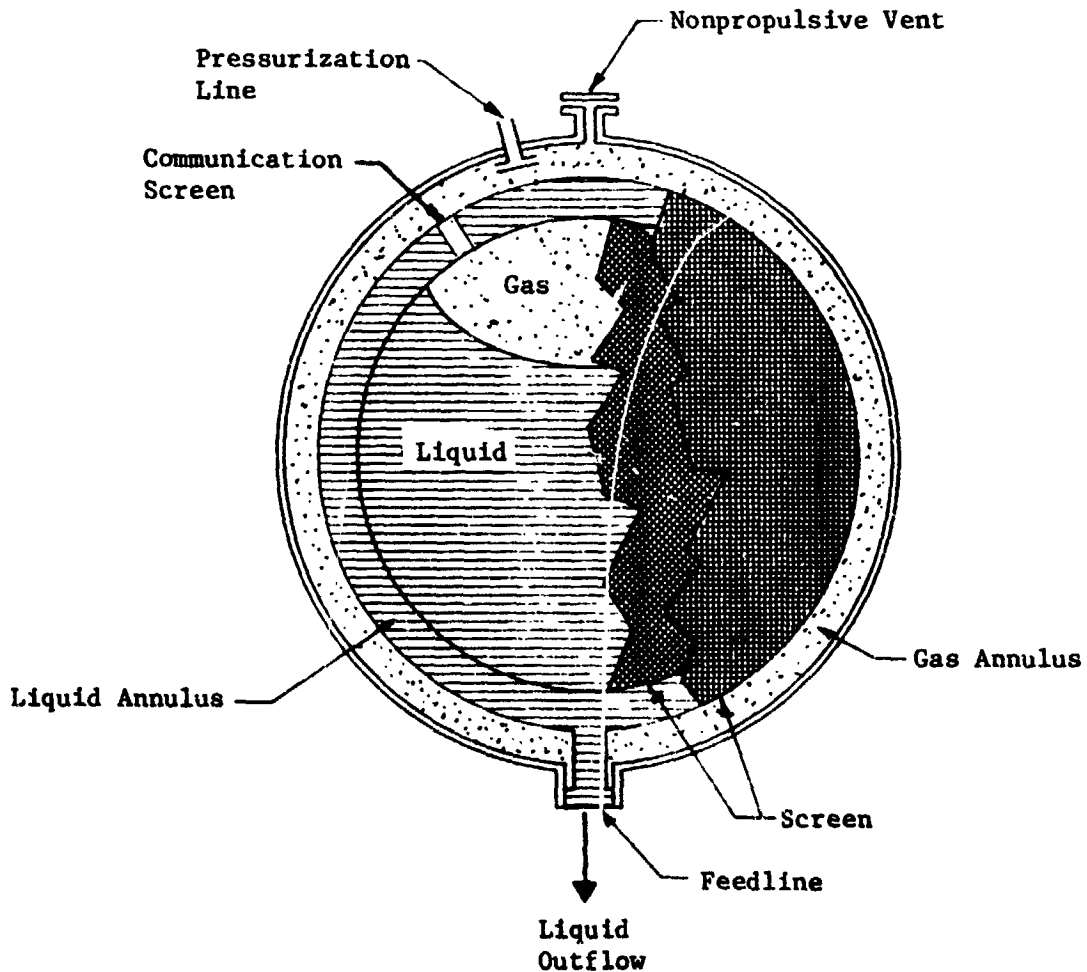


Fig. II-1 Basic DSL Concept

The liquid annulus is filled during tank loading and stabilized by the capillary retention capability of the screen so it will remain filled during the mission. The critical mission periods for stability are during high-g boost and low-g maneuvers. Factors affecting stability under these conditions are discussed in Section B.

The refilling problems associated with other trap concepts and start tanks do not affect the DSL. During an expulsion, bulk liquid flows through the liquid annulus to the tank outlet. Pressurization gas, including warm autogenous pressurant, may be introduced into either the bulk or gas annulus regions, with the latter tending to be the preferred method. Pressurant flows from the outer annulus through the passive communication ports and into the bulk region, displacing propellant into the liquid annulus. The screen liner filters gas out of the annulus until nearly the entire bulk region is emptied. At that point, the liquid entrance loss (bulk liquid entering the annulus through the screen) becomes excessive and the screen retention capability is exceeded. The retention capability, as determined from the bubble point of the screen, must be greater than (or at least equal to) the sum of the adverse pressure differences acting on the screen during the entire mission to continually stabilize the liquid/ullage interfaces at the pores. During low-g, the expulsion efficiency for the DSL is determined by the liquid remaining in the liquid annulus and in the bulk region when the entrance loss exceeds the pressure retention capability of the screen forming the liquid annulus.

Venting of the gas annulus must be performed within the bubble point of the screen liner to assure that liquid does not enter the vapor region during venting. Venting vapor from the tank and feedline requires that the bulk liquid be controlled. Passive communication devices (screen with a lower bubble point than that forming the controlled liquid volume) permit intermittent venting by providing a path of lower resistance for the vapor in the outer annulus to enter the bulk region rather than the liquid annulus. The absolute pressure level may be allowed to increase without causing screen breakdown, i.e., vapor will not enter the controlled liquid annulus region.

Support of the bulk propellant within the tank's central region is provided when the pressure in the gas annulus is greater than that of the central ullage region. This pressure difference must be adequate to support the hydrostatic head of the bulk propellant.

If some liquid is lost into the gas annulus, it will tend to be pushed back into the central portion of the tank because the liquid vaporization and the resulting pressure increase in the annulus will force the liquid into the bulk region. The DSL provides nearly continuous bulk propellant control under the dynamic conditions that may result from thrusting and docking maneuvers during low-g storage. A more detailed discussion of the critical parameters that influence the design of the DSL are presented in Section B.

## 2. Channel/Liner System

Since the expulsion efficiency of the DSL is based on the volume of the liquid annulus, expulsion efficiency and screen weight can be improved by using the channel/liner system shown in Fig. II-2. Instead of a complete liquid annulus, a number of separate screen channels are uniformly spaced around the tank perimeter extending the full length of the tank. The channels are manifolded at the tank outlet to provide gas-free liquid to the feedline. The region between the screen liner and the tank wall provides the gas annulus for venting. The screen between the channels provides passive communication between the gas annulus and the bulk region. The operating characteristics of this system are similar to the basic DSL. Structural support for the screen configuration is provided by coarser screen and/or perforated plate.

In addition to a lower hardware weight than the basic DSL, the channel/liner system reduces the residual propellant, thereby improving the expulsion efficiency. However, the geometry of the channel/liner system is limited by the wicking capability of the communication screen between channels. As an example, during pressurization, the liner may dry out (break down) while allowing gas to enter the bulk region. After pressurization, the liner must rewet if support of the bulk liquid is to be assured. Consequently, one consideration for spacing between channels is to limit the maximum distance to twice the wicking capability for the communication screen. This design constraint and others are discussed more fully in Section B.

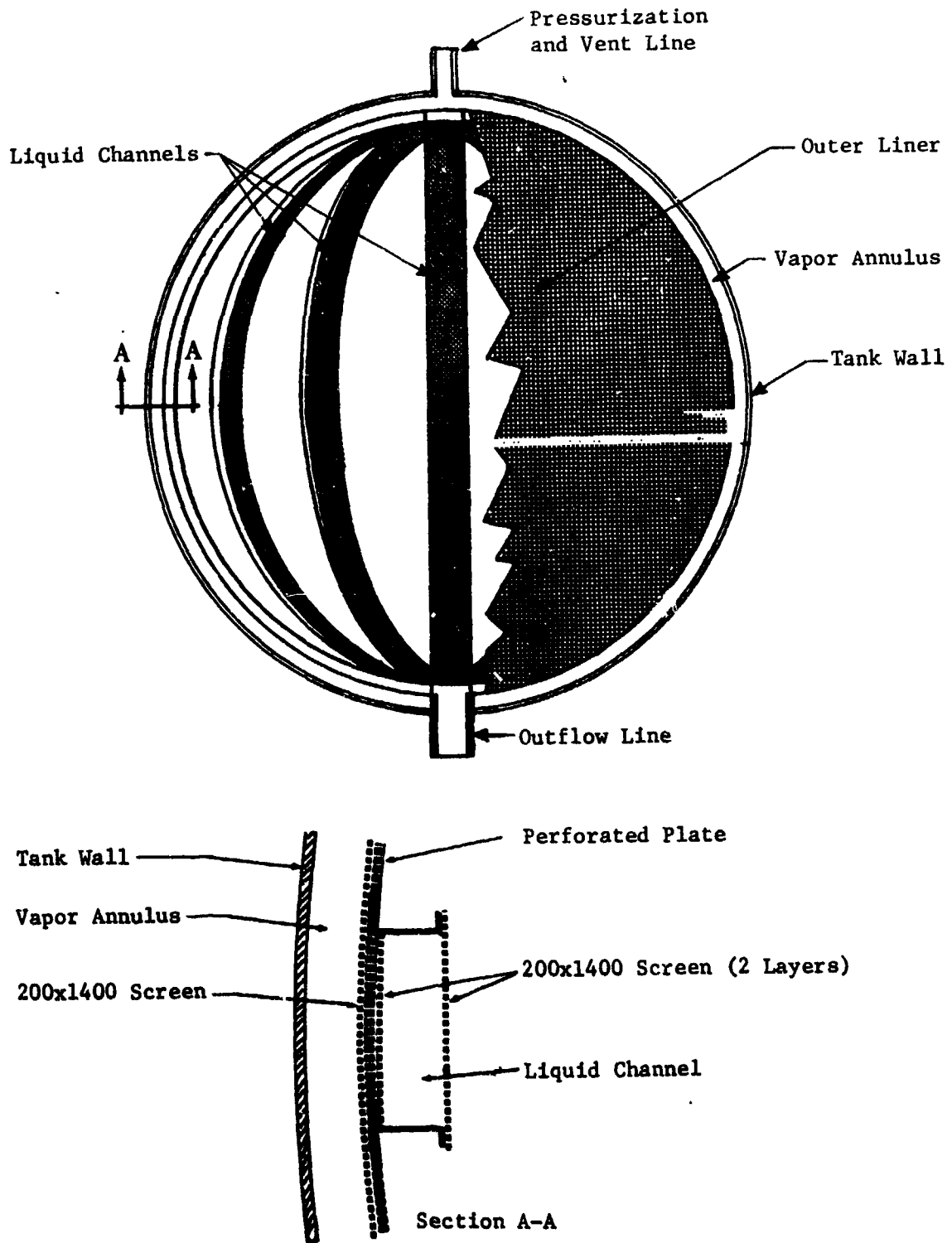


Fig. II-2 Channel/Liner System

### 3. Trap/Liner System

Another variation of the DSL is the refillable trap/liner system shown in Fig. II-3. The trap device is fabricated of fine mesh screen and contains a liquid annulus. The liquid annulus is connected to the tank outlet and is designed so that it is always full. The bulk liquid contained within the trap will contact the liquid annulus and displace liquid in the annulus during pressurization and liquid outflow. The device is refilled under a settling mode when vehicle acceleration during thrusting settles the propellant over the trap.

The region between the outer screen liner and the tank wall forms a gas annulus that allows venting at any time without the need for settling the propellant. Liquid is expelled by pressurizing the gas annulus until pressurant breaks through the screen liner and into the bulk propellant region. Continued pressurization will force the propellant into the controlled liquid region of the device and out the tank outlet. The trap volume is sized to provide gas-free liquid until settling occurs.

This variation of the DSL concept is particularly applicable for systems that experience relatively large longitudinal accelerations. Because the hydrostatic head approximately covers the tank length, the basic DSL system would require several layers of fine mesh screens to maintain stability under high accelerations. This, of course, results in additional hardware weights. The refillable trap uses the high longitudinal accelerations for refilling and the height of liquid that it must support can usually be that provided by a single layer of screen. The refillable trap, however, is mission-dependent and does not offer the flexibility provided by the basic DSL or channel/liner systems.

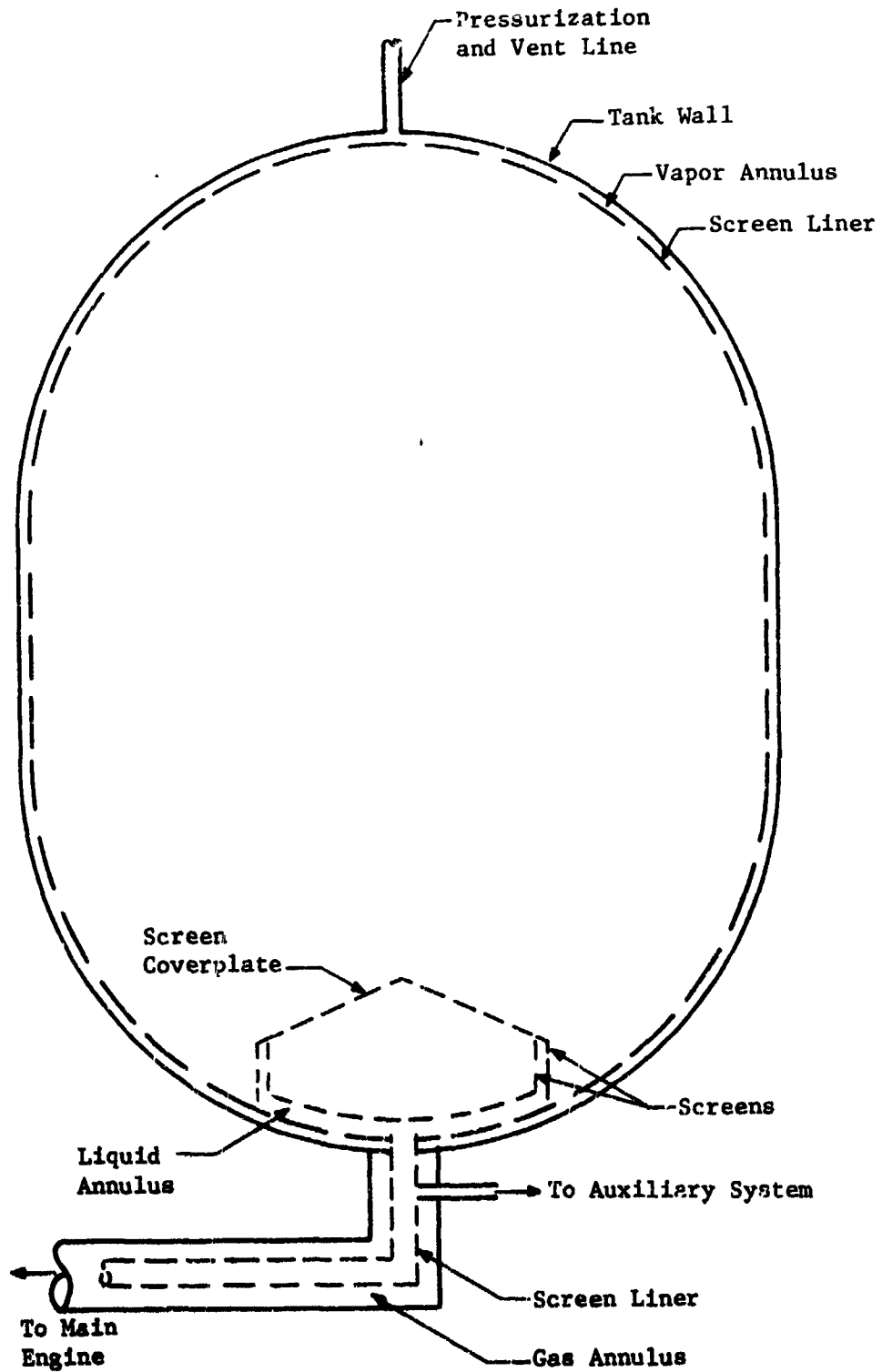


Fig. II-3 Trap/Liner System

#### 4. Eccentric Screen Liner

Another variation of the basic DSL is the eccentric-screen liner (ESL) shown in Fig. II-4 and II-5. It uses an eccentric positioning of the liners to afford the desired minimum surface energy conditions assuming that capillary forces will dominate and position the fluids. Both of the illustrated designs have three spherical-screened compartments. Liquid is expelled from the small central compartment. This compartment is designed so that it remains gas-free until the total liquid volume becomes less than the compartment volume. This is accomplished by the two outer screen liners, which keep liquid in contact with the screen of the central compartment at all times. The two outer screen liners are also sized to minimize hydrostatic head support required during high-g expulsions.

The dual-feedline design using the ESL concept is shown in Fig. II-4. Except during reentry, liquid is expelled from the central compartment through the feedline that is approximately on the X-axis of the vehicle. During reentry, the screens will break down and the liquid remaining in the tank will settle over the reentry feedline which is parallel to Y-axis of vehicle. This axis corresponds to the approximate direction of acceleration during reentry.

The single-feedline design using the ESL concept is shown in Fig. II-5. The outer and middle screen compartments are the same as those in the dual-feedline design. However, the central compartment consists of two hemispheres, one screen hemisphere and another thin-walled hemispherical dome with an outlet. This outlet is also parallel to the vehicle Y-axis. During reentry, the remaining liquid is retained in the central compartment. With these unique features, the ESL system can provide gas-free liquid expulsions during high-g periods, which is not possible with the basic DSL system. However, the three screen liners also result in more screen surface areas and larger hardware weight than that of the basic DSL system.

#### 5. Weeping Tank Concept

With the basic DSL, environmental heat input is intercepted by evaporation at the outer screen surface. Proper operation of this system depends on maintaining the pressure in the outer vapor annulus slightly higher than that in the liquid annulus. The pressure difference across the outer screen (between the

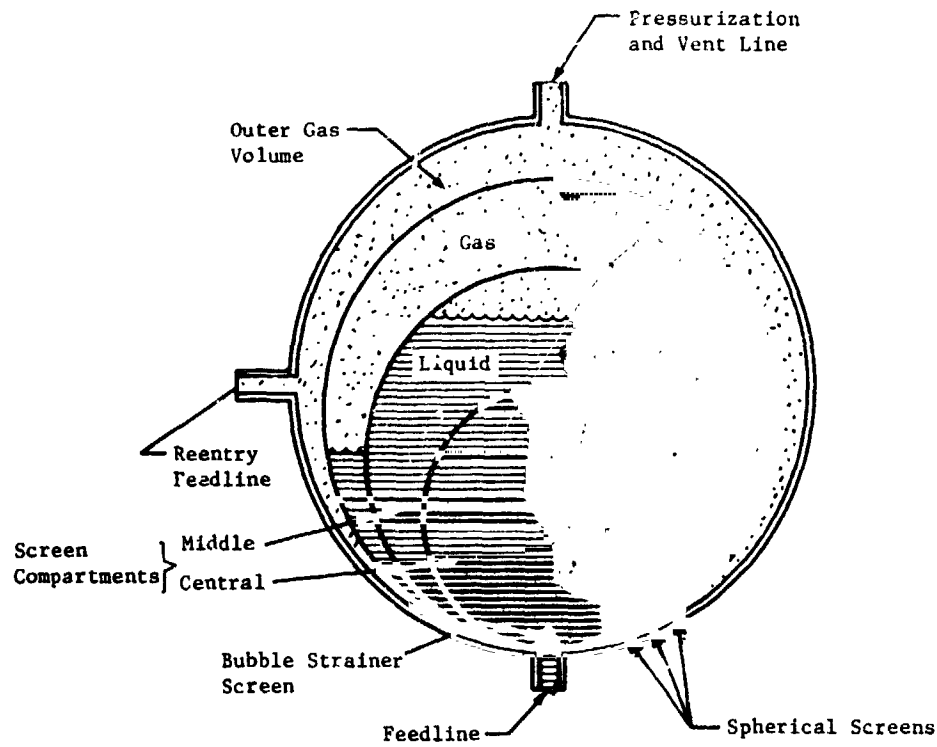


Fig. II-4 ESL Dual-Feedline Design

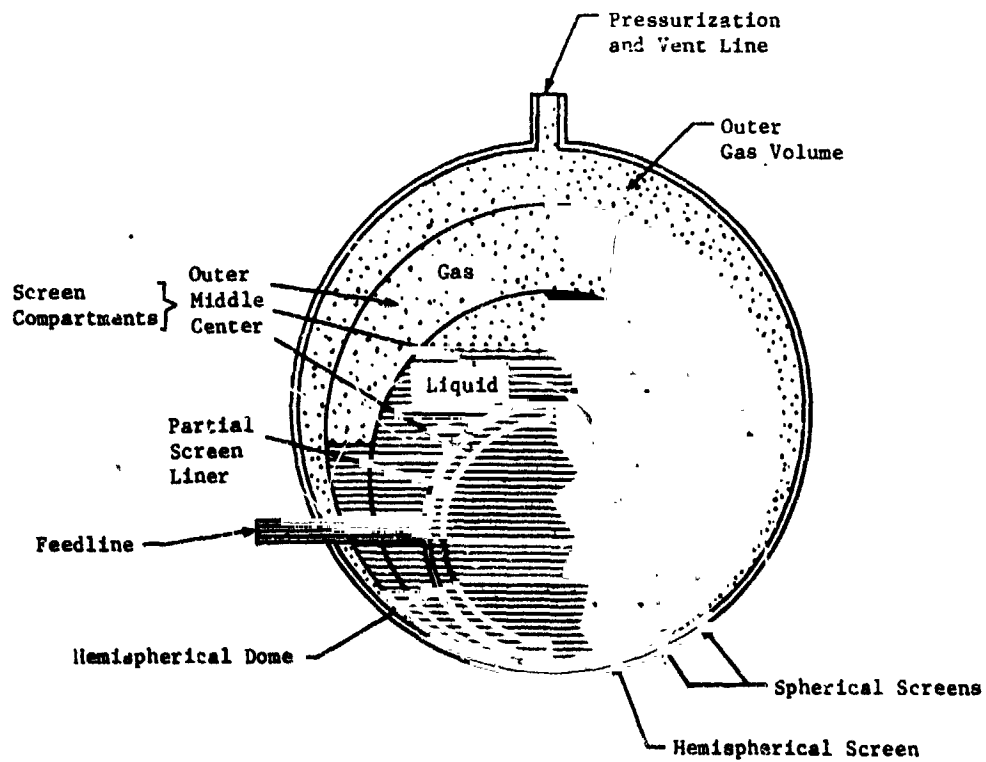


Fig. II-5 FSL Single-Feedline Design

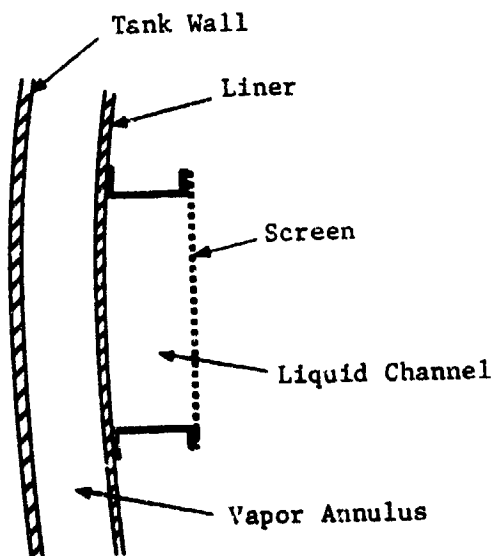
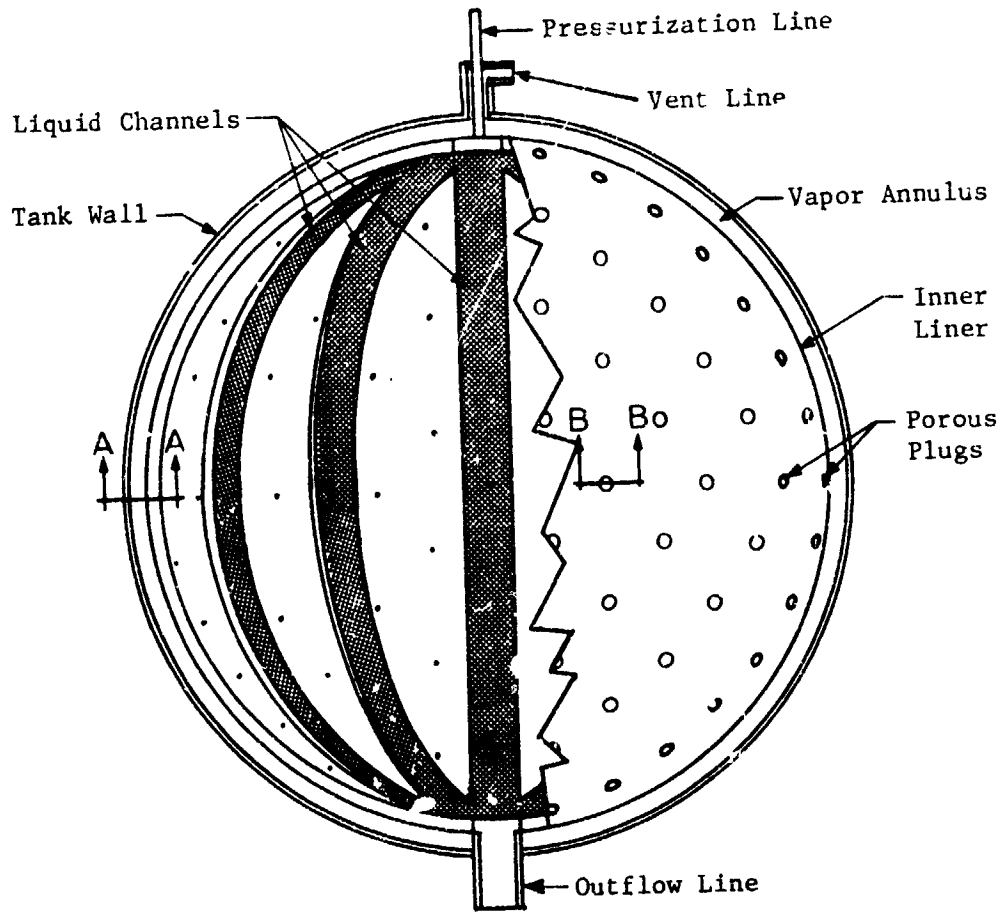
gas annulus and liquid annulus must not exceed the bubble point of the screen; except, of course, during pressurization. The weeping tank concept (Ref. 11-4) provides a means of circumventing the relatively narrow  $\Delta P$  variations of the DSL by allowing the pressure in the vapor annulus to drop below that in the liquid annulus. The resultant propellant leakage is controlled by greatly reducing the permeability of the outer screen. This permeability is chosen so the leakage rate is exactly required to maintain evaporative cooling equal to the net heat load.

The weeping tank concept, shown in Fig. II-6, has different venting characteristics from the basic DSL system. The outer liner is a solid shell (rather than a screen) with porous plugs or "visco jet" plugs to allow relatively slow propellant leakage into the vapor annulus. Screen channels provide gas-free liquid to the tank outlet as in the channel/liner system.

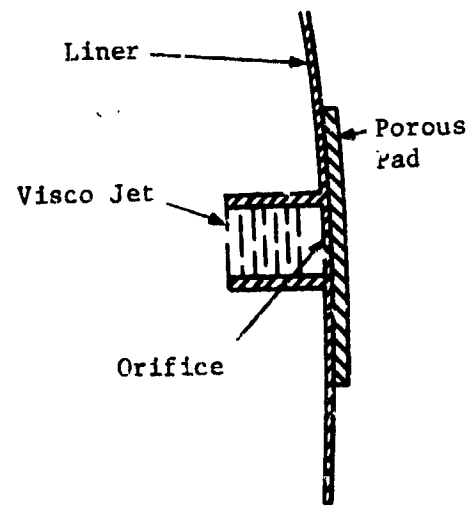
Two possibilities exist for controlling the vent rate with such a system--either controlled or uncontrolled. For an uncontrolled system, the vapor annulus is vented directly to space. The permeability is chosen to accommodate the anticipated heat load with variations in the heat load resulting in departures from the design of the tank operating pressures. The suitability of such a system depends on how well the heat load can be predicted. This type of system could be designed to operate with the pressure in the vapor annulus either above or below the triple point, depending on the pressure drop through the vent system. If operation is below the triple point, then the fluid will freeze somewhere within the permeable material and cooling will be by sublimation.

For the controlled system, venting occurs through a control valve (either on-off or continuous modulation). The vent rate is determined by the pressure difference between the liquid annulus and the vapor annulus. By closing the vent valve, the difference is reduced to zero. This type of system would probably always operate with the vapor annulus above the triple point. Also, the outer shell would have to be designed for the full tank pressure.

For heat inputs on the order of  $0.787 \text{ W/m}^2$  ( $0.25 \text{ Btu/ft}^2\text{-hr}$ ), the desired range of shell permeability is quite low. A cursory survey of porous materials disclosed no material suitable for a continuous permeable surface with reasonable thickness. However, this survey was far from exhaustive. Also, it is possible to use a permeable material intermittently. For example, discrete porous plugs may be spaced at suitable intervals in the tank wall. In



Section A-A



Section B-B

Fig. II-6 Weeping Tank Concept

this construction, cooling is localized, and the allowable temperature gradients in the wall are determined by the required porous plug spacing.

The weeping tank concept appears to offer an attractive alternative to the dual-screen liner for cryogenic low-g propellant storage systems. The same venting principle also appears suitable for feedlines.

6

#### Screen Feedlines

The DSL concept can also be applied to the cryogenic feedline design. As shown in Fig. II-7, a screen liner within the feedline provides a gas annulus and maintains a gas-free liquid core. The screen is supported by a perforated tube. Heat entering from the sides of the feedline vaporizes liquid at the screen liner, providing uniform cooling along the length of the feedline. The gas annulus, which is in communication with the gas annulus of the tank (Fig. II-8) can be vented to maintain the proper gas annulus pressure. Multilayer insulation (MLI) and a feedline vacuum jacket provide the thermal protection system.

The liner operation is similar to that discussed for the storage tank designs. It is attractive because it permits both wet and dry feedline conditions prior to liquid expulsions. Once the screen liner is wetted, the liner stabilizes the interface at its surface. Liquid between the liner and line wall tends to be positioned with the bulk liquid, provided it is in contact with the screen at some point. The controlled vapor region may or may not be in direct communication with the vapor region of the tank.

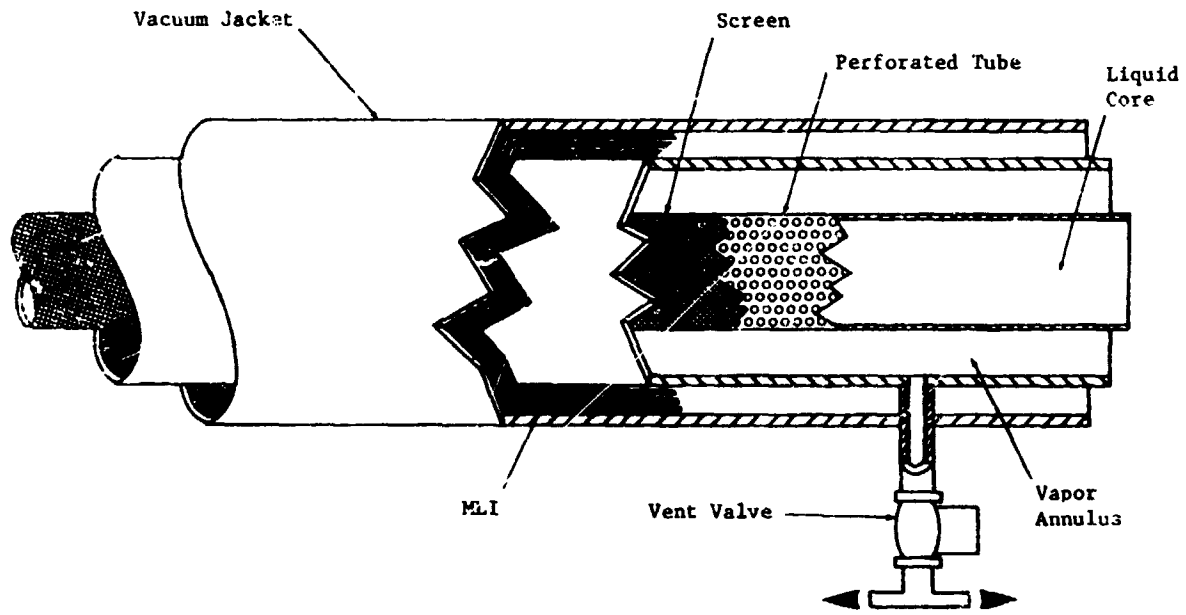


Fig. II-7 Screen Lined Cryogenic Feedlines

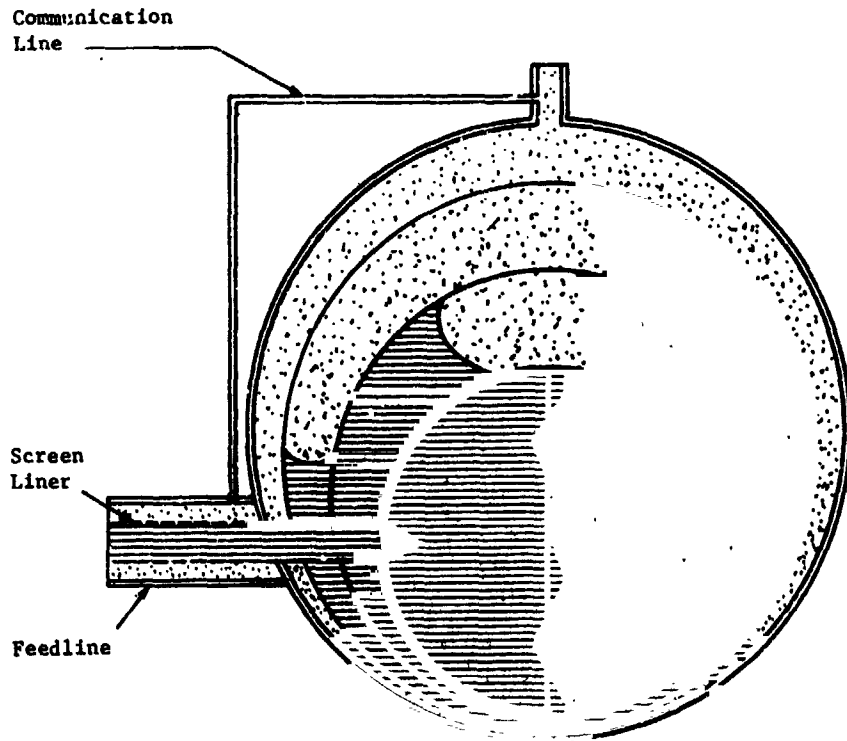


Fig. II-8 Screen Liner for Tank/Feedline System

## B. TECHNICAL AREAS AFFECTING SYSTEM DESIGN

The evaluation and design of a cryogenic acquisition/expulsion system required extensive knowledge of a number of important technical areas. Some of the information assembled during the course of the program, as an aid to selecting the ultimate design, was the result of literature searches and industry surveys. The bulk of the information, however, was collected from analytical and experimental investigations. These investigations were basic in nature and were directed toward answering the questions of--How passive cryogenic retention/expulsion systems could be used? What factors influenced the size, shape, weight performance, and service environment of the systems? This general information is presented here in four basic categories (1) Fluid Mechanics, (2) Thermal and Thermodynamics, (3) Structures, and (4) Configuration and Size.

### 1. Fluid Mechanics

The investigation of fluid mechanics, as related to cryogenic propellant acquisition/expulsion systems, included consideration of both static and dynamic fluid phenomena. Static phenomena investigations included analytical and experimental study of the nature of screen capillary stability. Dynamic phenomena included basic investigations of fluids flowing through capillary media together with computer dynamic system simulations and physical testing of representative system designs. Also included were start transient analyses and tests for representative systems, and analytical definition and test verification of wicking models.

*a. Capillary Stability* - The candidate concepts described in Section A may have functional differences, but they all rely on a common phenomenon for successful operation--the retention capability of the capillary media. All of the retention devices separate liquid regions from vapor regions in the tank and, generally, any ingestion of vapor into the controlled liquid region is undesirable and contrary to design philosophy. Thus, a complete knowledge of the capillary retention capabilities of the retention media in the devices is required.

When vapor passes through a screen or other capillary device into a controlled liquid region, the screen is said to have broken down. This breakdown phenomenon occurs when the sum of the pressure differentials associated with (1) the exposed hydrostatic

head of the device, (2) the viscous losses from fluid transfer across the screen, (3) the viscous losses from fluid transfer in the controlled liquid region, and (4) the velocity head at the point of breakdown, exceed the capillary retention capability of the device. Depending on the orientation of the acceleration vector, these terms can be additive.

Therefore, in Fig. II-9, when the acceleration settles the liquid away from the outlet, the differential pressures are additive for a screen of uniform pore size. Breakdown will first occur at the point near the outlet, as indicated. This is a worst-case condition because if the acceleration were in the opposite direction then the terms would not be additive.

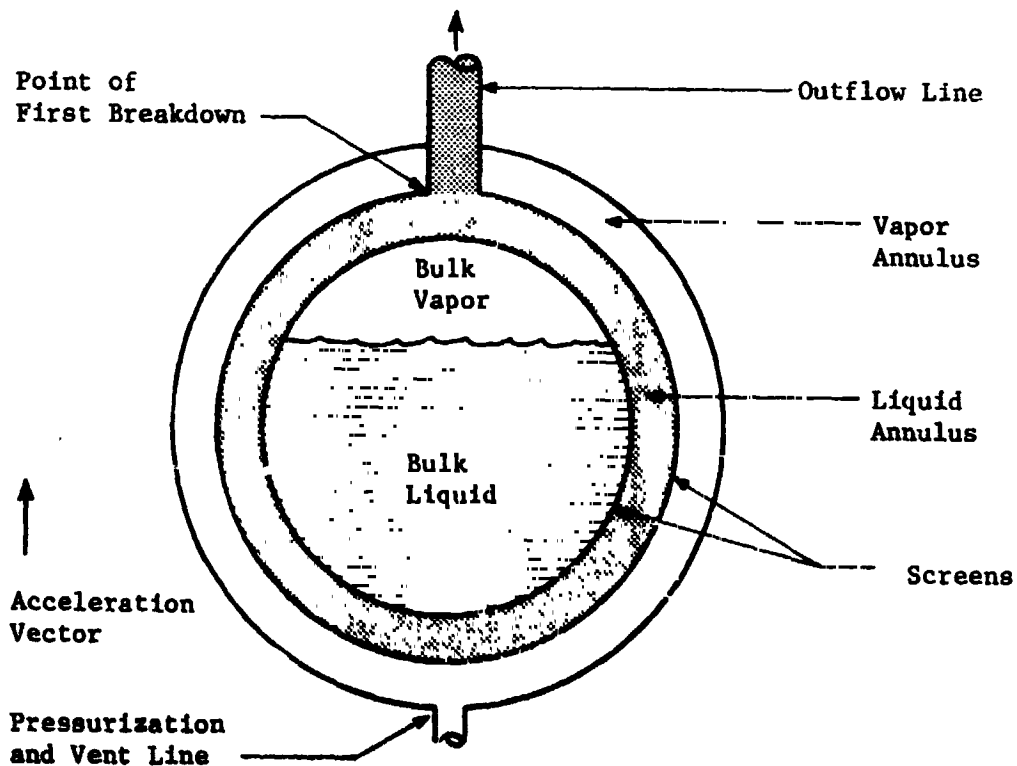


Fig. II-9 Screen Breakdown with Dual Screen Liner

The breakdown phenomenon can be represented mathematically by the algebraic inequality

$$\Delta P_c < \Delta P_{vh} + \Delta P_{fl} + \Delta P_{sl} + \Delta P_{sh} \quad [\text{II-1}]$$

where

$\Delta P_c$  = capillary retention pressure capability

$\Delta P_{vh}$  = velocity head

$\Delta P_{fl}$  = viscous flow losses in flow passage

$\Delta P_{sl}$  = viscous flow losses through screen

$\Delta P_{sh}$  = static head pressure differential

When the sum of all the terms on the right hand side of the equation is greater than the retention capability ( $\Delta P_c$ ) of the screen, breakdown will occur.

The velocity head term in Eq [II-1] is expressed simply by

$$\Delta P_{vh} = \frac{\rho}{g_c} \frac{V^2}{2} \quad [\text{II-2}]$$

The pressure drop in the flow passage is a function of the flow velocity and the nature of the flow passage. The standard expression for this is

$$\Delta P_{fl} = f K_1 \frac{\rho}{g_c} \frac{V^2}{2} \quad [\text{II-3}]$$

where  $K_1$  is a unique constant for a given system geometry and  $f$  is a friction factor, which can be functionally related to the Reynolds number ( $N_{Re} = \frac{\rho LV}{\mu}$ ). The pressure loss associated with flow through the screen can also be expressed in terms of a friction factor and velocity as

$$\Delta P_{sl} = f K V^2 \quad [\text{II-4}]$$

where  $K$  is a constant determined by the screen properties,  $V$  is

the velocity of the fluid approaching the screen, and  $f$  is the friction factor established by a screen Reynolds number.

The last term of [II-1] is the hydrostatic head term. This term represents the pressure differential that is present in a column of liquid in any gravitational environment and is expressed by

$$\Delta P_{sh} = \rho \frac{a}{g_c} h \quad \text{[II-5]}$$

where  $\rho$  = fluid density,  $\text{kg/m}^3$  ( $\text{lbm/ft}^3$ )

$a$  = local acceleration,  $\text{m/sec}^2$  ( $\text{ft/sec}^2$ )

$h$  = liquid height,  $\text{m}$  ( $\text{ft}$ )

$g_c$  = conversion factor,  $9.8 \frac{\text{kg} \cdot \text{m}}{\text{N} \cdot \text{sec}^2}$  ( $32.2 \frac{\text{lbm} \cdot \text{ft}}{\text{lbf} \cdot \text{sec}^2}$ )

In the case of a retention device with a vapor annulus, the liquid height across which the screen must remain stable is the diameter of the device in the direction of the acceleration, as shown in Fig. II-10.

However, in the case where a single screen liner is used, such as in the weeping tank concept, the inner capillary surface is the one subject to breakdown and the hydrostatic head is a function of liquid level in the bulk region, rather than being constant as in the previous case. This is illustrated in Fig. II-11.

*b. Hydrostatic Head* - The hydrostatic head is quite often the most important consideration of those previously outlined and expressed by Eq [II-1]. The acceleration environment, in which the capillary device must function, can have a first-order impact on the determination of the device size, shape, and configuration. An acceleration environment of sufficient magnitude may require the use of a capillary device (such as a trap), which encloses only a portion of the tank (thereby, reducing the hydrostatic head). There are cases where a screen device is designed so a part of the system will be unstable above certain acceleration levels. This is the case with a refillable trap design, where the trap cover must breakdown to allow liquid refill during certain mission maneuvers. Yet the same screen must not break down as a result of acceleration experienced in directions opposite or normal to the refill acceleration vector. These potential design requirements

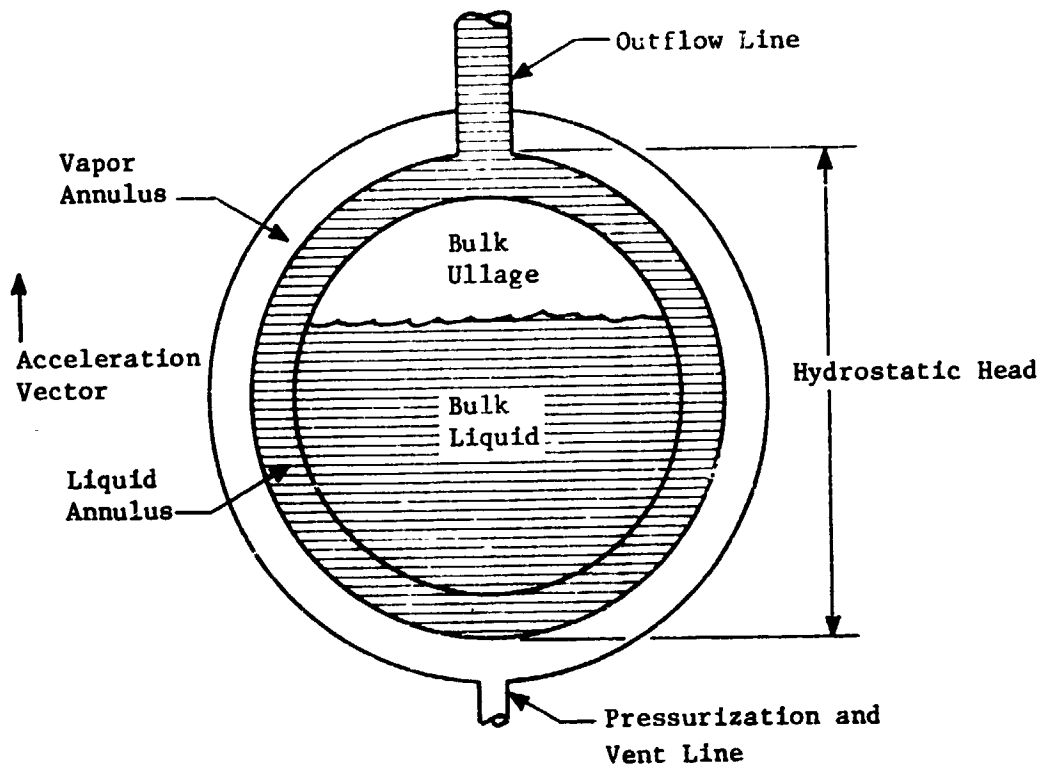


Fig. II-10 Hydrostatic Head with DSL

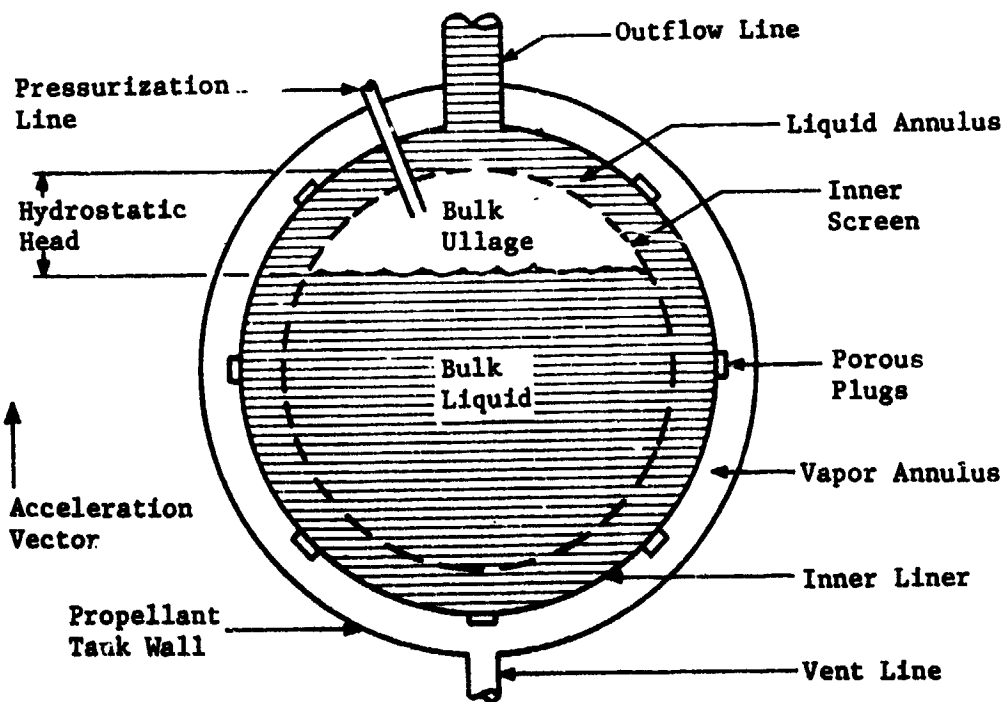


Fig. II-11 Hydrostatic Head with Weeping Tank Concept

illustrate the need for precise and detailed information on the capillary retention capabilities of fine mesh screen and other candidate capillary barriers.

The expression that predicts the pressure differential across a liquid-vapor interface is

$$\Delta P = \sigma \left( \frac{1}{r_1} + \frac{1}{r_2} \right) \quad [\text{II-6}]$$

where  $\sigma$  is the liquid surface tension and  $r_1$  and  $r_2$  are the principal radii of curvature measured at a point on the interface. For the small pores in capillary media these radii are essentially equal and the expression becomes

$$\Delta P = \frac{2\sigma}{r} \quad [\text{II-7}]$$

where  $r$  is the pore radius.

A large body of empirical data has been assembled that correlates well with the analytical predictions. However, little data have been available for bubble point values of screens tested in cryogens. Furthermore, data on the potential additive nature of multiple screen layers were unavailable for either noncryogens or cryogens. Therefore, a test program was initiated to establish the bubble point values for screens in cryogens and the bubble point values of multiple screen layers in cryogens as well as in the standard test fluid--methanol. These tests substantiated that bubble point values for screens in cryogens could be accurately predicted from the known values of fluid surface tension.

Curves showing the retention capability of selected fine mesh screens are presented in Fig. II-12 and II-13 for  $\text{LH}_2$  and  $\text{LO}_2$ , respectively. The tests also showed that when care was exercised to maintain a minimum gap between screen layers, bubble point values were additive for combinations of similar or dissimilar screens. These tests are discussed in detail in Volume III of this report. Based on these test results, the use of multiple screen layers to withstand large hydrostatic heads appears a reasonable solution to some design requirements.

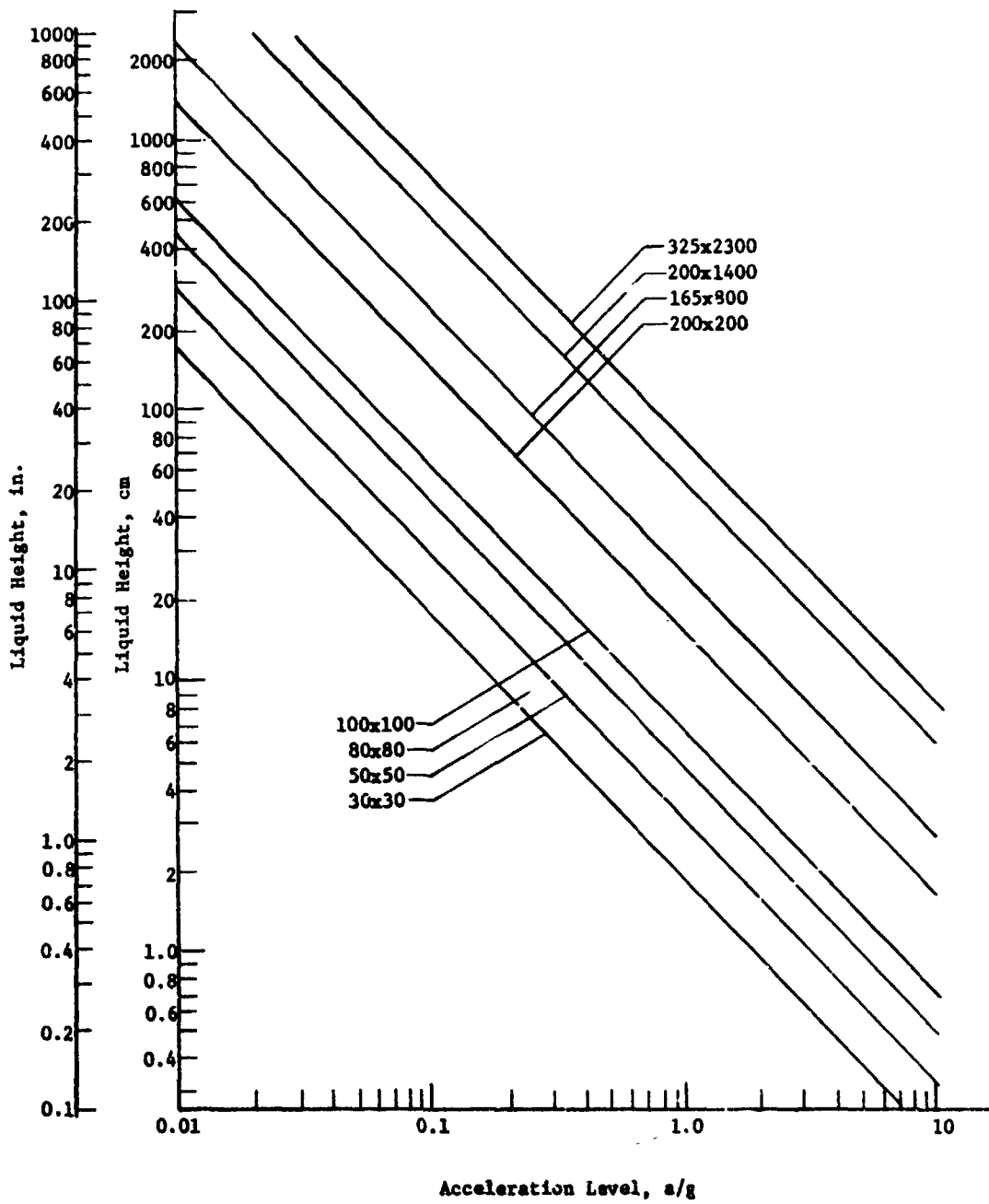


Fig. II-18 Maximum  $LH_2$  Hydrostatic Head vs Acceleration Level

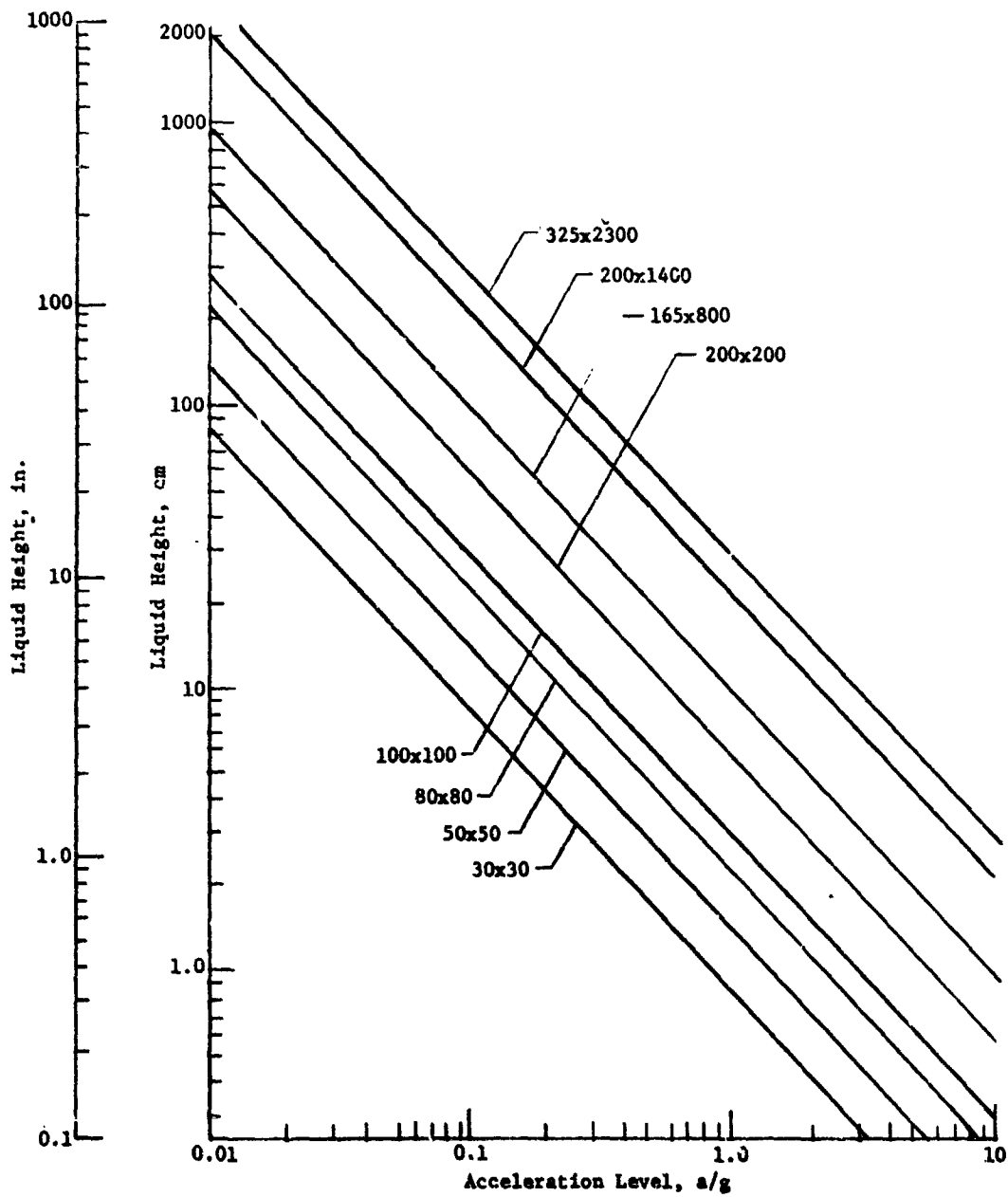


Fig. II-13 Maximum LO<sub>2</sub> Hydrostatic Head vs Acceleration Level

In some of the candidate systems use of communication screens poses another design consideration. The communication screen is broken down as an operational requirement during pressurization events. It must be able to recover, or regain, its capillary stability after the pressurization event is ended. Tests run with methanol indicate that the pressure differential across a screen must drop to approximately 57% of its bubble point value before the screen can recover. At that point the pressure differential supportable by the screen is again the bubble point of the screen.

These data are essential to the proper design of communication screens. The communication screen has a lower bubble point than the screens forming the controlled liquid regions; therefore, the wetted communication screen will break down before the other screens in the system and pressure will be equalized in the two adjacent vapor volumes. For the design to be successful, operational parameters must be carefully considered. Any liquid outflow event requires a certain pressurization flow rate. The communication screen must be sized so that this flow can pass into the bulk region without experiencing the large pressure drop that would result from an undersized communication screen area. The information gained from the communication screen tests, presented both here and in the Subsection c. on hydrodynamics, was used to estimate minimum communication screen areas for specific design applications.

The surface tension of cryogenics depends on the liquid temperature at the liquid/vapor interface. Because the bubble points of the screens are directly related to the surface tension of the wetting liquid, the temperature/surface tension dependency is an important design consideration. Curves illustrating this phenomenon for LH<sub>2</sub> and LO<sub>2</sub> are shown in Fig. II-14 and II-15.

These curves were generated using the empirically derived relationship

$$\sigma = \sigma_0 (1 - T_r)^{11/9} \quad [\text{II-8}]$$

where  $T_r$  is the reduced temperature,  $T/T_c$  and  $\sigma_0$  is an empirical constant, which may be regarded as the surface tension of a hypothetical supercooled liquid at 0°K. These values of surface tension agree within 2% of those presented in *Cryogenic and Industrial Gases* (Ref II-5). As shown in the figures, the surface tension of LH<sub>2</sub> (and therefore, the capillary retention capability of the devices) degrades rapidly with increased temperatures.

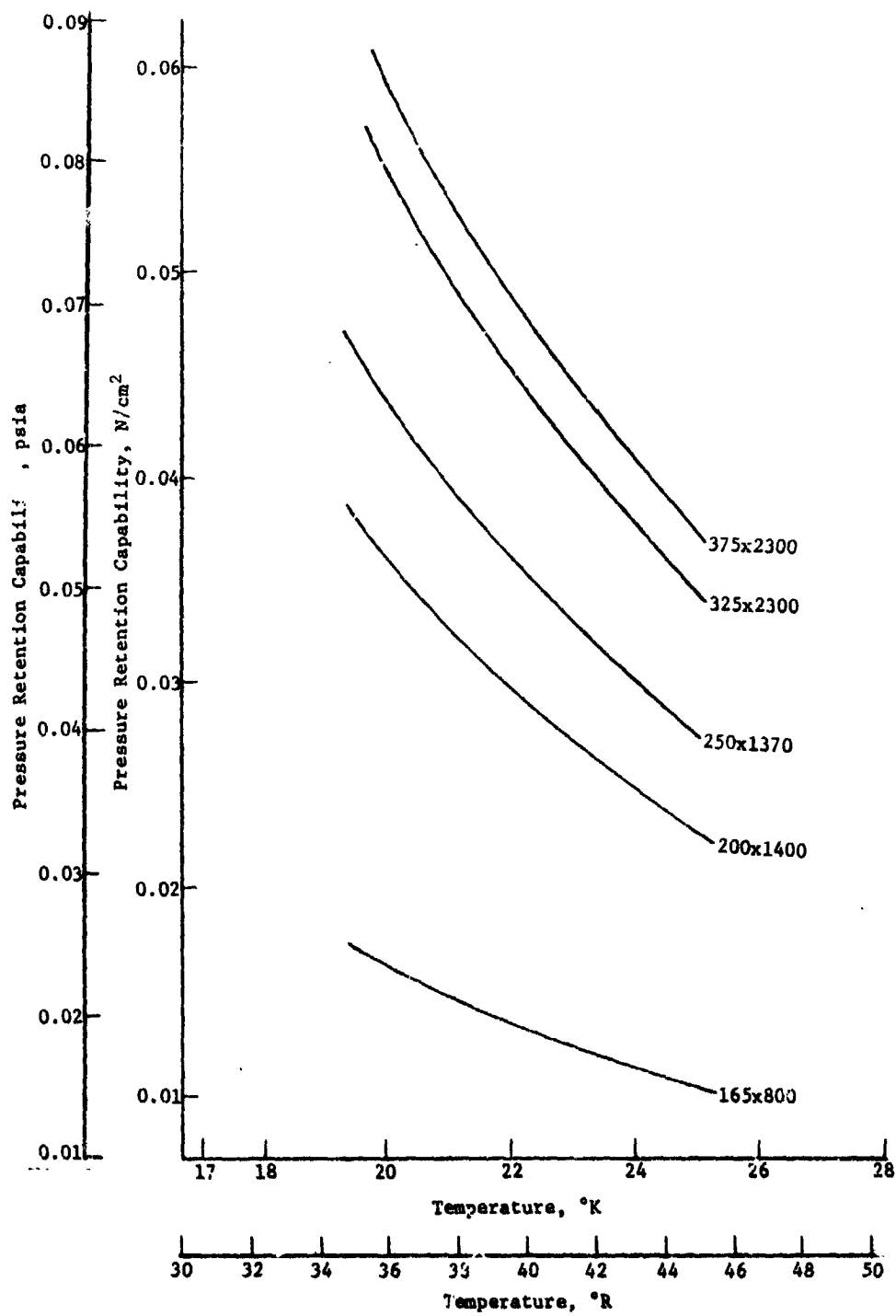


Fig. II-14 The Effect of Temperature on Screen Pressure Retention Capability in Hydrogen

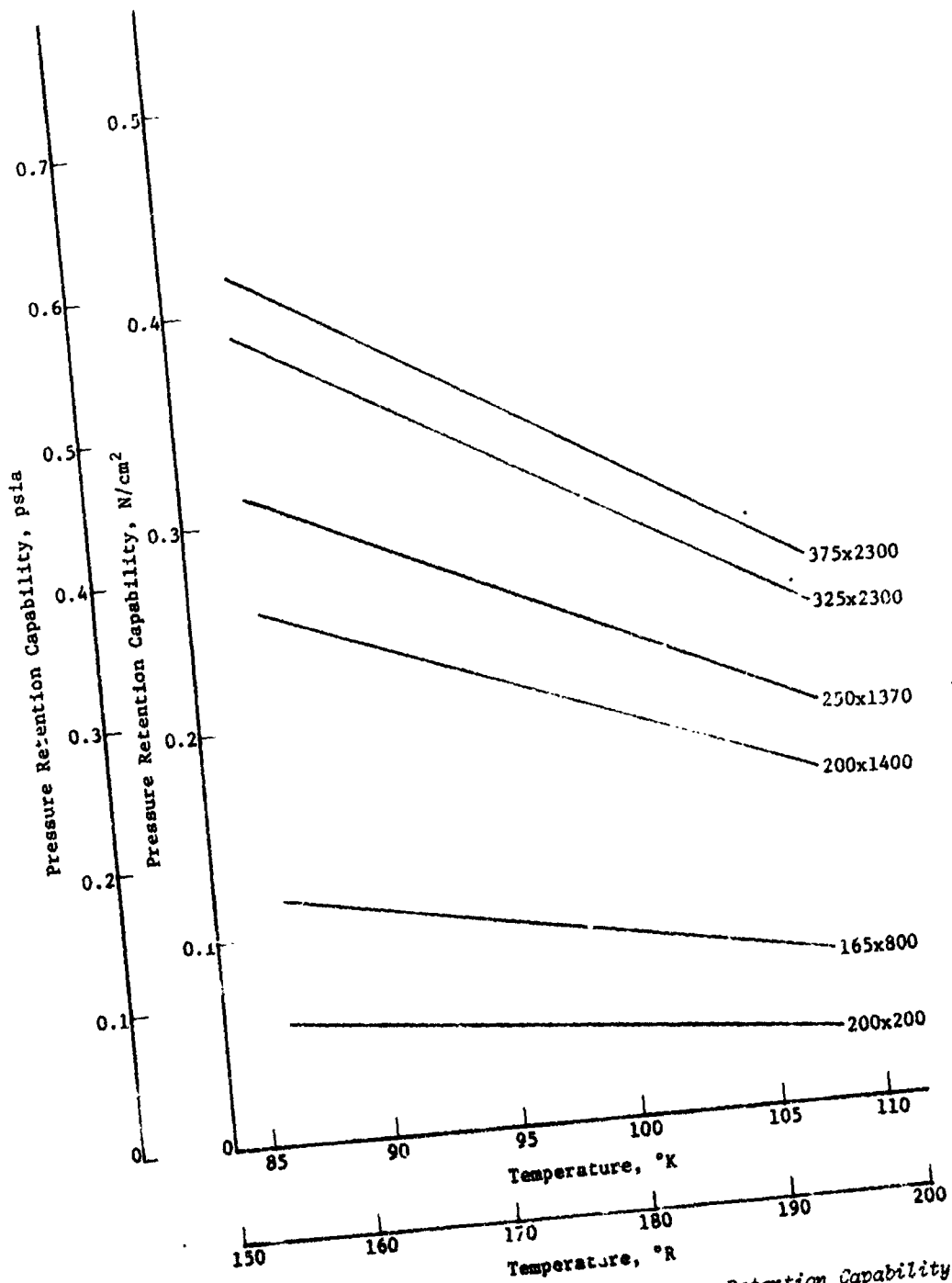


Fig. II-15 The Effect of Temperature on Screen Pressure Retention Capability in Oxygen

This same phenomenon is also present for oxygen, although not so pronounced. Each design was carefully analyzed over the entire mission duty cycle, for which it was intended, to ensure that it would function properly over the entire anticipated temperature excursion.

*c. Hydrodynamics*

1) General Considerations - The other major area of fluid mechanics that was treated extensively during the program was the general area of fluid dynamics. Three of the four terms contained in Eq [II-1] are dynamic terms. In the absence of an acceleration environment (i.e., with no hydrostatic head present), the dynamic conditions expressed by the three dynamic terms become the controlling factors in the performance of a capillary system. An understanding of these terms is crucial to selection and ultimate design of an acquisition/expulsion system.

The technical area of viscous losses experienced by the flow of liquids through screens and other porous media was considered through both experimental and analytical techniques. Losses for fluids in both the liquid and gaseous states were investigated over temperatures ranging from ambient to cryogenic. This information is an important determinant in the proper design of both the capillary surfaces defining the controlled liquid regions of the device and the capillary barriers which serve as communication devices between vapor regions.

Knowledge of the pressure losses experienced by fluid flowing across a screen or other capillary device is also important to the proper design of a capillary system. If not enough screen surface area is present in the system, situations may occur where the screen area, through which the fluid is flowing, may be small enough that the pressure drop experienced by the fluid exceeds the capillary retention capability of the screen. If this occurs, vapor will be ingested into the controlled liquid volume--a condition which is generally contrary to the design philosophy.

Relationships defining pressure losses experienced by fluids flowing through screens have been well established (Ref II-6). The possibility of incorporating multiple layer screen devices in certain designs poses the question of how pressure losses are related to the series of resistances that several screens in a flowing system represent. The only available literature suggested that the pressure loss was a multiple of the pressure loss experienced by a single screen of the same mesh; the

multiplying factor being the number of screens across which flow was occurring. This information was based on the testing of relatively coarse square-weave screens in series. Therefore, a series of tests was conducted to determine if this relationship held for fine mesh Dutch-twill screen as well. (These tests are discussed in detail in Volume III of this report). The results of these tests indicate that the pressure loss experienced by a series of similar fine mesh screens is predictable as a multiple of the loss through a single screen of the same mesh. Moreover, these data conformed to the predictions of Armour and Cannon (Ref II-6) and were found to hold for both gas and liquid. Therefore, in all analyses requiring the investigation of systems employing more than one layer of screen, these relationships were assumed.

In addition to screens, a number of other capillary materials were investigated analytically. Although from the onset fine mesh screens appeared to be the most reasonable, a comparative evaluation of all available capillary materials was performed. This evaluation is discussed in Subsection 4.c of this section, but the results of the flow loss analysis are presented briefly here.

A transfer function, independent of screen properties, was derived from the packed bed analysis for flowthrough screens developed by Armour and Cannon. Computer analysis of two candidate nonscreen materials with bubble point values comparable to fine mesh screens is shown for liquid hydrogen in Fig. II-16 and II-17.

The materials analyzed were various grades of Huyck Metals Company "Feltmetal," and Bendix Filter Division "Poroplate." The figures show that these two candidate materials produce pressure losses one to two orders of magnitude higher for the same flow rates than a representative fine mesh screen. Moreover, these materials are 7 to 8 times as heavy per square foot than screen. These data serve to enhance the desirability of fine mesh screens.

With the exception of the weeping tank concept, all of the proposed candidate capillary retention/expulsion concepts rely on some form of communication screen to regulate pressure differences between adjacent vapor regions. The communication screen passively regulates the pressure difference by allowing vapor to pass through it whenever the difference in pressure

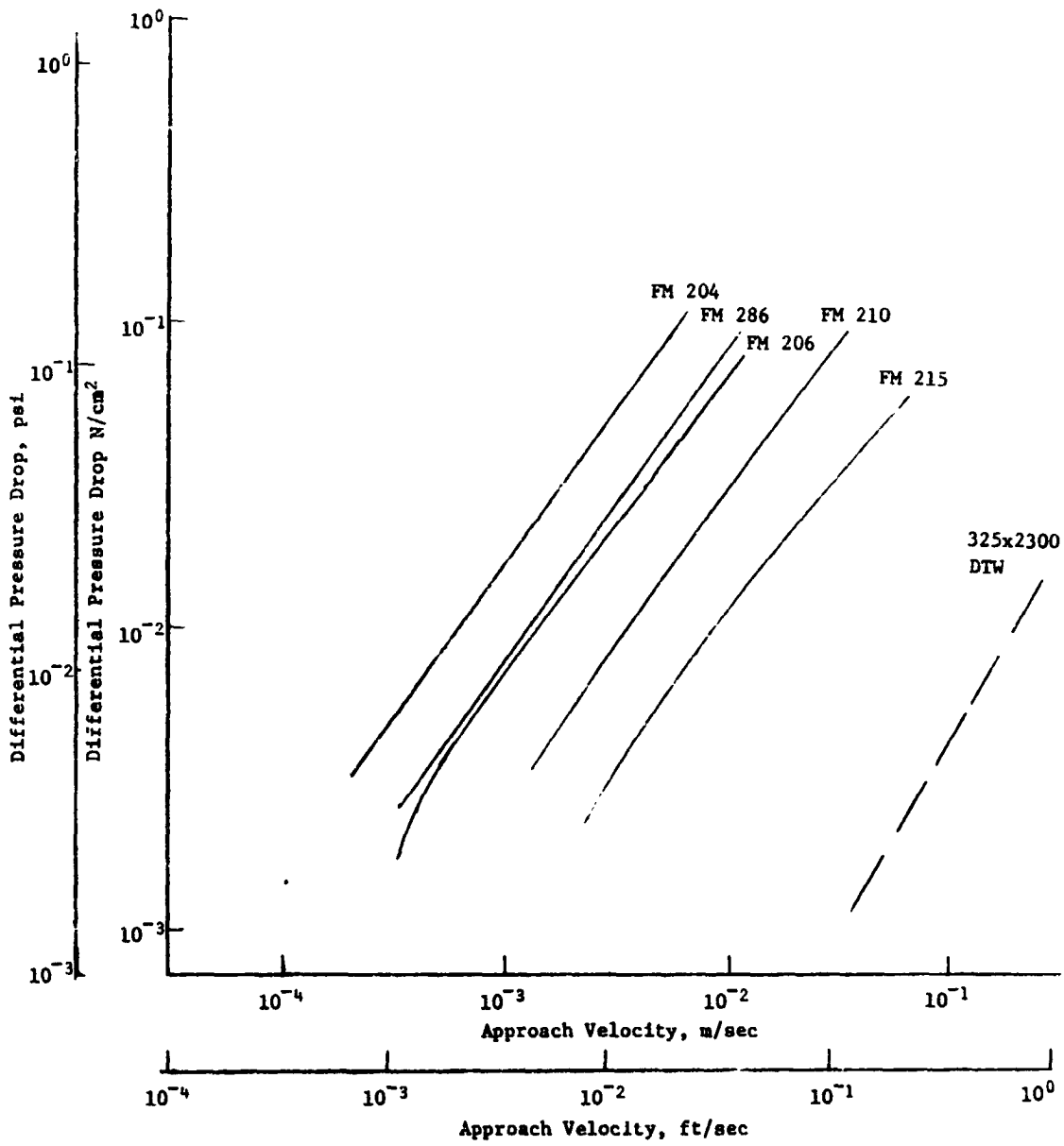


Fig. II-16 Differential Pressure vs Approach Velocity for LH<sup>2</sup> at 19°K (34.2°R), Hvyok Feltmetal Materials

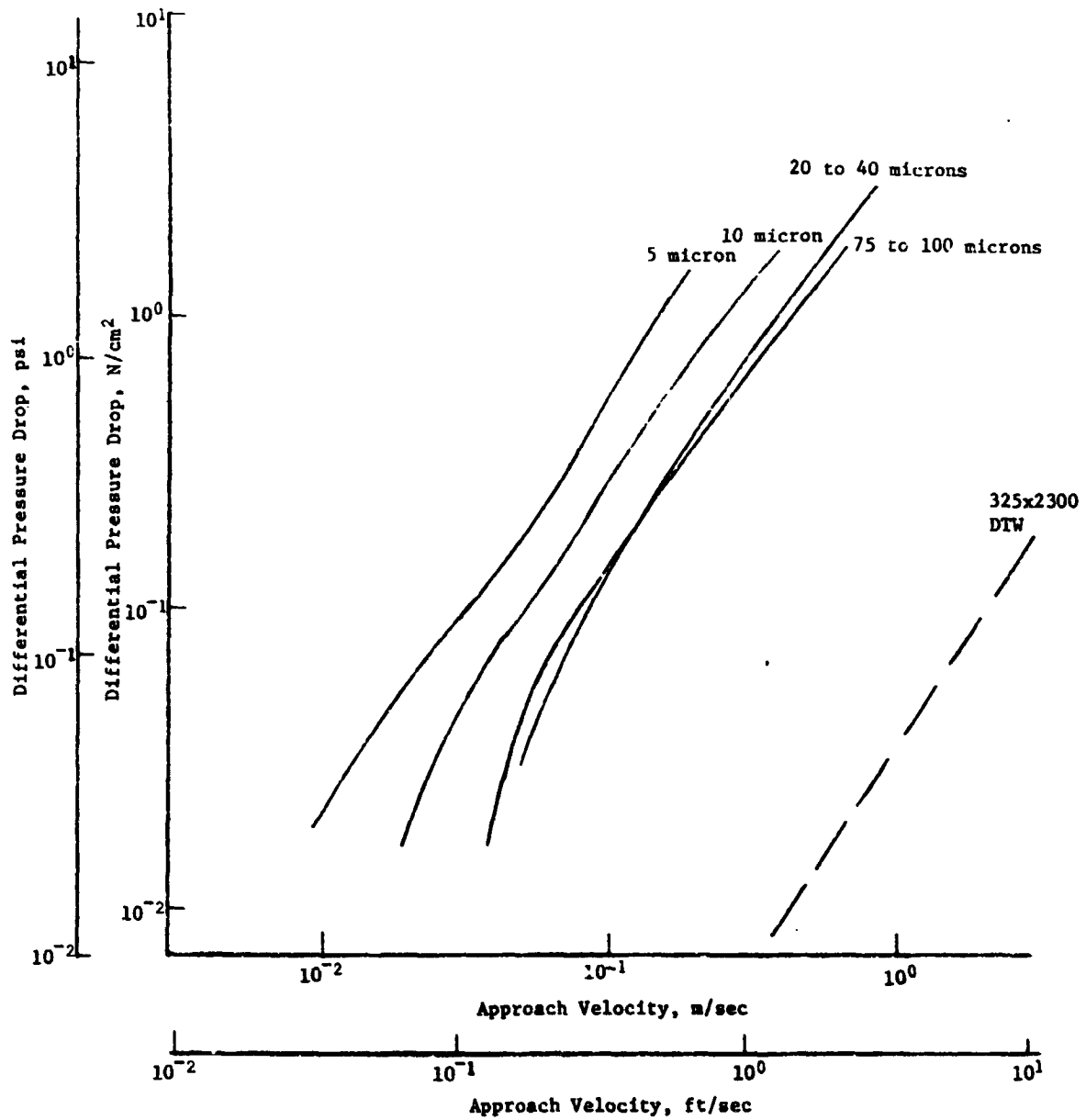


Fig. II-17 Differential Pressure vs Approach Velocity for LH<sub>2</sub> at 19°K (34.2°R), Bendix "Poroplate" Materials

between the two vapor regions exceeds the bubble point of the wetted screen.

A number of operational characteristics of communication screens were investigated experimentally and analytically. The pressure loss experienced by pressurant gasses passing through a communication screen was investigated by experiment with cryogenic gasses and by computer analysis.

When a communication screen first breaks down, it goes from a fully wetted condition to a partially wetted condition and eventually, if the pressure equalization event takes long enough, the screen becomes completely dry. The differences in pressure loss across the screen, which these variations in screen conditions could cause, were investigated. A necessary operational feature of communication screens is their ability to rewick or reseal after breakdown. Some knowledge of this re-sealing mechanism is desirable for the purposes of design and operational prediction; therefore resealing of communication screens was studied in the laboratory using cryogenic fluids.

The significant result obtained by testing communication screens in cryogenics was that pressurant flowing through a wetted screen will experience pressure losses of no more than 125% of the bubble point value of the screen. This result was established for liquid nitrogen, liquid oxygen and liquid hydrogen. This pressure loss value will not be exceeded as long as the screen through which gas is flowing can be resupplied with liquid so that it stays wetted. Experimental results and computer predictions show that once the screen has dried out, the pressure loss for gaseous flow through a screen is strictly an exponential function of the flow rate and has no upper bound. One other noteworthy result of the theoretical analysis was that the pressure loss due to flow across a screen was not necessarily a function of mesh size alone. As shown in Fig. II-18, 250x1370 Dutch twill produces a higher pressure drop at the same flow rate than does 325x2300 Dutch twill.

2) Feedline Considerations - The design of a capillary feedline is governed by the same relationships that are the basis for the design of any surface tension device. That is, the pressure differential across the screen device must never exceed the bubble point of the screen if gas-free liquid is to be maintained. Referring to Fig. II-19, the pressure difference between the liquid core at Point 1, Point 2, or anywhere along the entire

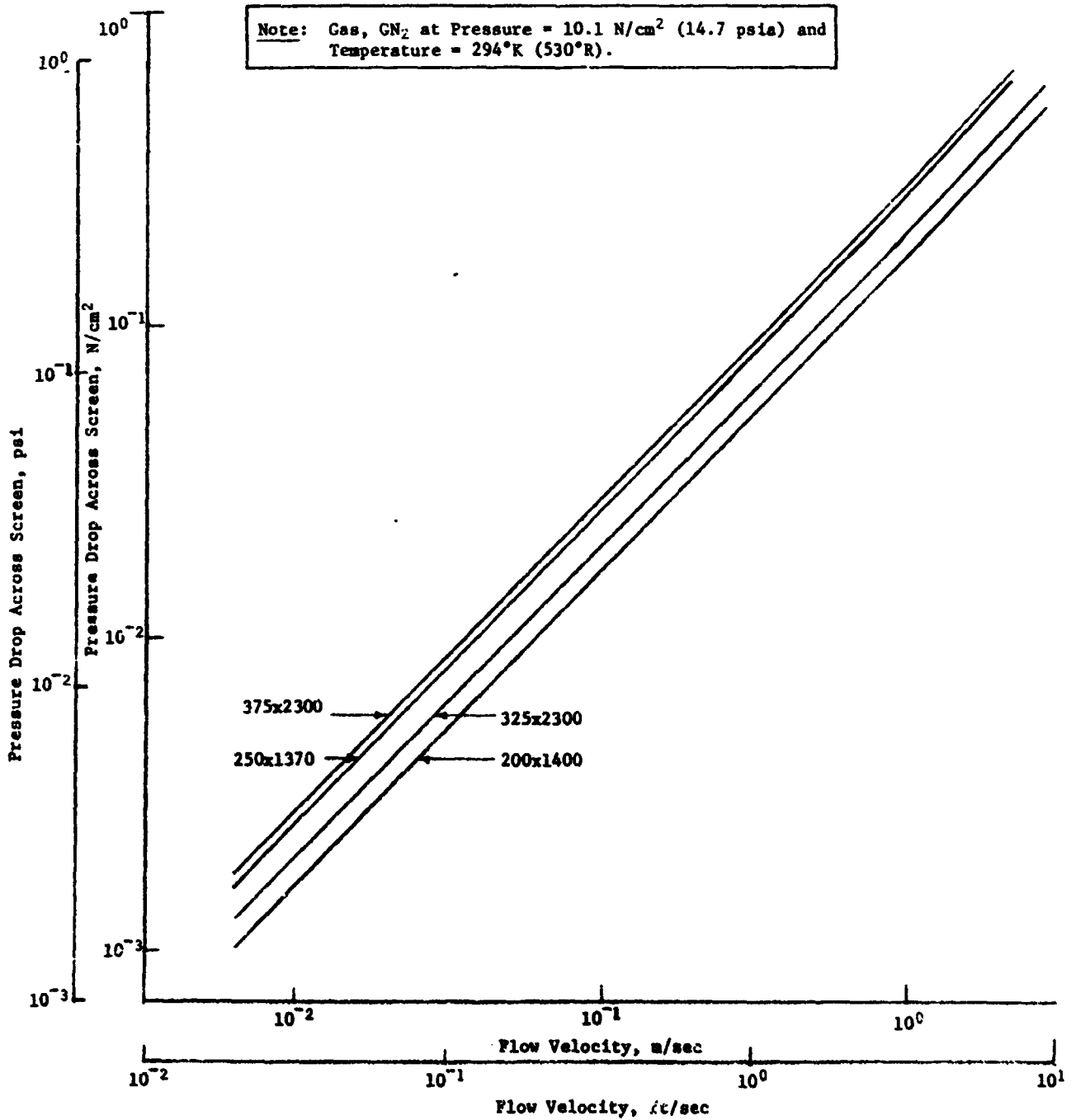


Fig. II-18 Theoretical Single Dry Screen Pressure Drop

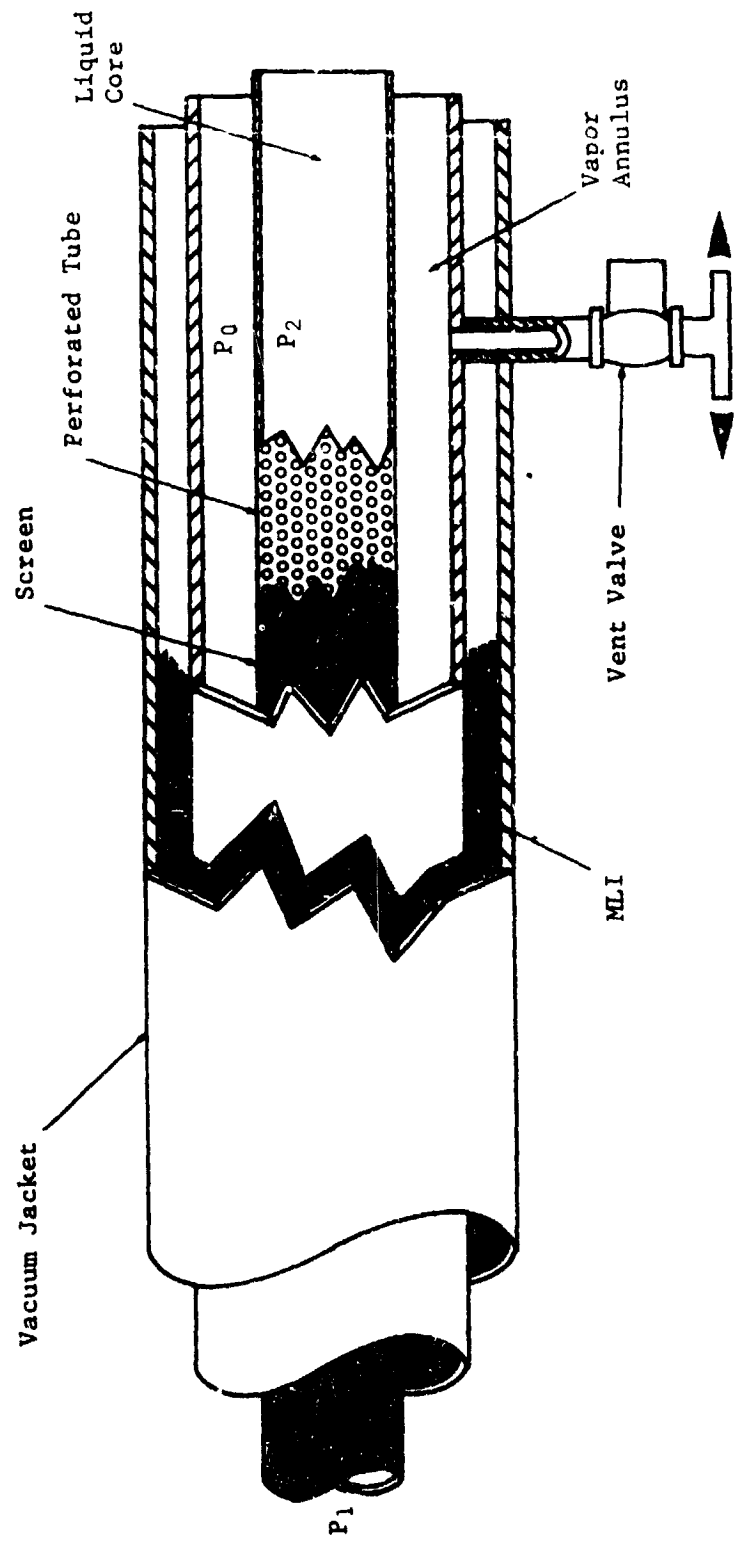


Fig. II-19 Screen Liner for Cryogenic Feedlines

length of the feedline and the vapor annulus must always be less than the bubble point of the screen. In equation form

$$BP \geq P_o - P_1, P_o - P_2, P_o - P_n \quad \text{[II-9]}$$

Under static conditions, the pressure along the line is constant and the only consideration is the pressure difference between  $P_o$  and  $P_1$ . During outflow, a pressure differential will exist throughout the length of the feedline due to frictional flow losses. Also a decrease in static pressure due to the velocity head will exist. With these considerations in mind the governing equation for feedline design in zero-g is

$$BP \geq (P_o - P_1) + \Delta P_{fl} + \Delta P_{vh} \quad \text{[II-10]}$$

where  $P_{fl}$  and  $P_{vh}$  are the pressure drops associated with frictional losses and velocity head, respectively.

Should the system be accelerated, the effect of the acceleration head,  $\rho gL$ , must be considered. For any given value of  $\rho gL$  the worst condition from a design standpoint would be an acceleration vector parallel to and in the direction of flow. The term,  $\rho gL$ , would be additive in the following equation.

$$BP \geq (P_o - P_1) + \Delta P_{fl} + \Delta P_{vh} \pm \rho gL \quad \text{[II-11]}$$

Depending on system geometry and basic design criteria, the first three terms of the right-hand side of the equation do not present any significant design problems. Since bubble points of screens are additive, the required number of screen layers may be determined to satisfy the equation. If the magnitude of  $\rho gL$  is comparable to the other terms in the equation, a realistic design may still be achieved. However, if the acceleration head is very large, the required number of layers of screen may exclude the capillary system as a practical design solution.

An acceleration vector opposite the direction of flow would aid the design because the acceleration head would reduce the effective pressure drop in the line. The term  $\rho gL$  would now become negative in Eq [II-11]. If the value of  $\rho gL$  is comparable but smaller than the other terms in the equation, the pressure gradient across the screen will be small and easily accommodated to assure that gas will not enter the liquid core. For a negative value of the equation ( $\rho gL$  larger than sum of other terms), liquid will be pushed into the vapor annulus to a level where equilibrium

is reached. However, gas-free liquid will still be available in the liquid region and system operation will not be impaired.

Equation [II-11] is the general equation governing the design of a capillary feedline system where  $P_1$  is the liquid core pressure at some point 1. This equation is valid at any distance,  $l$ , downstream of Point 1. It should be noted that the feedline distance,  $l$ , and acceleration head length,  $L$ , may be considerably different depending on feedline geometry and acceleration direction. When the equation is applied to a capillary propellant acquisition/expulsion system (storage tank and feedline), Point 1 is just before the feedline inlet and the viscous losses in the propellant acquisition/expulsion device are neglected. The term,  $P_0$ , is equal to the tank ullage pressure assuming communication between the feedline vapor annulus and storage tank.

The value of  $P_0 - P_1$  is constant for a given storage tank configuration. For a trap and screen liner storage tank system, it is the sum of the screen liner bubble point and the bubble point of the trap communication screen. The term,  $\Delta P_{vh}$ , represents frictional flow losses in the feedline due to pipe wall friction, bends, and other system plumbing. The dynamic pressure,  $\Delta P_{vh}$ , accounts for the reduction in inlet static pressure due to flow. Thus for a given flow rate, line geometry, and acquisition/expulsion device, these terms are constant and the number of screen layers required depends on the acceleration head term,  $agl$ .

At the inlet to the feedline, the frictional losses ( $\Delta P_{fl}$ ) are essentially zero and  $L$  reduces to the height of the storage tank device (assuming a positive acceleration vector with respect to the vehicle). Depending on the relative value of the terms involved, the required layers of screen may be less at the inlet to the feedline than at the outlet. Considerable weight savings as well as simplified fabrication may be realized by designing a capillary feedline as a function of feedline length. This approach was used in the feedline designs presented in the following chapters for the integrated OMS/RCS and Space Tug propulsion systems.

3) Candidate Concept Outflow Modeling - The basic expression for determining the local pressure in a capillary system was given in Eq [II-1]. Any one of the phenomena represented by the respective terms of that expression can, under certain circumstances, be sufficiently large to cause breakdown of the capillary barrier.

Normally, however, breakdown will be precipitated by the combined influence of all the terms.

Several computer models were constructed to predict outflow capabilities of capillary systems. These computer models basically balance the two sides of Eq [II-1], the variables being the system geometry, outflow rate, fluid level in the tank, mesh size and number of the screen layers, and acceleration environment. Figures II-20 through II-25 show typical results of these analyses. In all cases the acceleration vector was assumed to settle propellant away from the tank outlet, thereby creating a worst-case condition.

The curves show results for typical cryogenic Shuttle tanks. The curve for each respective acceleration level defines the boundary between the regions where stable outflow is possible and the region where breakdown will occur. In all cases the curves tend to merge into a single horizontal line near the abscissa. The intersection of this line with the ordinate defines the fraction of the tank volume enclosed by the particular screen system and is, therefore, a measure of expulsion efficiency. A comparison of Fig. II-20 for the 2.59 m (8.5 ft) LO<sub>2</sub> dual-screen liner and Fig. II-24 and II-25 for the 2.59 m (8.5 ft) 16-channel variation of the dual-screen liner concept, illustrates the variations in outflow capability of these similar systems as determined by changes in system geometry. These curves also serve to demonstrate the versatility of these computer programs as tools for system comparisons and optimization studies.

4) Dynamic System Testing - In addition to the system performance predictions provided by the computer models, two subscale DSL systems were tested with noncryogenics in the low-gravity environment of the KC-135 aircraft. The qualitative tests were designed as functional tests of the DSL components to evaluate: (1) the vapor annulus as a pressurization space; (2) the communication screen as a path for the pressurant between the vapor annulus and the bulk vapor space; (3) the liquid annulus as an effective discriminator between vapor and liquid that is able to deliver gas-free liquid to the outlet.

The tests successfully demonstrated the soundness of the basic concepts. Complete gas-free liquid expulsions were accomplished in the low-g aircraft environment and in minus 1-g bench tests prior to the aircraft tests. Expulsions were completed in times on the order of 30 seconds. These tests are described in detail in Volume III of this report.

Note: 1. Tank, 2.6 m (8.5 ft) dia.  
 2. Fluid, LO<sub>2</sub>.  
 3. Vapor Annulus = 1.27 cm (1/2 in.).  
 4. Liquid Annulus = 2.54 cm (1 in.).  
 5. Screen = 325x2300.

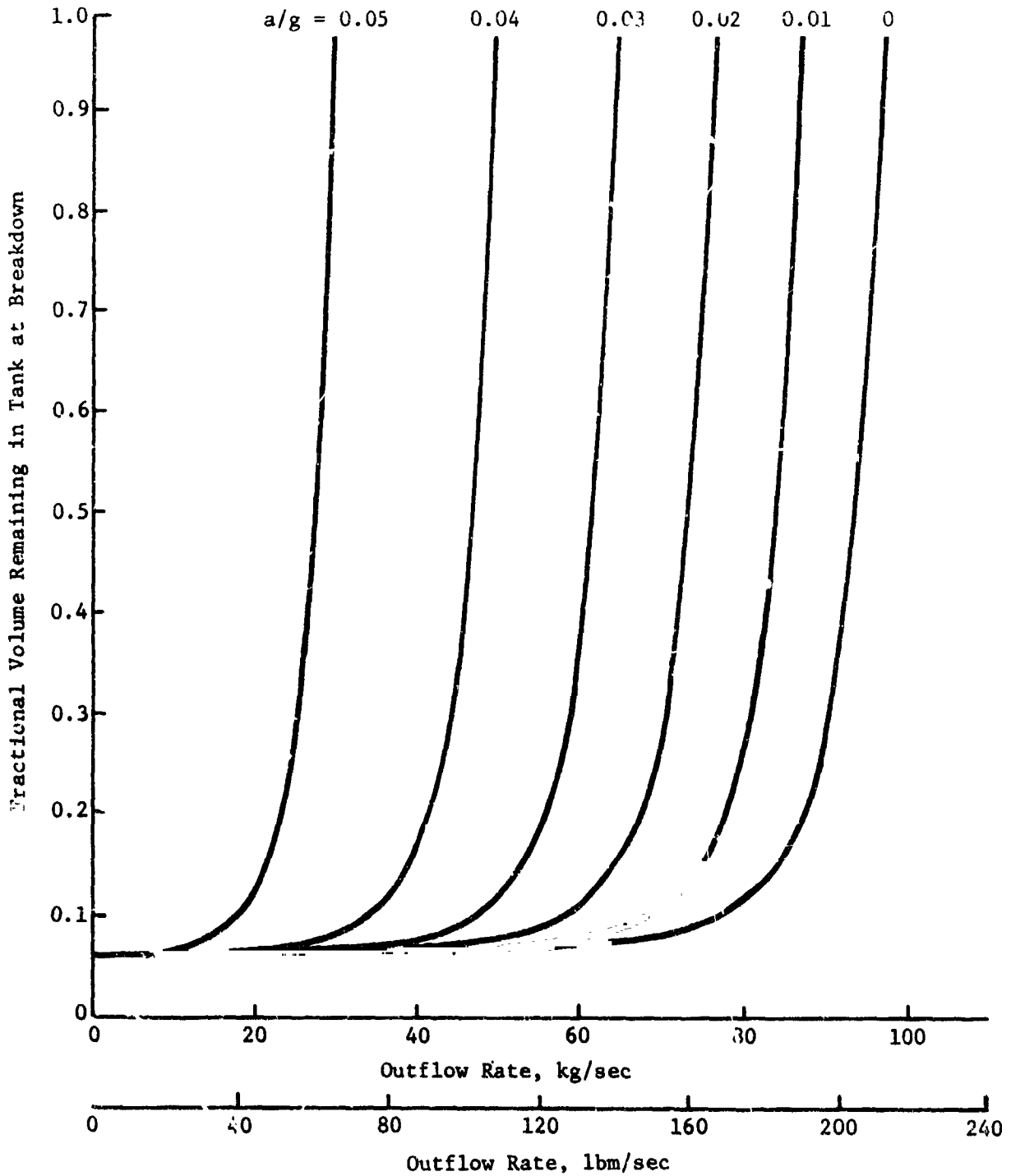


Fig. II-20 Outflow Capability of a Spherical Dual Screen Liner with Liquid Oxygen

Note: 1. Tank, 3.81 m (12.5 ft.) dia.  
 2. Fluid, LH<sub>2</sub>.  
 3. Vapor Annulus = 7.62 cm (3in.)  
 4. Liquid Annulus = 2.54 cm (1 in.)  
 5. Screen = 325x230C

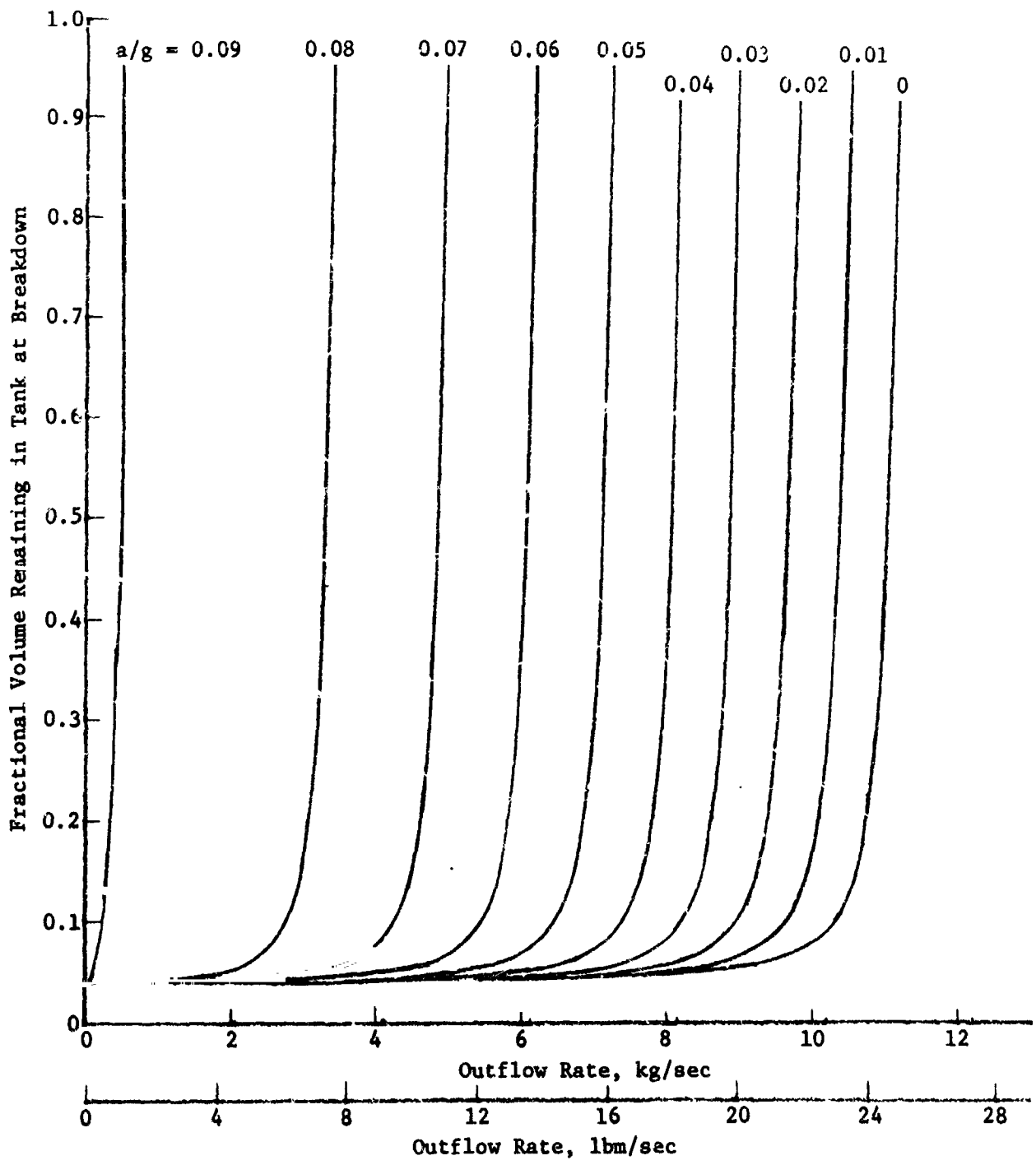


Fig. II-21 Outflow Capability of a Spherical Dual-Screen Liner in Liquid Hydrogen

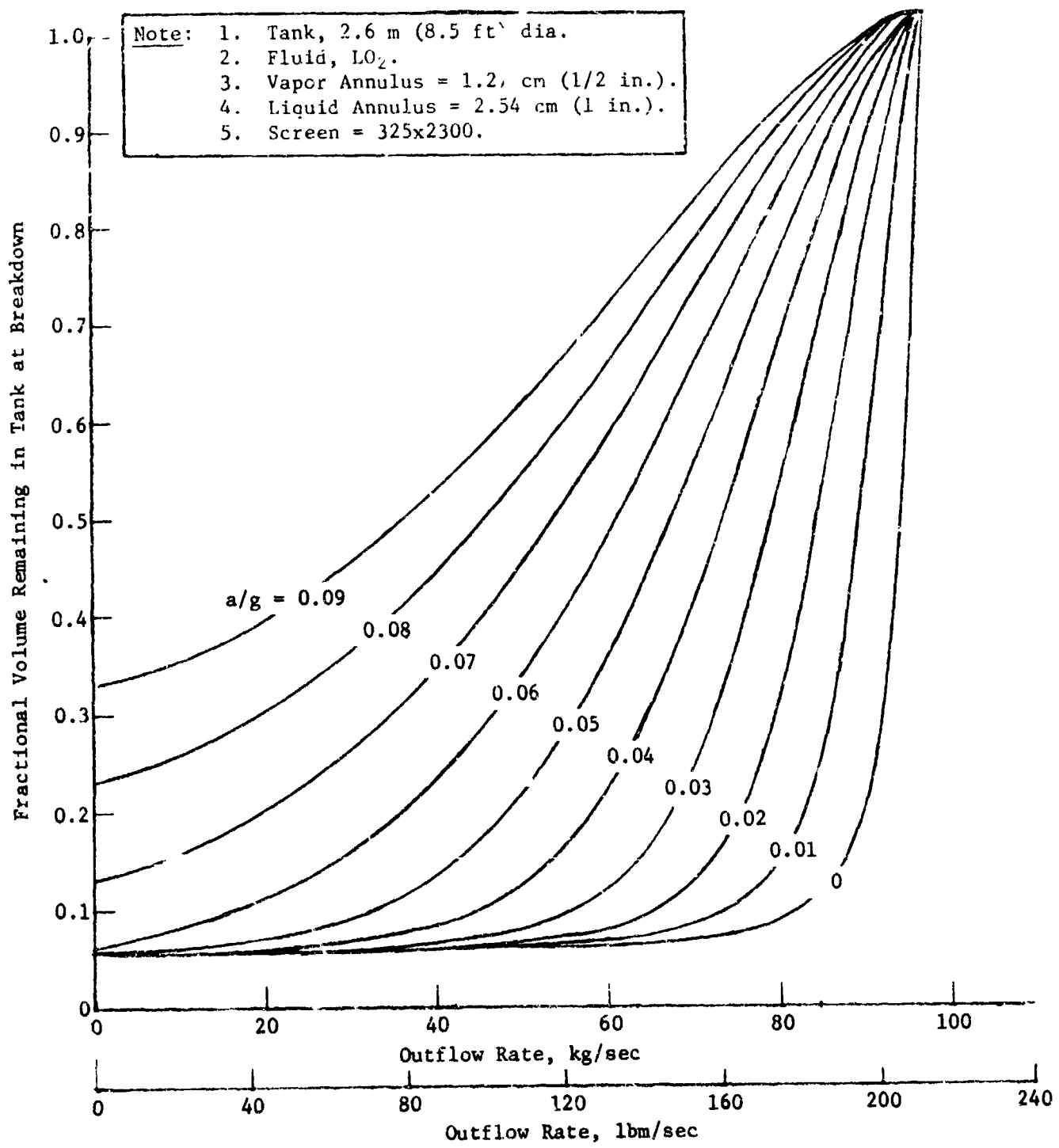


Fig. II-22 Outflow Capability of a Spherical Weeping Tank with Liquid Oxygen

Note: 1. Tank, 3.81 m (12.5 ft) dia.  
 2. Fluid, LH<sub>2</sub>.  
 3. Vapor Annulus = 7.63 cm (3 in.).  
 4. Liquid Annulus = 2.54 cm (1 in.).  
 5. Screen = 325x2300

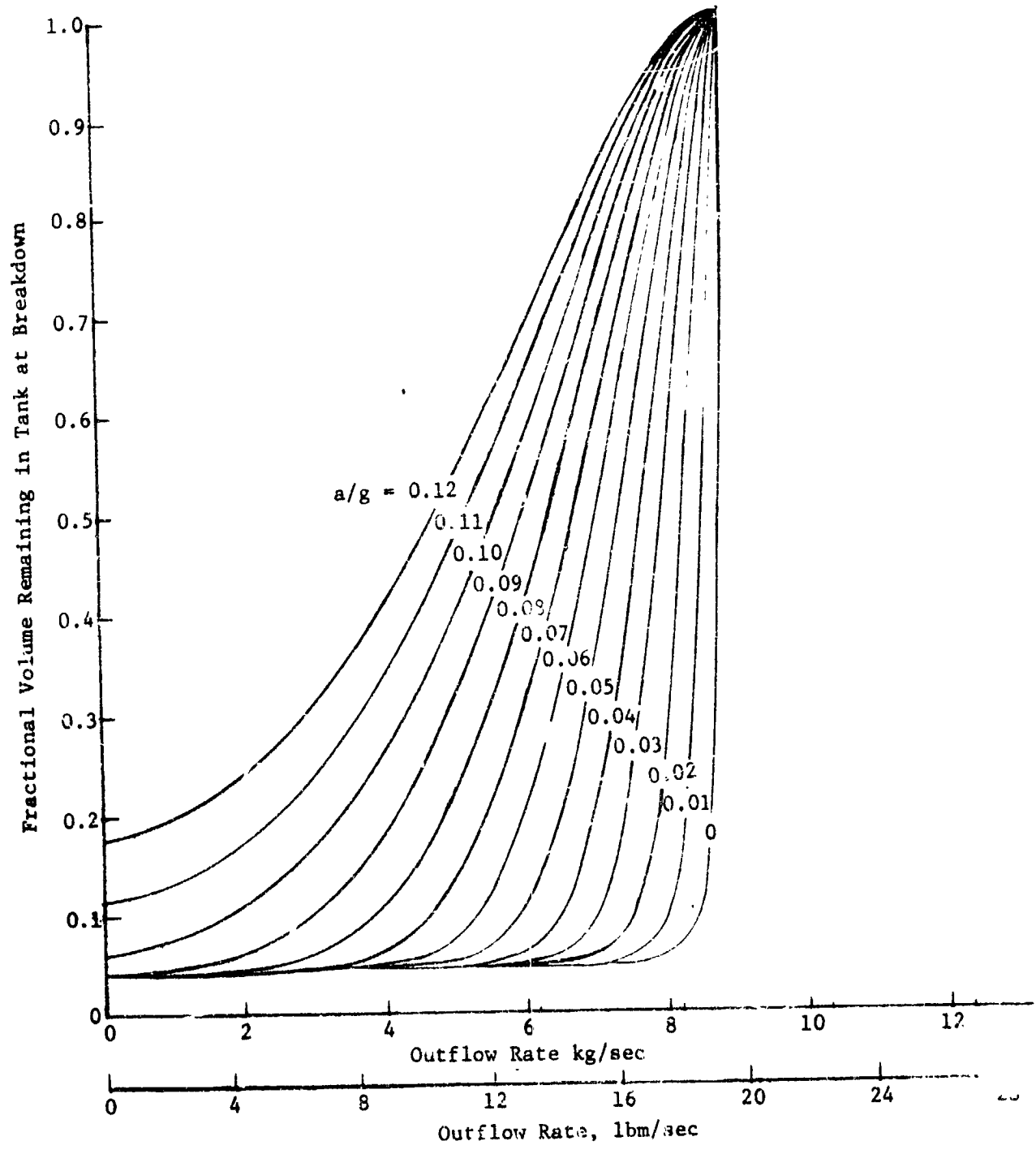


Fig. II-23 Outflow Capability of a Spherical Weeping Tank with Liquid Hydrogen

- Note:
1. Tank, 2.6 m (8.5 ft) dia.
  2. Fluid, LO<sub>2</sub>.
  3. Vapor Annulus = 1.27 cm (1/2 in.).
  4. Liquid Annulus = 2.54 cm (1 in.).
  5. Screen = 325x2300.
  6. 16 channels.
  7. Channel Spacing, 0.304 m (1 ft).

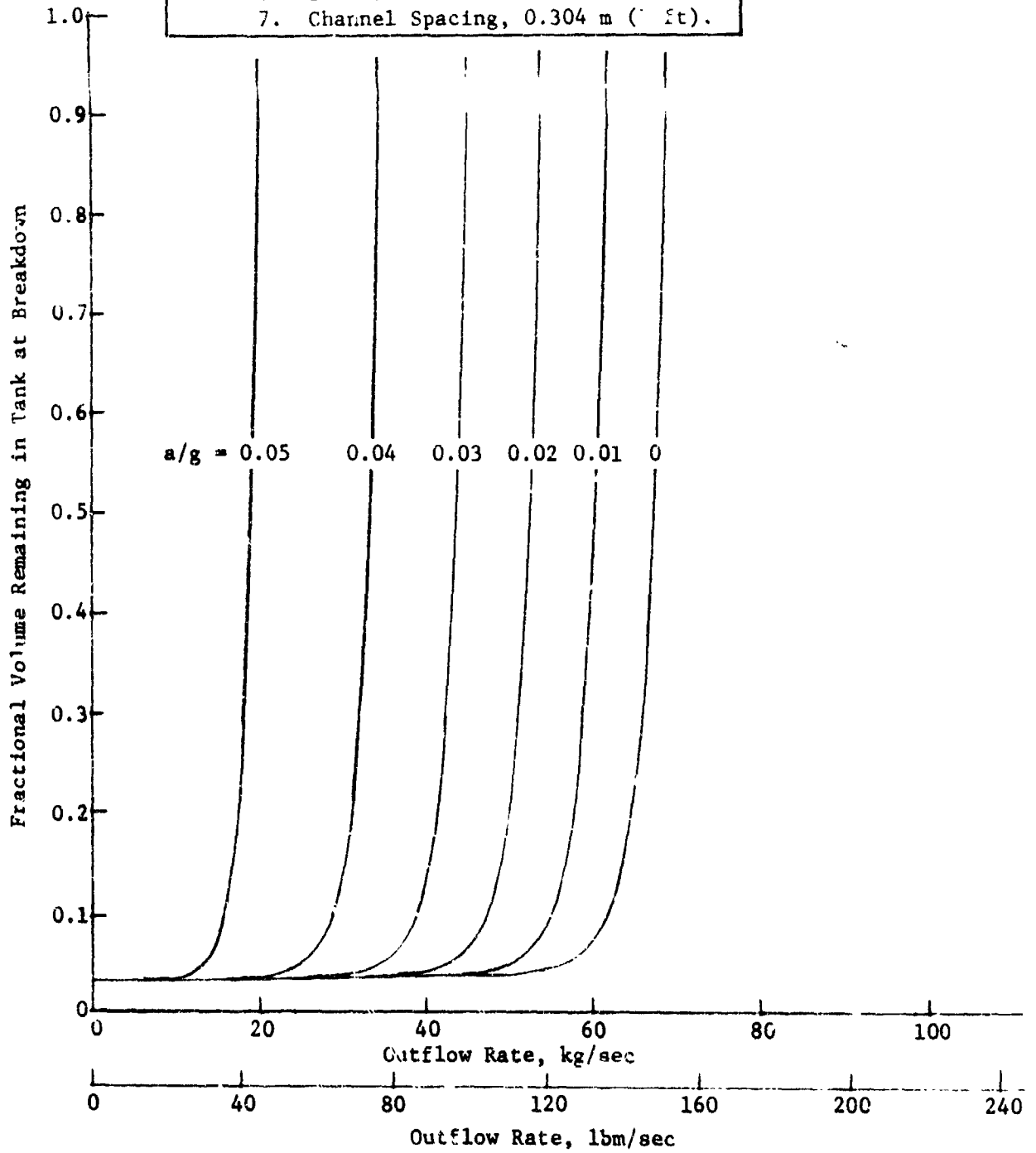


Fig. II-24 Outflow Capability of a Spherical Channel System with Liquid Oxygen

- Note:
1. Tank, 2.6 m (8.5 ft.) dia.
  2. Fluid, LO<sub>2</sub>.
  3. Vapor Annulus = 1.27 cm (1/2 in.).
  4. Liquid Annulus = 3.18 cm (1 1/4 in.).
  5. Screen = 325x2300.
  6. 16 channels.
  7. Channel Spacing = 0.304 m (1 ft.).

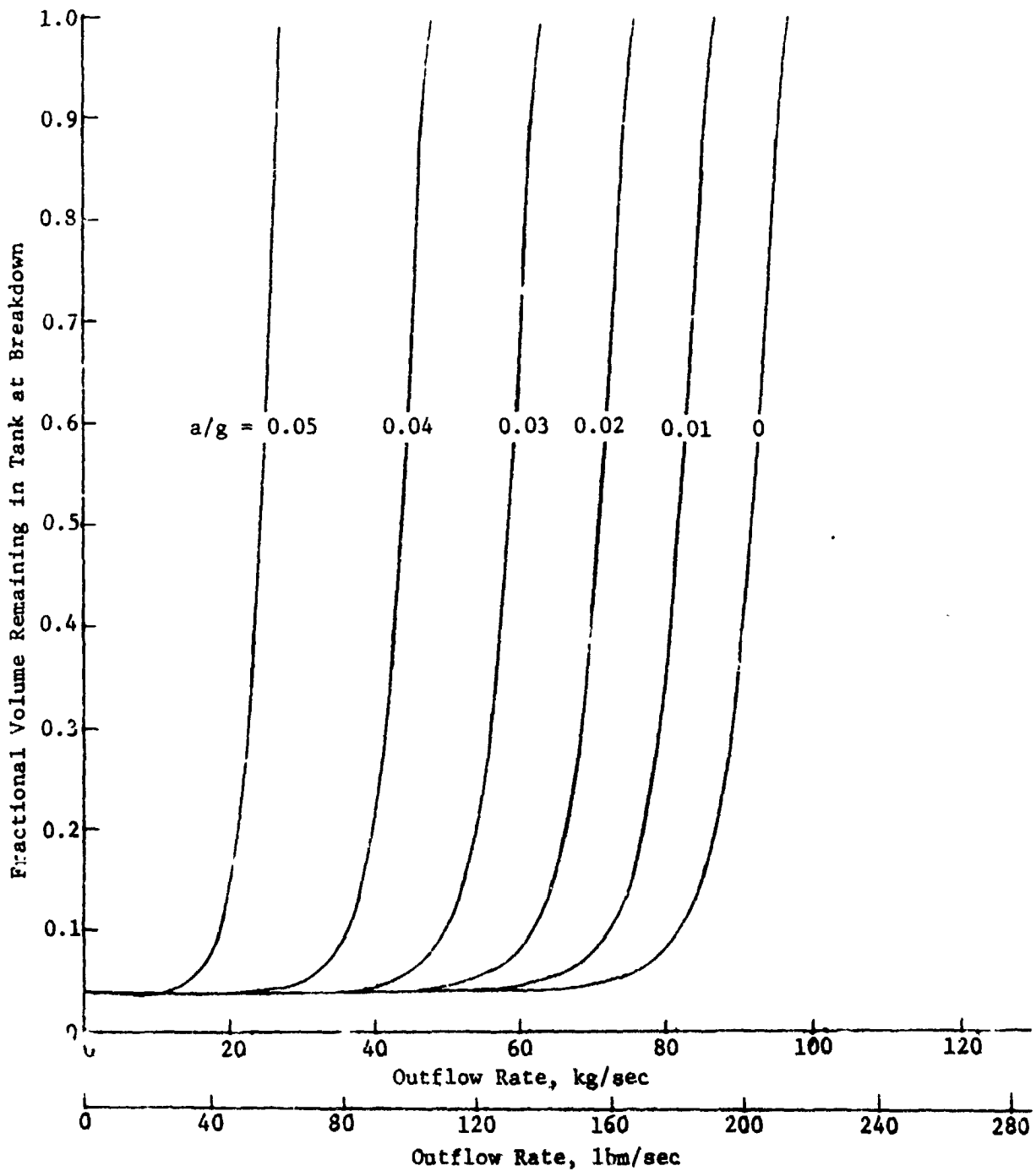


Fig. II-25 Outflow Capability of a Spherical Channel System in Liquid Oxygen

In addition to these noncryogenic tests, a successful series of tests was performed with a typical channel design in cryogenics. The design was a full liner and channel system, containing eight channels in a 63.5-cm (25-in.) spherical design. Test liquids were LN<sub>2</sub> and LH<sub>2</sub>. Detailed discussions of the device and the test procedures are included in Volume III. Tests performed covered all the operational requirements of an actual in-service device that could be modeled in a one-g bench test. Tests included fill and refill of the device, heat leak evaluation, liquid outflow with outer annulus pressurization using condensible and noncondensable pressurants, and venting evaluations. These tests demonstrated the design adequacy of the channel/liner concept to meet the requirements of cryogenic storage and feed systems in low-g environments.

d. *Start Transient Analysis* - The transient condition occurring in a fluid system by the initiation or termination of flow is an important parameter in system pressure load considerations. Pressure pulses caused by the rapid opening or closing of a valve can be sufficiently large to break down a capillary barrier or even cause structural damage to the capillary device. An analysis of this problem was conducted using the parameters of a typical capillary system.

When a valve at the end of a pipeline filled with static fluid is suddenly opened, a decompression wave is generated and transmitted down the pipeline, accelerating the fluid toward the valve. The magnitude of the decompression wave is given by the following equation (Ref II-7 and II-8).

$$\Delta H = a/g \Delta V \quad [II-12]$$

where

$\Delta H$  = magnitude of pressure wave, m (ft) of fluid;

$a$  = fluid sonic velocity, m/sec (ft/sec);

$\Delta V$  = velocity increase, m/sec (ft/sec);

$g$  = acceleration of gravity.

In terms of pressure,  $P$ , the equation, assuming constant density is

$$\Delta P = \frac{\rho a}{g} \Delta V \quad [II-13]$$

where  $\rho$  = fluid density.

This equation is applicable when the valve opening time is equal to or less than the time required for the wave to travel to the end of the pipe and back to the valve. That is, the valve opening time is less than the wave transport time according to the following

$$t \leq 2L/a$$

[II-14]

where  $t$  = valve opening time, sec

$L$  = pipe length, m (ft);

$a$  = fluid sonic velocity, m/sec (ft/sec).

If the valve opening time is greater than  $2L/a$ , the wave front will have been reflected from the end of the pipe and returned to the valve before the valve is fully opened. The result is that the maximum head or pressure difference will not have been produced.

The effects these pressure surges would have on the fine mesh screen is not well understood. Because the pressure pulses are generally of large amplitude but short duration, a nonsteady flow analysis is required. In addition, the porosity of the screen may allow some relaxation of the pressure pulse by passing liquid or the screen may absorb some of the pulse energy in elastic deformation.

A hydraulic transient analysis computer program, using the hydrodynamic criteria outlined in previous sections, was used to investigate the problem. The system modeled was a  $LO_2$  OMS tank and feedline system, which presents the more stringent requirements of the two propellant systems for this analysis. The feedline diameter was 10.16 cm (4 in.), tank pressure was  $24.1 \text{ N/cm}^2$  (35 psi) and the steady-state flow rate was 13.16 kg/sec (29 lbm/sec). The feedline length was 18.28 m (60 ft) and the valve opening time was assumed to be 0.137 sec. This valve opening time is based on an analysis (Ref II-9), which defined valve opening times that would yield linear changes in velocity corresponding to the maximum required mass acceleration levels of the propellant. These accelerations were  $289 \text{ kg/sec}^2$  (88 lbm/sec<sup>2</sup>) for  $LH_2$  and  $227 \text{ kg/sec}^2$  (500 lbm/sec<sup>2</sup>) for  $LO_2$ . A 25.4-cm (10-in.) diameter 200x1400 fine mesh screen trap was simulated on the tank bottom. A schematic of this system is shown in Fig. II-26. The results of the study are shown in Fig. II-27 through II-29. Figure II-27 illustrates the pressure transients in the system that are associated with the initiation of flow. Figure II-28 shows the expected system velocities; Fig. II-29 shows that the pressure differential across the screen trap levels off at approximately

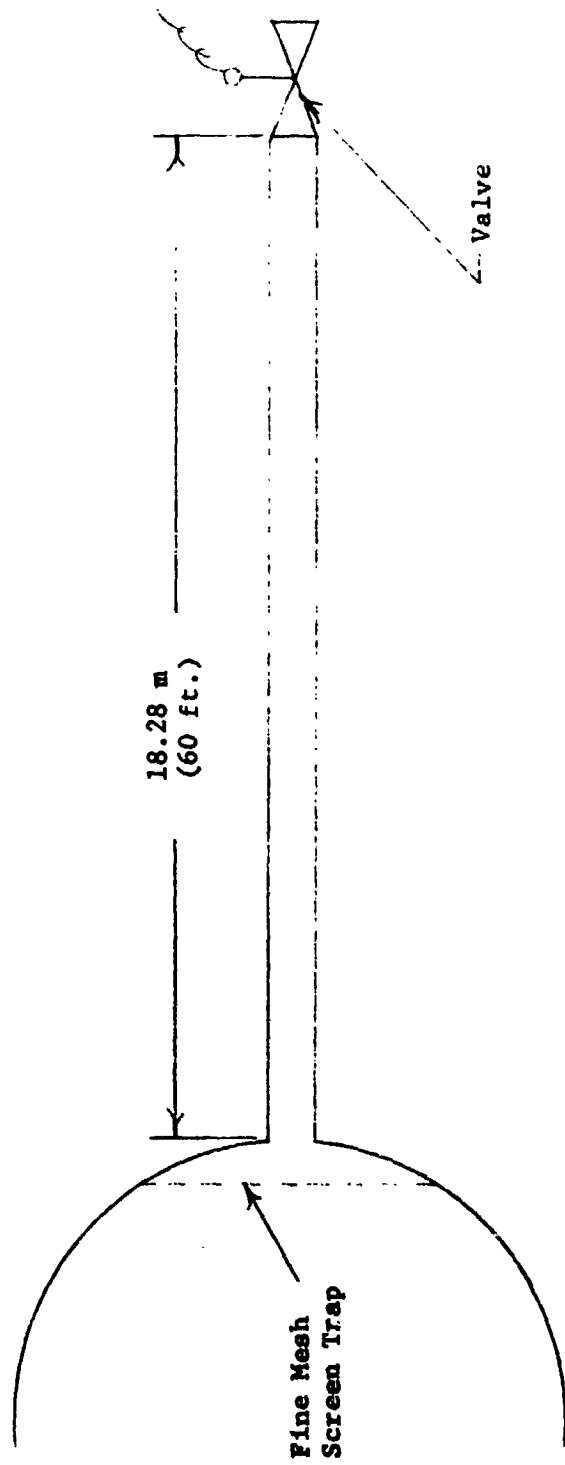


Fig. II-26 L02 OMS Feedline Start Transient Model Design

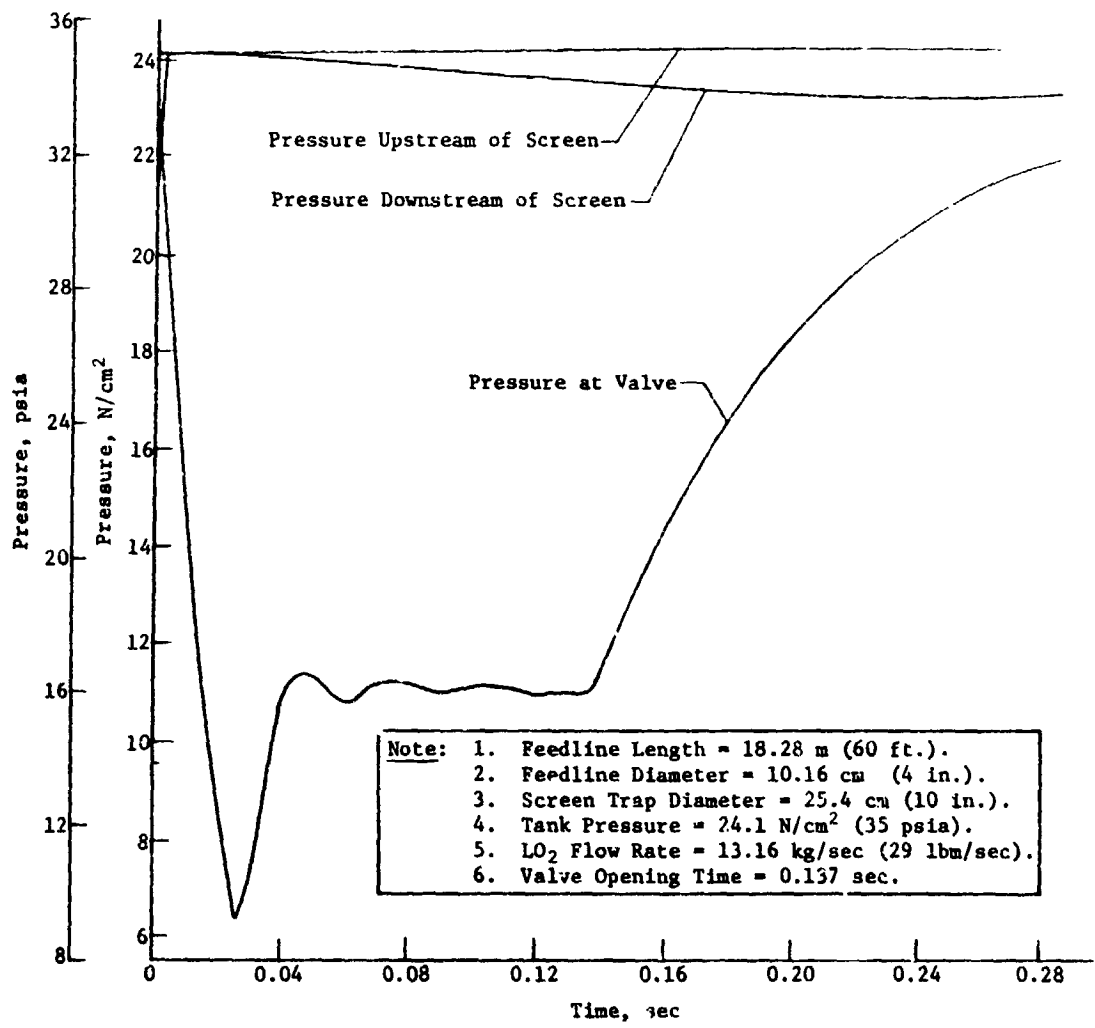


Fig. II-27 OMS LO<sub>2</sub> Tank Feedline Pressure Transients

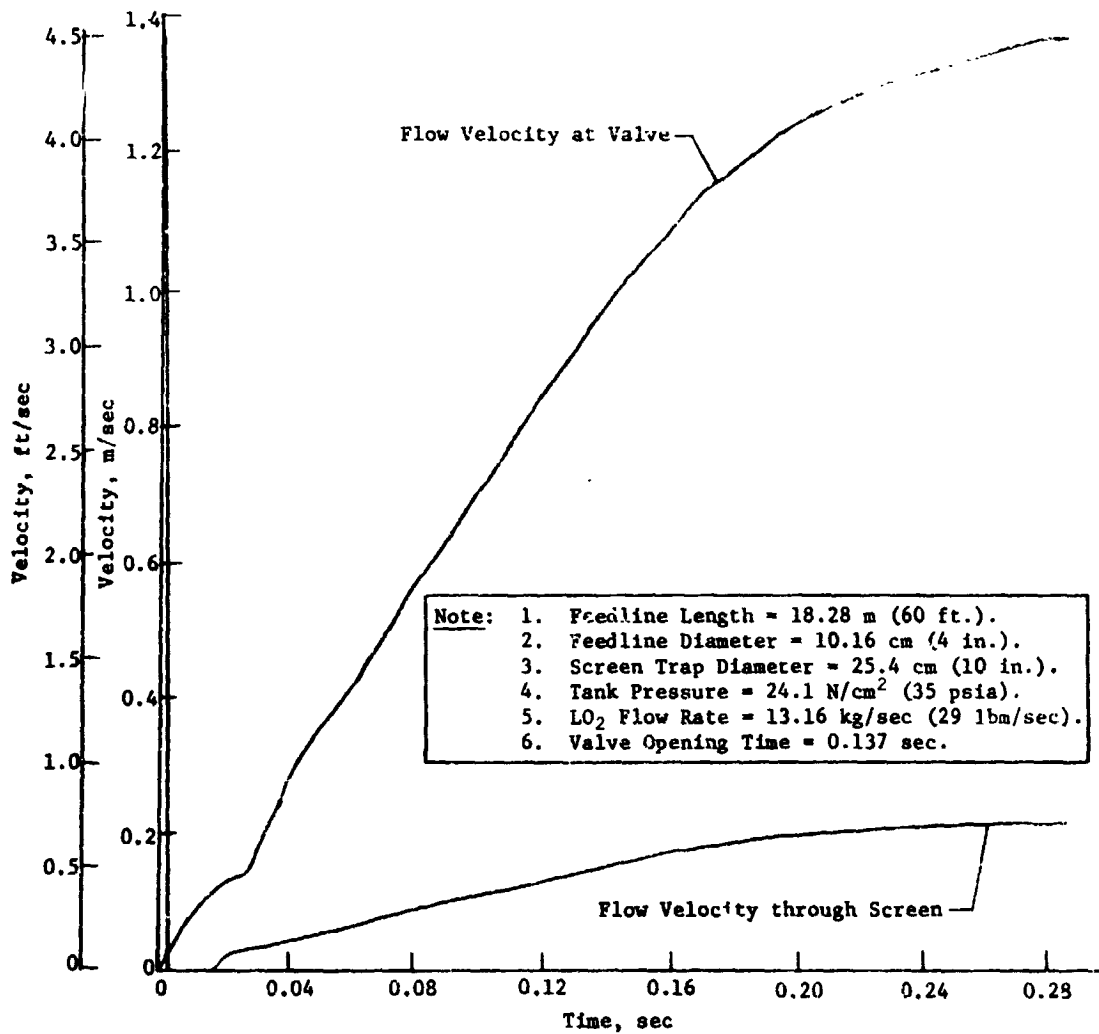


Fig. II-28 OMS LO<sub>2</sub> Tank Feedline Flow Velocity Transients

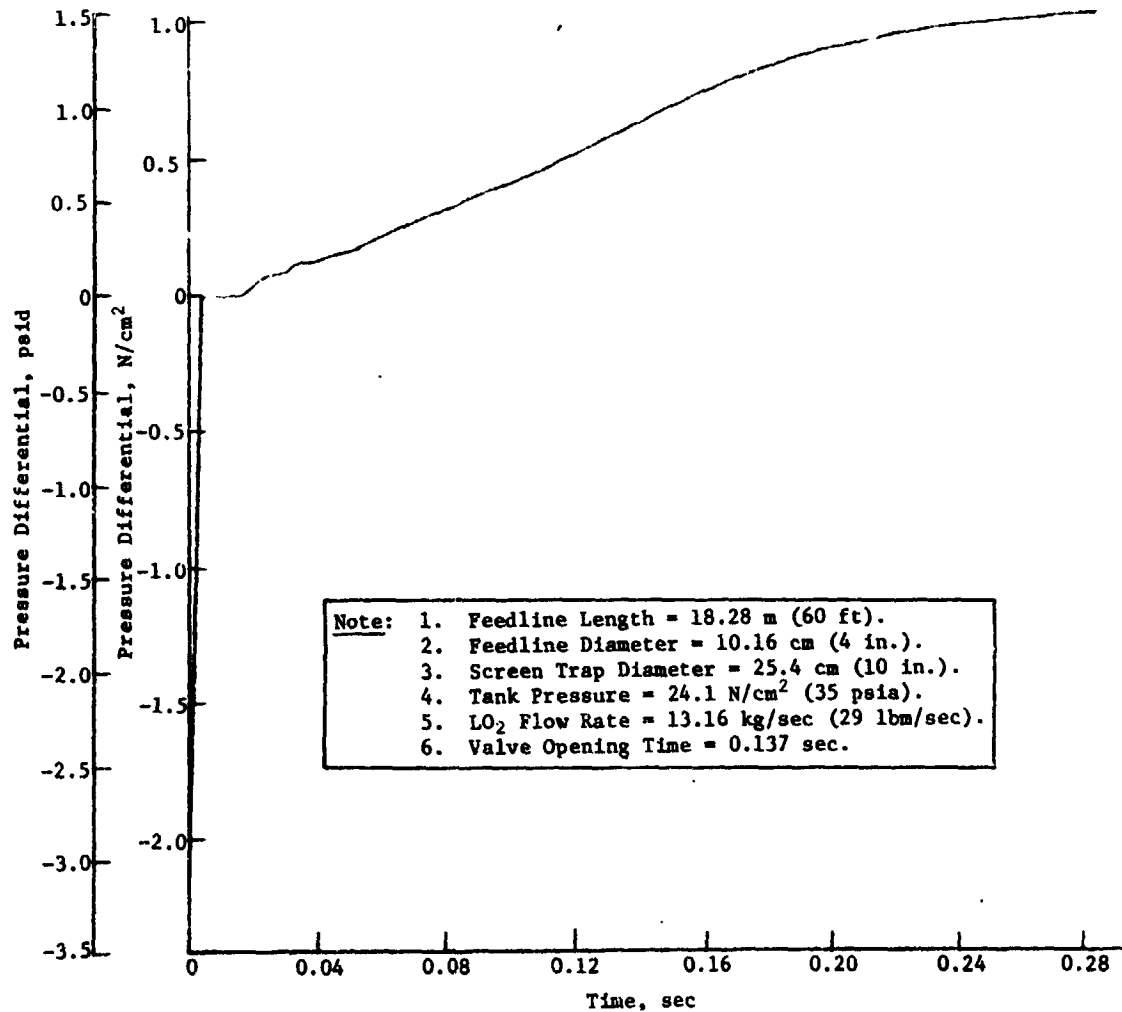


Fig. II-29 OMS LO<sub>2</sub> Tank Pressure Differential across 25.4-cm (10-in.) 200x1400 Fine Mesh Screen Trap

1.03 N/cm<sup>2</sup> (1.5 psid). It should be noted that this screen device is much smaller than any of the anticipated designs and, therefore, experiences pressure losses far in excess of any which might reasonably be expected in the candidate systems.

The results of the analysis indicate that although start transients must be considered in the design, the phenomenon does not appear to be a serious or restrictive design consideration. These conclusions were substantiated during testing of the noncryogenic transparent feedline which is detailed in Volume III. During these tests, start transients caused some liquid to drop out of the feedline screen core.

*e. Wicking Analysis* - The containment of liquid within a capillary retention device depends on the existence of a stable liquid meniscus across each capillary pore of the screen. With cryogenic propellants, heat transfer through the tank wall will cause a continuous evaporation of liquid from the screen surface. Wicking of the propellant along the screen must supply enough liquid to meet this evaporation rate and keep the screen wet. During pressurization with relatively warm gas, higher evaporation rates may occur locally. Should the screen dry out under these evaporation rates, wicking velocities must be high enough to rewet the screen in a reasonable length of time.

Previous work (Ref II-10, II-11, II-12) has shown that the wicking velocity in a single layer of screen can be characterized by

$$V = \frac{c \sigma}{l \mu} \quad \text{[II-15]}$$

where V = wicking velocity

c = wicking constant

l = wicking distance

σ = surface tension

μ = viscosity

Wicking velocities in a single layer of screen are quite low. By comparison, the wicking velocity in a narrow channel can be several orders of magnitude greater. Such a channel is formed between a screen and the perforated plate which is often used for support.

With vaporization occurring either along a wick or at a concentrated heat input located some distance away from the reservoir,

an equilibrium is reached in which the capillary forces are balanced by the frictional and gravitational body forces. If the frictional losses or the heat load for a wick are sufficiently high, the wick will not wet completely. The distance between the reservoir and the liquid interface is called the dryout limit. Although wicking velocities are of interest, dryout limits are critical to the design of the cryogenic acquisition/expulsion device. Therefore, an analytical and an experimental program were undertaken to determine dryout limits of screen and screen-plate wicks.

The analytical investigation considered both steady-state and transient wicking phenomena. The analysis produced the expression for wicking limits

$$S = \sqrt{\frac{\rho g_c h_{fg} \sigma K(a+b)}{Q\mu}} \quad \text{[II-16]}$$

where  $S$  = the dryout limit of the wick, m (ft)

$$K = \frac{C\phi + b^2/6}{a+b}, \text{ m (ft)}$$

$\phi$  = porosity of the screen

$a$  = thickness of the screen, m (ft)

$b$  = thickness of the gap between the screen and plate, m (ft)

$Q$  = heat flux,  $W/m^2$  (Btu/hr-ft<sup>2</sup>)

$h_{fg}$  = heat of vaporization, W-sec/kg (Btu/lbm)

$\mu$  = viscosity, kg/m-sec (lbm/ft-sec)

$\sigma$  = surface tension, Dyne/cm (lbf/ft)

$\rho$  = density, kg/m<sup>3</sup> (lbm/ft<sup>3</sup>)

$$C = \frac{4 D_a^2}{D_{BP} A_w}, \text{ m (ft)}$$

Wicking lengths for various screens without perforated plate are plotted in Fig. II-30 and II-31. Equation [II-16] is plotted in Fig. II-32 and II-33 for liquid hydrogen and liquid oxygen, respectively, for various values of screen-plate gap ( $b$ ) with 200x1400 screen. The value  $b = 0$  represents a screen by itself. Note the significant jump in the dryout limit when plate (signified by a finite value of  $b$ ) is added to the screen. This is due to the relatively large volume of liquid being supplied by the channel between the screen and plate.

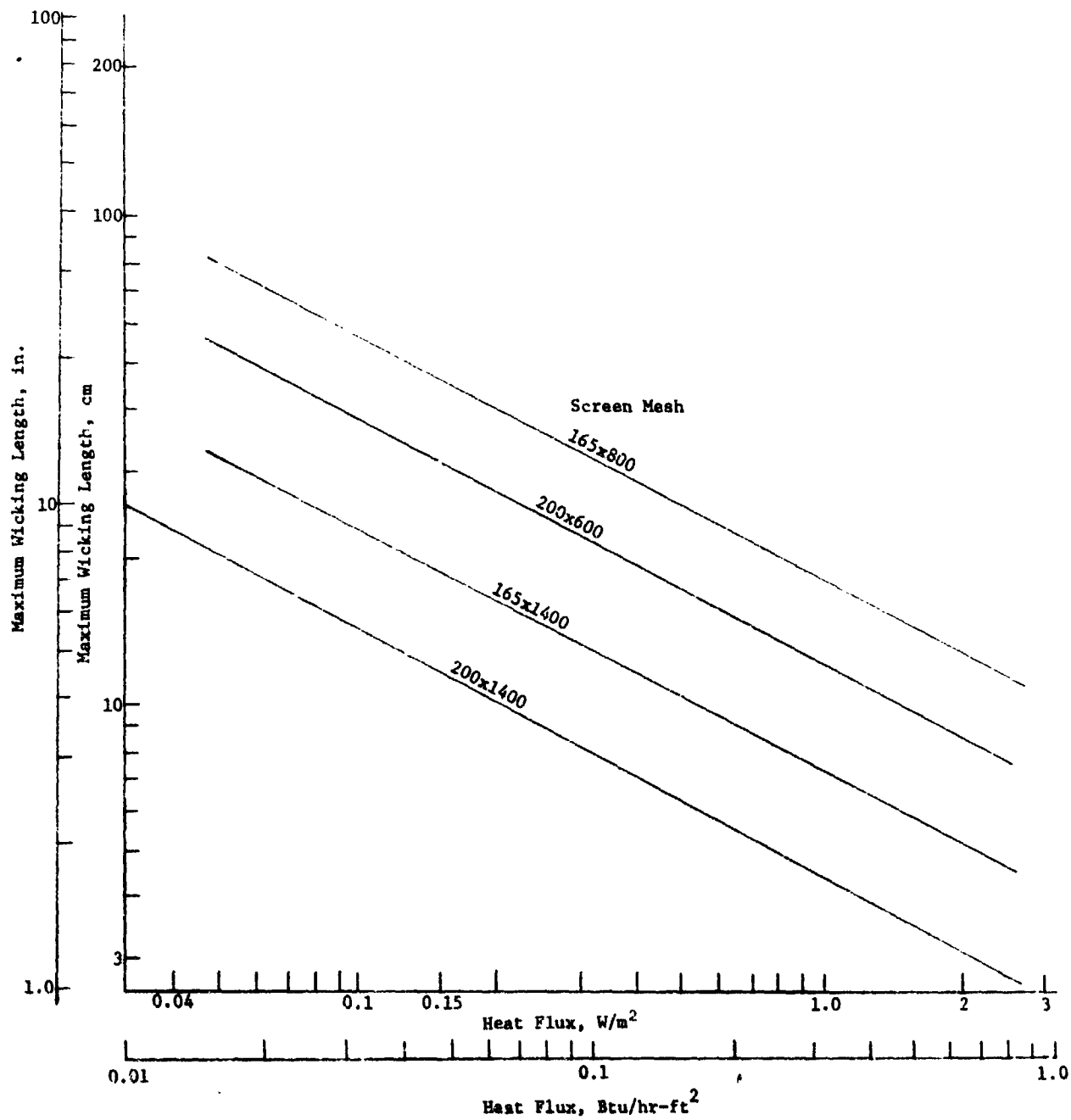


Fig. II-30 Maximum Wicking Length for Liquid Hydrogen as a Function of Heat Flux

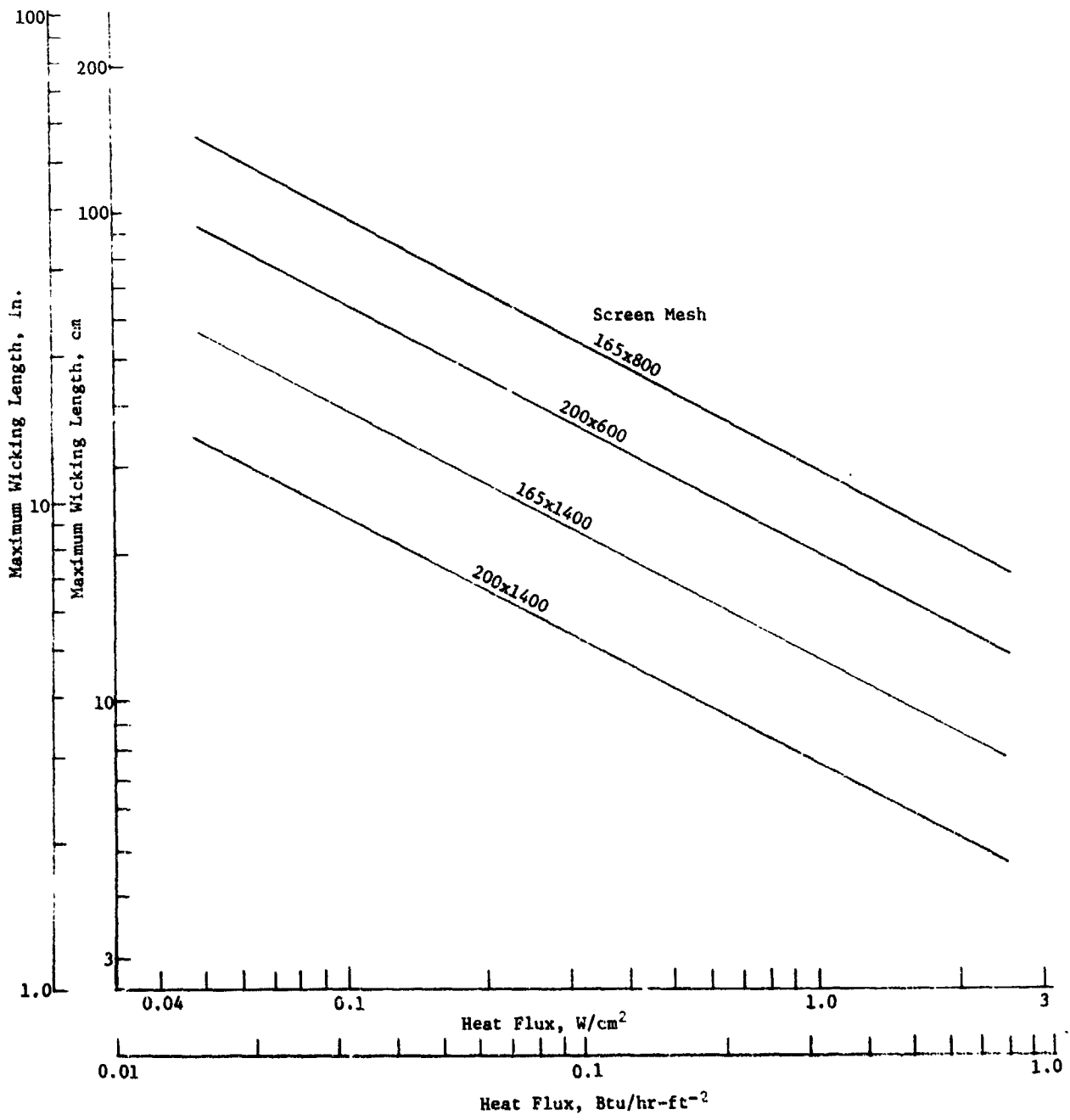


Fig. II-31 Maximum Wicking Length for Liquid Oxygen as a Function of Heat Flux

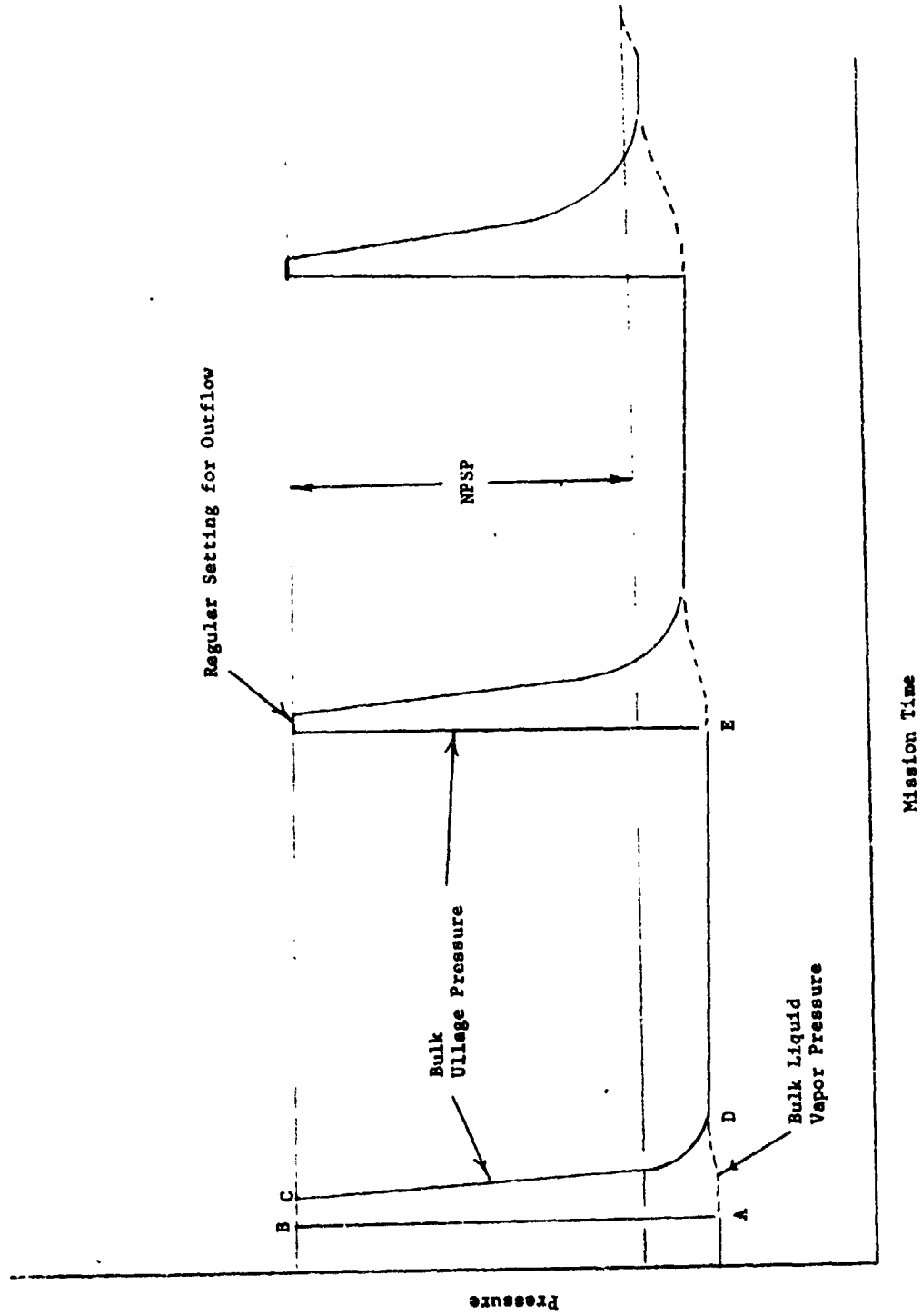


Fig. II-35 DSL Tank Pressure History

Mission Time

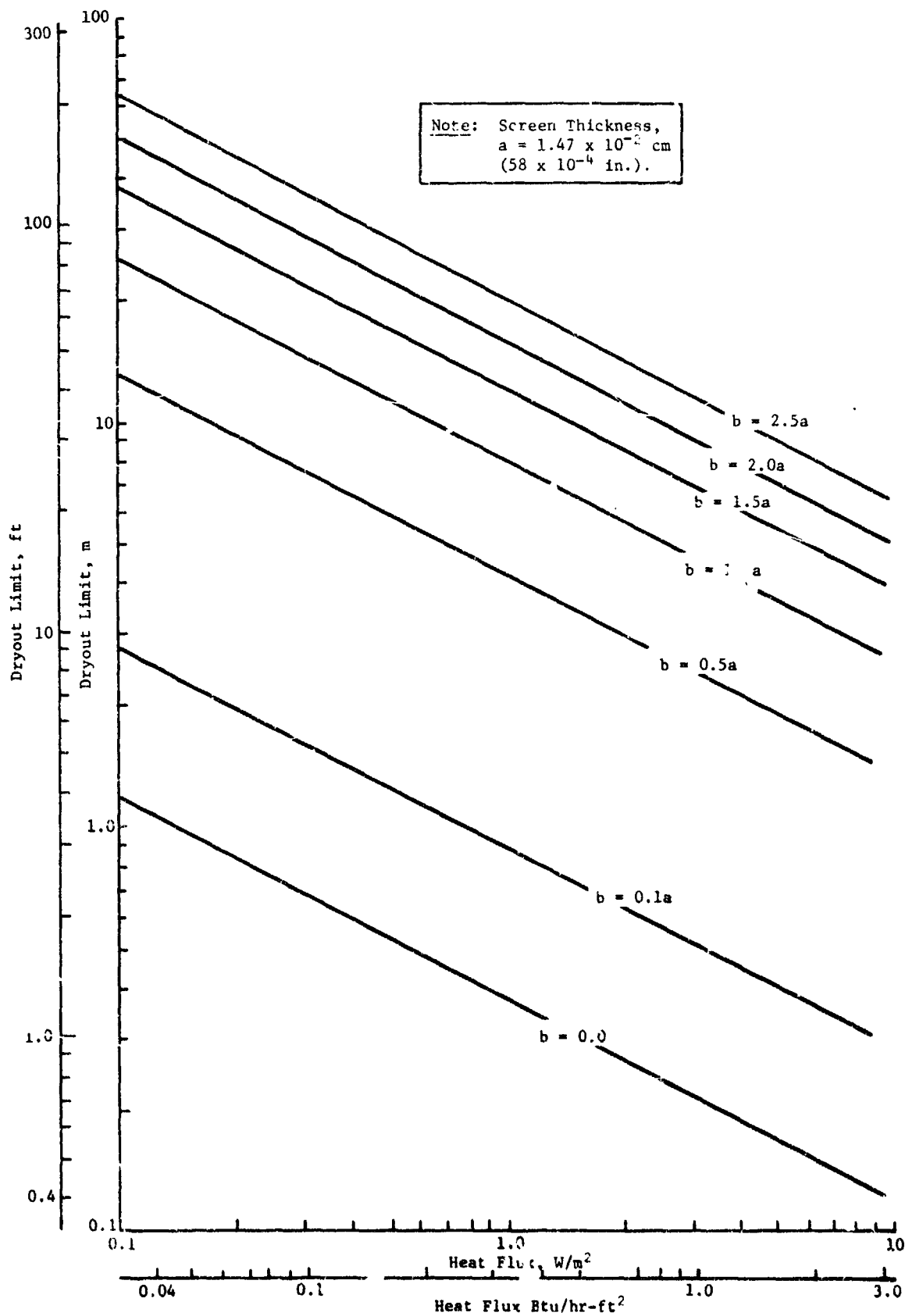


Fig. 11-50 Dryout Limit for  $b/a$  with 200#1400 Screen on Plate

The development of Eq [II-16] assumed a constant velocity along the screen. The consideration of evaporation along the screen surface implies a velocity gradient along the screen. A computer model was used to more accurately represent the wicking phenomenon. This program uses finite differences to solve the heat transfer problem and a method of excess degrees (Ref II-13) to model the evaporation. The evaporation rate is then used to determine the wicking velocity. Figure II-34 shows a plot of the liquid/vapor interface location as determined by this model. For the conditions considered, the curve approaches a constant value predicted by Fig. II-32.

An experimental program, described in Volume III, was conducted to augment the wicking analysis. The results of these tests correlated well with analytical predictions, substantiating the validity of the analytical model.

On the basis of these tests and analyses, the wicking problem does not appear to be more than a design consideration and the wicking limits for fluids of interest do not appear to be restrictive.

## 2. Thermal and Thermodynamic Effects

The design of any cryogenic acquisition/expulsion system is significantly affected by several thermal and thermodynamic processes. In this study, the thermal and thermodynamic processes affecting the design of the DSL system were analyzed to yield design approaches and guidelines. The analyses conducted were primarily in the areas of pressurization and venting. An evaluation of the collapse of hydrogen and oxygen vapor bubbles was conducted, which included analytical and experimental investigations. These studies and the computer program used in the pressurization and venting analyses are presented in the following paragraphs.

*a. Analytical Model* - An analytical model was developed to specifically analyze the DSL baseline concept. The DSL computer program was developed and used extensively under previous studies (Ref II-14 and II-15) to simulate the performance characteristics of DSL systems for various cryogenic propellants and mission duty cycles. Under this program the model was modified, improved, and used to predict the pressure and temperature histories of the cryogenic storage systems for specific mission duty cycles of the Space Shuttle Orbiter and the Space Tug.

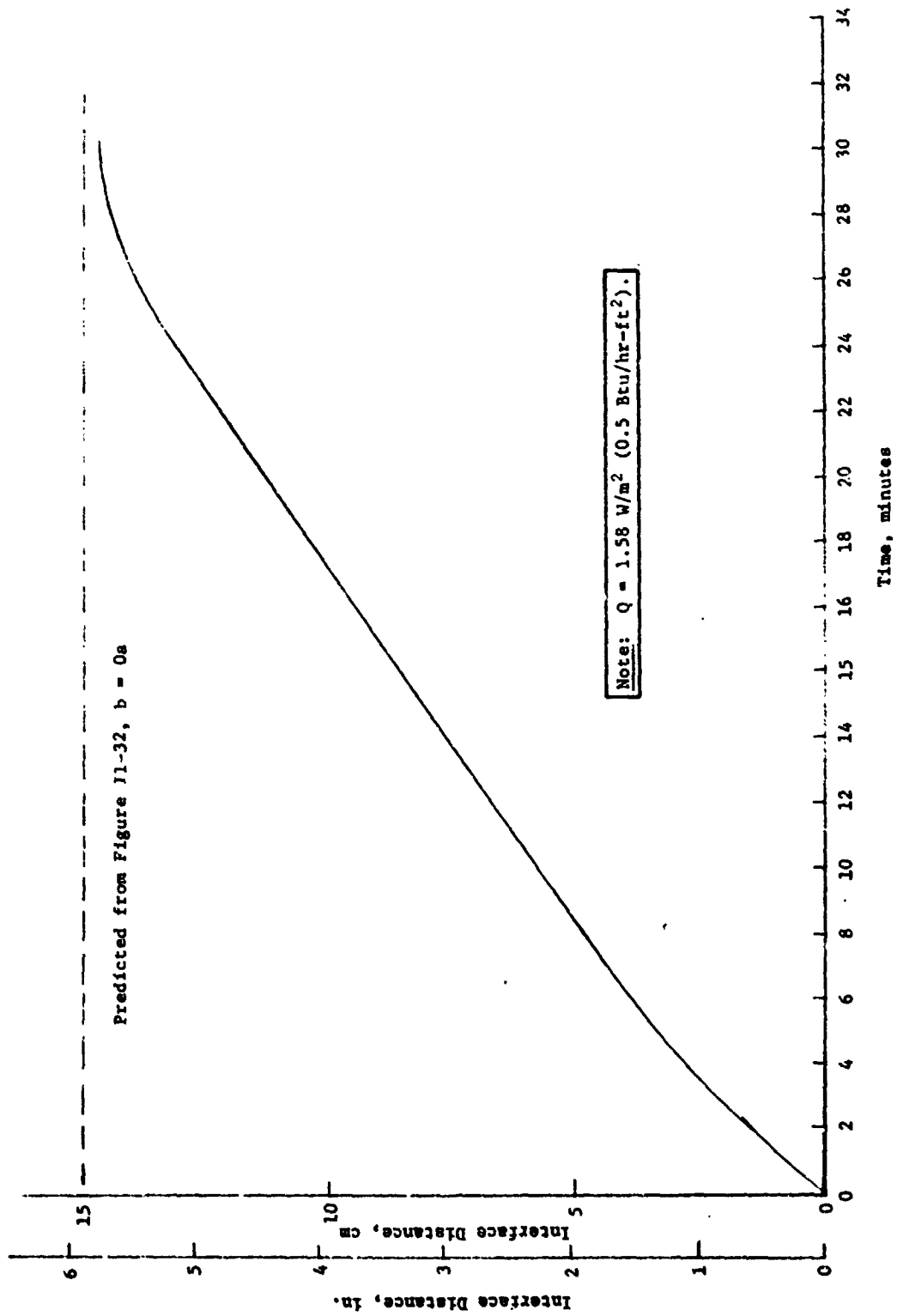


Fig. II-34 Transient Movement of Vapor-Liquid Interface of  $Lh_2$  in a 200x1400 Screen Wick

The analytical model simulates the pressurization and venting characteristics of the DSL system. The program considers three concentric compartments divided into five nodes--an outer annulus vapor volume; a liquid and vapor volume in the bulk region; and two liquid volumes within the controlled liquid annulus one sees the gas and the other sees the liquid in the bulk region. The communication screen is simulated by specifying a screen with a bubble point less than that of the controlled liquid annulus screens. This simulation allows for propellant and pressurant mass transfer between the outer annulus and the bulk region.

Briefly, the model can simulate the following operations

- 1) Tank pressurization in either the vapor annulus or bulk region with either autogenous or inert gas;
- 2) Coast periods with external heating and venting, using several vent control schemes;
- 3) Liquid outflow, maintaining a specified NPSP and controlled by a regulator.

The model assumes natural free-convection heat transfer through the tank and uses the standard hydrodynamic and hydrostatic relationships for predicting pressure drops throughout the system. Because the hydrostatic head and natural free-convection heat transfer coefficients are functions of acceleration, the model simulates a low-g environment by using an acceleration value near zero. The model will not handle the diffusion of a two-component gas mixture in the bulk region. The condensation and vaporization are assumed to occur at a flat interface.

The thermodynamic and transport properties for the fluids are calculated from curve fit equations. With the exception of hydrogen, all the vapors are considered to be an ideal gas. For hydrogen, the Redlich-Kwong equation of state was used to calculate densities. This equation of state was checked out for  $\text{GH}_2$  and was determined to be within 5% of published data for pressures up to  $103.3 \text{ N/cm}^2$  (150 psia) and for a temperature range of  $19^\circ\text{K}$  ( $35^\circ\text{R}$ ) to  $294^\circ\text{K}$  ( $530^\circ\text{R}$ ). A more detailed description and discussion of this analytical model is presented in References II-14 and II-15.

*b. Pressurization System Characteristics* - The previous section briefly described the operating characteristics of the DSL system during pressurization and liquid expulsion. This section

presents the important pressurization considerations that affect the design of a cryogenic acquisition/expulsion system. For the cryogenic Space Shuttle OMS and the Space Tug, the propulsion systems are baselined as pump-fed with the exception of the dedicated OMS (LO<sub>2</sub>) system, which could also be a pressure-fed system. Therefore, the pressurization system considerations were primarily those associated with a pump-fed system.

For a pump-fed system, the single most important pressurization system requirement is that of satisfying NPSP as dictated by the turbopump. This requirement can be met using either an autogenous gas or helium as the pressurant. Helium pressurant is slightly more complex, requiring an additional storage tank, valving, and plumbing. Also trade studies have shown that autogenous pressurization has a slight weight advantage over helium. For the integrated OMS/RCS and the Space Tug, autogenous pressurization was therefore baselined. In these systems, the pressurant supply is provided by the gaseous accumulators, which also provide the propellants for the RCS propulsion system. The gaseous accumulators are recharged using liquid from the main propellant tanks; the liquid is conditioned by the turbopump and heat exchanger assemblies.

The pressurization characteristics for the preferred DSL concept are illustrated in Fig. II-35. This curve shows a tank pressure history for the DSL system during a multiburn and coast duty cycle. The tank prepressurization occurs between points A and B and the pressurization and liquid expulsion (burn period) occurs between points B and C. As previously mentioned, during liquid expulsion the pressurant gas enters the outer annulus and then communicates into the bulk liquid via the communication screen. Following the burn period, the tank pressure drops from point C to D, which is caused by the warm ullage cooling down. During the burn and pressure collapse period, there is an increase in the bulk liquid temperature, illustrated by a corresponding increase in vapor pressure. This temperature increase is due to the energy exchange between the warm ullage and the bulk liquid, point D. Following the completion of a burn and during the pressure collapse, the DSL vent system is activated and venting continues until the next prepressurization period, point E. The cycle is then repeated.

The curve also shows that the NPSP is satisfied for every burn period with the last burn period being the most critical, i.e., if NPSP is satisfied in the last burn, it will be satisfied for all burn periods. This is due to the bulk liquid temperature



rise being inversely proportional to the quantity of liquid present and, of course, the quantity of liquid is the smallest during the last outflow period. It is, therefore, important to predict the tank pressure and bulk liquid temperature histories as functions of pressurant temperature, heat flux, initial conditions, etc, for a representative mission duty cycle.

As previously mentioned, these predictions can be made using the DSL computer program. In addition, estimates for pressurant use and pressurant mass flow rate are considered important and affect the system design. The pressurant mass flow rate is important because it affects the design of the communication screen. The communication screen surface area must be large enough so that the pressure drop during pressurization does not exceed the bubble point of the liquid annulus screens. The pressurant usage is most important because it affects the size of the propellant conditioning unit and gaseous accumulator.

*c. Stratification Effects* - The stratification effects have been investigated both analytically and experimentally in both 1-g and low-g environments during the past few years (Ref II-16 and II-17). In a 1-g environment, the typical vertical stratification results from heat entering the storage tank through the walls and penetrations. Buoyant forces establish the convective flow, of the liquid within the storage tank. This convective flow, which could be turbulent depending on the magnitude of the heat rates, deposits warm liquid at the gas/liquid interface. The stratified liquid layer continues to grow as a function of heat flux, type of cryogen, configuration of storage tank, etc. At the warm gas/liquid interface, vaporization occurs, thus cooling the bulk liquid.

For the same cryogenic propellants in reduced gravity, the free-convection circulation is significantly reduced. At the same heat flux, the surface temperature rise will be much faster under the reduced gravity conditions than under the 1-g environment. The creation of nucleation sites on or near the heating surfaces must be considered. Following nucleation, the vapor bubbles generated will grow rapidly because of the continued heat addition and vaporization which results. This creates a condition that produces high tank pressure rise rates.

The DSL cryogenic acquisition/expulsion system incorporates capillary barriers that thermally isolate the bulk liquid from the heating surfaces, using a complete screen liner. The superheating of the liquid and the inception of nucleation is circumvented. The pressure rise within the tank is controlled by

providing a large gas/liquid interface directly opposite the heating surfaces and allowing normal vaporization of the liquid at the screen surfaces. This cools the bulk liquid. The tank pressure is relieved by venting from the controlled outer gaseous volume.

The thermal stratification for the DSL system becomes radial rather than the vertical orientation of the standard gravity environment. The pressurization of the DSL during expulsion also tends to enhance this condition because the warm pressurant is introduced in the outer annulus. Under this stratified condition, the bulk liquid can be passively maintained in a subcooled condition without the use of mixers or heat exchangers.

*d. Vent System Characteristics* - Under Contract NAS9-10480 (Ref II-15), analytical trade studies were conducted that identified many of the operational characteristics of the baseline DSL concept. In particular, a preferred DSL vent system was selected based on a parametric analysis that considered weight and thermal performance tradeoffs. During this study, the analyses of the previous contract were continued and supplemented with experiment data.

The preferred vent system is illustrated in Fig. II-36 for both  $LH_2$  and  $LH_2$ . Using this vent system, the stratification condition discussed in the previous section is maintained. The tank pressure can be controlled while maintaining the bulk liquid in a subcooled condition. The tank pressure is controlled by venting liquid-free vapor from the outer annulus. The outer annulus pressure is controlled between two levels. The lower pressure level (when the valve is closed) is approximately the bulk pressure and the upper pressure limit (when the valve is opened) is the bulk pressure plus the bubble point of the communication screen. The upper limit was established to prevent the communication of the warm vapors from the outer annulus into the bulk region, thereby minimizing the energy input to the bulk liquid.

The lower pressure limit corresponds to the pressure required in the outer annulus to support the liquid in the bulk region. With a negligible hydrostatic head in a low-g environment, the lower limit pressure is approximately the bulk pressure. The vent band would, therefore, be reduced in an acceleration environment where the hydrostatic head becomes significant. Figure II-36 shows the difference in the outer annulus vent bands for  $LH_2$  and  $LO_2$  systems. The vent band for  $LO_2$  is much greater than that

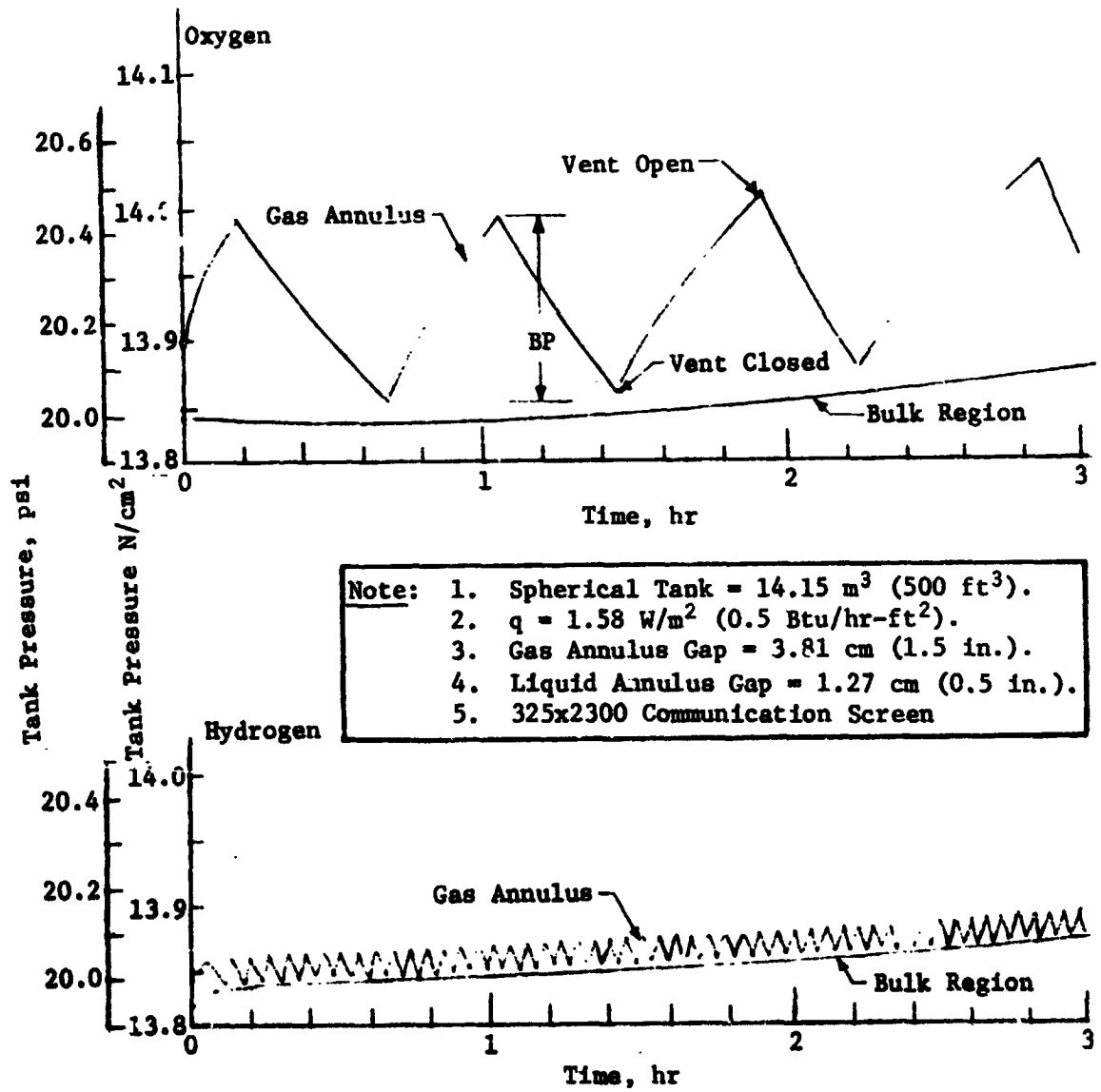


Fig. II-36 Tank Pressure Illustrating DSL Vent System

for LH<sub>2</sub> because of the corresponding differences in the bubble points of the communication screens. Also, as expected, the vent frequencies between the two systems show the same differences.

The operation of the preferred vent system does not depend on the tank pressure. The system is activated following the completion of an outflow period and its operation is terminated prior to the prepressurization of the tank for the next outflow. The venting system requires a sensor for sensing the pressure differential between the outer annulus and the bulk region. The sensor operation would be similar to a pressure switch and will actuate a vent control (solenoid) valve. The desired vent rate would be achieved by orificing the vented gas downstream of the vent control valve.

The parameters most affecting the performance of the DSL vent system are:

- 1) external heat flux,
- 2) outer annulus gap,
- 3) pressure drop during venting,
- 4) vent rate,
- 5) valve open time.

The performance of the vent system for a LH<sub>2</sub> or LO<sub>2</sub> tank, independent of tank size and geometry is presented in Fig. II-37. The annulus gap,  $\Delta r$ , is presented as a function of the group parameter,  $q\theta/\Delta P$ , where  $q$  is the external heat flux,  $\Delta P$  is the pressure drop in the outer annulus during a vent cycle, and  $\theta$  is time the vent valve is open. The parameter  $K$  is the ratio of the vent rate to evaporation rate. For hydrogen, the values of  $K$  presented range between 1.1 to 4; for oxygen, a wide range of 1.1 to 20 is presented.

Before discussing the performance curve, a more detailed explanation of the critical performance parameters and how they are established is required. The annulus gap is generally sized by the initial ullage volume and cases where the initial ullages are small, force the annulus gap to be small. For the fixed propellant loaded volumes, the only way to increase the annulus gap is to increase the tank volume, which is generally undesirable.

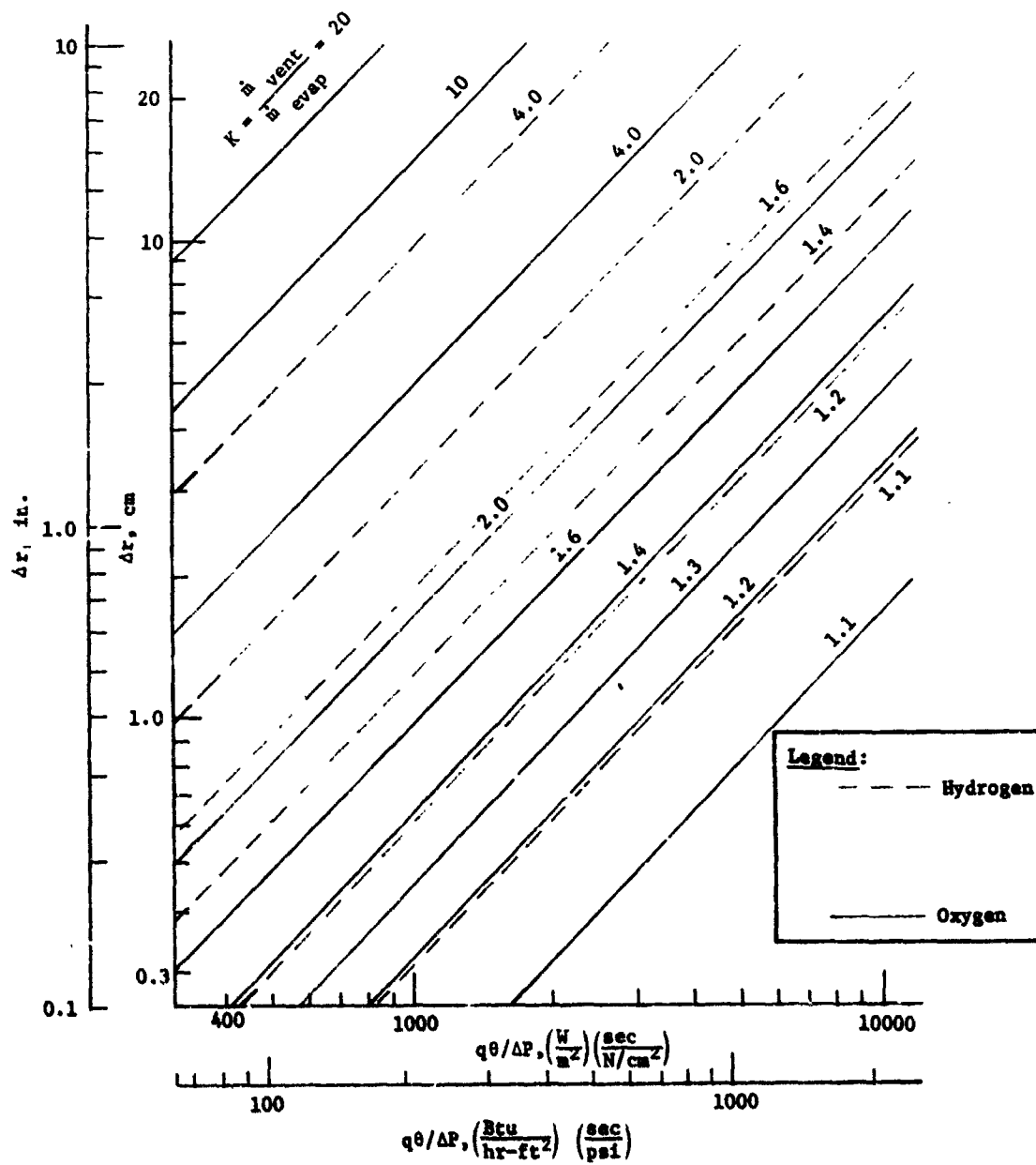


Fig. II-37 DSL Vent System Performance Characteristics

For mission duty cycles that use propellants early in the mission, the annulus gap can be increased to accommodate the smaller propellant volume following these initial burn periods. The larger the annulus gap, the better the performance of the vent system. Increasing the annulus gap increases the superheat of the vented vapor, thereby reducing the vent vapor mass. Increasing the annulus gap also reduces the number of vents required as shown in Fig. II-38.

During low-g the  $\Delta P$  term is a function of the bubble point of the communication screen. As mentioned earlier, the communication screen mesh and size are determined by the design of the liquid annulus screens.

For a fixed heat flux, the vent valve open time is inversely proportional to the vent rate and directly proportional to  $\Delta r$  and  $\Delta P$ . Because  $\theta$  has a direct influence on vent frequency, it is desirable to have as large a  $\theta$  as possible. Since it is the ratio of vent rate to evaporation rate, the parameter  $K$  is influenced by several considerations. First, the vaporization rate is, of course, a function of the heat flux and the propellant. The vent rate is determined by considering both the size of the vent orifice and the vent frequency. The exit vent pressure is very near vacuum; therefore, the vent orifice sizing considers sonic flow, which means that the vent rate can be changed only by changing the orifice size. To avoid plugging, the orifice should be as large as possible. However, as shown in Fig. II-38, reducing the vent rate reduces the number of vents; this is also desirable. Therefore, a tradeoff between orifice size and number of vents must be made in order to establish the vent rate.

To further illustrate the performance characteristics of the DSL vent system, consider a vent system design where the  $\Delta r$ ,  $\Delta P$ ,  $\theta$ , and vent rate have been established for a specific heat flux,  $q$ . First, assume that the  $q$  has doubled, which also doubles the evaporation rate. This means that unless the initial value of  $K$  was greater than or equal to two, the vent system will not be able to control the tank pressure increase resulting from the increase in  $q$  unless the vent orifice is increased. If the initial value of  $q$  were reduced by one-half, the value of  $K$  would double, but the vent system would still be capable of handling this change. The only significant effect produced by this change would be an increase in the vent frequency.

This example illustrates that the preferred vent system is very sensitive to an increase in  $q$  and the design must be capable of increasing the orifice size. This increase can be accomplished

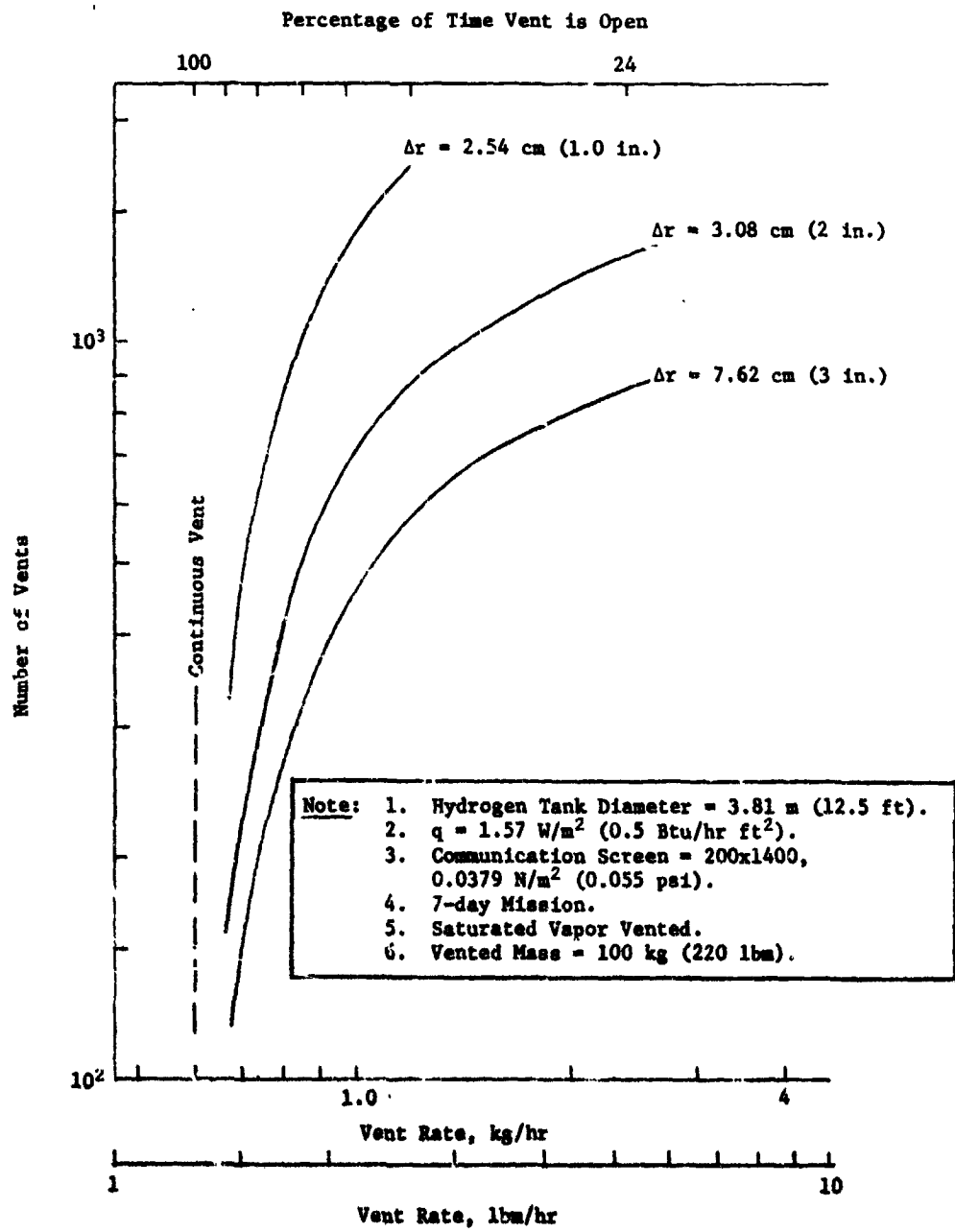


Fig. II-38 Effect of Gas Annulus Gap on Vent Rate

by incorporating additional orifices in parallel with the design orifice. Initially isolated, the additional orifices would be activated as required to accommodate an increase in heat flux. The additional orifices would not be used if a decrease in  $q$  occurred unless the vent frequencies became excessive.

Although fine mesh screen has been the focus for most DSL system designs, various foraminous materials with higher bubble points were evaluated to determine their effect on vent system performance. Pressure rise and quantity of vapor mass vented are presented for several bubble points and for both the LO<sub>2</sub> and LH<sub>2</sub> storage systems in Table II-1. The 7-day coasting period with venting (no pressurization or liquid outflow) produced relatively small pressure increases. This allows the cryogens to be stored with little increase in temperature despite appreciable external heating. Venting, as usual, is initiated just before the pressure differential between the outer annulus and the bulk region would cause breakdown of the communication screen. Venting was terminated when pressure differential fell to 0.034 N/cm<sup>2</sup> (0.05 psi).

LH<sub>2</sub> cases considered a 63.67 m<sup>3</sup> (2250 ft<sup>3</sup>) sphere with a 3-in. outer annulus gap and 20% total ullage and a 28.18 m<sup>3</sup> (995 ft<sup>3</sup>) cylinder with hemispherical end domes, 30% total ullage, and a similar gas annulus gap. Heat leak to both tanks was 1.57 W/m<sup>2</sup> (0.5 Btu/hr-ft<sup>2</sup>). As the bubble point was increased from 0.048 to 6.89 N/cm<sup>2</sup> (0.07 to 10.0 psi), the pressure rise at the end of the seven days also increased. However, venting was less frequent with the higher bubble point material and the vapor vented had a greater amount of superheat, yielding a smaller mass vented during the seven-day simulation. The vent rate shown in the table is the actual vent rate during the vent period. The seven-day pressure rise and vapor mass vented for the low bubble point cases were extrapolated because the computer interval needed to maintain such a narrow pressure control band would require a long and costly computer simulation. The vapor mass vented at the end of the three-hour period was zero because the tank was not vented during that interval. The ullage pressures for the large 6.895 N/cm<sup>2</sup> (10 psi) tank case, are presented in Fig. II-39. The tank was vented about 20 times during the 7-day mission. The upper curve shows the amount of liquid in the central region as a percentage of the initial quantity. The venting simulation for the large 0.69 N/cm<sup>2</sup> (1.0 psi) tank case is shown in Fig. II-40. Vent frequency is slightly over 1 vent per hour. The pressure history for the 28.18 m<sup>3</sup> (995 ft<sup>3</sup>) LH<sub>2</sub> tank is shown in Fig. II-41.

Table II-1 Effect of Bubble Point on Venting, External Heat Rate  $1.57 \text{ W/m}^2$   
( $0.5 \text{ Btu/hr-ft}^2$ )

Simulated Cases	Vent Rate during Vent, kg/hr (lbm/hr)	7-Day Period	
		Pressure Rise, $\text{N/cm}^2$ (psi)	Mass of Vapor Vented, kg (lbm)
Case 1 Bubble Point, $\text{N/cm}^2$ (psi)			
0.048 (0.07)	1.63 (3.6)	Constant	170.7 (376)*
0.689 (1.0)	1.63 (3.6)	0.579 (0.84)*	134.4 (296)*
6.89 (10.0)	2.27 (5.0)	4.84 (7.03)	114.8 (253)
Case 2 Bubble Point, $\text{N/cm}^2$ (psi)			
6.89 (10)	2.53 (5.57)	6.0 (8.69)	69.5 (153)
Case 3 Bubble Point, $\text{N/cm}^2$ (psi)			
0.365 (0.53)	0.994 (2.19)	0.689 (1.0)*	119.8 (264)*
0.689 (1.0)	1.00 (2.21)	0.689 (1.0)*	112.1 (245)*
2.41 (3.5)	1.12 (2.47)	2.31 (3.36)	27.2 (60)
3.44 (5.0)	No Vent	3.13 (4.54)	No Vent
0.365 (0.53)	0.994 (2.19)	0.689 (1.0)*	119.4 (263)*
Case 4 Bubble Point, $\text{N/cm}^2$ (psi)			
1.72 (2.5)	1.04 (2.29)	1.12 (1.63)*	69.5 (153)*
3.44 (5.0)	No Vent	3.15 (4.58)	No Vent
Case 1: Hydrogen Spherical Tank, Volume = $63.76 \text{ m}^3$ ( $2250 \text{ ft}^3$ ); Gas Annulus = 7.62 cm (3.0 in.); Liquid Annulus = 2.54 cm (1.0 in.); 20% Initial Ullage, including 7.5% in Gas Annulus.			
Case 2: Hydrogen Cylindrical Tank with Hemispherical End Domes, Volume = $28.15 \text{ m}^3$ (995 ft <sup>3</sup> ); Gas Annulus = 7.62 cm (3.0 in.); Liquid Annulus = 2.54 cm (1.0 in.); 30% Initial Ullage, including 10% in Gas Annulus.			
Case 3: Oxygen Spherical Tank, Volume = $14.15 \text{ m}^3$ (500 ft <sup>3</sup> ); Liquid Annulus = 1.27 cm (0.5 in.); Gas Annulus = 3.81 cm (1.5 in.); 20% Initial Ullage, including 7.44% Ullage in Gas Annulus.			
Case 4: Oxygen Spherical Tank, Volume = $14.15 \text{ m}^3$ (500 ft <sup>3</sup> ); Liquid Annulus = 1.27 cm (0.5 in.); Gas Annulus = 1.27 cm (0.5 in.); 20% Initial Ullage, including 2.4% in Gas Annulus.			
*Extrapolated data, based on 3-hr vent period.			

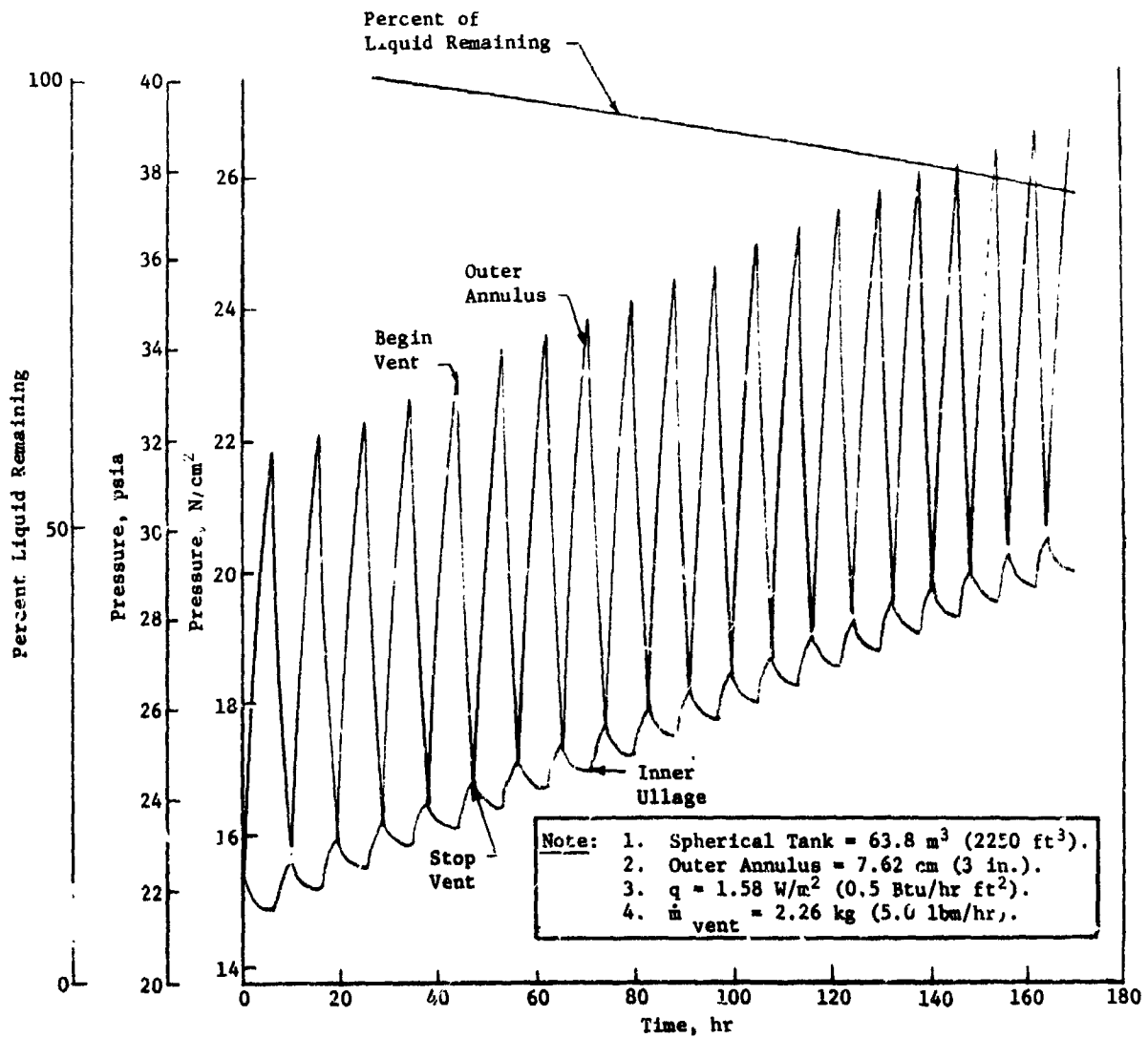


Fig. II-39 Pressure Rise Rate in a Spherical Hydrogen Tank, BP = 6.9 N/cm<sup>2</sup> (10 psi)

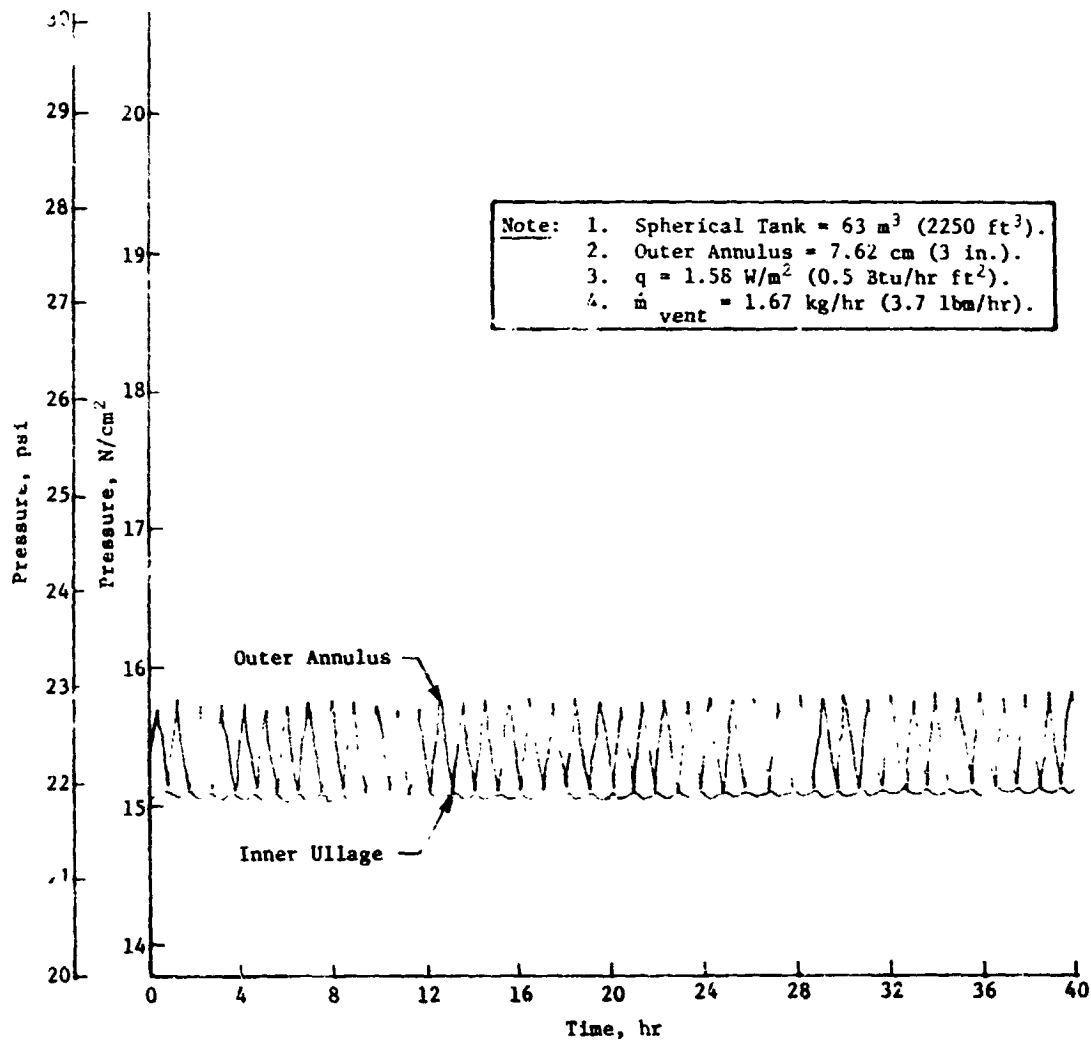


Fig. II-40 Pressure Rise Rate in a Spherical Hydrogen Tank, BP = 0.69 N/cm<sup>2</sup> (1.0 psia)

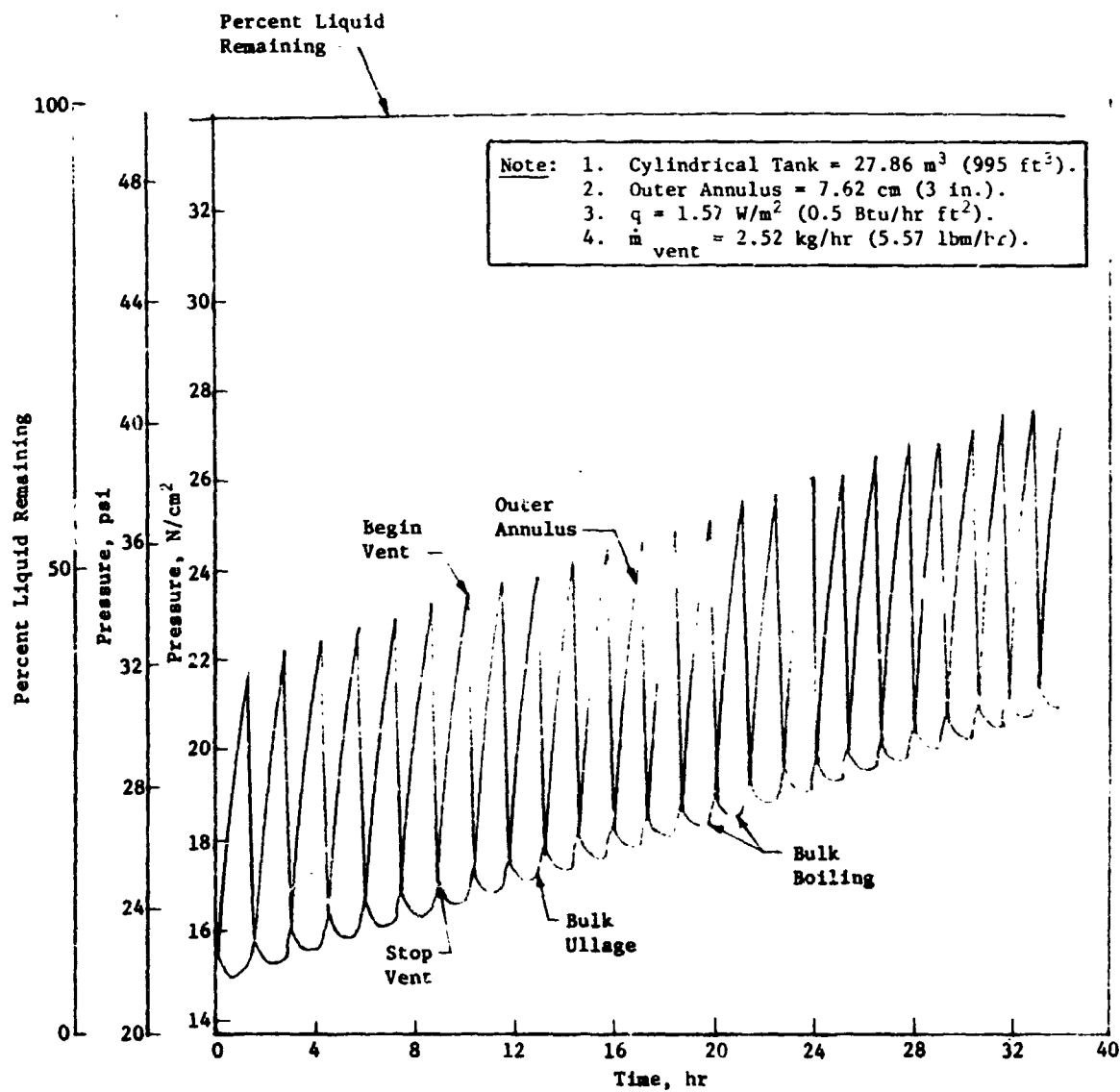


Fig. II-41 Pressure Rise Rate in Cylindrical Hydrogen Tank, BP = 6.9 N/cm<sup>2</sup> (10 psia)

The effect of bubble point variation for a  $14.15 \text{ m}^3$  ( $500 \text{ ft}^3$ ) spherical liquid oxygen tank is shown for gas annulus widths of 1.27 (0.5 in.) and 3.81 cm (1.5 in.). The same effect is seen for the oxygen case, i.e., the pressure rise increased with increasing BP; however, the vapor mass vented decreased. In addition, it is clear that the venting performance is insensitive to the vapor annulus gap size for the two sizes considered. It should also be noted that for bubble points greater than about  $2.62 \text{ N/cm}^2$  (3.8 psi), the tank was not vented because the pressure differential between the bulk ullage and the gas annulus did not exceed this value during the seven-day period. Although the tank was not vented, the tank pressure rise was less than  $3.44 \text{ N/cm}^2$  (5 psi) as shown in Table II-1.

The results of this BP variation study tend to indicate that venting performance is not a primary factor in selecting the liner material because satisfactory performance can be obtained over the range of bubble points considered. The higher BP materials do, however, require a less stringent vent control and, correspondingly, less sophisticated vent control devices. However, considerations such as wetting of the foraminous material and weight tradeoffs become more significant with regard to selecting the foraminous material for the outer liner.

*e. Vapor Bubble Collapse Analysis* - The existence of vapor bubbles in the controlled liquid region of a cryogenic propellant acquisition system prior to pressurization may be a problem, depending on how long it takes for these bubbles to collapse after pressurization. This discussion is restricted to the case when no non-condensable gas (i.e., helium) is present anywhere in the system. In such a case, a vapor bubble can only exist (in more than a transitory way) if the surrounding liquid is at the local boiling point; that is, the local NPSP is zero. Prior to starting a pump, the liquid must be pressurized to provide a positive NPSP, which will cause the bubble to collapse. This section presents some data on the time it takes for this collapse to occur as a function of the initial diameter and the applied NPSP.

Several investigations, both theoretical and experimental, have been made of vapor bubble collapse in a subcooled liquid. (See Ref II-18 through II-21 for a representative sample). The main emphasis here is on those situations where the bubble collapse rate is controlled, primarily, by heat transfer rather than by liquid inertia or surface tension. Liquid inertia is important only for very large  $\Delta P$ , and surface tension only for very small  $\Delta P$  or very small bubbles.

The theoretical analyses are based on calculating the conduction rate of the latent heat of condensation from the bubble surface into the liquid. The problem is complicated by the moving boundary and by the presence of heat convection due to the radial liquid flow, and the solutions obtained are of a numerical type or are based on simplifying approximations. Florschütz and Chao (Ref II-18) give examples of both types. They give two solutions based on different simplifying approximations; the simpler (which also seems to fit the experimental data better) being expressed as

$$\gamma = 1 - \tau_H^{1/2} \quad \text{[II-17]}$$

where  $\gamma$  (nondimensional radius) =  $r/r_0$

$$\tau_H \text{ (nondimensional time)} = \frac{4}{\pi} Ja^2 \frac{\alpha t}{r_0^2}$$

$$Ja \text{ (Jacob number)} = \frac{\rho_l C_{p_l} \Delta T}{\rho_v \lambda}$$

$\alpha$  = thermal diffusivity of liquid

$t$  = time

$r$  = bubble radius

$r_0$  = bubble radius at  $t = 0$

$$\Delta T = T_{\text{sat}} - T_l$$

$\lambda$  = latent heat of evaporation

The numerical solutions, which also include the effects of liquid inertia, are not very useful, because they are difficult to generalize. They do, however, tend to follow the approximate solutions, with the addition of a slight oscillatory behavior.

Prisnyakov (Ref II-19), by adopting a different set of simplifying approximations, arrives at the equation

$$\gamma = 1 - 2 \epsilon \sqrt{\tau_H} \quad \text{[II-18]}$$

where the factor  $\epsilon = 1 + \frac{\rho_v}{\rho_l} (2Ja - 1)$  is very nearly unity for

most cases of interest. This solution, therefore, gives collapse times that are essentially four times greater than those of Eq [II-17].

Experimental data have been obtained by Hewitt and Parker (Ref II-20), using LN<sub>2</sub> at 1 g, and by Florschuetz and Chao, using water and ethanol in a 1.83-m (6-ft) (0.6 sec) zero-g drop facility. Both of these investigations were subject to experimental difficulties and exhibit considerable scatter. The LN<sub>2</sub> bubbles at 1 g were subject to forced convection while rising in the liquid. The water and ethanol bubbles always contained some air, coming from the air dissolved in the liquid, which slowed the bubble collapse rate in the later stages, and thus total collapse of these bubbles was never observed. Also, because of the short zero-g time available in these tests, the initial bubble motion was never completely arrested prior to initiation of bubble collapse.

Prisnyakov compares both Eq [II-17] and [II-18] with the above mentioned LN<sub>2</sub> data and with some other 1-g water data, and shows that Eq [II-18] gives a better fit. This is also the case with the Florschuetz and Chao ethanol data; however, their water data tends toward Eq [II-17]. Hewitt and Parker give an empirical correlation of their LN<sub>2</sub> data as

$$\gamma = 1 - \sqrt{\tau_S} \quad \text{[II-19]}$$

$$\text{where } \tau_S = \tau_H \left(\frac{1}{\gamma}\right)^2 \left(\frac{2.6^\circ\text{R}}{\Delta T}\right)^{1.5}$$

This correlating parameter decreases the data scatter significantly.

Figure II-42 shows the results of applying Eq [II-18] to two different degrees of subcooling, corresponding to 1.37 (2 psi) and 6.89 N/cm<sup>2</sup> (10 psi), to LO<sub>2</sub> and LH<sub>2</sub>. It should be noted that the experimental data are all restricted to small bubbles, on the order of 0.254 cm (0.1 in.) diameter, and extrapolation to much larger sizes is, therefore, very risky. Florschuetz and Chao noticed a tendency for larger bubbles with high ΔP's to exhibit unstable collapses, in which the bubble ultimately shattered into many smaller bubbles.

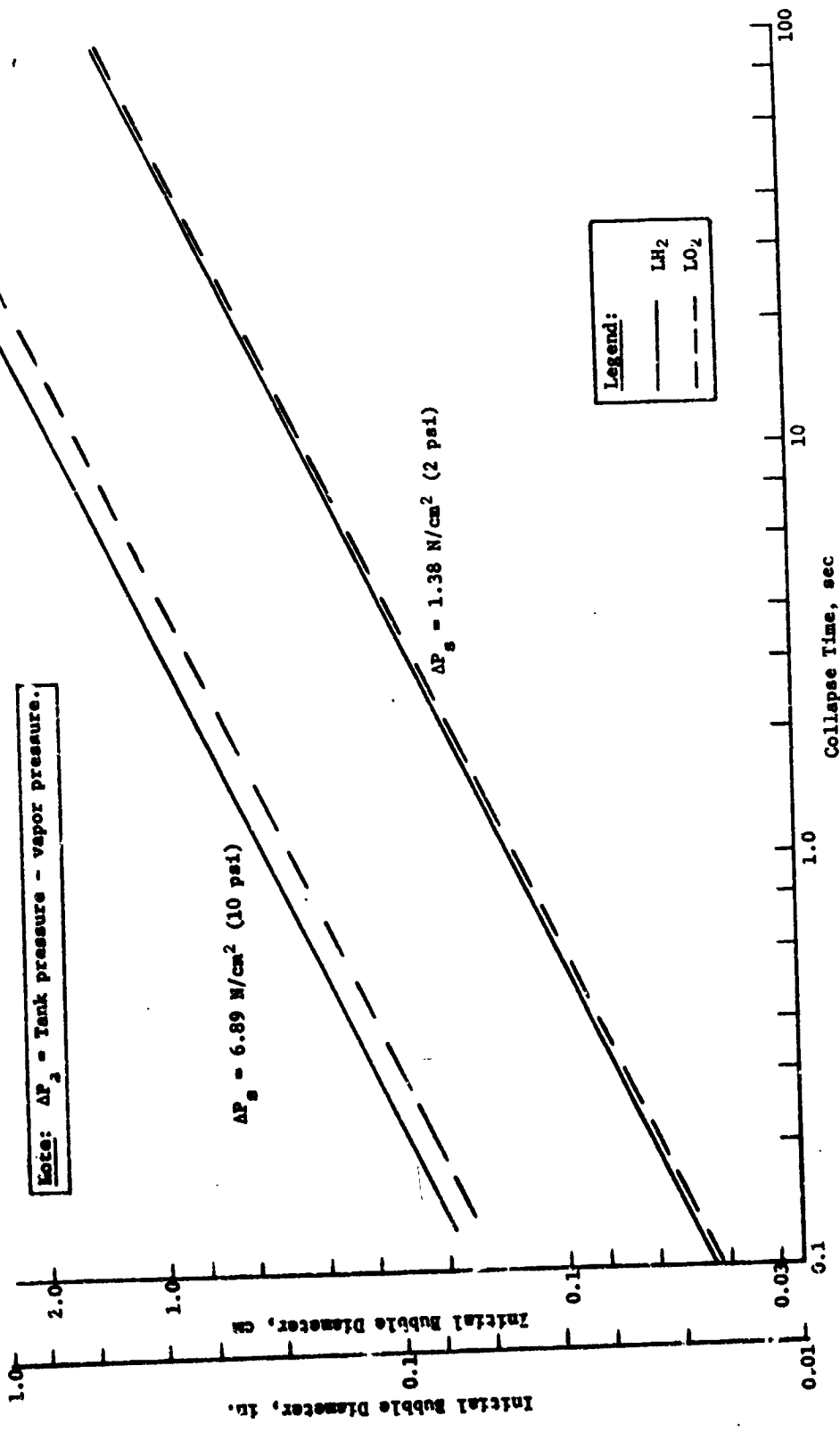


Fig. II-42 Collapse Time for Spherical Vapor Bubble in Subcooled Liquid (Prisnyakov)

These analyses showed a need for additional experimental data, particularly at low-g and with large bubbles. An experimental program was, therefore, conducted to further verify the analytical predictions. The details of these tests are presented in Volume III of this report. The experimental and analytical results showed generally good agreement. It is, therefore, concluded that hydrogen and oxygen vapor bubbles with diameters of 1-in. or less can be collapsed within a reasonable time period by pressurizing the tank.

*f. Weeping Tank Thermal Analysis* - In a cryogenic tank using the weeping tank cooling system where evaporation of the liquid occurs in small localized areas distributed over the tank surface and the heat input to the tank wall is more or less uniformly distributed, temperature gradients will result from heat flow within the tank wall. A simplified analysis was performed to permit estimation of the magnitude of these temperature gradients.

To simplify the analysis, a few approximations are made. The thickness and curvature of the tank wall are neglected, and the cooling spots are assumed to be distributed on equilateral triangles as shown in Fig. II-43. For this geometry, and assuming uniform heat flux, each cooling spot is surrounded by a hexagonal adiabatic boundary as shown. Approximating each hexagonal cell by a circle of equal area, and assuming the circular boundary to be isothermal, the heat flow becomes purely radial. The resulting equation for the steady state is

$$\frac{d^2T}{dr^2} + \frac{1}{r} \frac{dT}{dr} + \frac{q/A}{kt} = 0 \quad \text{[II-20]}$$

where  $q/A$  is the incident heat flux,  $k$  is the thermal conductivity, and  $t$  is the thickness of the wall. The derivation of this equation is illustrated in Fig. II-44. For the adiabatic boundary condition

$$\frac{dT}{dr} = 0 \text{ at } r = a, \quad \text{[II-21]}$$

the solution is

$$T - T_a = \frac{q/A a^2}{2kt} \left\{ \ln \frac{r}{a} + \frac{1}{2} \left[ 1 - \left( \frac{r}{a} \right)^2 \right] \right\} \quad \text{[II-22]}$$

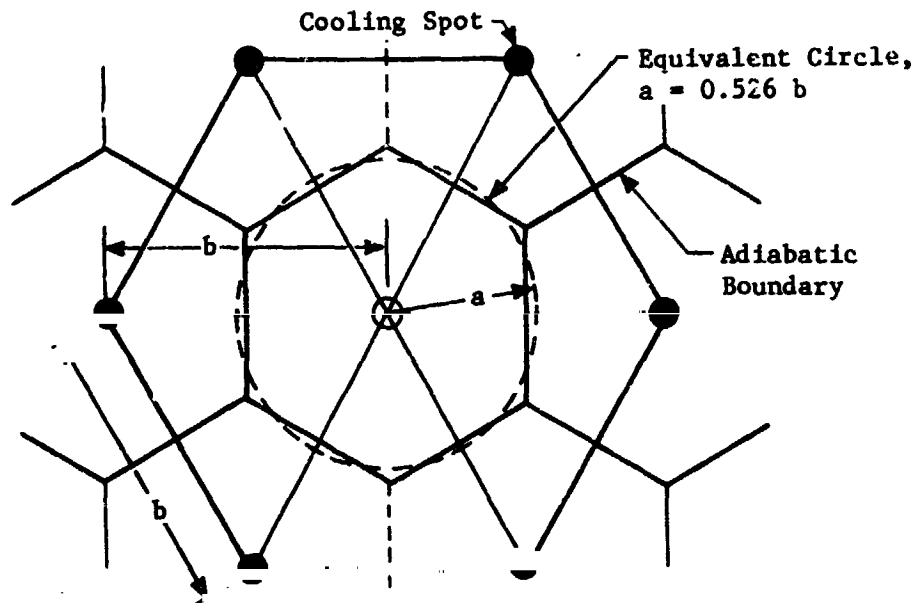
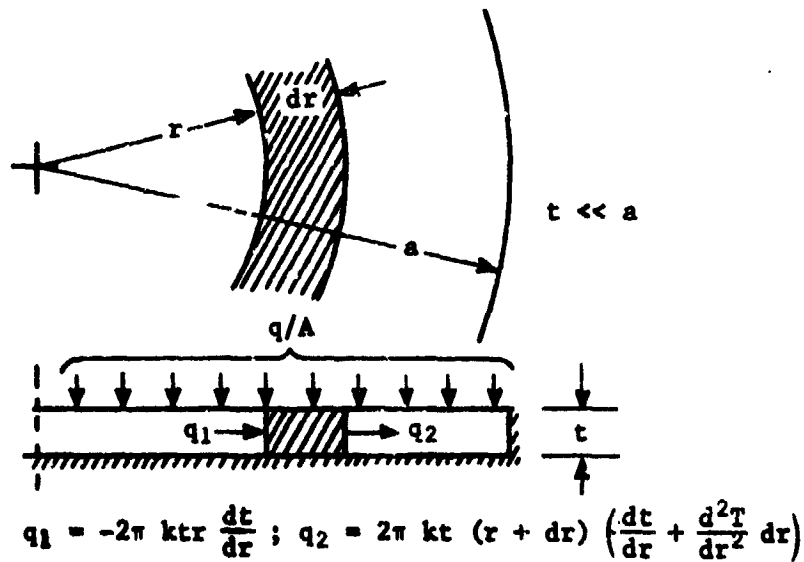


Fig. II-43 Spot Cooling Geometry



$$q_1 = -2\pi ktr \frac{dt}{dr} ; q_2 = 2\pi kt (r + dr) \left( \frac{dt}{dr} + \frac{d^2T}{dr^2} dr \right)$$

$$q_1 + 2\pi r dr (q/A) - q_2 = 0$$

$$\frac{d^2T}{dr^2} + \frac{1}{r} \frac{dT}{dr} + \frac{q/A}{kt} = 0$$

Fig. II-44 Simplified Analysis

$$\text{or } \frac{\theta}{\theta_0} = \ln \rho + \frac{1}{2} (1 - \rho^2)$$

[II-23]

$$\text{where } \theta = T - T_a$$

$$\theta_0 = \frac{q/A a^2}{2kt}$$

$$\rho = \frac{r}{a}$$

This function is plotted in Fig. II-45.

Values of  $\theta_0$  are plotted in Fig. II-46 against "a" for various wall thicknesses at a heat flux of  $1.57 \text{ W/m}^2$  ( $0.5 \text{ Btu/ft}^2\text{-hr}$ ). The tank wall is assumed to be aluminum with thermal conductivities of  $0.173$  and  $0.640 \text{ W/cm} \cdot ^\circ\text{K}$  ( $10$  and  $37 \text{ Btu/ft-hr-}^\circ\text{F}$ ) at  $\text{LH}_2$  and  $\text{LO}_2$  temperatures, respectively.

In the above analysis, the heat conduction in the liquid adjacent to the tank wall is neglected. An order of magnitude estimate of the resulting error can be obtained from the ratio of the wall thermal conductivity to that of the liquid. For  $\text{LH}_2$ , this ratio is 150 and for  $\text{LO}_2$  it is 465. The thickness of a liquid layer of the same thermal resistance as a  $0.101 \text{ cm}$  ( $0.040 \text{ in.}$ ) thick tank wall is, therefore,  $15.24 \text{ cm}$  ( $6 \text{ in.}$ ) for  $\text{LH}_2$  and  $47 \text{ cm}$  ( $18.5 \text{ in.}$ ) for  $\text{LO}_2$ . The effect of liquid conduction would be appreciable for cooling spot spacings that are large compared with these dimensions.

As an example of the use of these data, consider an aluminum  $\text{LO}_2$  tank of  $0.101 \text{ cm}$  ( $0.04 \text{ in.}$ ) wall thickness and a cooling spot spacing of  $30.48 \text{ cm}$  ( $1 \text{ ft}$ ). The radius,  $a$ , of the equivalent circle is then  $16.03 \text{ cm}$  ( $0.526 \text{ ft}$ ) and, for a heat flux of  $1.57 \text{ W/m}^2$  ( $0.5 \text{ Btu ft}^2\text{-hr}$ ), Fig II-46 gives a  $\theta_0$  of  $255.67 \text{ }^\circ\text{K}$

( $0.56^\circ\text{F}$ ). Arbitrarily assigning a maximum temperature difference of  $254.25 \text{ }^\circ\text{K}$  ( $-2^\circ\text{F}$ ), gives  $\theta/\theta_0 = -3.58$  and Fig. II-45 shows that

the minimum  $r/a$  is approximately  $0.017$ , so that  $r_{\text{min}} = 0.274 \text{ cm}$

( $0.009 \text{ ft}$ ) or  $2.74 \text{ mm}$  ( $0.11 \text{ in.}$ ). This means that each cooling spot must be  $5.48 \text{ mm}$  ( $0.22 \text{ in.}$ ) diameter. If porous plugs are used to control the bleed rate in such a way that evaporation is completed within the plug, then the plug diameter must equal this value.

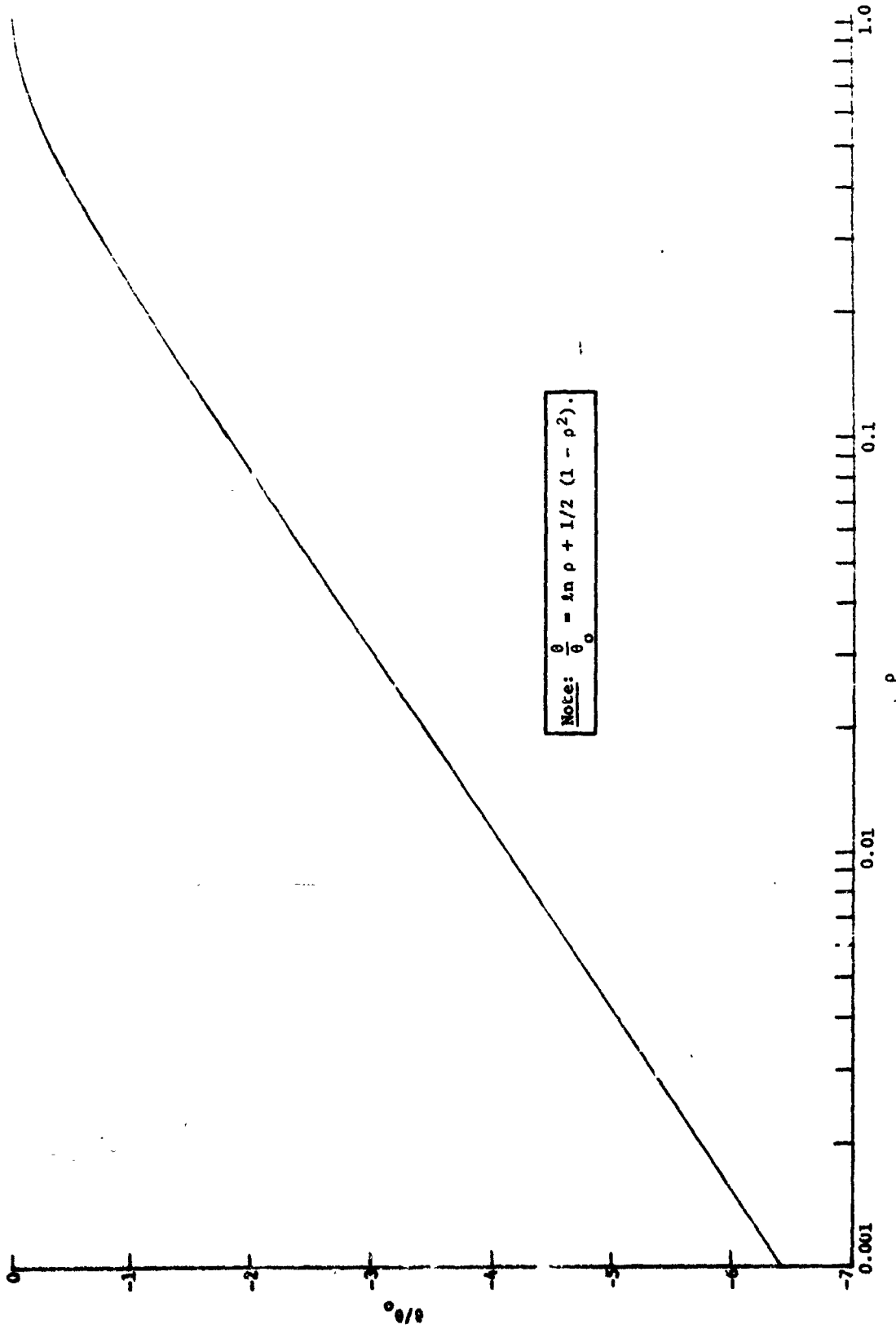


Fig. II-45 Predicted Thermal Performance of Heeping Tank

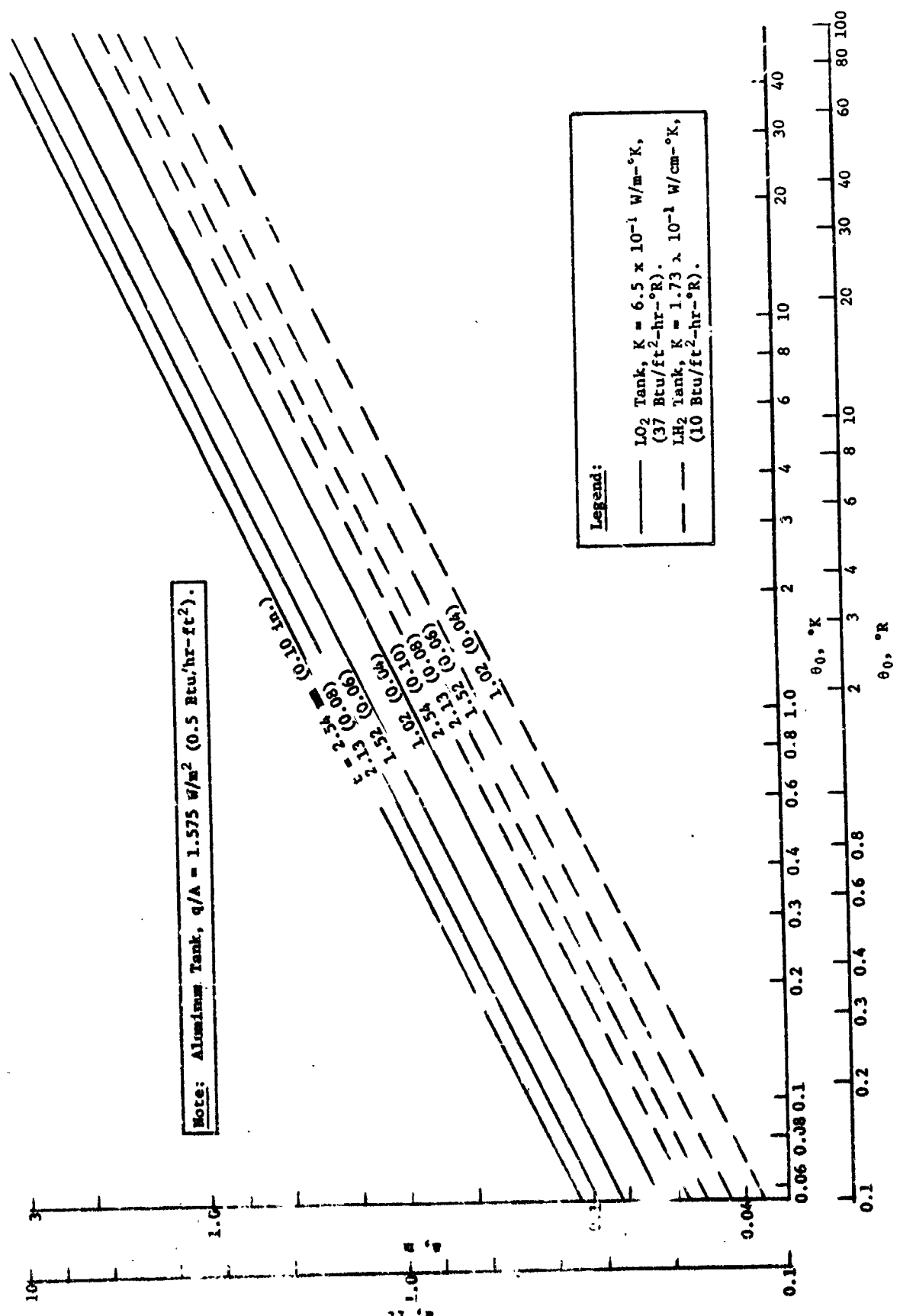


Fig. II-46 Effect of Wall Thickness on Keeping Tank Thermal Performance

The tank wall area associated with each spot is  $\pi a^2 = 8.08 \times 10^{-2} \text{ m}^2$  (0.87 ft<sup>2</sup>), so the cooling load is 458.6 W (0.435 Btu/hr). This gives a bleed rate of  $2.15 \times 10^{-3} \text{ kg/hr}$  ( $4.75 \times 10^{-3} \text{ lbm/hr}$ ) for each plug. The necessary length and porosity of the plug can then be determined for any desired pressure drop.

### 3. Structural Considerations

One of the attractive features of capillary propellant management systems is their potential for extremely lightweight construction. To take maximum advantage of this potential, a number of analytical and experimental investigations were undertaken to determine the structural characteristics of screens and proposed structural support techniques and to perfect techniques for system fabrication. The information evolving from these studies was successfully applied to several hardware articles during the course of the study.

With the exception of the weeping tank concept, all of the proposed candidate systems are designed so that a pressure gradient exists that causes a collapsing force to be exerted on the capillary device. This external buckling pressure is determined by the bubble point capability of the capillary media employed. This pressure would normally be that sustainable by the communication screen, which is designed to break down before any other part of the system. The first structural consideration must, therefore, be that the system maintain structural integrity under these types of loads.

The pressure bearing surfaces of the capillary systems are also subject to the intermittent pressure cycling due to pressurization and venting operations. These cyclic pressure excursions affect cyclic screen deflections having the potential for causing screen fatigue failure. The presence of a possible intermittent vibration environment associated with propulsion system firings suggests an additional potential cause of structural fatigue. These considerations must also be evaluated in the design of capillary systems.

The requirement that the acquisition/expulsion systems be flight hardware implies that the system weight be the minimum consistent with accepted design practices and mission requirements. Potentials for system weight reductions exist when fine mesh screen can be employed without the necessity of additional structural support over the entire screen surface. But to effect this type of design, reliable predictions of screen stress/strain characteristics are required.

Information necessary in evaluating these technical areas was produced under several study efforts including--(1) computer analyses and specimen tests of polyspherical support structures; (2) unsupported screen structural characteristics tests and analyses; (3) cyclic pressure-induced screen structural fatigue tests; and (4) fabrication and cleaning techniques of capillary structures.

a. *Polysphere Support Structure* - In the past, capillary devices have been fabricated by one of two methods--(1) by pleating the screen to provide additional strength, or (2) by attaching the screen to a structural member, generally perforated plate. For the screen device to conform to the contours of a tank interior, especially a dome area, the screen must be formed into a compound curvature. This has been accomplished on a small scale with pleating as shown in Fig. II-47. Forming singly-curved surfaces presents fewer fabrication problems and this technique seems more feasible for very large tanks--typically, those tanks envisioned for Space Shuttle and Space Tug. A convenient method for approximating the compound curved surfaces of tank domes with singly curved surfaces is to use gore sections of screen and perforated plate formed into a polysphere.

The DSL and its variations present at least two problems for which polysphere configurations may offer solutions. The first of these is the necessity of providing capillary liners that are lightweight and can withstand an external application of pressure approximately equal to their bubble point. Secondly, this barrier must be made, as nearly as practical, to conform to the geometry of the enclosing tank. Generally, propellant tanks will be of spherical or hemisphere/cylinder configuration because of their favorable volume to weight ratios. Therefore, capillary barriers must also have hemispherical shapes.

Forming hemispherical shapes from flat stock is not an unusual or new technology and can be done by drawing or spinning. However, the additional requirement to form these shapes of porous material such as perforated plate makes these routine forming operations very difficult. Spincraft, a vendor of spun domes, indicated that any attempt to form domes of perforated plate stock would result in the development of cracks between the holes. Moreover, aside from pleating, no techniques have been successfully developed for forming compound curvatures from fine mesh screen.



*Fig. II-47 Pleated Screen Sphere*

It is physically possible to form a compound curvature of fine mesh screen; however, the bubble point is generally degraded so that the screens are no longer capable of maintaining adequate hydrostatic heads.

A computer analysis and a test program were conducted on the octosphere (see Fig. II-48.), an eight-sided member of the polysphere family. The computer analysis was executed for octospheres of typical tank sizes to determine the applicability of this technique to lightweight systems.

The octosphere is a member of a class of shell-type structure called polygonal domes. A polygonal dome consists of a number of cylindrical sectors joined in such a manner that horizontal sections lie along the generators of the cylindrical sectors and form a regular polygon. They are transversely loaded and, due to the abrupt curvature change at the sector intersections, are generally supported at these intersections by ribs and along their base by a foot ring. If the top of the dome is open, another ring is usually provided at the top. The ribs essentially carry only axial forces and the rings are required for shear and bending. If the tangent to the sectors is perpendicular to the base, there are no bending moments in the plane of the ring, only transverse to the plane.

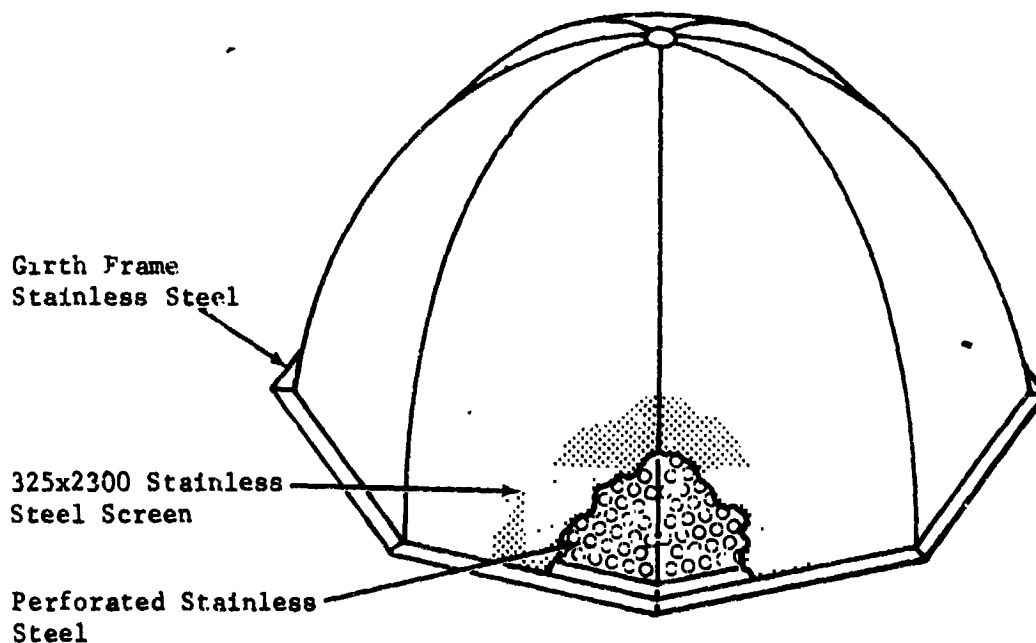


Fig. II-48 Octosphere Capillary Screen Structure

The state of stress is essentially that for a membrane. The stresses in the structure are determinable from statics alone, as long as the loading is symmetric. Examples of symmetric loadings are vertical inertia loads including weight and external pressure loading. Once the stresses are known, the deformation can be obtained by numerical integration. For nonsymmetrical loadings, approximations are required but the analysis is similar.

Parametric analyses were conducted to evaluate the effect of symmetrical loads, due primarily to different pressure differences across the capillary material, and critical design parameters such as material thickness, percent open area, size, and number of supporting ribs. Trade studies yielding structural weight as a function of critical buckling pressure loading (the bubble point of the screen) are presented in Fig. II-49 through II-51.

The test program involved fabricating a small octosphere, subjecting it to a buckling load, and measuring the deflection at various points on the octosphere surface over a range of pressure loads. Two octosphere shells were fabricated, one of 0.635 mm (0.025 in.) thick stainless steel perforated plate and one of 0.396 mm (0.0156 in.) thick stainless steel perforated plate. The tests were conducted to determine the structural adequacy of the configuration and to evaluate the fabrication techniques for both the shell structure and the screen cover. The shells were sealed with a plastic material so that a vacuum could be drawn on the inside. The results of the tests showed that both the deflection measurements and the ultimate failure load agreed well with the predictions of the analytical computer model. The tests verified the adequacy of the technique and, as a result, a dodecasphere (12 sides) was selected as the configuration for the 1.77m (70 in.) diameter channel/liner fabrication program. Details of both test programs are presented in Volume III of this report.

Despite the positive results of this effort it should be noted that the results presented in the screen structural characteristics section indicate that a construction method using unsupported screen is also feasible. The equal applicability of the two fabrication concepts emphasizes the advisability of conducting comparative studies of the two techniques for each design, for which both can be considered. Since weight minimization is a crucial factor for flight designs, these weight comparisons would be required to help select the lowest weight fabrication technique for each application.

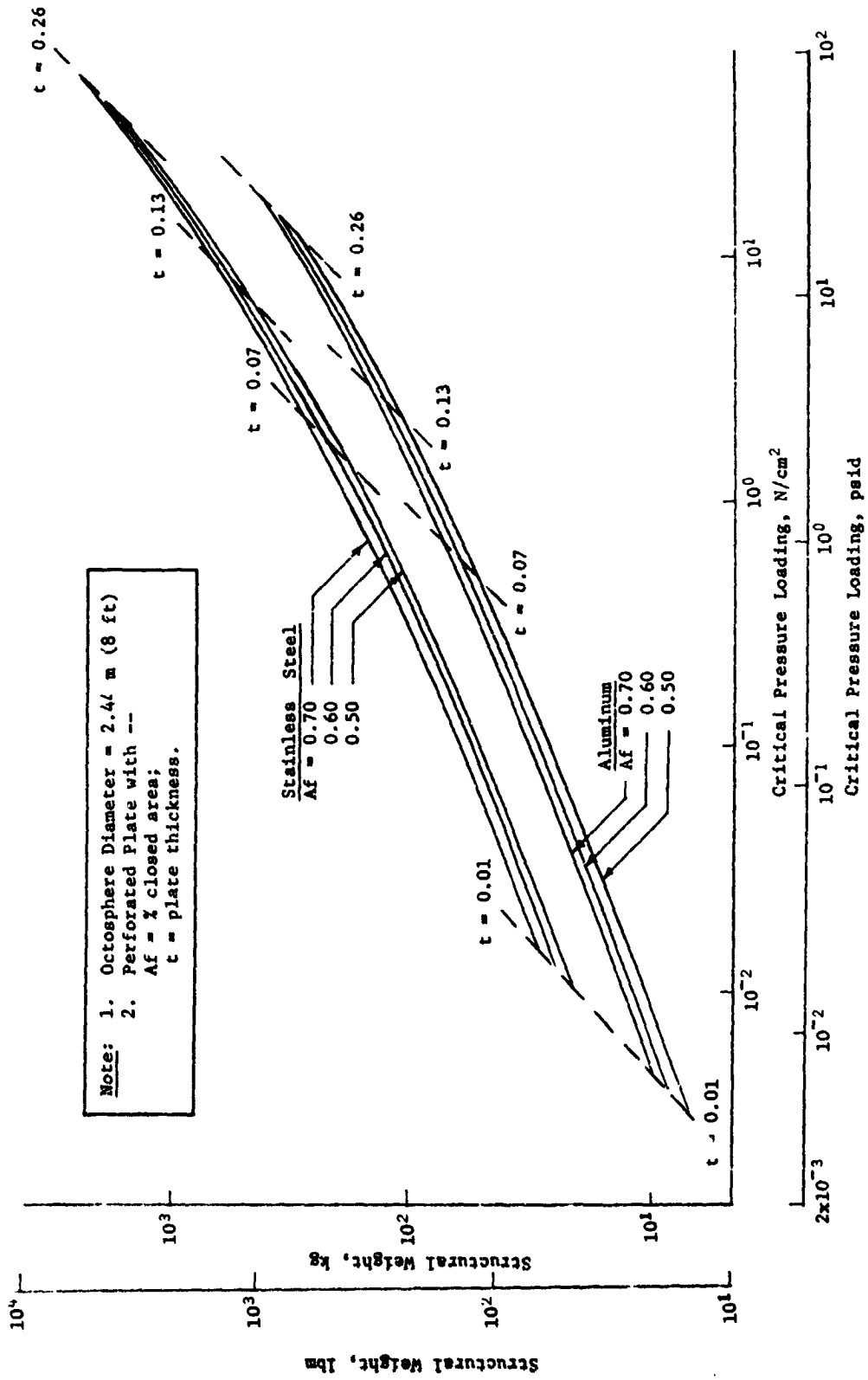


Fig. II-49 Structural Weight Estimate for 2.44 m (8 ft) Diameter Octosphere

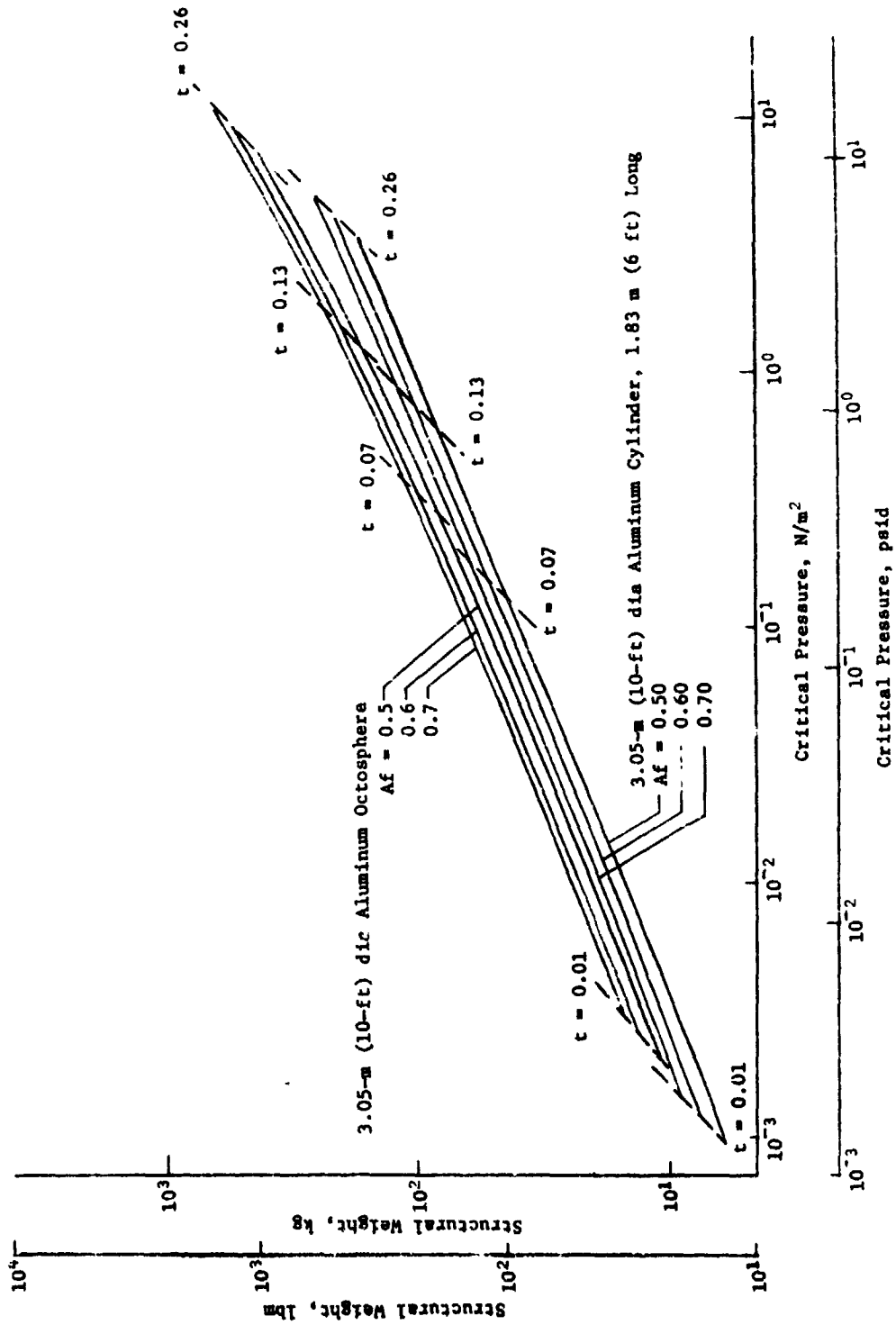


Fig. II-50 Structural Weight Estimate for 3.05-m (10-ft) Diameter Octosphere

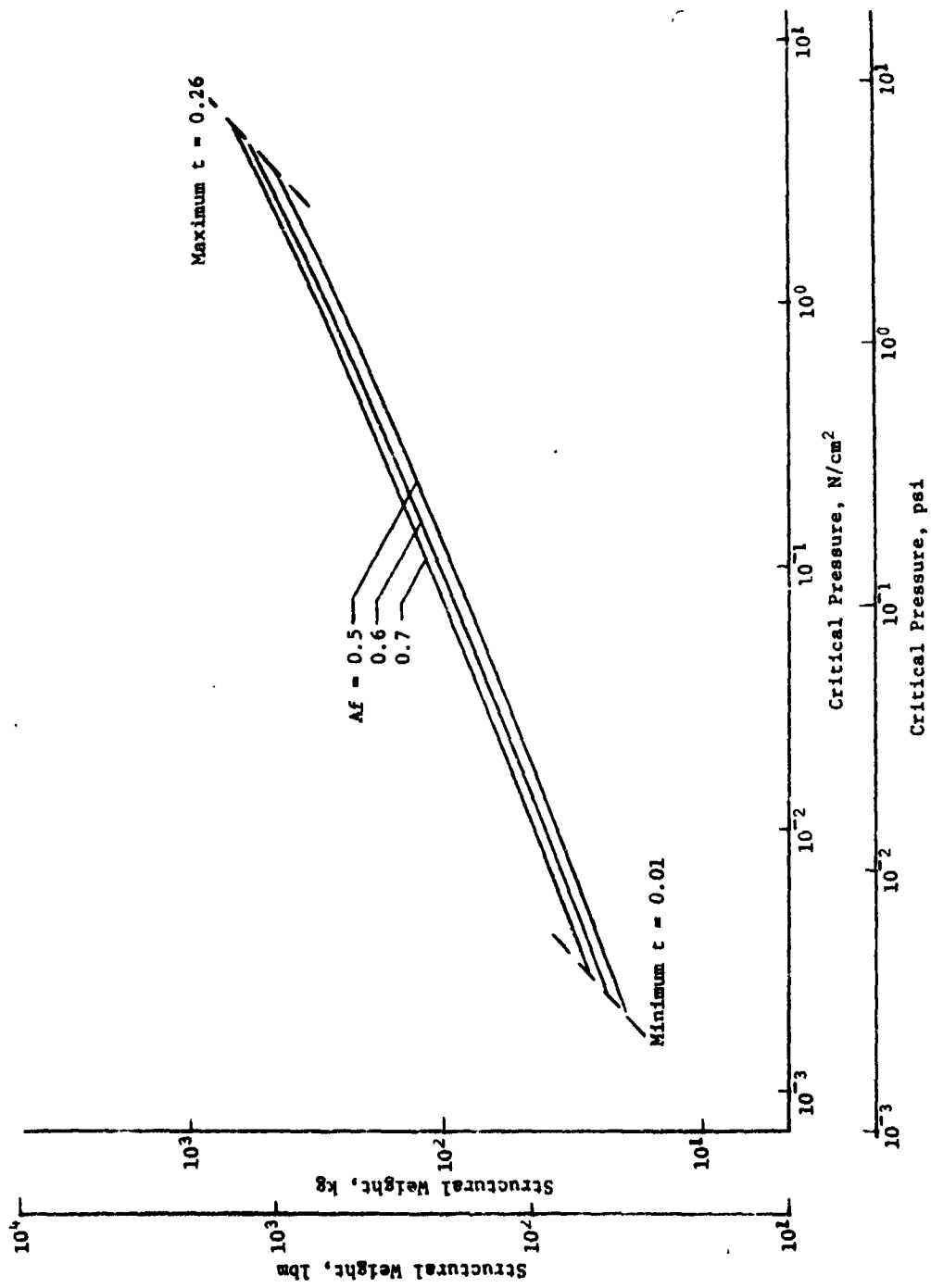


Fig. II-51 Structural Weight Estimate for a 3.05-m (10-ft) Diameter, 4.88-m (16-ft) Long Cylindrical Tank with Octospherical End Domes

b. *Unsupported Screen Characteristics* - The use of screen unsupported by perforated plate offers the opportunity for lightweight capillary device construction. Since lightweight construction and weight savings are a prime concern in the design of flight articles, a coordinated analysis and testing program was performed to establish design criteria and predict performance characteristics of unsupported screen.

Empirical results were incorporated into the analytical treatment of screen structural characteristics. The test results and a discussion of the test program appear in Volume III. Analyses were performed for both circular and rectangular screen sections. Using the Rayleigh-Ritz calculus of variations method, equations for maximum deflections and maximum stress were derived. Maximum screen deflection obeys the following dependencies on pressure load and screen segment size and shape for circular segments:

$$W_o = 0.815 \left( \frac{\Delta P R^4}{K} \right)^{1/3} \quad \text{[II-24]}$$

where  $W_o$  = maximum screen deflections, cm (in.)

$\Delta P$  = pressure differential, N/cm<sup>2</sup> (lbf/in.<sup>2</sup>)

$R$  = circular radius, cm (in.)

$K$  = screen constant, N/cm<sup>2</sup> (lbf/in.)

For rectangular screen segments, deflection is determined by

$$W_o = 0.452 \left( \frac{\Delta P b^4}{K (\alpha^4 + 1)} \right)^{1/3} \quad \text{[II-25]}$$

where  $b$  = long side of rectangle, cm (in.),

$\alpha$  = ratio of long to short side of rectangle,  $\alpha = b/a$ .

K factors for the screens tested are

- 1) 325x2300 stainless steel, 18,738 N/cm (10,700 lbf/in.);
- 2) 250x1370 stainless steel, 23,082 N/cm (13,180 lbf/in.);
- 3) 200x1400 stainless steel, 45,533 N/cm (26,000 lbf/in.);
- 4) 200x1400 aluminum, 13,958 N/cm (7,970 lbf/in.).

The deflection dependencies are only valid up to a transition point, which is defined as the point where maximum stress in the screen segment exceeds an experimentally determined critical stress. For a circular screen segment

$$N_{\max} = \xi \sigma t = 0.281 (K \Delta P^2 R^2)^{1/3}$$

where  $N_{\max}$  = maximum stress, N/cm<sup>2</sup> (lbf/in.<sup>2</sup>),

$\xi$  = cross-sectional area ratio term,

$\sigma$  = critical stress for individual screens, N/cm<sup>2</sup> (lbf/in.<sup>2</sup>),

$t$  = screen thickness, cm (in.).

For a rectangular section of screen

$$N_{\max} = \xi \sigma t = 0.582 \left[ \frac{K \Delta P^2 b^2}{(\alpha^4 + 1)^2} \right]^{1/3}$$

[II-27]

The values of  $\xi$  and  $\sigma$  are

	$\xi$	$\sigma$
325x2300 stainless steel	0.351	16,548 N/cm <sup>2</sup> (24,000 psi)
250x1370 stainless steel	0.362	18,134 N/cm <sup>2</sup> (26,300 psi)
200x1400 stainless steel	0.352	7,171 N/cm <sup>2</sup> (10,400 psi)
200x1400 aluminum	0.354	3,378 N/cm <sup>2</sup> (4,900 psi)

Plots of screen size as a function of critical stress pressure are shown in Fig. II-52. These curves are used by assuming the critical pressure is the bubble point of the screen and determining the maximum screen size from the curve at that pressure value.

Figure II-52 can be used to find either the maximum screen segment size that can safely support a specific pressure, or inversely, the maximum pressure that a specific screen segment can support without failure. For the first case, assume, for example, a pressure differential of 2.06 N/cm<sup>2</sup> (psi). Read the proper shape curve for the corresponding universal radius or short span. For a rectangular screen with an aspect ratio of  $\alpha = 0.7$  the corresponding value of  $b_u$  would be 1.04 cm (0.41 in.). From the

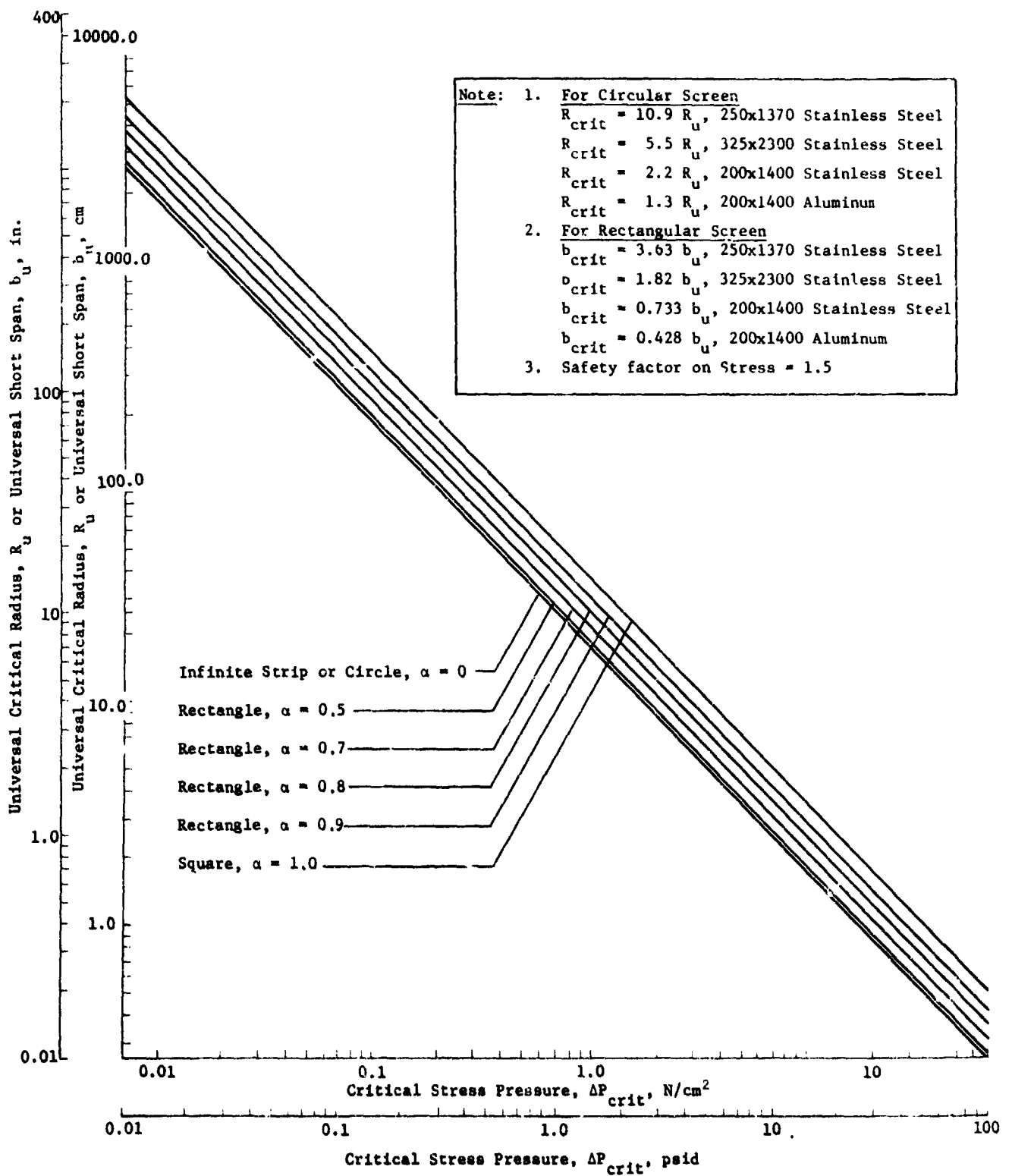


Fig. II-52 Screen Radius or Short Span at Critical Stress

criteria for rectangular screens included on the figure,  $b_u$  of 1.04 cm (0.41 in.) would mean a screen dimension of 3.78x5.41 cm (1.49x2.13 in.) is the largest 250x1370 screen that could support 2.06 N/cm<sup>2</sup> (3 psid) without exceeding the critical stress.

Inversely, to find the maximum pressure a 25.4-cm (10-in.) diameter screen circle could safely support, first determine the corresponding universal critical radius. From the formula listed for 325x2300 stainless steel screen, this would be 2.31 cm (0.91 in.). Using the curve for  $\alpha = 0$ , the corresponding maximum  $\Delta P$  for  $R_u = 2.31$  cm (0.91 in.) would be approximately 0.744 N/cm<sup>2</sup> (1.08 psid).

Basically, the results of this analysis show that fine mesh screens offer considerable structural strength when uniformly loaded as flat screen segments. However, screen offers essentially no strength when loaded in a buckling mode. The upper design limit can be determined and is a predictable function of pressure differential raised to the one-third power

$$[W_o = K \Delta P^{1/3}].$$

*c. Cyclic Pressure-Induced Screen Structural Fatigue* - The repeated pressurization and venting cycles experienced by the screen device in an operational system subject the unsupported screens to a cyclical pressure loading. Structured materials which undergo repeated or cyclic loads are subject to fatigue failures. Therefore, a test was conducted to investigate the structural characteristics of screens undergoing repeated pressure loading. The pressure difference across the screen during the cycling events was maintained at a level below the pressure that corresponded to the transition point.

A screen sample loaded over 100,000 times at intervals of from 14 to 20 seconds showed no degradation of bubble point when it was checked at the conclusion of the test. Moreover, the maximum deflection of the pressurized screen did not change during the test and no permanent strain was observable. From the results of these tests, we concluded that screen structural fatigue is not a serious design problem and that attention to other failure modes in design criteria will ensure the adequacy of screen to resist fatigue.

d. *Fabrication and Cleaning Techniques*

1) *Fabrication Techniques* - Fabrication and cleaning techniques are presented briefly to complete the discussion of structural considerations for screen devices. This section represents only a summary of the details and results presented in Volume III of this report.

Fabrication and assembly techniques for successful manufacture of capillary screen devices (especially large devices) were investigated and verified during this study. The investigations included basic forming and joining techniques, assembly methods, and quality assurance and control procedures. These methods were tested and refined during the fabrication of two complete cryogenic acquisition/expulsion systems. A 63.5-cm (25-in.) channel and liner test article was designed and fabricated under this contract for liquid hydrogen service and a 177.8-cm (70-in.) screen liner and channel model was designed and fabricated under an IR&D program.

Under both contractual and IR&D programs, Martin Marietta has pioneered the technology of screen system fabrication. In assembling a screen system, two joining methods are possible--screen joined to screen or screen joined to some structural member, such as perforated plate. Satisfactory methods have been developed by Martin Marietta to effect these kinds of joints by either welding or brazing. During the course of this study, two additional methods of joining and repairing screens were investigated under an IR&D program (see Vol III, Chap. IV).

The first of these methods was a spray metal overlay technique. With this process, high velocity molten metal particles are sprayed by a special gun over the faying surfaces of two sheets of metal. Three types of metal overlays were tested--copper, monel, and aluminum. They were used to join stainless steel screen to stainless steel structure, stainless steel screen to aluminum structure, aluminum screen to stainless steel structure, and aluminum screen to aluminum structure. Acceptable bonds were achieved with all of these combinations. The fabrication samples showed no degradation of the screen bubble point.

Unsupported screen samples, which were attached to test structures by spray-metal applications, were tested by pressurizing to rupture. Generally, the failure occurred in the spray-metal bond rather than in the screen itself. However, these failures occurred at

relatively high pressures, 20.6 to 34.4 N/cm<sup>2</sup> (30 to 50 psid), which are far beyond any pressure currently envisioned in even the most severe operating ranges of screen devices. Spray-metal application was selected as one of the methods used for fabricating the 25.4-cm (10-in.) screen device.

Silver solder was also tested as a joining candidate. Stainless steel screen was joined to a stainless steel structure using zinc silver solder. A high quality bond was achieved which did not degrade the screen capillary retention capability and which functioned well in cryogenics. Although this joining technique also shows promise in screen system fabrication, there is a potential disadvantage associated with its incompatibility with liquid oxygen. This technique was the basic method for attaching the screens to the supporting structure of the 63.5-cm (25-in.) diameter liquid hydrogen test model.

The majority of screen attachments performed in fabrication of the 177.8-cm (70-in.) diameter screen liner were welds. Resistance welding has been particularly successful in joining one fine mesh screen to another and to supporting structures. During fabrication of 177.8-cm (70-in.) liner, an automated process was developed for attaching large screen segments to the support structure using a resistance seam welder controlled by a photoelectric pattern follower.

It should be emphasized here that welding is considered the superior method for joining screens. Other successful methods are considered only as alternate joining methods or as techniques for repairing screens.

Techniques and facilities were developed for testing the bubble point of the large screen surfaces after they were welded to the perforated plate structural member. There are 24 of these gore sections in the 177.8-cm (70-in.) liner. Testing must be done after each manufacturing process to assure that the process has not degraded the screen bubble point. In addition, the weld or other joint must be leaktight. Special fixtures and procedures were tested and verified to satisfy this objective. Procedures were also developed and tested to assure the integrity of the completed assembly. Tests verified that an entire assembled hemisphere could be bubble point tested by flowing an alcohol film across the screen.

Special fixtures and procedures were implemented for the process of joining the individual gore sections into a hemisphere. Lip welding proved to be the best method and was used to make all closure welds on the device. The closure process, as well as the screen welding process, was automated.

2) *Penetration Design* - The design of any capillary propellant management system requires penetration of the capillary barrier one or more times to provide for the feedline, pressurization and vent lines, pressure taps, and instrumentation wiring. There are advantages to being able to penetrate the screen barrier at will without any requirement of predetermined location. Such penetrations generally must exclude welding or brazing because they are difficult to implement after assembly of the screen/perforated plate laminate. Welded penetration methods were used successfully when they had been included in the screen system design prior to fabrication. The added ability to effect screen penetrations without elaborate preplanning can greatly enhance the flexibility of capillary systems. An additional feature of these types of mechanical penetrations is their ability to accommodate dissimilar materials, such as an aluminum tank wall penetrated by a stainless steel feedline.

A test program was implemented to evaluate mechanical penetration designs. Three basic types of penetrations were evaluated: (1) a pressed-type design (shown in Fig. II-53) where the parts were forced together with a hydraulic press; (2) a screw-type (shown in Fig. II-54) which is torqued together; and (3) a riveted type (also shown in Fig. II-54). Each of these devices featured a copper compression gasket, which was seated into the stainless steel screen to effect a proper seal. Aluminum gaskets were used with aluminum screens.

Tests were conducted after fabrication of the penetration to determine if the bubble point of the screen had been degraded by the fabrication process or if the penetration assembly itself leaked gas before the surrounding screen broke down. The samples were also immersed in liquid nitrogen and then rechecked by bubble point test to evaluate any leaks that might have developed.

The results of the testing, discussed in detail in Volume III, showed no significant change in the screen bubble point when compared with the "as received" screen after fabrication and after each cryogenic exposure. All three types of mechanical penetrations appear to be candidates for application with penetrating tubes in the 0.635 to 7.62 cm (1/4 in. to 3-in.) range that was tested.

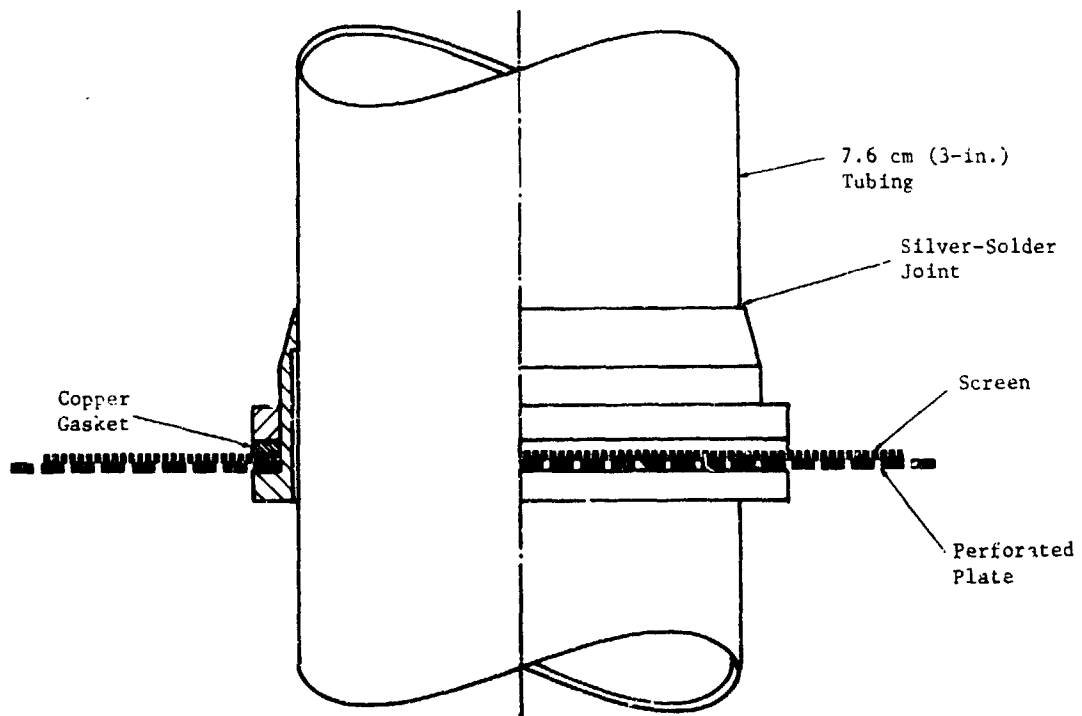
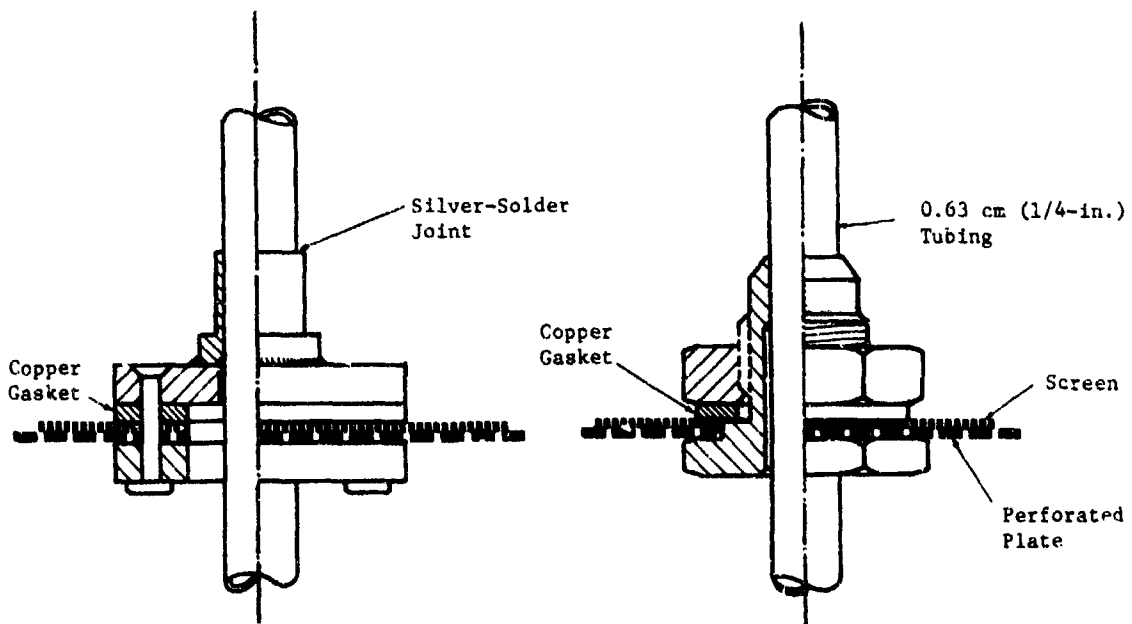


Fig. II-53 Pressed-Type Penetration Design



Riveted Type

Screwed Type

Fig. II-54 Riveted and Screw Type Penetration Designs

3) *Cleaning Techniques* - Martin Marietta has gained considerable experience in cleaning and handling fine mesh screen systems for propellant management applications. Experience has shown that the cleaning and handling requirements are strongly influenced by the nature of the test liquid or propellant, the construction, materials, and the complexity of the system hardware. The inclusion of fine mesh screen in the system does not significantly complicate cleaning or handling techniques. Also, cleaning methods do affect screen performance. Vapor degreasing, ultrasonic cleaning, normal chemical procedures, high temperature vacuum annealing, and chemical cleaning followed by vacuum annealing have all been used successfully. The last three techniques listed have been used successfully to clean fine mesh screen for service in liquid fluorine. Based on previous work (Ref II-22), no problems in cleaning the screen systems are anticipated.

#### 4. Configuration and Size

The final technical areas affecting system designs concern the basic question of the gross physical characteristics of cryogenic propellant acquisition/expulsion systems. The size of a propellant system has significant effect on the particular design details and the functional characteristics of the capillary system included for propellant management. Therefore, the topics of configuration and size are closely interrelated.

a. *One Tank vs Two Tanks* - The impact of various environmental parameters on the choice of tank size was investigated. The basic environmental constraint or Shuttle mission parameter that affects tank size is the acceleration spectrum in which the tank containing a screen device must function. For the cryogenic Shuttle studies, the hydrogen system could include tankage comprising a single 4.72-m (15.5-ft) diameter spherical LH<sub>2</sub> tank or two 3.81-m (12.5-ft) diameter spherical LH<sub>2</sub> tanks. It is obvious from the hydrostatic considerations discussed earlier that two screen devices fabricated of the same mesh screen would have different hydrostatic head capabilities in the two different tank sizes. The ratio of the maximum acceleration level, in which each could operate, would compare as the inverse of the ratios of the tank diameters. Therefore, the smaller tanks could operate in a higher acceleration environment. This fact alone would tend to make a two-tank system a more desirable design.

To further substantiate this argument, computer analyses were performed on both the one-tank and two-tank configurations to determine the effect of tank size on outflow capability. The

results (Fig. II-55 and II-56) show that although the larger tank does exhibit slightly more propellant delivery capability at zero-g, it is not twice the capability of the smaller tank; and the smaller tank only contains half the volume of the larger. Moreover, as the acceleration level increases, the outflow capability for each of the two smaller tanks quickly overtakes that of the larger tank, and as expected, continues after the larger tank capillary device has broken down. These results heavily favor the two-tank system. Therefore, the two-tank concept was assumed in all further considerations of the study.

b. *Parallel vs Series Tankage* - Assuming that the long-term cryogenic storage system for the Shuttle Orbiter consisted of two separate tanks per propellant, additional configuration definition studies were required. Propellant can be emptied from two or more tanks either by simultaneously draining all tanks at once into a common manifold of a parallel feed system, or by cascading all tanks through a single outlet in a series feed system. The differences between these parallel and series feed systems that could significantly affect the propellant acquisition system were evaluated.

The comparison criteria used were--relative complexity, performance or weight, and technology cost or risk. Complexity is related to reliability and was evaluated qualitatively by the number of components required and the relative simplicity of operation. Maximum performance was assumed to be indicated by minimum weight. Technology cost or risk was evaluated qualitatively for each new or unproven concept.

Three systems were considered in the study: (1) parallel feed systems; (2) series-start tank systems; and (3) series-common systems. These systems were all analyzed with fail operational/fail safe criteria, which imply triple redundancy.

The parallel system concept considered was a sequenced drain of two separate tank systems as shown in Fig. II-57. A schematic of the series/start tank concept is shown in Fig. II-58. The start tank concept implies that Tank 2 is always available for supplying the subsystems, with refill possible at convenient times from Tank 1. The series-common concept, shown in Fig. II-59, utilizes the unique features of the multiple screen liner concept by coupling both tanks functionally into a simple common system.

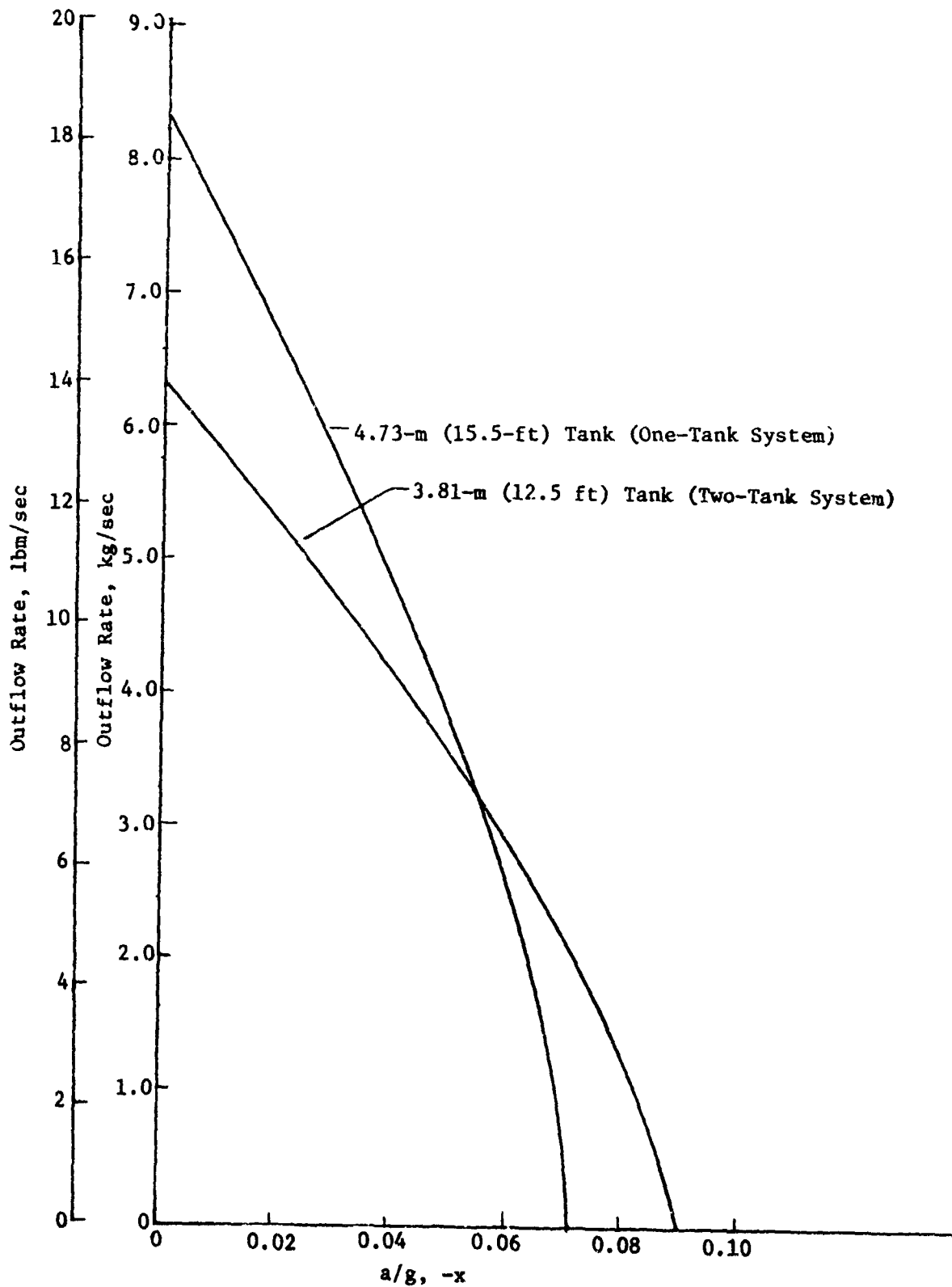


Fig. II-55 Comparison of Outflow Capability of One-Tank and Two-Tank System for Liquid Hydrogen

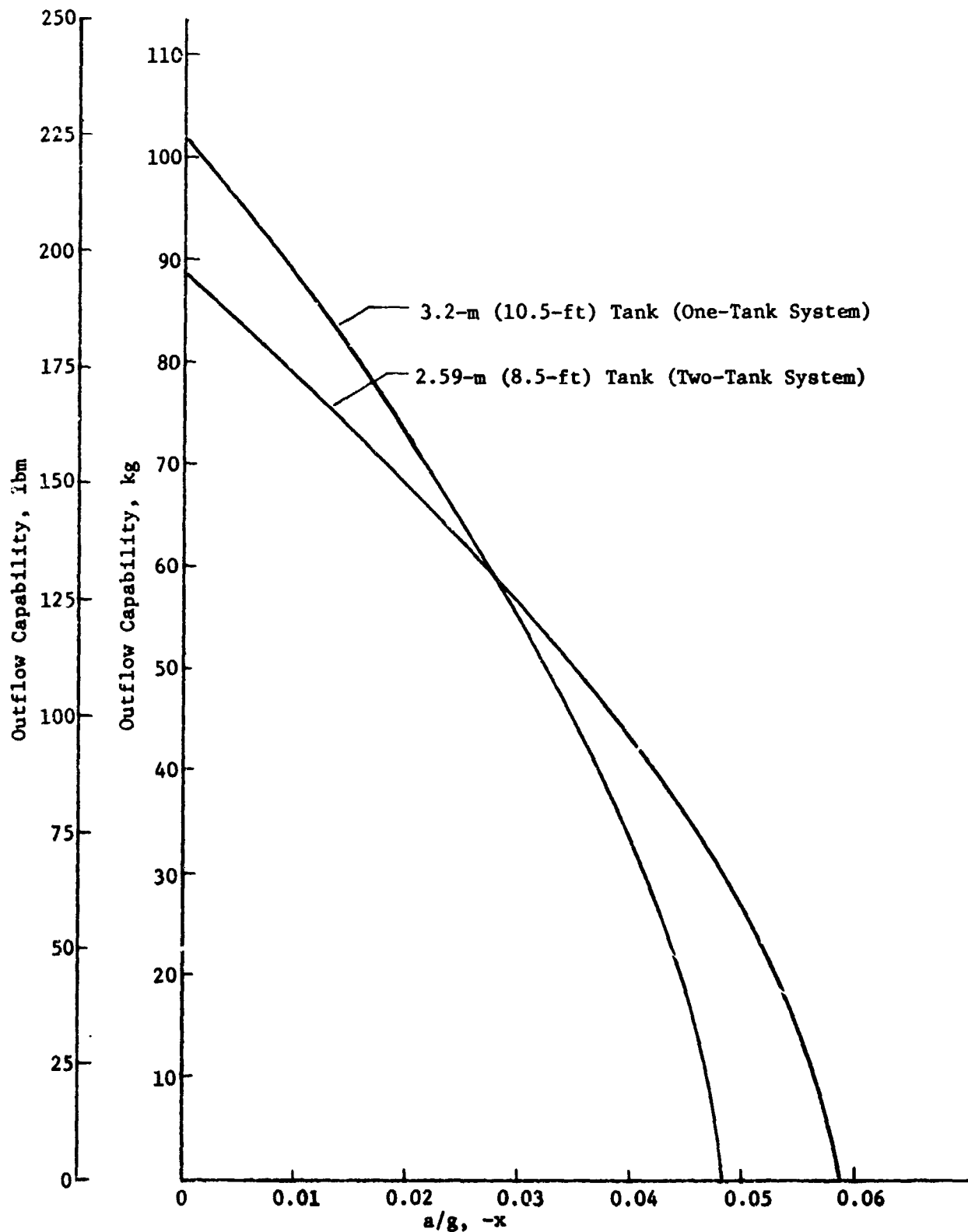
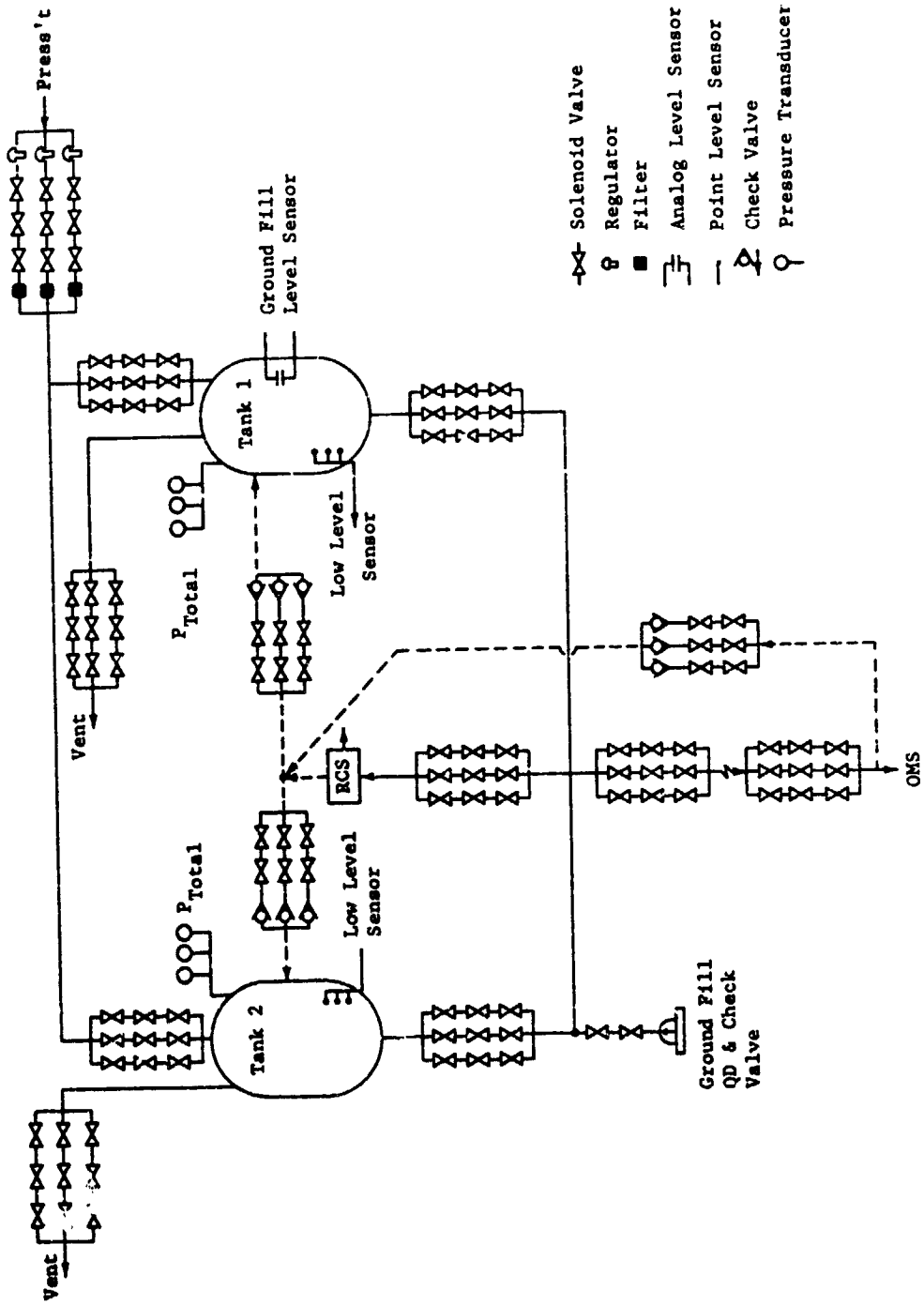


Fig. II-58 Comparison of Outflow Capability of One-Tank and Two-Tank System for Liquid Oxygen



- ⊗ Solenoid Valve
- ⊕ Regulator
- Filter
- ⊞ Analog Level Sensor
- ⊖ Point Level Sensor
- ⊔ Check Valve
- ⊙ Pressure Transducer

Fig. II-57 Parallel-Sequenced Drain Concept, Two-Tank System

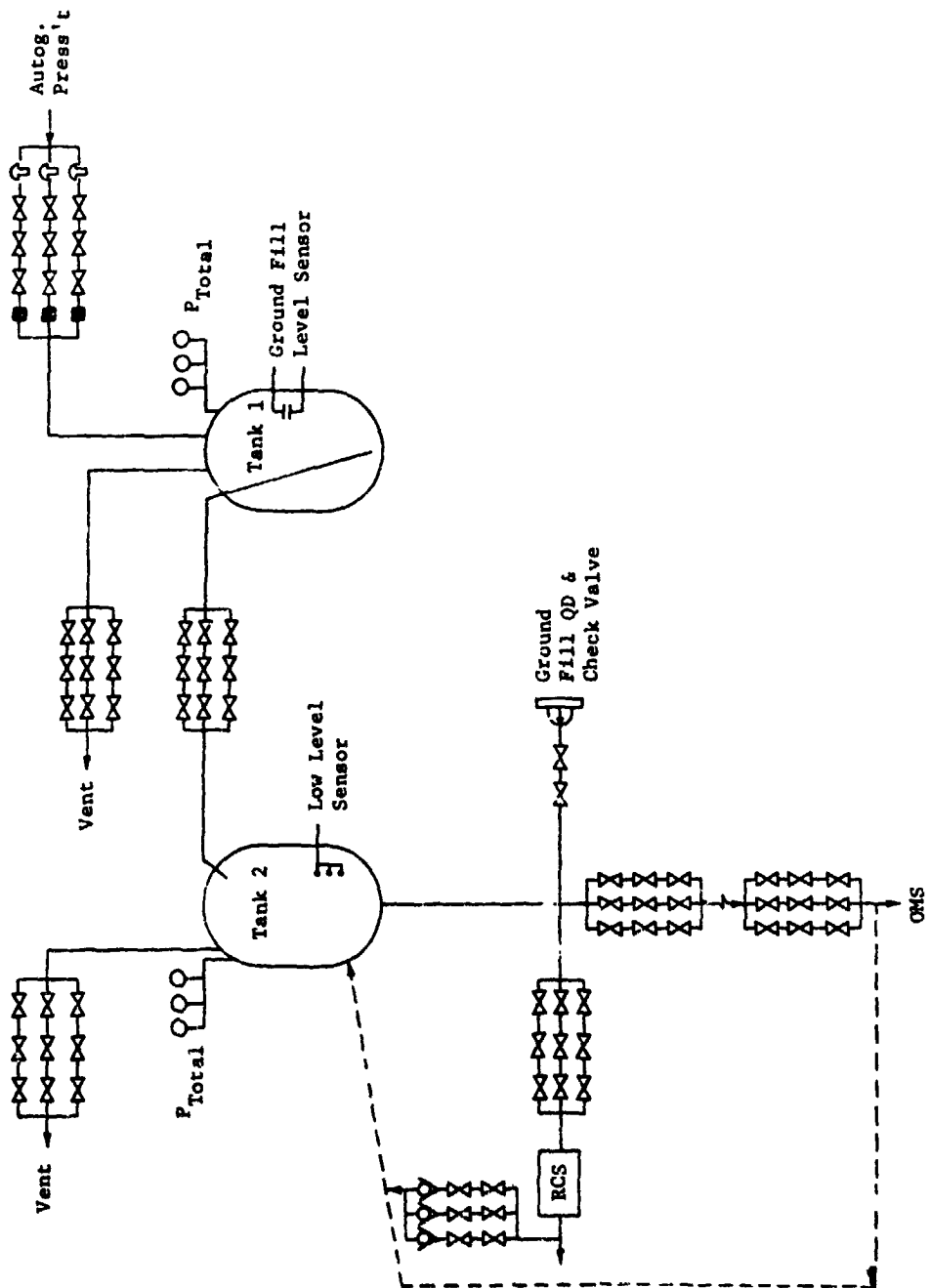


Fig. II-58 Series/Start Tank Concept, Two-Tank System

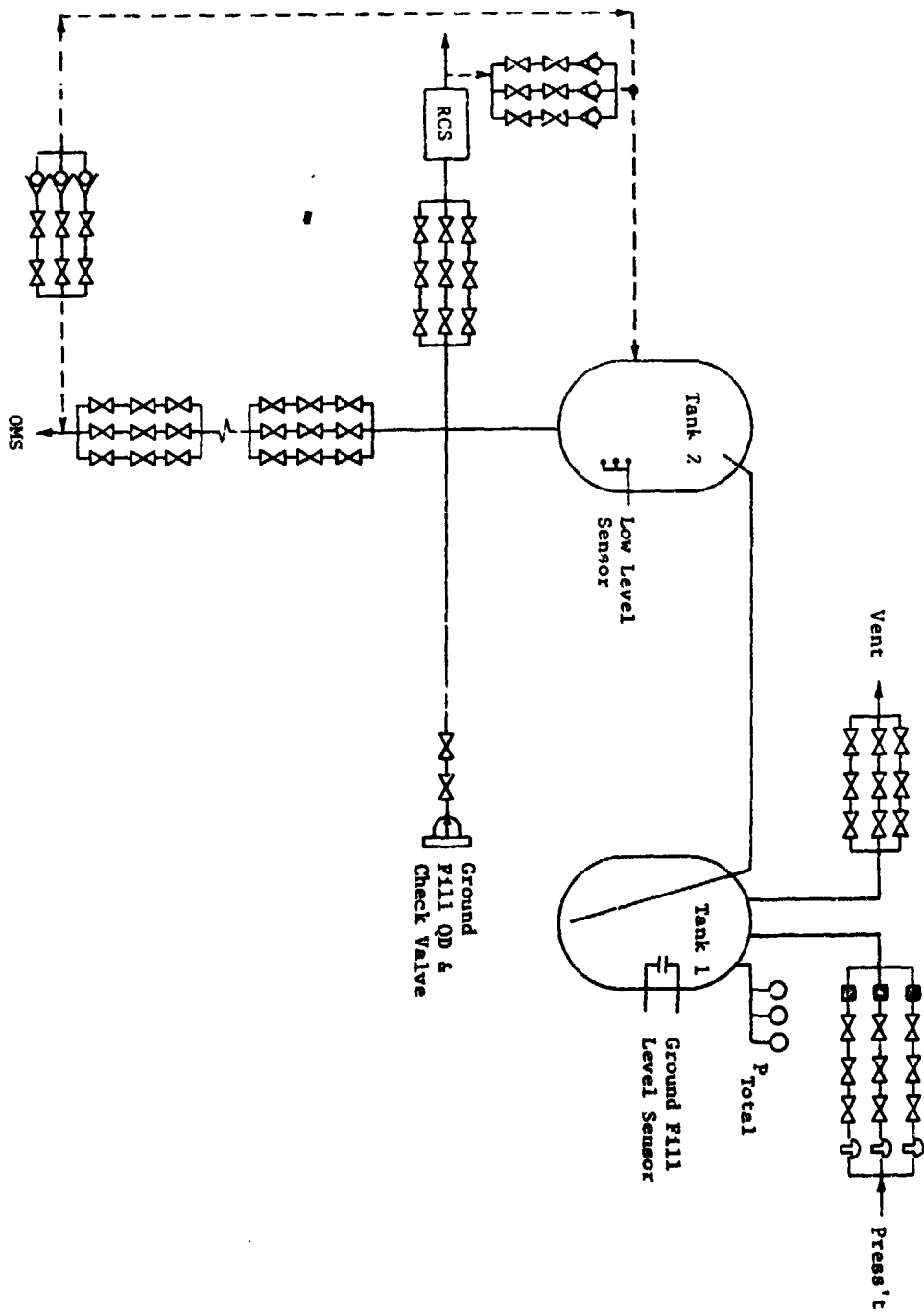


Fig. II-59 Series/Common Drain Concept, Two-Tank System

The results of the comparison studies are summarized in Tables II-2 through II-4. The comparisons were made on the basis of complexity, weight, and technical risk. A recirculation feedline concept was assumed to be representative of the plumbing and control complexity required for this function. Two separate pressurant gas systems were assumed for the series-start tank concept (Fig. II-58) to minimize helium usage and to maximize complexity in this comparison. Helium pressurant alone could be used for both tanks, but considerable development on the potential pressure collapse in Tank 2 would be required before autogenous pressurant gas could be recommended for both tanks.

The complexity comparison is shown in Table II-2. The total number of active elements in these systems is lowest for the series common concept and highest for the sequenced-parallel feed systems.

The weight performance comparison appears in Table II-3. The totals of the weights also show a clear preference for the series concepts. Technology cost/risk comparisons are shown in Table II-4 with assessments of the subsystems indicated.

The results of this study do not collectively favor parallel feed systems for on-orbit cryogenic propulsion systems. Series systems provide less complexity and lower weight with little discrimination in technical risk.

*c. Foraminous Materials Survey* - Suppliers were surveyed to identify candidate capillary materials for use in device fabrication. In all, nine different materials were evaluated. Although there are considerably more than nine capillary materials commercially available, many were immediately eliminated (e.g., they were not compatible with the propellants of interest). Ten properties were evaluated for each candidate and each property was assigned a rating according to the following criteria.

Property Rating Factor, r

- |   |  |
|---|--|
| 1 | Unacceptable; not usable without major design compromise and associated performance penalty. |
| 2 | Poor; significant design compromise required with some penalty.                              |
| 3 | Fair; moderate design compromise and little penalty.   |
| 4 | Good; little design provision and no penalties.  |

Table II-2 Complexity Comparison

ACTIVE COMPONENTS	SEQUENCED PARALLEL		SERIES-START TANKS		SERIES-COMMON TANKS	
	Mech	Elec	Mech	Elec	Mech	Elec
Valves	110	440	89	356	57	228
Check Valves	9	36	3	12	6	24
Filters	--	--	3	--	3	--
Pressure Regulators	3	12	3	12	3	12
Pressure Sensors	6	24	6	24	3	12
Low Level Sensors	6	24	3	12	3	12
Ground Fill Level	1	4	1	4	1	4
Totals	138	540	108	420	76	292

Table II-3 Weight and Performance Comparison

COMPONENT	SEQUENCED PARALLEL		SERIES-START TANK	kg (lbm)	SERIES-COMMON TANK		kg (lbm)
	Qty.	Size			Qty.	Size	
Valves and Check Valves, One Propellant Feedline	27,	- 10.1 cm (4 in.) dia	27,	98.1 (216)	27,	- 10.1 cm (4 in.) dia	98.1 (216)
	18,	- 7.62 cm (3 in.) dia		49.0 (108)			
Pressure Vent	45,	- 7.62 cm (3 in.) dia	27,	122.6 (270)	27,	- 7.62 cm (3 in.) dia	73.6 (162)
Recirculation System	18,	- 5.08 cm (2 in.) dia	6,	40.9 (90)	6,	- 5.08 cm (2 in.) dia	13.7 (30)
Total, (Two Propellants)				621 (1368)			390.6 (816)
Vacuum Feedline, Pressurant, line dumps, etc							
H <sub>2</sub>	15.8 m (52 ft),	7.62 cm (3 in.) dia	12.2 m (40 ft),	212.4 (468)	12.2 m (40 ft),	7.62 cm (3 in.) dia	127.1 (280)
O <sub>2</sub>	11.3 m (37 ft),	6.35 cm (2.5 in.) dia	12.2 m (40 ft),	369.5 (814)	12.2 m (40 ft),	6.35 cm (2.5 in.) dia	72.6 (160)
Residuals, Liquid							
H <sub>2</sub>	3X, 4810 kg (106,000 lbm)		3X, 2405 kg (5330 lbm)	145.3 (320)	3X, 2405 kg (5330 lbm)		72.6 (160)
O <sub>2</sub>	3X, 18,500 kg (40,700 lbm)		3X, 9250 kg (20,350 lbm)	553.8 (1220)	3X, 9250 kg (20,350 lbm)		276.0 (610)
Total				1902 (4180)			938.9 (2026)

Table II-4 Technology Cost/Risk Comparison

SYSTEM	SEQUENCED PARALLEL	SERIES-START TANK	SERIES-COMMON TANK
Acquisition-Expulsion	Minimal	Minimal	Backflow
Pressurization	Minimal	Low Risk	Receiver Collapse
Pressurant Systems	One	Two	One
Low-Level Gaging	Crucial	Minimal	Minimal
Feedline Conditioning	Crucial	Minimal	Minimal

- 5            Excellent; no design compromise, provision, or penalty.

Each property was also assigned a weighting factor based on its importance to the system design.

Weighting Factors, w

- 1            Noncritical; even where  $r = 1$ , could be tolerated in the system.
- 2            Semicritical; unacceptable to poor ( $r = 1$  or  $2$ ) characteristics could not be tolerated in the system.
- 3            Critical; characteristics must be fair to excellent ( $r = 3$  to  $5$ ) in order to be usable.

The properties and their weight factors are listed below

<u>Property</u>	<u>Factor, w</u>
a) bubble point	3.0
b) gross weight	2.5
c) volume	2.0
d) compatibility	3.0
e) formability	2.0
f) joining	2.0
g) cleanability	1.5
h) durability	2.0
i) wicking	2.0
j) cost	1.0

Each of the nine materials selected had at least one outstanding attribute that warranted evaluation. These materials are discussed in the following paragraphs.

1) *Steel Screen* - This material has been used more often than any of the others because it rates high in most of the critical areas. Despite only a moderate bubble point and no inherent bending strength, it is the most promising material in this study.

2) *Polyester Screen* - Inexpensive and light in weight, this material might find application in some other system. Low bubble point and incompatibility rule it out in this study.

3) *Porous Ceramic* - A very high bubble point and basic inertness make this material attractive. Its chief disadvantages are weight and fabrication difficulty.

4) *Sintered Fiber* - This is a promising material in most respects, although weight and volumetric efficiency could be a problem.

5) *Laminate* - Strength and durability are favorable factors for screen laminates. Bubble points were lower than expected and weight is a definite problem.

6) *Perforated Plate* - Although this material has no appreciable bubble point, it has been used with good results as a structural backup for other capillary candidates.

7) *Metal Foam* - This material produces good bubble points and has good strength. However, it is heavy and difficult to form.

8) *Porous Teflon* - This relatively new material is lightweight and has a moderate bubble point. Fabrication and wicking are problem areas.

9) *Electroformed Mesh* - This material has good weight and joining properties, but low bubble points and poor wicking.

The overall rating factor, R, for each material is obtained from

$$R = \frac{rw}{R_{\max}}$$

[II-28]

where r is the property rating factor,

w is the weighting factor,

$R_{\max}$  is the maximum possible rating of 105.

The results of the survey are shown in Table II-5. The rating factors are shown in the lower right corner of each matrix element and the weighting factors are shown at the top of each column (where applicable). The last column of the matrix lists the overall rating factors for each material.

The matrix shows that woven steel screen is the best material choice, but it possibly needs some structural backup. The second highest rating was scored by perforated plate. Although it was regarded unacceptable because of its low bubble point, other characteristics were rated high enough to result in a high overall mark. Based on this survey, stainless steel woven screens backed with stainless steel perforated-plate were used as the primary construction material.

Table II-5 Foraminous Materials Rating Matrix

TYPE	DESCRIPTION	PORE SIZE, $\mu$	BUBBLE POINT, N/cm <sup>2</sup> (in. H <sub>2</sub> O) (3.0)	WEIGHT, kg/cm <sup>2</sup> (lb/ft <sup>2</sup> )	CROSS WEIGHT, * kg/cm <sup>2</sup> (lb/ft <sup>2</sup> )	VOLUME, cm <sup>3</sup> /m <sup>2</sup> (in. <sup>3</sup> /ft <sup>2</sup> )	COMPATIBILITY, Cryogenic Strainers (3.9)	FABRICABILITY FORMING (2.0)	SEALABILITY (1.5)	DURABILITY (2.0)	WEIGHING (2.0)	COST PER SQ. FT. (1.0)	OVERALL RATING FACTOR, R
Screen, Metal	Woven, Stainless Steel, Dutch Weave	2 to 3	0.647 (26)	4.88 x 10 <sup>-2</sup> (0.10)	15.34 (0.65)	880.4 (5.0)	OK	Good	Good	Good	Good	372.00 (30)	0.600
Screen, Plastic	Woven, Polyester, Nylon, Dutch Weave	4 to 6	0.423 (17)	7.32 x 10 <sup>-2</sup> (0.13)	16.52 (0.70)	4	OK	Good	Good	Good	Good	53.75 (11)	0.653
Ceramic	Porous Ceramic Cast, 0.317 cm (0.125-in.) Thick	11 to 20	1.1 to 2.40 (50 to 100)	4.88 x 10 <sup>-2</sup> (1.0)	23.6 (1.0)	3169.4 (18)	OK	Good	Fair	Good	Good	215.00 (2.0)	0.705
Fiber, Metal	Compressed Stainless Steel, 0.150 cm (0.063-in.) Thick	2 to 10	0.6119 (30)	7.8 x 10 <sup>-2</sup> (1.7)	37.76 (1.6)	1507.11 (8.9)	OK	Good	Fair	Good	Good	215.00 (2.0)	0.705
Laminate	Five Layers of Stainless Steel, Bonded	2	0.3926 (20)	9.76 x 10 <sup>-2</sup> (2.0)	47.2 (2.0)	1584.7 (9.0)	OK	Good	Fair	Good	Good	215.00 (2.0)	0.705
Plate	Perforated Sheet, Stainless Steel, 0.040 cm (0.016-in.) Holes, 26 Gage	400	0.924 (-1)	2.68 x 10 <sup>-2</sup> (0.55)	12.98 (0.55)	633.88 (3.0)	OK	Good	Excellent	Good	Fair	5.75 (1)	0.653
Metal Foam	Porous Nickel, 0.150 cm (0.063-in.) Thick	10	0.6219 (-20)	9.27 x 10 <sup>-2</sup> (1.9)	44.84 (1.9)	1507.11 (8.9)	OK	Fair	Fair	Good	Good	215.00 (2.0)	0.705
Sheet TFF	Porous Teflon, 0.040 cm (0.016-in.) Thick	2	0.1906 (-20)	9.7 x 10 <sup>-2</sup> (3.02)	13.45 (0.57)	1034.8 (5.9)	OK	Good	Good	Fair	Fair	215.00 (2.0)	0.705
Electroformed Mesh	Nickel, 4x10 <sup>4</sup> Holes per Square Inch	20	0.190 (-10)	1.46 x 10 <sup>-2</sup> (0.03)	13.68 (0.58)	860.4 (5.9)	OK	Fair	Fair	Fair	Fair	215.00 (2.0)	0.705

\*Includes structural backup material, if required.

## C. RESULTS AND CONCLUSIONS

The investigations discussed in this chapter form the basis for the three specific acquisition/expulsion system design studies presented in Chap. III, IV, and V. The general investigations described here can be applied to any cryogenic acquisition/expulsion system design. The five systems identified in this chapter have characteristics that can satisfy varied mission requirements and design criteria. In general, the systems are variations of the basic DSL cryogenic storage concept. The passive characteristics of this concept make it one of the most desirable approaches for the long-term storage of cryogens in space.

Four of the five candidate storage systems are identical in their venting characteristics. Their expulsion characteristics differ slightly. These four systems are the basic DSL, the channel/liner, the trap/liner and the ESL. The different expulsion characteristics make these systems more attractive for some particular missions than for others. For a specific mission some of the candidate systems can be eliminated by requirements such as acceleration environment. Candidate systems can be further evaluated by conducting appropriate trade studies to yield the preferred system for the specific mission.

The weeping tank concept, however, is a special case. This system relies on a completely different vent system for achieving tank pressure control. Its primary advantage is the venting flexibility allowed by the wider vent band. The preliminary analyses conducted have pointed out its capabilities and limitations. Although this concept has potential, it needs further development to achieve the state-of-the-art level of the other candidate systems. Additional analyses are required to identify porous plug designs and venting characteristics. In addition, testing is required to substantiate these analyses. The primary advantage of the weeping tank concept did not appear significant to warrant further analyses and testing during this study. For these reasons, this concept was not considered a candidate for the three specific designs accomplished under this program.

The results of the analytical and experimental investigations conducted during this study represent a significant contribution to the knowledge required for evaluating and designing cryogenic capillary expulsion systems. The results represent answers to many questions that affect the design of passive cryogenic propellant management systems. Critical data were compiled in the

four technical areas that influence the size, shape, weight, and performance of cryogenic acquisition/expulsion systems.

In the fluid mechanics area, the critical parameters affecting the capillary stability of these cryogenic systems were identified and modeled. Experimental data verified design approaches in the areas of retention capability of multilayered screens and pressure losses associated with both gas and liquid flow through fine mesh screens. Wicking analyses were conducted and experimentally verified to provide data used in the design of the DSL vent systems. The results of the start transient analyses indicate that typical start transients do not present significant design problems for capillary propellant management systems.

Thermal and thermodynamic effects are considered critical for cryogenic system design. The investigations in this area centered primarily on pressurization and venting. Pressurization system characteristics for the DSL systems were established. The use of either autogenous gas or helium pressurants was experimentally verified over a wide pressurant temperature range. The preferred DSL vent system was identified and its operational characteristics and sensitivity to changes in heat flux, vent pressure band, etc., were established. Although the vent characteristics were not experimentally verified because of the 1-g thermal stratification effects, a vent control scheme was developed for the small vent control band required for the liquid hydrogen system. The results of the thermal stratification investigation show that low-g thermal stratification will favor the DSL concept. The collapse of any vapor bubbles within the controlled liquid volume of a propellant management system was investigated both analytically and experimentally. These results indicate that bubbles of 2.54-cm (1-in.) diameter or less can be collapsed during tank pressurization.

From the structural investigations, two approaches are available for the structural design of capillary propellant management systems. A polysphere structure that uses perforated plate for supporting screens under collapsing loads was developed. Also the structural characteristics of unsupported screens were investigated both analytically and experimentally. The test results from the cycling of pressure loads on unsupported screen indicate that this is not a serious design problem.

Other potential problem areas such as cleaning, inspection, and maintenance of capillary acquisition/expulsion devices were investigated, but revealed no critical design problems. The

screen joining techniques developed under a related Martin Marietta IR&D program are considered more than adequate to satisfy the critical sealing requirements of the fine mesh screen systems. Of the several joining methods investigated, the preferred method is resistance welding although other methods look promising for making screen repairs.

The system configuration and size investigations yielded three important conclusions.

- 1) The results of the one versus two propellant tank comparison favor the two-tank system.
- 2) For a two-tank system, a series feed has advantages of lower weight and greater reliability over a parallel feed system.
- 3) Results from the foraminous material survey and comparison showed that the fine mesh metal screens are preferred over all other materials investigated.

The results of these investigations yield the data for designing various cryogenic acquisition/expulsion systems. For all of these critical investigations, the consistent approach followed was to experimentally verify analytical techniques and models. This approach adds credibility and confidence to the information and data compiled and to the designs based on the data. The next three chapters present detailed discussions of specific designs for the integrated Orbital Maneuvering System/Reaction Control System (OMS/RCS), the dedicated OMS (LO<sub>2</sub>), and the Space Tug.

### III. INTEGRATED OMS/RCS DESIGN

---

This chapter discusses the analysis and design of the cryogenic acquisition/expulsion systems for the integrated OMS/RCS propellant tanks of the cryogenic-fueled Space Shuttle. Comparative evaluations were made among the most promising candidate systems described in Chapter II. The comparisons were made using mission parameters and criteria for typical Space Shuttle missions. The most promising concept was analyzed in greater detail and a detailed design of the system was accomplished. The ability to fabricate, assemble, and check out systems similar in design and size to the proposed integrated OMS/RCS design was developed. These topics are discussed under three headings.

- (1) Mission Requirements and Design Criteria;
- (2) Preliminary Design Analysis;
- (3) Detail Design.

#### A. MISSION REQUIREMENTS AND DESIGN CRITERIA

The cryogenic Space Shuttle vehicle configurations and related mission requirements that were used to design the acquisition/expulsion system for the integrated OMS/RCS cryogenic storage system are outlined here. These vehicle configuration and mission requirements reflect the Space Shuttle Phase B study results (Ref III-1 and III-2). These data were continually updated during the study to assure that the acquisition/expulsion system design satisfied the configuration and mission requirements. The design approach did not favor one particular vehicle and mission, but rather met a worst-case set of criteria.

##### 1. General Requirements

The following general performance and design requirements were to be satisfied within the existing Space Shuttle design philosophy. The systems were designed for easy inspection, checkout, and maintenance while making maximum use of aircraft design practice. The integrated OMS/RCS system was designed to operate satisfactorily throughout the range of acceleration and thermal environments anticipated during Shuttle operation. The designs

included provisions for a minimum service life of 100 missions over a 10-year period. For each of these missions, at least 7 days of self-sustaining lifetime were provided for, with the additional capability of extending the on-orbit stay to 30 days. The useful storage capacity of the tanks provided for 609.6 m/sec (2000 fps) delta velocity. The capability for receiving propellants while on orbit was also included.

2. Design Missions

Three specific Shuttle missions were used as a baseline. The three missions are: 1) an easterly launch; 2) a polar launch; and 3) a space station resupply. Typical propellant and delta velocity requirements for these missions are shown in Tables III-1 through III-4 (Ref III-1). None of these missions approaches the baseline tankage capacity of 609.6 m/sec (2000 fps) delta velocity. However, a nearly fully-loaded condition at liftoff (5% initial ullage) was considered to incorporate future growth requirements into the acquisition/expulsion system design.

3. Tankage and Feedline Geometry

The Shuttle Phase B study results (Ref III-1 and III-2) were used to establish a representative set of tank and feedline dimensions and geometries. The baseline design parameters are shown in Table III-5 under the headings, Tankage and Feedlines.

4. Thermal Criteria

The thermal criteria of primary importance to this study are listed in Table III-5 under the heading, Heat Leaks. Other criteria were defined in the Design Requirements Document (Ref III-3).

5. Propellant Utilization Criteria

The expulsion duty cycle for the cryogenic storage system is based on satisfying (1) the OMS engine requirements; (2) the RCS gaseous accumulator pump requirements; and (3) the thermal conditioning needs. These duty cycles are outlined in Tables III-2 through III-4.

The acquisition/expulsion systems were designed to provide gas-free liquid instantaneously on demand, without relying on propellant settling. The systems were designed so that neither the duration nor the number of expulsion events is limited by the design. The systems were also designed to assure maximum

Table III-1 Summary of Design Missions

MISSION PHASE	RCS PROPELLANTS, kg (lbm)		OMS ΔV, m/sec (fps)	
<u>Easterly Launch</u>				
Orbit Injection	180.1	(396.7)		
Hohmann (2)	---		46.42	(152.3)
Deployment	482.4	(1,062.6)		
Wait in Orbit	302.2	(665.6)		
Hohmann (2)	---		51.75	(169.8)
Phase	195.7	(431.1)		
Hohmann and TPI	---		20.7	(68.0)
Rendezvous	665.0	(1,464.9)		
Retrieval	157.5	(346.3)		
Deorbit	171.2	(377.1)	101.5	(333.0)
Preentry	71.8	(158.2)		
Entry	544.8	(1,200.0)		
<b>Total</b>	<b>2,770.8</b>	<b>(6,103.1)</b>	<b>220.4</b>	<b>(723.1)</b>
<u>Polar Launch</u>				
Orbit Injection	179.6	(395.6)		
Hohmann (2)	---		73.2	(240.0)
Deployment	533.2	(1,174.5)		
5-Day Mapping or	15,572.0	(34,300.0)		
Weather Reconnaissance	1,167.1	(2,570.8)		
Deorbit	---		64.0	(210.0)
Preentry	70.8	(156.1)		
Entry	544.8	(1,200.0)		
<b>Total</b>	<b>17,519.7</b>	<b>(38,589.8)</b>	<b>137.2</b>	<b>(450.0)</b>
	<b>2,660.7</b>	<b>(5,860.6)</b>		
<u>Space Station Resupply</u>				
Orbit Injection	340.9	(750.9)		
Hohmann (3)	---		156.4	(513.0)
Rendezvous	563.7	(1,241.6)		
Hohmann (1)	---		41.7	(137.0)
TPI	---		8.2	(27.0)
Docking	212.1	(467.1)		
5-Day Stationkeeping	315.1	(694.0)		
Redocking	282.3	(621.7)		
Deorbit	115.3	(254.0)	132.5	(435.0)
Preentry	67.8	(149.4)		
Entry	544.8	(1,200.0)		
<b>Total</b>	<b>2,441.9</b>	<b>(5,378.7)</b>	<b>338.4</b>	<b>(112.0)</b>

Table III-2 Space Station Resupply Mission Timeline

Event	Mission Time, hr:min:sec	Event Time, sec	LO <sub>2</sub>				LH <sub>2</sub>				Total Propellant		Total Mass		
			$\dot{m}$ , kg/sec	$\dot{m}$ , lbm/sec	$\dot{m}$ , kg	$\dot{m}$ , lbm	$\dot{m}$ , kg/sec	$\dot{m}$ , (lbm/sec)	$\dot{m}$ , kg	$\dot{m}$ , lbm	kg	lbm	kg	lbm	
Launch	00:00:00	425			6033	13,290			1208	2661	7241	15,951	161,601	355,951	
RCS	00:07:05				6033	13,290			1708	2661	7241	15,951	161,601	355,951	
					(-53)	(-138)			(-12.7)	(-28)	(-75)	(-166)			
					5971	13,130			1195	2633	7166	15,785	161,526	355,785	
Hohmann 1	00:50:40	120	13.2	(29.0)	(-1570)	(-3,458)	2.7	(6.0)	(-314)	(-692)	(-1884)	(-4,130)			
OMS ΔV					4401	9,694			881	1941	5282	11,635	159,642	351,635	
RCS	00:52:40				(-81)	(-178)			(-16.3)	(-36)	(-97)	(-214)			
					4320	9,510			865	1905	5185	11,421	159,545	351,421	
Circularize	01:35:06	53	13.2	29.0	(-691)	(-1,523)	2.7	(6.0)	(-138)	(-305)	(-830)	(-1,828)			
OMS ΔV					3628	7,793			726	1600	4355	9,593	158,715	348,593	
RCS	01:35:59				(-138.5)	(-305)			(-27)	(-61)	(-166)	(-366)			
											4189	9,227	158,549	349,227	
Payload Release	20:00:00				Release 18,200 kg (40,000 lbm) Payload							0	0		
RCS ΔV	20:01:00				3490	7,688			698	1539	4189	9,227	140,389	309,227	
					(-45)	(-99)			(-9)	(-20)	(-54)	(-119)			
					3445	7,589			689	1519	4135	9,108	140,335	309,108	
RCS	20:11:00				(-72)	(-158)			(-14.5)	(-32)	(-86)	(-190)			
					3373	7,431			675	1487	4048	8,918	130,248	308,918	
RCS ΔV	24:00:00				(-44.5)	(-98)			(-9)	(-20)	(-53)	(-118)			
					3329	7,333			666	1467	3995	8,800	140,195	308,800	
RCS ΔV	24:10:00				(-110)	(-2,445)			(-222)	(-489)	(-1332)	(-2,934)			
					2219	4,888			444	978	2663	5,866	138,863	305,866	
Deorbit	166:48:39	130	13.2	(29.0)	(-1706)	(-3,758)	2.7	(6.0)	(-341)	(-752)	(-2048)	(-4,510)			
OMS ΔV					513	1,130			102	226	615	1,356	136,815	301,356	
RCS	166:50:49				(-513)	(-1,130)			(-102)	(-226)	(-615)	(-1,356)			
					0	0			0	0	0	0	136,260	300,000	
Land	168:07:04														

Table III-3 Space Station Resupply Mission Timeline

Event	Mission Time, hr:min:sec	Event Time, sec	LO <sub>2</sub>				LH <sub>2</sub>				Total Propellant		Total Mass	
			$\dot{m}$ , kg/sec	$\dot{m}$ , lbm/sec	$\dot{m}$ , kg	$\dot{m}$ , lbm	$\dot{m}$ , kg/sec	$\dot{m}$ , (lbm/sec)	$\dot{m}$ , kg	$\dot{m}$ , lbm	kg	lbm	kg	lbm
Launch	00:00:00	421		0	12,177	26,823			2436	5366	14,614	32,189	162,163	357,189
Insertion	00:07:01	--			12,177	26,823			2436	5366	14,614	32,189	162,163	357,189
RCS					(-62.6)	(-138)			(-12.7)	(-28)	(-75)	(-166)		
Hohmann 1	00:50:36	66	13.1	29	11,115	26,685	2.7	6	2423	5338	14,538	32,023	162,088	357,023
OMS ΔV					(-86.3)	(-1,900)			(-173)	(-380)	(-1,035)	(-2,280)		
RCS	00:51:42	--			11,252	24,785			2251	4958	13,503	29,743	161,053	354,743
					(-104)	(-230)			(-21)	(-46)	(-125)	(-276)		
					11,148	24,555			2230	4912	13,378	29,467	160,928	354,467
Hohmann 2	23:22:28	103	13.1	29	1,354	(-2,983)	2.7	6	(-271)	(-597)	(-1,625)	(-3,580)		
OMS ΔV					9,794	21,577			1960	4315	11,752	25,887	159,302	350,887
RCS	23:24:11	--			(-80)	(-177)			(-16)	(-35)	(-96)	(-212)		
					9,713	21,705			1943	4280	12,110	26,675	159,206	350,675
Hohmann 3	24:07:21	197	13.1	29	(-2,588)	(-5,700)	2.7	6	(-518)	(-1140)	(-3,105)	(-6,840)		
OMS ΔV					7,126	15,695			1426	3140	8,551	18,835	156,101	343,835
RCS	24:10:38	--			(-93)	(-205)			(-19)	(-41)	(-111)	(-246)		
					7,032	15,490			1407	3099	8,439	18,589	155,989	343,589
Hohmann 4	24:53:54	96	13.1	29	(-1,263)	(-2,783)	2.7	6	(-253)	(-557)	(-1,516)	(-3,340)		
OMS ΔV					5,769	12,707			154	2542	6,923	15,249	154,473	340,249
RCS	24:55:30				(-65)	(-143)			(-13)	(-29)	(-78)	(-172)		
					5,704	12,564			1141	2513	6,845	15,077	154,394	340,077
TPE Burn	25:39:20	19	13.1	29	(-253)	(-558)	2.7	6	(-51)	(-112)	(-304)	(-670)		
OMS ΔV					5,450	12,006			1090	2401	6,540	14,407	151,090	339,407
RCS	25:39:39				(-60)	(-132)			(-12)	(-26)	(-69)	(-153)		
					5,390	11,874			1078	2378	6,469	14,249	154,019	339,249
TPE Burn	26:12:30	55	5.4	12	(-252)	(-556)	0.91	2	(-50)	(-111)	(-302)	(-667)		
RCS ΔV					5,138	11,318			1028	2264	6,166	13,582	153,716	338,582
RCS	26:13:25	5 days			(-807)	(-1,777)			(-161)	(-356)	(-968)	(-2,133)		
Dork					4,331	9,541			866	1908	5,198	11,449	152,747	336,449
Deorbit	163:53:00	290	13.1	29	(-3,821)	(-8,417)	2.7	6	(-764)	(-1683)	(-4,585)	(-10,100)		
OMS ΔV					510	1,124			102	225	612	1,349	148,162	326,349
RCS	163:57:50				(-510)	(-1,124)			(-102)	(-225)	(-612)	(-1,349)		
Land	165:14:00												147,550	325,000

Table III-4 Easterly Launch Mission Timeline

Event	Mission Time hr:min:sec	Event Time sec	LO2			LiF <sub>2</sub>			Total Propellant		Total Mass	
			m, kg/sec	m, lbm/sec	m, kg	m, lbm	m, kg/sec	m, lbm/sec	kg	lbm	kg	lbm
Launch	00:07:00				9189 (-63)	20,240 (-138)	1839 (-13)	4051 (-28)	11,028 (-75)	24,291 (-166)	176,738 (-166)	389,291 (-166)
Rohmann 1 OMS ΔV RCS	00:50:35	95	13.1	29.0	9126 (-1246)	20,102 (-2,744)	1826 (-249)	4023 (-348)	10,953 (-1,495)	24,125 (-3,292)	176,662 (-3,292)	389,125 (-3,292)
Rohmann 2 RCS	00:52:10				7880 (-81)	17,358 (-179)	1577 (-16)	3475 (-16)	9,458 (-98)	20,833 (-215)	175,168 (-215)	385,833 (-215)
Deployment RCS 1	01:34:48	25	13.1	29.0	7468 (-7.2)	16,451 (-16)	1495 (-1.3)	3293 (-3)	8,964 (-8.6)	19,744 (-19)	175,127 (-19)	384,744 (-19)
Deploy	02:25:00				7461 (-98)	16,435 (-217)	1495 (-19.5)	3200 (-43)	8,955 (-1,180)	19,725 (-260)	174,665 (-260)	384,725 (-260)
Deployment RCS 2	03:00:00		(29,510 kg) 65,000 lbm Payload						8,837 (0)	19,465 (0)	174,547 (0)	384,465 (0)
Deployment RCS 2	03:01:00				7363 (-302)	16,218 (-665)	1474 (-60)	3247 (-133)	8,837 (-362)	19,465 (-798)	145,037 (-798)	319,465 (-798)
Hold in Orbit	04:18:00				7061 (-252)	15,553 (-554)	1413 (-111)	3114 (-302)	8,473 (-665)	18,663 (-665)	144,673 (-665)	318,663 (-665)
RCS	134:49:00				6809 (-56)	14,934 (-124)	1363 (-11)	3003 (-25)	8,171 (-68)	17,998 (-149)	144,371 (-149)	317,998 (-149)
Rohmann 3 OMS ΔV RCS	135:00:00	28	13.1	29.0	6753 (-364)	14,875 (-802)	1350 (-73)	2978 (-160)	6,741 (-436)	14,849 (-962)	144,303 (-962)	317,849 (-962)
Rohmann 4 OMS ΔV RCS	135:00:28				6389 (-83)	14,073 (-182)	1280 (-17)	2818 (-37)	1,667 (-99)	16,887 (-219)	143,866 (-219)	316,887 (-219)
Rohmann 5 OMS ΔV RCS	135:54:41	81	13.1	29.0	6306 (-1070)	13,891 (-2,357)	1262 (-214)	2781 (-472)	7,567 (-1,284)	16,668 (-2,829)	143,767 (-2,829)	316,668 (-2,829)
Rendezvous RCS 1	135:56:02				5236 (-23.6)	11,334 (-52)	1048 (-5)	2309 (-11)	6,283 (-74)	13,839 (-163)	142,482 (-163)	313,839 (-163)
Rendezvous RCS 1	136:18:44				5213 (-56)	11,482 (-123)	1043 (-11)	2298 (-25)	6,254 (-67)	13,776 (-148)	142,454 (-148)	313,776 (-148)
Rohmann 5 OMS ΔV RCS 2	136:29:44	30	13.1	29.0	5157 (-394)	11,359 (-869)	1032 (-79)	2273 (-174)	6,187 (-473)	13,628 (-1043)	142,387 (-1043)	313,628 (-1043)
Rendezvous RCS 2	156:30:14				4762 (-105)	10,490 (-231)	953 (-21)	2099 (-46)	5,714 (-125)	12,585 (-277)	141,913 (-277)	312,585 (-277)
TPI	138:26:48	14	13.1	29.0	4657 (-177)	10,239 (-390)	932 (-35)	2053 (-78)	5,588 (-212)	12,308 (-468)	141,787 (-468)	312,308 (-468)
Rendezvous RCS 3	138:27:02				4480 (-393)	9,869 (-866)	897 (-78)	1975 (-173)	5,377 (-472)	11,844 (-1,039)	141,577 (-1,039)	311,844 (-1,039)
Retrieval RCS	139:19:33				4087 (-131)	9,003 (-289)	818 (-26)	1802 (-58)	4,905 (-156)	10,805 (-347)	141,105 (-347)	310,805 (-347)
Satellite	140:05:00				3956	8,714	792	1744	4,748 (0)	10,458 (0)	140,947 (0)	310,458 (0)
Deorbit RCS	153:56:00				3956 (-143)	8,714 (-314)	792 (-28)	1744 (-63)	4,748 (-171)	10,458 (-377)	170,457 (-377)	375,458 (-377)
Deorbit OMS ΔV RCS	154:16:00	250	13.1	29.0	3813 (-3300)	8,400 (-7,268)	763 (-660)	1681 (-1455)	4,576 (-3,960)	10,081 (-8,723)	170,286 (-8,723)	375,081 (-8,723)
Land	4:20:10				514 (-514)	1,132 (-1,132)	103 (-103)	226 (-226)	616 (-616)	1,358 (-1,358)	166,326 (-1,358)	366,358 (-1,358)
Land	155:36:20				0	0	0	0	0	0	165,710	365,000

Table III-5 Integrated OMS/RCS Baseline Design Parameters

	LH <sub>2</sub>	LO <sub>2</sub>
<u>Tankage</u>		
Total Tank Volume, m <sup>3</sup> (ft <sup>3</sup> )	58 (2046)	16.5 (585)
Tank Diameter, m (ft)		
One Spherical Tank	4.78 (15.7)	3.10 (10.4)
Two Spherical Tanks	3.8 (12.5)	2.51 (8.25)
Two Cylindrical Tanks, 1.84 (6.05 ft) Long Barrel	3.05 (10)	
<u>Feedlines</u>		
Diameter, cm (in.)		
OMS	10.2 (4)	10.2 (4)
RCS	10.2 (4)	10.2 (4)
Length, m (ft)		
OMS	18.3 (60)	4.57 (15)
RCS	3.05 (10)	3.05 (10)
<u>Operating Conditions</u>		
Tank Pressure, N/cm <sup>2</sup> (psia)	10.3 to 34.5 (15 to 50)	10.3 to 34.5 (15 to 50)
NPSP for Steady-State OMS and RCS, N/cm <sup>2</sup> (psf)	1.38 (2)	2.76 (4)
OMS Engine Start Pressure, N/cm <sup>2</sup> (psia)	16.5 (24)	24.1 (35)
OMS Flow Rates, kg/sec (lbm/sec)	2.7 (6)	13.2 (29)
RCS Flow Rates, kg/sec (lbm/sec)	0.9 to 2.72 (2 to 6)	5.44 to 8.17 (12 to 18)
<u>Heat Leaks</u>		
Storage Tanks, W/m <sup>2</sup> (Btu/hr-ft <sup>2</sup> )	1.57 (0.5)	1.57 (0.5)
RCS-TPA Interface, watts (Btu/hr)	27.8 (95)	22.3 (76)

expulsion efficiency. The propellant flow rates considered are included in Table III-5 under the heading, Operating Conditions.

6. Acceleration Criteria

The three different Shuttle Phase B configurations were used to generate a worst-case on-orbit local acceleration profile. This profile was used to design the acquisition/expulsion system. The ascent and reentry accelerations were essentially the same regardless of orbiter configuration. These criteria are shown in Table III-6.

Table III-6 Acceleration Environment

Maneuver	Orbit-To-Orbit Maneuvers				Tank
	Subsystem Employed	Acceleration Direction			
		X	Y	Z	
OMS Translational	One RL-10 Engine	+0.07§			LH <sub>2</sub> /LO <sub>2</sub>
RCS Translational	RCS Thrusters	±0.024†	+0.046†	±0.044*	LH <sub>2</sub> /LO <sub>2</sub>
RCS Rotational	RCS Thrusters	+0.046†	+0.027†	+0.018*	LH <sub>2</sub>
		-0.086*	-0.012§	-0.020§	
Abort (Translational)	Two RL-10 Engines	+0.056†	+0.027†	+0.015*	LO <sub>2</sub>
			-0.014§	-0.022§	
Launch		+0.14§			LH <sub>2</sub> /LO <sub>2</sub>
Reentry		+3.0		-2.3	LH <sub>2</sub> /LO <sub>2</sub>

\* Ref III-2.

† Ref III-1.

§ Ref III-3.

7. Pressurization and Venting

Pressure control for the OMS/RCS LH<sub>2</sub> and LO<sub>2</sub> tanks is accomplished through proper pressurization and venting. Pressurant is introduced through a diffuser to prevent impingement of the pressurant on the screen surfaces. Venting is based on the system's ability to keep liquid away from the vent so that only liquid-free gas is vented.

Pressurization was assumed to be autogenous with NPSP for RCS pumps and OMS steady-state operation of  $1.38 \text{ N/cm}^2$  (2 psid) for hydrogen and  $2.76 \text{ N/cm}^2$  (4 psid) for oxygen.

The vented fluid is 100% vapor and is vented through a nonpropulsive vent from a maximum tank pressure of  $34.4 \text{ N/cm}^2$  (50 psia). The vent is designed to operate during all nonpressurization events of the entire mission, including the high-g prelaunch and the low-g on-orbit operations.

#### 8. Structural Design Criteria

The acquisition/expulsion systems were designed:

- 1) for minimum mass and volume;
- 2) to provide a minimum number of thermal paths to the fluid through structural supports;
- 3) for compatibility with both  $\text{LO}_2$  and  $\text{LH}_2$ ;
- 4) for service through 100 missions of 7 to 30 days each;
- 5) for structural integrity through all the mission-imposed shock, vibrational, acoustic, and operational loads.

#### B. PRELIMINARY DESIGN ANALYSIS

A series of studies were conducted during the preliminary design phase of the integrated OMS/RCS design effort to define the most appropriate acquisition system. The first study involved definition of the system geometry. This definition was accomplished by comparing different system configurations according to their ability to deliver propellants within the constraints of the mission acceleration criteria. From these comparisons, optimum configurations were determined on the basis of maximum outflow with minimum propellant residuals and minimum system hardware weight. Additional studies were done to determine thermodynamic characteristics of the systems, specifically with regard to system pressurization and venting. Preliminary design analyses were also conducted to identify a feedline configuration. The results of these studies were used as the basis of a detailed design effort for the  $\text{LH}_2$  and  $\text{LO}_2$  integrated OMS/RCS cryogenic Shuttle acquisition/expulsion systems.

1. System Configuration Definition Study

The first goal of the system definition study was to define the type of system to be used for the integrated OMS/RCS. Based on data presented in the Chapter II, two equal volume spherical tanks were assumed for each of the two cryogenic propellants. The LH<sub>2</sub> tanks were 3.81 m (12.5 ft) in diameter and the LO<sub>2</sub> tanks were 2.6 m (8.5 ft) in diameter. The tank volumes were consistent with the 609.6 m/sec (2000 ft/sec) delta velocity requirement. It was also assumed that they would be arranged in a series-feed configuration.

Of the five candidate acquisition/expulsion systems, the trap systems were immediately eliminated because the baseline missions did not lend themselves well to trap designs. The RCS propellant requirements between OMS settling maneuvers included as much as 20% of the total initial propellant load. Moreover, it was difficult to determine which maneuvers could be defined as settling maneuvers because some RCS maneuvers could result in potentially higher accelerations in a nonsettling direction (-x) than any available acceleration in the settling direction (+x).

Two candidate systems appeared to be applicable to the unique requirements of the integrated OMS/RCS designs. These were the basic dual-screen-liner (DSL) and the channel/liner systems. Both systems offer the flexibility required to meet the varied mission requirements of the Shuttle operational concepts. Therefore, the initial comparative analysis concentrated on defining the differences between the two systems within the framework of Shuttle requirements to select the most promising system.

Defining the system geometry of a channel/liner design included specifying both the number of channels and the distance between them. The size of the communication screen or the distance between the flow channels is a direct function of the ability of the communication screen to wick the wetting fluid. At the time of this initial study, final results from the wicking analysis and wicking tests were not available. From a preliminary analysis based on information from other sources (Ref III-4), it was estimated that a 15.24 cm (6 in.) wicking distance for both LH<sub>2</sub> and LO<sub>2</sub> was reasonable. Therefore, a distance of 0.305 m (1 ft) between flow channels was specified for the channel/liner design. The results of more detailed analyses showed that this channel spacing estimate was slightly conservative for the LO<sub>2</sub> system, but was essentially an optimum wicking distance between channels for the LH<sub>2</sub> system. Therefore, these channel spacing dimensions were retained in the final design.

The DSL and the channel/liner systems were analyzed to determine the configurations necessary to satisfy the mission requirements. Several channel/liner designs with different numbers of channels were considered. The basic comparison criteria were the amount of propellant residuals inherent in each design and the estimated weight of the designs. The propellant residuals included the volume of propellant contained within the retention device and the predicted additional propellant that might be trapped in the bulk propellant region when breakdown occurred. Considerable conservatism was included in the analyses, including the conservative assumptions incorporated in the computer programs. A 2.0 factor of safety was applied to the capillary retention capability of the screens analyzed. During the initial phases of the analysis, all screens defining controlled liquid regions were assumed to be 325x2300 Dutch-twill stainless steel. In all cases the diameter of the screen liner was held constant so that comparison would be based on the same volume of enclosed liquid.

The computer model assumed that the channels in the channel/liner configurations were rectangular in cross-section and had parallel surfaces along their entire lengths. Therefore, the greatest distance between the channels occurred at the equator. The distance between the channels decreases as the reference point moves from the liner equator toward the poles. The channels join to form a manifold in the vicinity of the poles. Therefore, as the distance between the channels at the equator decreases, the device approaches the limiting case of the DSL. For a given wicking distance and a constant liquid annulus or channel depth, the amount of trapped propellant within the device should decrease as the number of channels increases. This comparison of ideal expulsion efficiency was the first comparison made between the DSL and various channel/liner designs.

The comparison of ideal expulsion efficiency between the DSL and channel/liner designs consisting of 8, 16, and 20 channels for both the LH<sub>2</sub> and LO<sub>2</sub> systems are shown in Fig. III-1 and III-2. The results demonstrate the advantage of a channel system with a large number of channels compared to the basic DSL. For example, for the LO<sub>2</sub> system analyzed with a 8.64 cm (3.4 in.) annulus gap, the difference in ideal expulsion efficiency between the DSL and a 20-channel configuration is approximately 3%. With a total LO<sub>2</sub> propellant load of nearly 18,160 kg (40,000 lbm), that difference amounts to approximately 544.8 kg (1200 lbm). Neither the percentage difference nor the weight

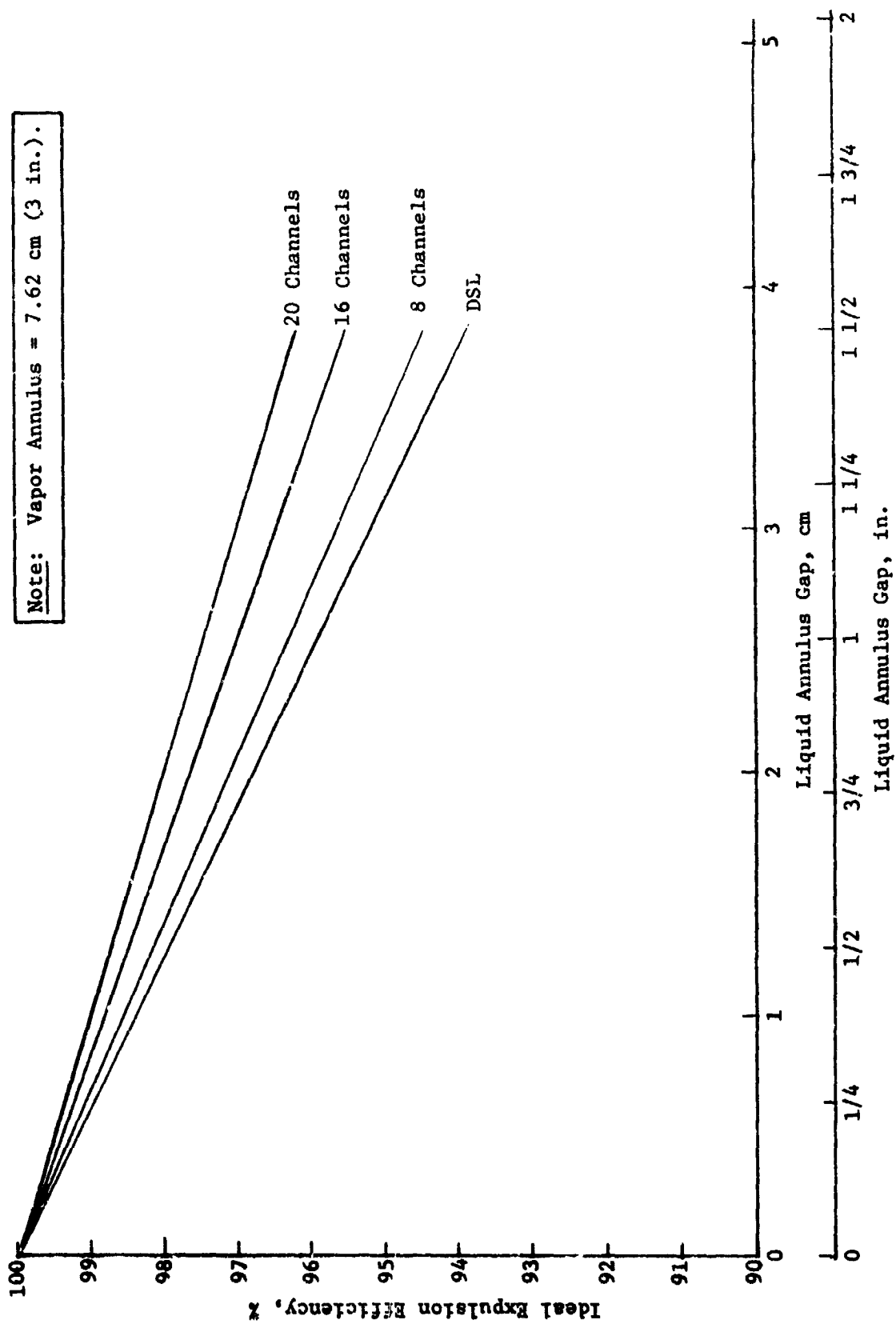


Fig. III-1 Ideal Expulsion Efficiency of Screen Systems in a 3.8-m (12.5-ft) Diameter Spherical LH<sub>2</sub> Tank

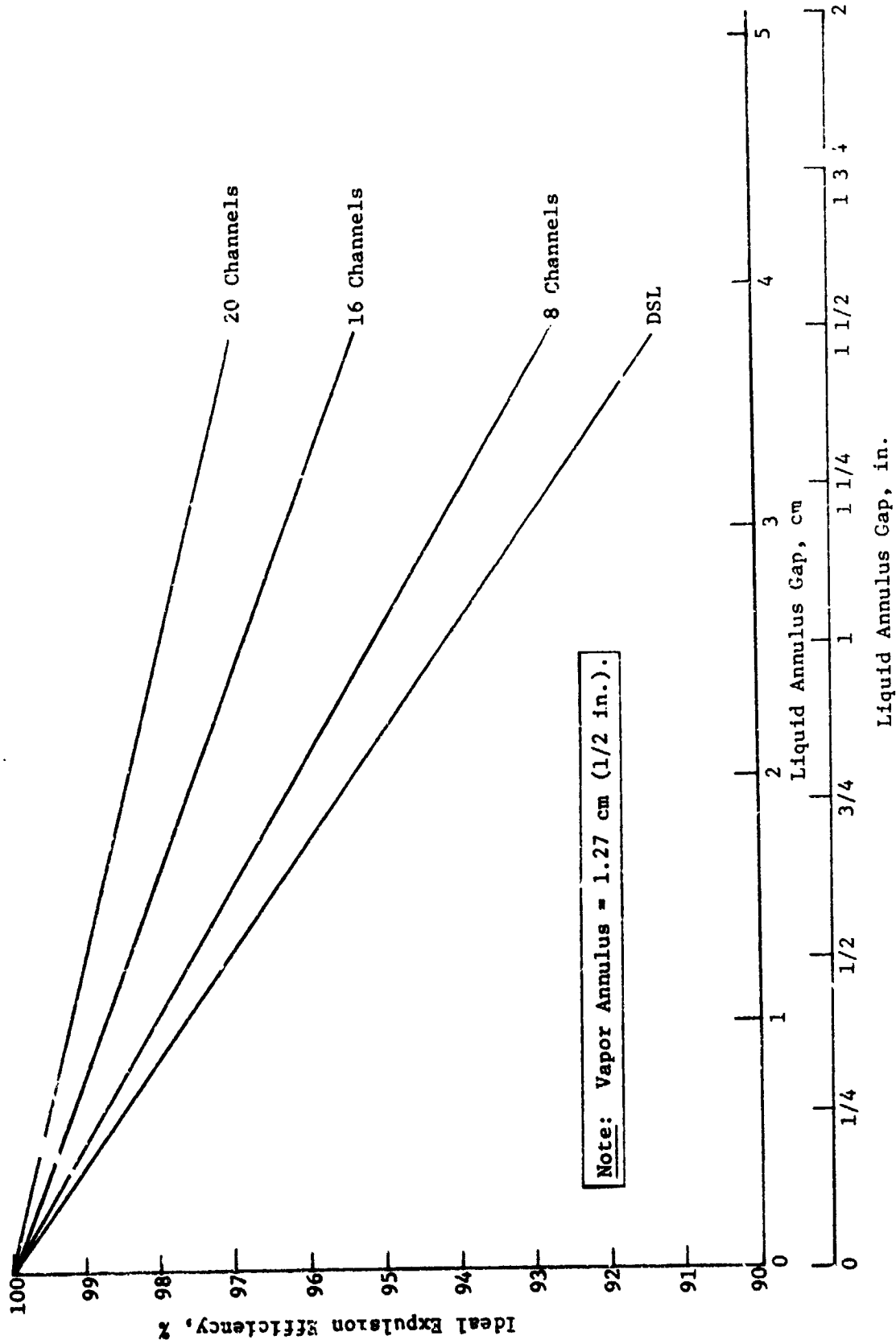


Fig. III-2 Ideal Expulsion Efficiency of Screen Systems in a 2.58-m (8.5-ft) Diameter Spherical LO<sub>2</sub> Tank

difference is as large for the  $\text{LiH}_2$  system; however, the results clearly indicate the advantage of the channel concept in terms of ideal expulsion efficiency.

To compare the outflow capabilities of the candidate systems, the computer models described in Chapter II were used. A worst-case analysis was conducted to demonstrate the ability of the systems to meet the basic mission requirements. For these systems, the worst-case is the requirement to deliver vapor-free propellant under an acceleration that tends to settle propellant away from the tank outlet (-x direction). As the bulk propellant flows into the device and out of the tank, the propellant volume decreases, as does the area it contacts on the screen device. For a constant flow rate, as this contact area decreases, the associated pressure loss across the screen increases.

Eventually the sum of the pressure losses in the system will exceed the capillary retention capability of the screen device and breakdown will occur. The computer models consider this phenomenon and compute the volume of propellant remaining in the bulk propellant region. The sum of this volume plus the device volume is then comparable for any set of constant conditions (such as acceleration and outflow rate) for any candidate device. The sum of these two volumes represents a measure of the actual expulsion efficiency.

During the course of the analysis, a number of system configurations was investigated. The volumes of the screen devices in these systems were seldom the same for any two systems. Therefore, the ideal expulsion efficiencies also differed because ideal expulsion efficiency is determined by:

$$EE_I = \frac{V_T - V_D}{V_T} \quad \text{[III-1]}$$

where  $EE_I$  = ideal expulsion efficiency,

$V_T$  = total volume enclosed by screen liner,

$V_D$  = volume enclosed by screen retention device.

The actual expulsion efficiency is expressed by:

$$EE_A = \frac{V_T - V_D - V_B}{V_T} \quad [III-2]$$

where  $EE_A$  = actual expulsion efficiency,

$V_B$  = volume remaining in the bulk propellant region at screen breakdown.

Comparing different system outflow capabilities on the basis of an arbitrarily fixed value of actual expulsion efficiency is not a useful comparison method because the systems with larger ideal expulsion efficiencies are unduly penalized. For example, a system with 98% ideal expulsion efficiency would have some finite outflow capability that would cause breakdown with 0.9% of the fluid remaining in the bulk region. Thus, the actual expulsion efficiency for that specific flow rate would be

$$EE_A = \frac{100 - 2 - 0.9}{100} = 97.1\%$$

It is impossible to compare this particular system case to another system that has an ideal expulsion efficiency of, for instance, 97% because it is physically impossible for the 97% system to have any outflow at 97.1%.

It was decided that a better comparison of outflow capabilities could be made on the basis that the actual expulsion efficiency would always be a fixed percentage of the ideal expulsion efficiency for any system. For example, if that fixed percentage of the ideal expulsion efficiency were 200%, the comparisons between two systems would always be made (at the points where the combined effect of the pressure losses caused the systems to break down) when the amounts of fluid remaining in the respective bulk regions were equivalent to the volumes contained in respective screen devices themselves, i.e.,  $V_D = V_B$ ,  $V_D + V_B = 200\% V_D$ .

Essentially two criteria were chosen for making these outflow comparisons. These were the breakdown points where the remaining propellant (representing the sum of the screen device volume plus the propellant remaining in the bulk region) was 101% of the screen device volume (i.e., the channel volume) and also 110% of the screen device volume. Thus, these criteria were called the 1.01 criterion and the 1.10 criterion.

To illustrate these criteria, consider a system with an ideal expulsion efficiency of 98%. Two percent of the propellant would be trapped in the device. The criteria, when applied to this device, would call for comparisons when breakdown occurred with 2.02% remaining for the 1.01 criterion and 2.2% remaining for the 1.10 criterion. The relationship of ideal to actual expulsion efficiency for these criteria is illustrated in Fig. III-3. These criteria are stringent measures of the capabilities of a device; they were useful in demonstrating the wide range of applicability of the acquisition/expulsion devices proposed.

Using these criteria, a systematic evaluation of the candidate systems was performed. Figures III-4 and III-5 show typical comparative results for LH<sub>2</sub> systems; Fig. III-6 and III-7 show similar comparisons for LO<sub>2</sub>. For both systems, configurations containing more than 20 channels showed sharply degraded outflow capabilities, but designs with up to 20 channels compared favorably with the DSL. Therefore, no results for configurations with more than 20 channels are shown. The differences in the flow rate capabilities between the two criteria also illustrate two points: (1) the reduced capability shown by the 1.01 criterion when compared to the 1.10 criterion shows the difficulties that will be encountered in outflowing to complete depletion, and (2) the 1.10 criterion shows that the devices can deliver propellant flow rates that will satisfy mission requirements in worst-case conditions until the propellant is very close to depletion.

Figure III-8 further illustrates the fact that the devices do not vary in outflow capability until they are almost totally depleted. For the DSL described, the outflow capability is nearly constant in the -x direction until only 10% (2.5 criterion) of the total initial propellant load remains. This is seen from the fact that the 20% and 10% curves are nearly the same. Since the ideal expulsion efficiency of this device is approximately 96%, a 90% actual expulsion efficiency implies that approximately 6% of the usable propellant remains when outflow capability begins to degrade, namely:

$$EE_A = 90\% = \frac{100 - 4 - 6}{100} \text{ for } V_D = 4\% \text{ and } V_B = 6\%.$$

The maximum outflow of the device at zero-g is approximately 10.9 kg/sec (24 lbm/sec) and is still 7.5 kg/sec (16.5 lbm/sec) or about 70% of maximum when only 0.4% ( $V_B = 0.4\%$ ) of the usable

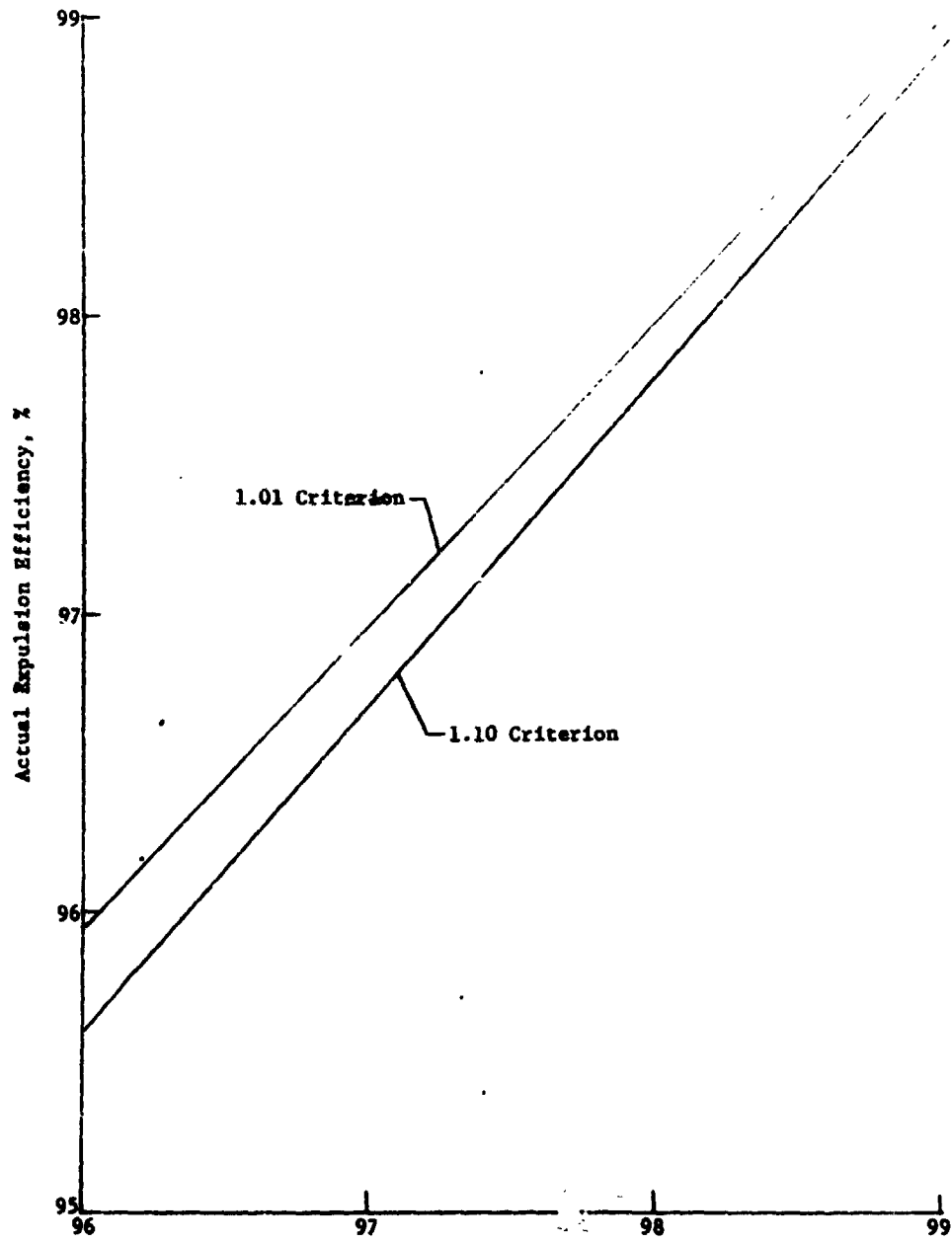


Fig. III-3 Relationship of Actual to Ideal Expulsion Efficiency for Two Outflow Capability Comparison Criteria

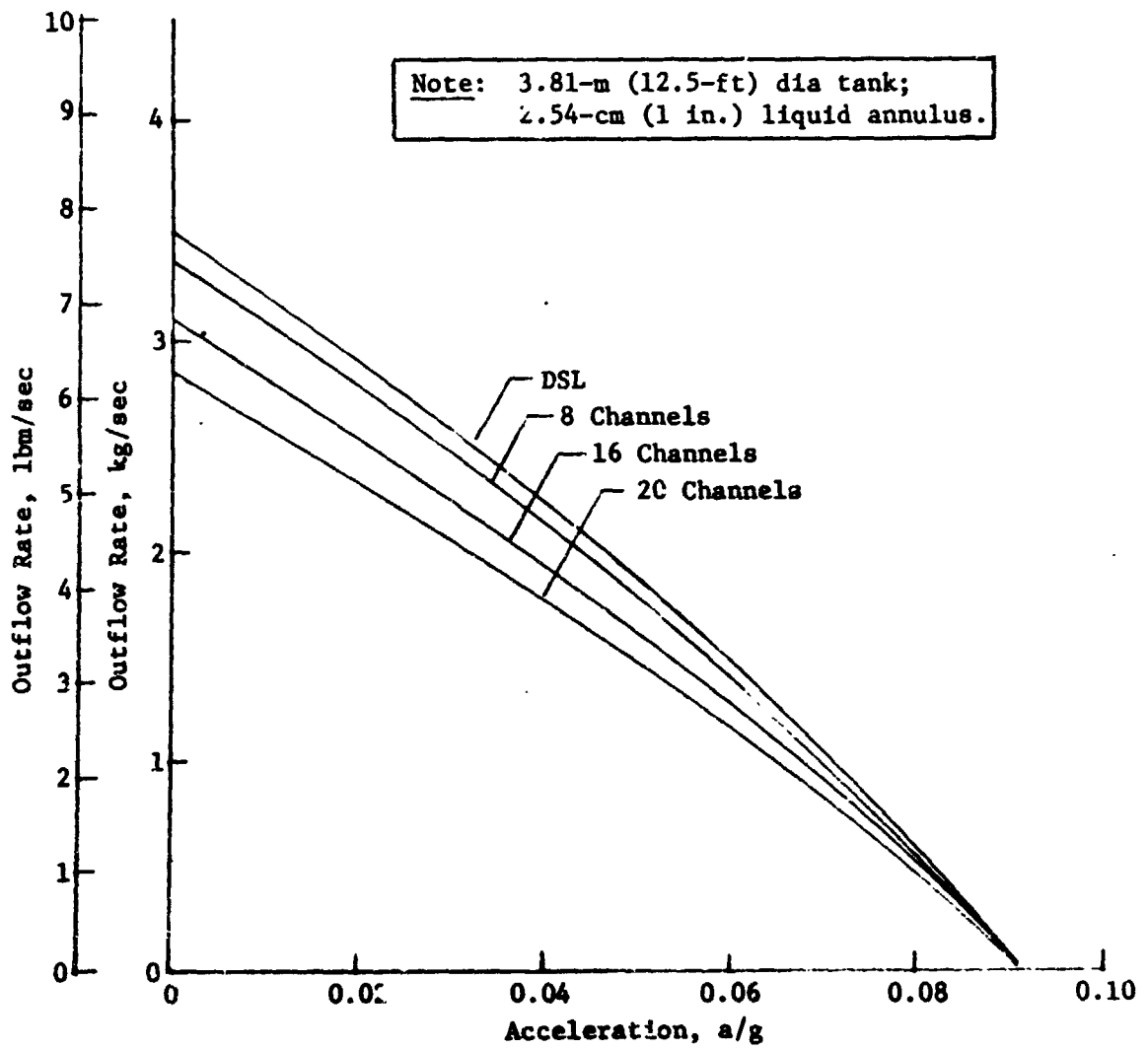


Fig. III-4 LH<sub>2</sub> Outflow Rate Capability Comparison for Screen System Using the 1.01 Criterion

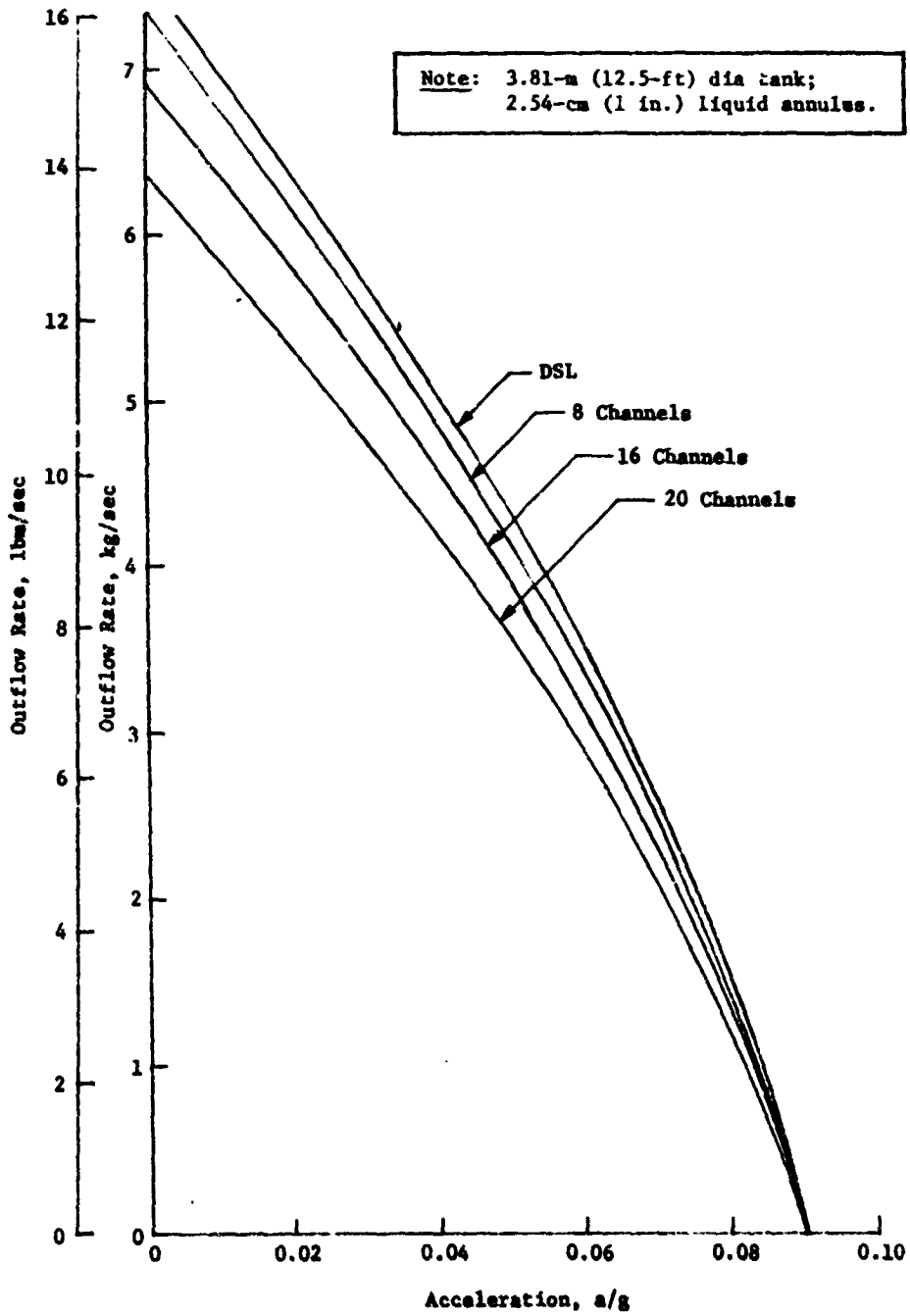


Fig. III-6  $LH_2$  Outflow Rate Capability Comparison for Screen System Using the 1.10 Criterion

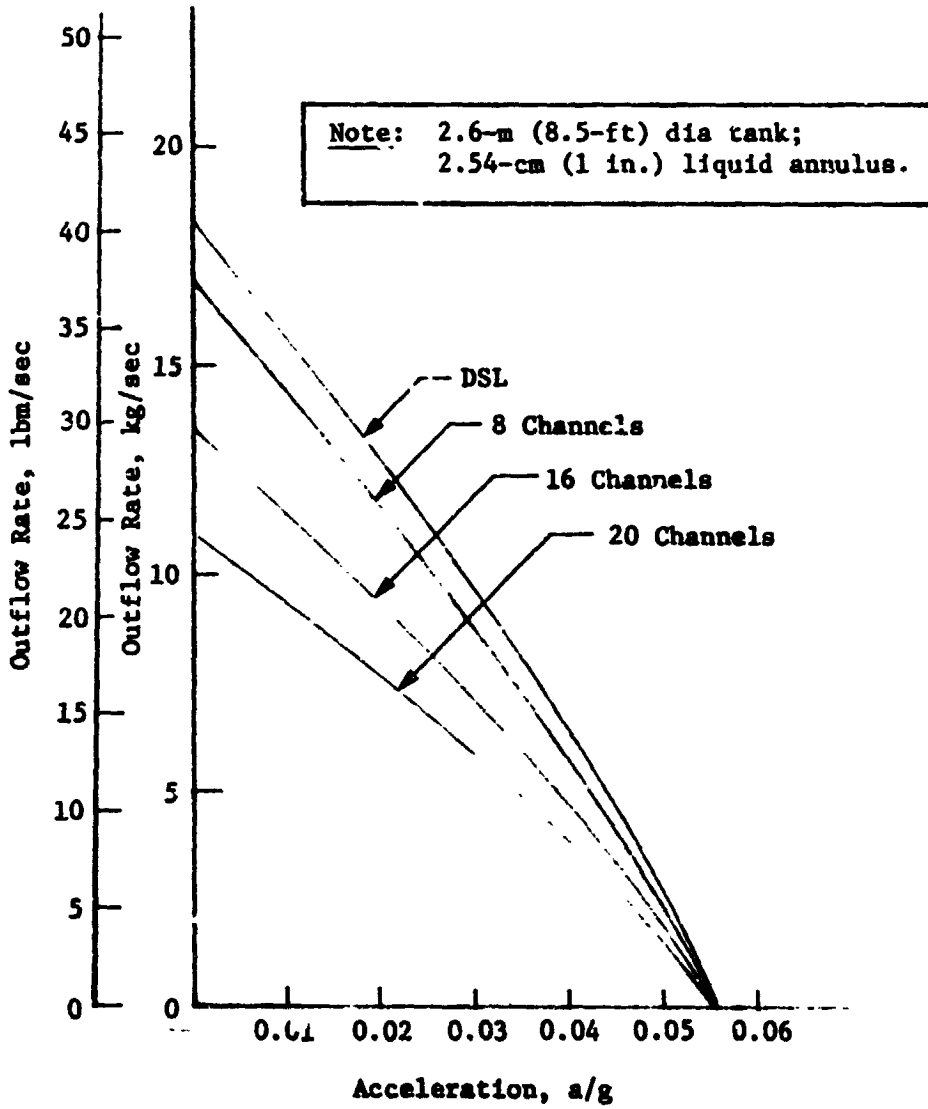


Fig. III-6  $LO_2$  Outflow Rate Capability Comparison for Screen Systems Using the 1.01 Criterion

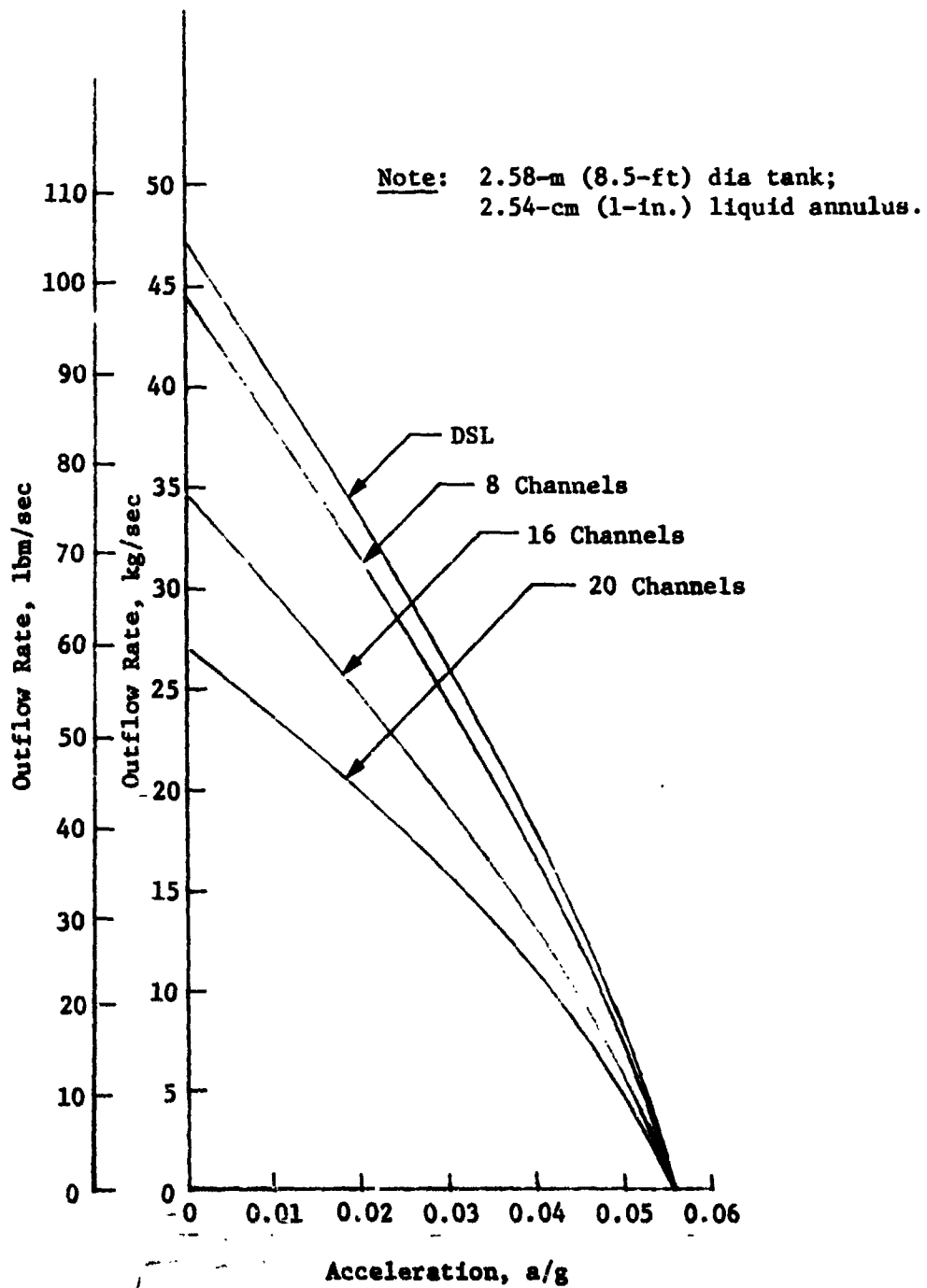


Fig. III-7  $LO_2$  Outflow Rate Capability Comparison for Screen Systems Using the 1.10 Criterion

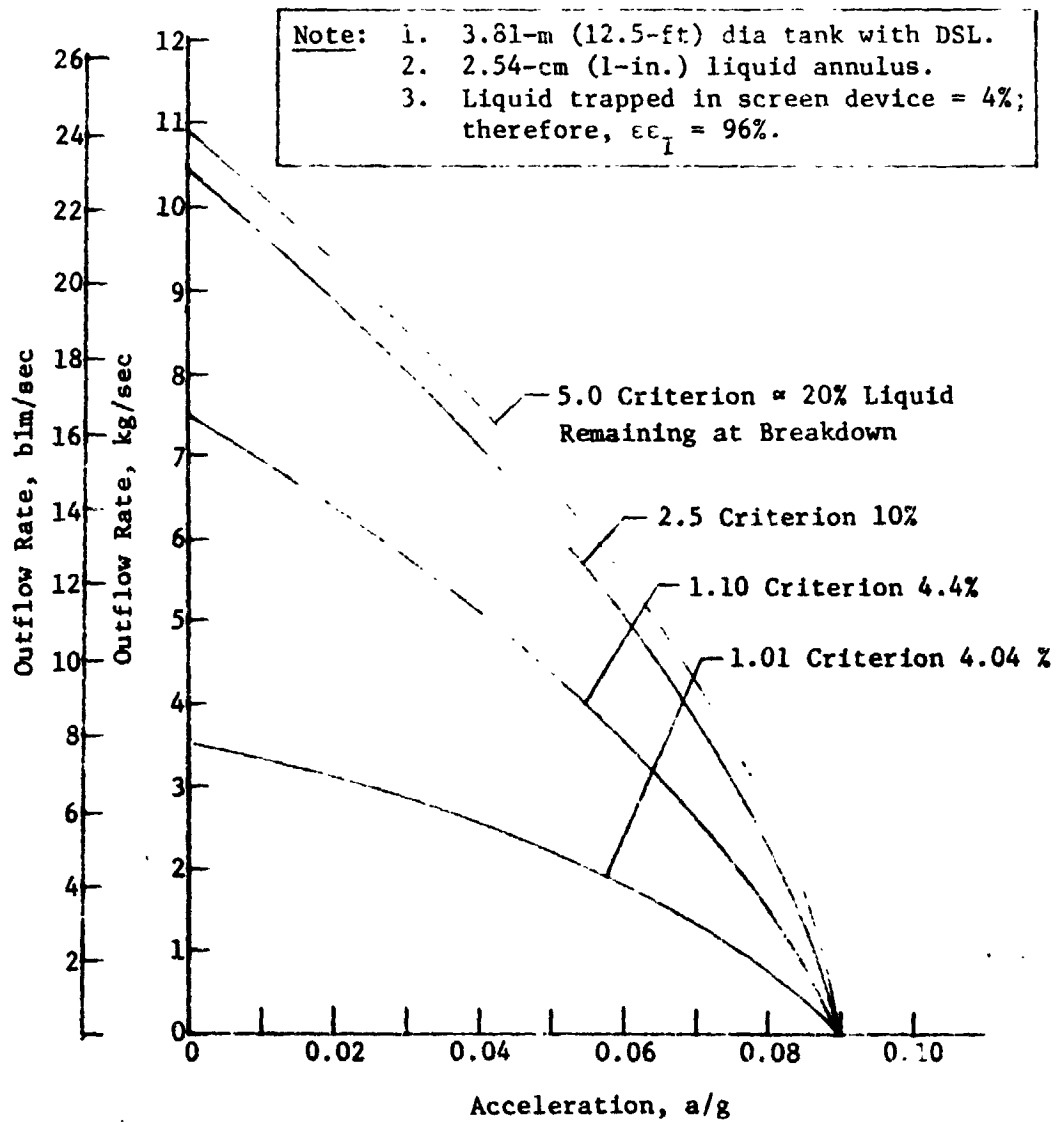


Fig. III-8 LH<sub>2</sub> Outflow Rate Capability Comparison with Varying Amounts of Propellant Remaining in Tank

propellant remains. It should also be noted that this example is not necessarily representative of the final selections because they have expulsion efficiencies in the 98 to 99% range. Therefore, they would show improved capabilities over the example in Fig. III-8.

From the results of this initial configuration definition study, it was concluded that the retention device could be designed with a 20-channel configuration. The DSL does not offer significantly increased outflow capability when compared to the 20-channel system (as shown in Fig. III-4 through III-7) and the channel design has a significantly better expulsion efficiency.

Once the initial configuration of the devices for both the LH<sub>2</sub> and the LO<sub>2</sub> tanks was determined, additional analysis was performed to determine the channel depth required to provide the necessary outflow rates. Figures III-9 and III-10 show typical results from the analysis. All parameters were held constant while the channel depth was varied. The results show a relatively linear increase in outflow capability with respect to linear increases in channel depth.

Examination of the ideal expulsion efficiency curves in Fig. III-1 and III-2 shows that a 2.54 cm (1-in.) channel depth should be near the upper limit of gap sizes because efficiencies of approximately 98% or greater, provided by channels of that depth, are reasonable and desirable goals. Reexamination of Fig. III-9 and III-10 show that the LH<sub>2</sub> system with a 2.54 cm (1-in.) channel depth can satisfy all but one of the requirements for outflow, and the LO<sub>2</sub> system meets all requirements. It should be noted that the OMS flow rate requirements are associated only with a +x acceleration vector. The capability of the LH<sub>2</sub> system can be improved by using a multiple layer screen fabrication technique. This method is described in Section C of this chapter.

From the study results, it was also concluded that the full-liner systems could not be conveniently designed to function during the high-g reentry maneuvers of the Shuttle missions. To circumvent this problem, a noncapillary reentry tank was included in one of the two tanks for each propellant. The reentry tank would have a volume sufficient to satisfy the propellant requirements during the reentry phase of the mission.

Information provided by these studies was the basis for detail design of the integrated OMS/RCS cryogenic acquisition/expulsion devices, as follows:

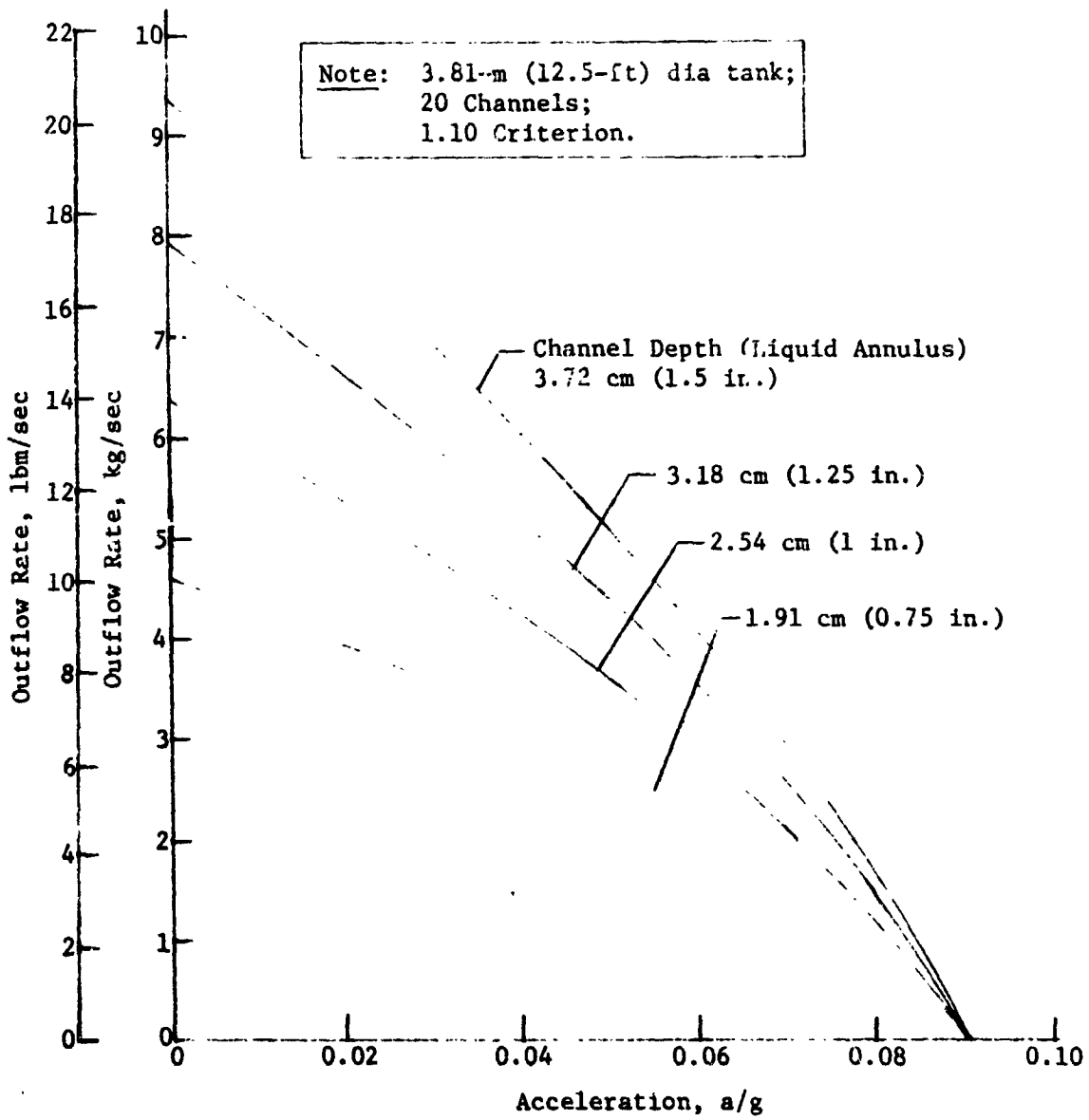


Fig. III-9 LH<sub>2</sub> Outflow Rate Capability Comparison for Varying Channel Depths

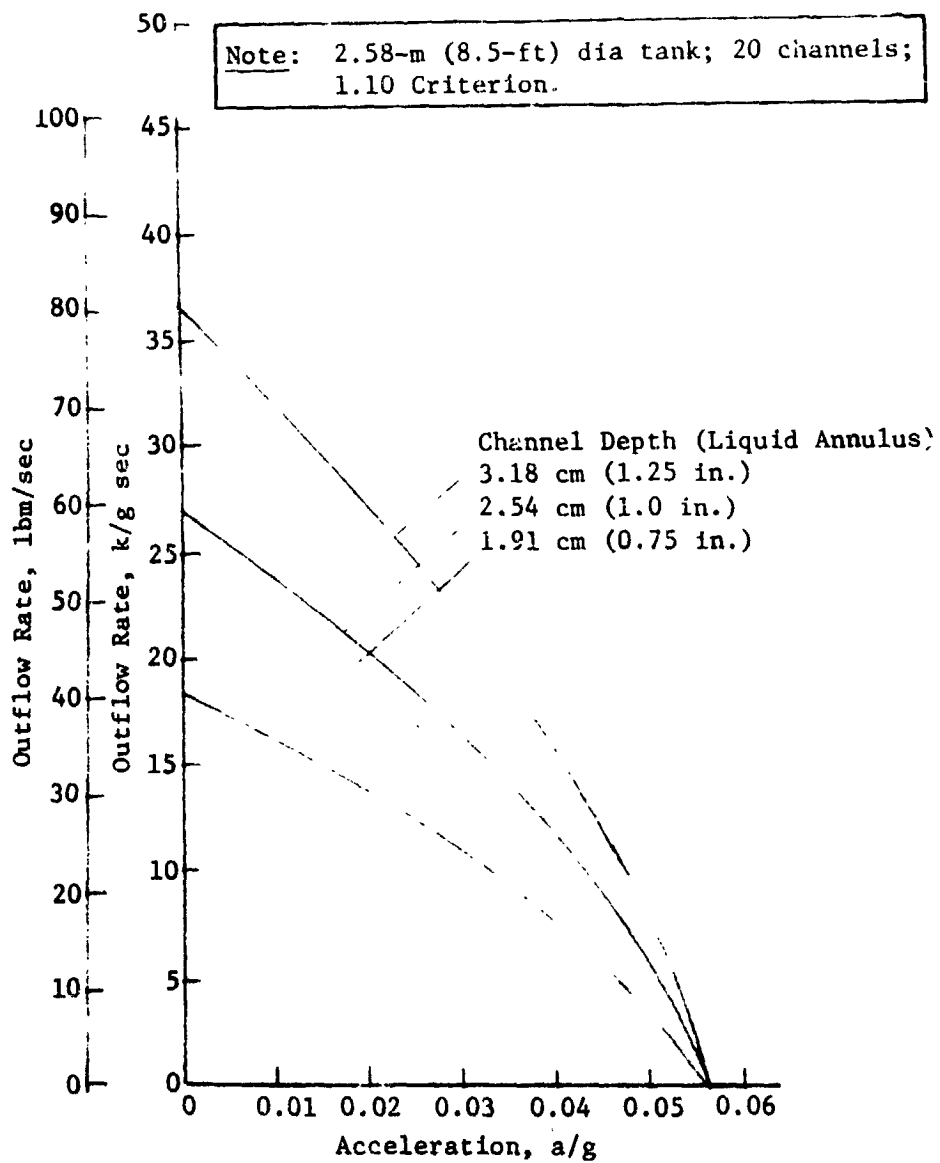


Fig. III-10  $LO_2$  Outflow Rate Capability Comparison for Varying Channel Depths

- 1) Two spherical tanks for each propellant, 3.81 m (12.5 ft) in diameter for LH<sub>2</sub> and 2.6 m (8.5 ft) in diameter for LO<sub>2</sub>;
- 2) Full screen liners, each with 20 channels, for each tank;
- 3) Channel spacing was set at 30.5 cm (12 in.) at the equator with channel depths no greater than 2.54 cm (1 in.);
- 4) A noncapillary reentry tank inside the primary tank of each propellant system was also identified.

Details and refinements of the design, including final screen selections, final configurations, material selections, and weight estimates are included in Section C.

## 2. Pressurization and Venting Analyses

The analytical approach and computer model discussed in Section B of Chapter II were used to predict the pressurization/venting requirements and performance characteristics of the selected LH<sub>2</sub> and LO<sub>2</sub> systems. The predictions were made for a representative Shuttle mission of seven days duration. The results of these analyses are shown in Table III-7 for both propellant systems. The mission simulation included all propellant outflow demands specified by the mission timeline and the pressurization usage was modeled to produce those expulsion events.

Venting was accomplished within the vent bands indicated as determined by the communication screen capillary retention capability in the two propellants. The cycle frequency differences for the two systems illustrates the effect the vent band magnitude has on the requirement for venting. The vent band magnitude of the LO<sub>2</sub> system is nearly an order of magnitude greater than that of the LH<sub>2</sub> system and the vent frequency for LO<sub>2</sub> is, correspondingly, an order of magnitude smaller. Nevertheless, the 20-cycles-per-hour vent rate of the hydrogen tank is not considered a concern.

Over the seven-day duration of the mission the temperature of the stored LH<sub>2</sub> rises only 0.67°K (1.2°R), corresponding to a pressure rise of 2.2 N/cm<sup>2</sup> (3.0 psi). These values for stored LO<sub>2</sub> are 0.89°K (1.6°R) and 2.07 N/cm<sup>2</sup> (3.0 psi). The total temperature rise for the propellants is significant when considering liquid surface tension degradation as a function of temperature rise. The numbers indicate that the surface tension decay and, therefore, the reduction in capillary retention capabilities of the integrated OMS/RCS LH<sub>2</sub> and LO<sub>2</sub> system screens, are of minimal concern.

Table III-7. Comparison of Venting Test Results

Parameters	LO	LH
Tank Sizes, m (ft) dia, each of two tanks	2.5 (8.25)	3.8 (12.5)
Pressurant Temperature, °K (°R)	222 (400)	111 (200)
Initial Pressure, N/cm <sup>2</sup> (psia)	13.8 (20)	15.0 (21.8)
Initial Liquid Temperature, °K (°R)	93.6 (168.5)	21.7 (39)
Vent Bandwidth (200x1400 A2 Screen), N/cm <sup>2</sup> (psi)	0.206 (0.30)	0.031 (0.045)
Vent Frequency, cycles/hr	2	20
Vent Mass,* kg (lbm)	108.9 (240) GO <sub>2</sub>	189.7 (418) GH <sub>2</sub>
Pressurant Mass,* kg (lbm)	42.7 (94) GO <sub>2</sub>	45.4 (100) GH <sub>2</sub>
Pressure at End of 7 Days, N/cm <sup>2</sup> (psi)	15.8 (23.0)	17.2 (25.0)
Bulk Liquid Temperature at End of 7 Days, °K (°R)	94.6 (170.1)	22.35 (40.2)
*Values are totals for both tanks.		

### 3. Offloading and Filling

a. *Offloading* - The shuttle tanks were designed to provide the capability of loading an amount of propellant equivalent to a 609.6 m/sec (2000 ft/sec)  $\Delta V$  budget. However, none of the three missions used as the baseline in Section A includes this  $\Delta V$  requirement.

The propellant loads for the three previously defined missions are: (1) seven-day polar mission, 7,241.7 kg (15,951 lbm); (2) space station resupply mission, 14,613 kg (32,189 lbm); and (3) due east mission, 11,028 kg (24,291 lbm). The total load capacity of the propellant tanks is 21,710 kg (47,820 lbm). Therefore, the tanks must be offloaded. Since an operational requirement of the channel system is that the channels remain filled with liquid throughout the mission, an offloaded tank can present a problem where the propellant level during the high-g boost phase is low enough to expose a hydrostatic head sufficient to cause screen breakdown.

This problem can be circumvented by using the series-start tank approach to propellant delivery. This approach assumes that the primary tank (tank 1) containing the reentry tank is loaded to capacity and the offloading occurs in the remaining tank (tank 2). The screen device in tank 2 will then break down during the boost phase of the mission; however, tank 2 will remain fully operational and will be capable of delivering any propellant outflow requirements on demand. Tank 1 can be supplied from tank 2 at any time a favorable acceleration exists, such as during the OMS  $\Delta V$  maneuvers, which would settle propellant over the outlet.

A small amount of propellant can be offloaded from tank 1. This offloading can be done until the liquid level exposes the height of screen that can remain stable under the 3-g boost acceleration. A maximum offloaded condition is depicted in Fig. III-11. By offloading tank 1 in the  $LH_2$  system, the maximum offload that can be accommodated is 47.85%. For the  $LO_2$  system, this percentage is 49.01%.

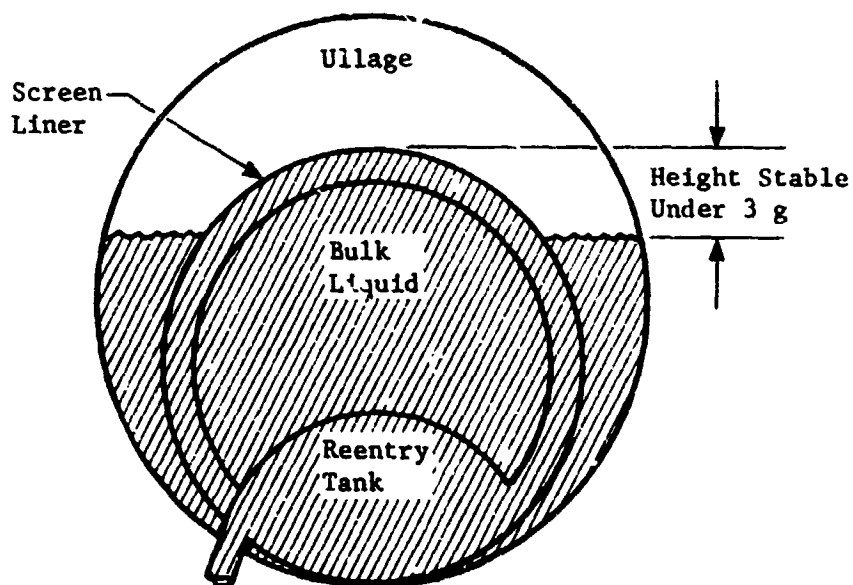


Fig. III-11 Tank in Offloaded Condition

The offload requirements for the Space Station resupply mission and the due east mission are 66% and 50.8%, respectively. These missions would be flown with the primary tank fully loaded (including 5% ullage) and the remaining 16% for the resupply mission and 0.8% for the due east mission loaded in tank 2. In the case of the due east mission, the small amount in tank 2 would be used for the orbital insertion maneuvers during the first 1 hr and 35 minutes of the mission. In the case of the seven-day polar mission, which calls for a 33.4% offload, propellant in excess of the mission requirements would have to be loaded because the minimum offload is approximately 49%. However, the minimum propellant requirements are cited for the 7-day polar mission. The polar mission is designed to perform a variety of functions that require additional propellant. For example, a 5-day mapping segment of the polar mission would raise the propellant requirements to a full capacity load. Therefore, the 49% offloading minimum is not viewed as a realistic restriction to the baseline missions.

*b. Filling* - Filling the tanks and devices can be accomplished by either of two separate methods. One method was successfully demonstrated during cryogenic testing of the 63.5-cm (25-in.) diameter test model. This method included purging the system with propellant vapors before the propellants were introduced into the tank. The purge was carried out through several pressurization and blowdown cycles to assure that all inert or undesirable gaseous elements (such as air) were eliminated from the tank. Following the purge, the subcooled cryogen was flowed into the tank until filling was completed. At ambient pressure, the cryogen must be subcooled to prevent vapor formation in the channels. If the cryogen is filled in an ambient saturated condition, vaporization can readily occur with even small heat leaks and vaporization could occur in the channels. Loading subcooled propellants helps to eliminate this concern.

The second procedure is vacuum loading. The tanks are vacuum-jacketed, so vacuum loading presents no problems from a structural standpoint. Vacuum loading is also an attractive loading option for on-orbit refilling because the tanks can be easily vented to the vacuum of space prior to the loading event.

#### 4. Feedline Analysis

Normal design practice for capillary systems involves selecting the finest mesh screen (largest pressure retention capability)

to minimize the number of screen layers required. However, analysis of the storage tank design showed a weight saving by using aluminum screen (200x1400 mesh) and supports, rather than using the 325x2300 mesh stainless steel screen. A similar analysis was performed as part of the feedline design analysis. The results showed that a similar weight saving could be realized with 200x1400 mesh aluminum screen, although the savings are less significant. For the LH<sub>2</sub> feedline, a maximum saving of 12%\* is possible for the OMS and 16%\* for the RCS. For LH<sub>2</sub> feedlines, a saving of approximately 25% may be realized for both systems. However, weight is not the only factor to be considered in the screen selection. Material compatibility, fabricability, and structural considerations are also important.

The integrated OMS/RCS feedlines are stainless steel, presenting possible incompatibility and thermal expansion problems if aluminum screen is used. The lower pressure retention capability of aluminum screen requires a larger number of screen layers for the same design conditions, compared with the stainless steel screen. However, minimization of screen layers is advantageous from the standpoint of fabrication and system reliability. Based on these considerations, 325x2300 mesh stainless steel screen was selected for the integrated OMS/RCS capillary feedline designs. The design considerations presented in Chapter II for a feedline with a screen liner were applied to the integrated OMS/RCS feedline systems. Analyses were conducted to identify feedline designs for the OMS and RCS acquisition/expulsion systems for both LO<sub>2</sub> and LH<sub>2</sub>. The number of layers of 325x2300 Dutch-rail screen required to maintain a gas-free liquid core was established and the propellant boiloff from each liner estimated.

a. *OMS Feedline Design Analysis* - Tables III-5 and III-6 showed the baseline design parameters and acceleration environment for the integrated OMS/RCS. As shown in Table III-6, the OMS operational acceleration is always in the +x direction (tending to settle propellant in the aft end of the tanks). This is an optimum design condition because the term  $\rho g L$  becomes negative, helping to decrease the resulting pressure drop in the feedline.

---

\* These numbers are based on the assumption that the spacer material density is the same as that of the screen material.

Under these conditions, from a design standpoint, the worst case is not maximum, but minimum acceleration during system operation, because this will maximize the pressure differential that must be sustained by the screen device. This minimum acceleration is +0.05 g.

The selected acquisition/expulsion system for the integrated OMS/RCS is the channel/liner system which provides a low-g venting capability. The liner design assures hydrostatic stability for most of the orbit-to-orbit maneuvers and possibly throughout the entire mission. Therefore, the feedlines must be designed to provide gas-free liquid with a liquid-free vapor annulus.

The OMS flow rates (Table III-5) result in feedline velocities of 4.97 m/sec (16.3 ft/sec) and 1.46 m/sec (4.8 ft/sec) for the LH<sub>2</sub> and LO<sub>2</sub> systems, respectively. Using these values the pressure drop terms of Eq [II-10] were calculated for both systems at the feedline inlet and outlet. For the LH<sub>2</sub> OMS, 19 screen layers are required at the feedline outlet and three layers at the inlet. The LO<sub>2</sub> OMS feedline requires only two screen layers at the outlet and one layer at the inlet. These numbers conservatively represent the number of screen layers necessary to assure gas-free liquid in the feedline core. The relatively large number of screen layers required for the LH<sub>2</sub> system is caused by the excessive length of the feedline, 18.3 meters (60 ft), and associated frictional losses.

From this discussion, several advantages may be realized by designing the liner as a function of feedline length. Assuming that the number of screen layers required varies linearly with feedline length,  $\bar{n}$ , the average number of screen layers is simply the arithmetic mean of the required layers at the feedline outlet and inlet. For the LH<sub>2</sub> and LO<sub>2</sub> OMS this corresponds to 11 and 2 layers (rounded off to highest whole number) of 325x2300 mesh stainless steel Dutch-twill screen. This results in a significant weight saving for the LH<sub>2</sub> as will be discussed later.

*b. RCS Feedline Design Analysis* - The acceleration environment for the RCS imposes different design criteria than does the OMS. Accelerations in any direction result in a worst-case design condition for the capillary feedlines; i.e., an acceleration vector such that the term  $\rho g L$  becomes additive in the basic feedline equation. In this situation the maximum acceleration must be considered. This also implies that the system will operate with a dry vapor annulus because liquid could not be forced into the annulus even if the tank liner were unstable.

RCS flow rates result in velocities of 4.97 m/sec (16.3 ft/sec) and 0.92 m/sec (3.00 ft/sec) for the LH<sub>2</sub> and LO<sub>2</sub> system, respectively. Based on feedline lengths of 3.05 m (10 ft) for both systems, an acceleration of ±0.046 g and an approach similar to that of the OMS, a capillary feedline design consistent with the candidate acquisition/expulsion system was established. The resulting design for the LH<sub>2</sub> RCS requires eight and three layers of screen at the feedline outlet and inlet, respectively. Once again the predominant terms are the friction losses and velocity head associated with liquid hydrogen flow. The small density of LH<sub>2</sub> results in large velocities, which are predominant in the resulting pressure loss terms. An average of six layers of screen are adequate for proper system design.

The lower velocities associated with liquid oxygen flow result in insignificant frictional and velocity head terms as compared to the other terms in the equation. Although the acceleration head is now significant, the increased screen pressure retention capability in LO<sub>2</sub> results in fewer screen layers and a more desirable design solution. Consequently, only two layers of screen are required at the feedline outlet and a single layer at the inlet for the LO<sub>2</sub> RCS. This is sufficient to prevent gas ingestion into the liquid core. The hardware weights associated with these screen layers are presented in Section C.

*c. Boiloff Analysis* - With low operating pressures and the small vapor-annulus gaps associated with feedline design, the effective cooling capacity of the capillary system is reduced to the heat of vaporization of the liquid propellant. During coast conditions (no flow), the amount of propellant boiloff can be estimated by the heat of vaporization of the fluid divided by the heating rate,  $q$ .

Feedline boiloff rates were obtained from Ref III-5. The values used were 4.1 kg/m (2.76 lbm/ft) and 4.6 kg/m (3.092 lbm/ft) for the LH<sub>2</sub> and LO<sub>2</sub> systems, respectively. These numbers are based on vacuum-jacketed stainless steel lines. For the feedline lengths specified in Table III-8, corresponding boiloff is 55.4 kg (122 lbm) and 21.3 kg (47 lbm) for the LH<sub>2</sub> and LO<sub>2</sub> OMS, respectively. The RCS boiloff is 9.5 kg (21 lbm) for LH<sub>2</sub> and 14.1 kg (31 lbm) for LO<sub>2</sub>. The resulting total boiloff for the LH<sub>2</sub> feedline is 65 kg (143 lbm) and for the LO<sub>2</sub> feedline 35.4 kg (78 lbm).

The integrated OMS/RCS capillary feedline design is summarized in Table III-8.

Table III-8 Integrated OMS/RCS Feedline Summary

GEOMETRY	LH <sub>2</sub>		LO <sub>2</sub>	
	OMS	RCS	OMS	RCS
Feedline Length, m (ft)	18.3(60)	3.05(10)	4.6(15)	3.05(10)
Number of 90° Bends (Estimated)	3	3	3	3
Screen Liner-Inner Diameter, cm (in.)	10.2(4)	10.2(4)	10.2(4)	10.2(4)
Maximum Layers of 325x2300 Screen*	19	8	2	2
Minimum Layers of 325x2300 Screen *	3	3	1	1
Average Layers of 325x2300 Screen	11	6	2	2
<b>PERFORMANCE CHARACTERISTICS</b>				
Pressure Drop during Outflow, N/cm <sup>2</sup> (psi)	0.31(.45)	0.61(.89)	0.29(.42)	0.86(1.25)
Maximum g in -x Direction for Hydro- static Stability	0.047	0.079	0.347	0.347
Feedline Boiloff, Kg/m (lbm/ft)	55.4(122)	9.5(21)	21.3(47)	14.1(31)
Liquid Usage for TPA Cooldown, kg (lbm)	28.6(63)	N/A	9.5(21)	N/A
* Maximum layers of screen are required at feedline outlet and minimum at feedline inlet.				
Note: All feedlines use 300 series stainless steel for vacuum jacket, inner line, and screen liner.				

C. DETAILED DESIGN

Various aspects of the detailed design effort, including discussions of final material selection, system capabilities, system weight, and operational characteristics are presented here. Detailed configuration drawings and dimension summaries are also included for the screen systems in both the tanks and the capillary feedlines.

1. Storage Tank Design

The preliminary design and configuration tradeoffs discussed in Section B defined the integrated OMS/RCS in a general manner to include the following features: (1) two spherical tanks for each of the propellants, with the hydrogen tanks 3.8 m (12.5 ft) in diameter, and the oxygen tanks approximately 2.6m (8.5 ft) in diameter; (2) full screen liners for each of the tanks with 20 channels evenly spaced at a distance of 30.4 cm (12 in.) at the equator; (3) channel depths of no more than 2.54 cm (1 in.); and (4) a noncapillary reentry tank in the primary tank (tank 1) of each propellant system with a capacity sufficient to satisfy the propellant requirements during the reentry phase of a Shuttle mission.

One of the primary objectives of the detailed design effort was to minimize the weight of the retention device as much as possible while meeting structural requirements and propellant demand. All of the initial system capability analyses were conducted for structures that were assumed to be stainless steel 325x2300 Dutch twill screen supported by a stainless steel perforated plate back-up structure. The octosphere structural analysis presented in Chapter II and the results shown in Fig. II-49 and II-50 indicate that for both stainless steel and aluminum, the perforated plate thickness, which would be structurally adequate, is less than the gage thicknesses normally considered minimum for these types of applications. On this basis, even though the stainless steel minimum gage is less than that of aluminum, the density of aluminum (one-third that of stainless steel) makes it an attractive structural material option. The disadvantage of aluminum is that it is not commercially available in Dutch twill screens with as fine a mesh as stainless steel. The finest available aluminum screen is 200x1400 mesh. One layer of 200x1400 aluminum screen cannot provide the capillary retention capability of the one layer of the 325x2300 stainless steel screen used in the preliminary analysis. However, the added capabilities of two layers of 200x1400 aluminum screen exceed the capability of a single layer of

325x2300 mesh screen while weighing less. This, together with the additional weight savings achieved by using an aluminum support structure, makes aluminum the primary candidate material for the retention devices

The outflow capabilities of the systems using two layers of 200x1400 screen are compared with the same systems using one layer of 325x2300 in Fig. III-12 and III-13. The comparisons show that although the two-layer system cannot deliver the propellant volumes at zero-g that the single-layer system can, this condition is reversed as the acceleration level increases so that the overall capability of the two layers of 200x1400 is significantly better.

The curves presented in Fig. III-12 and III-13 illustrate the capabilities of the two tank designs in an adverse acceleration condition (-x direction). They indicate that the aluminum designs can meet the entire mission propellant demand when nearly depleted (1.10 criterion) in a negative acceleration environment with the exception of the 13.2 kg/sec (29 lbm/sec) outflow of  $LO_2$  for an OMS burn at 0.07 g. However, all OMS burns produce accelerations in the +x direction. To account for the differences in the interaction of the various pressure loss terms for this condition, additional outflow predictions were developed. Figure III-14 illustrates these results for the  $LH_2$  system. As shown, the capability to outflow propellant is increased when the acceleration vector is in the +x direction. Similar predictions are shown for  $LO_2$  in Fig. III-15.

The curves for  $LO_2$  show that the 13.2-kg/sec (29-lbm/sec) requirement cannot be met by the 1.10 criterion for 0.07 g in the +x direction. A criterion of approximately 1.5 must be applied to show sufficient system performance to deliver 13.2kg/sec (29 lbm/sec) at + 0.07 g. The ideal expulsion efficiency of the oxygen device is 98.1%; therefore, applying a 1.5 criterion to the system implies that the actual expulsion efficiency for an OMS outflow at 0.07 g would be 97.2%. This represents an ability to outflow an OMS propellant demand until 0.9% of the usable propellant remained in one tank, an equivalent of 0.45% of the total potential usable propellant load of the Shuttle  $LO_2$  tanks. It should be noted that none of the potential Shuttle missions calls for an OMS propellant demand when the volume of propellant remaining is that low.

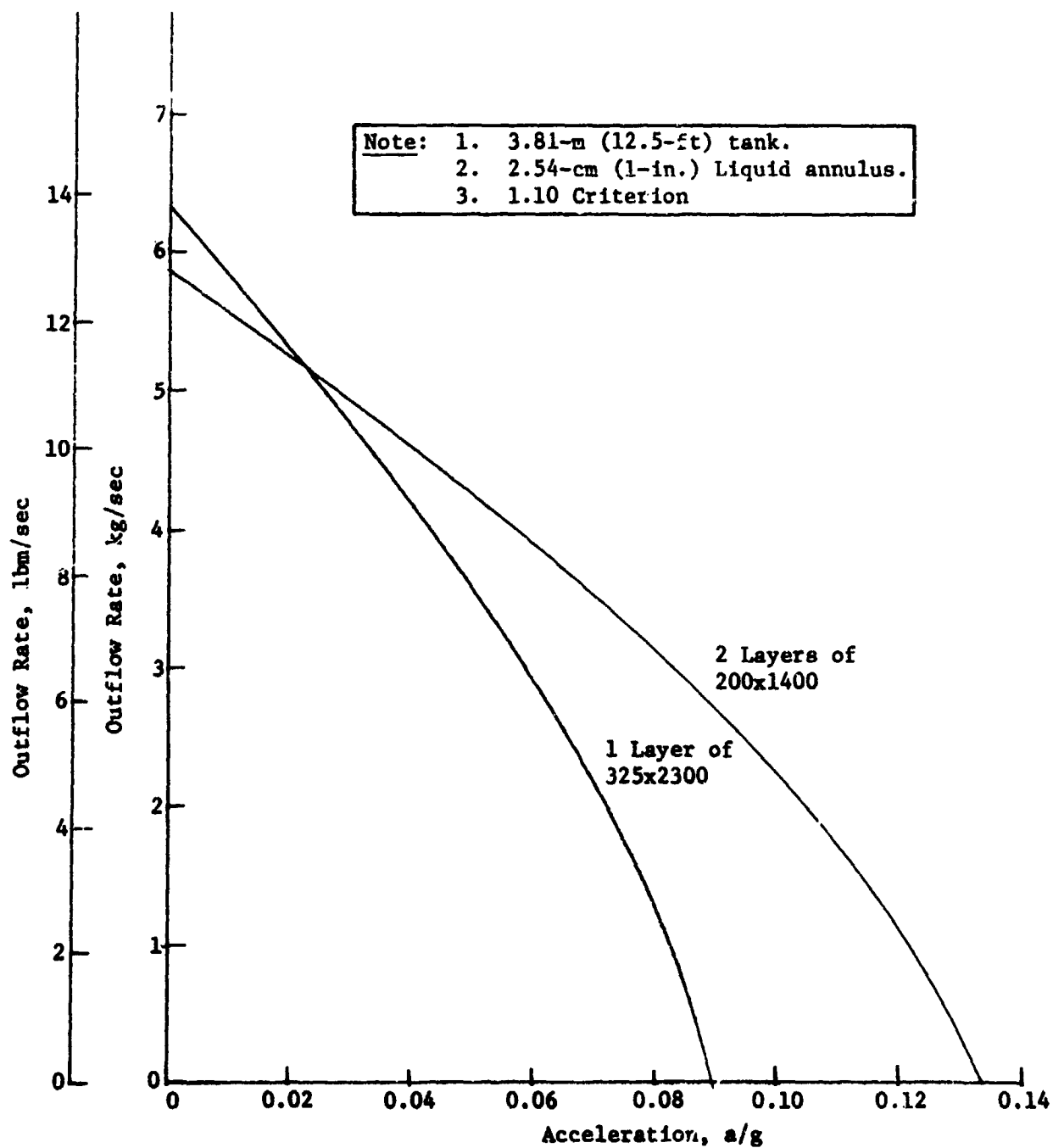


Fig. III-12 LH<sub>2</sub> Outflow Rate Capability Comparison between Single- and Double-Layer Screen

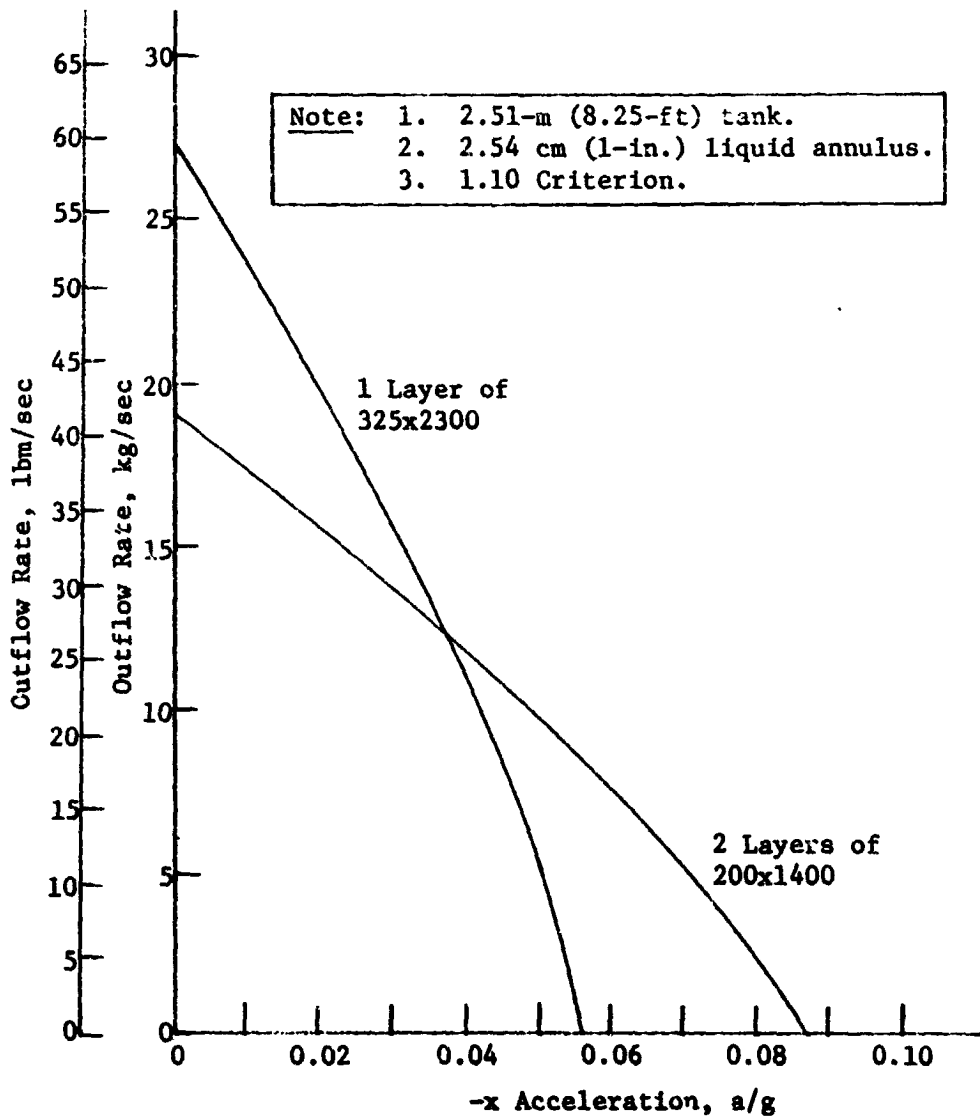


Fig. III-13 *LO<sub>2</sub> Outflow Rate Capability Comparison between Single- and Double-Layer Screen*

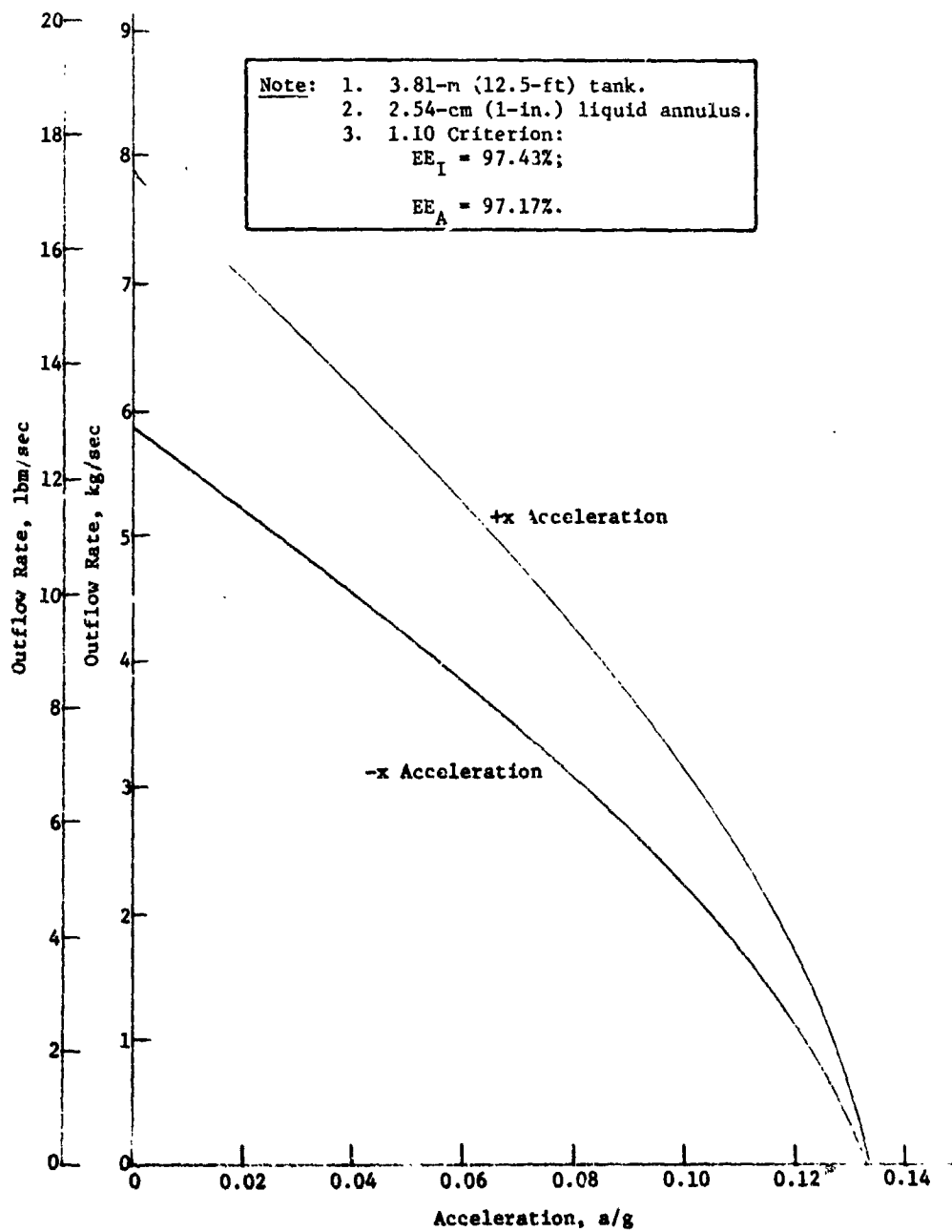


Fig. III-14  $LH_2$  Outflow Rate Capability Comparison for Positive and Negative Accelerations

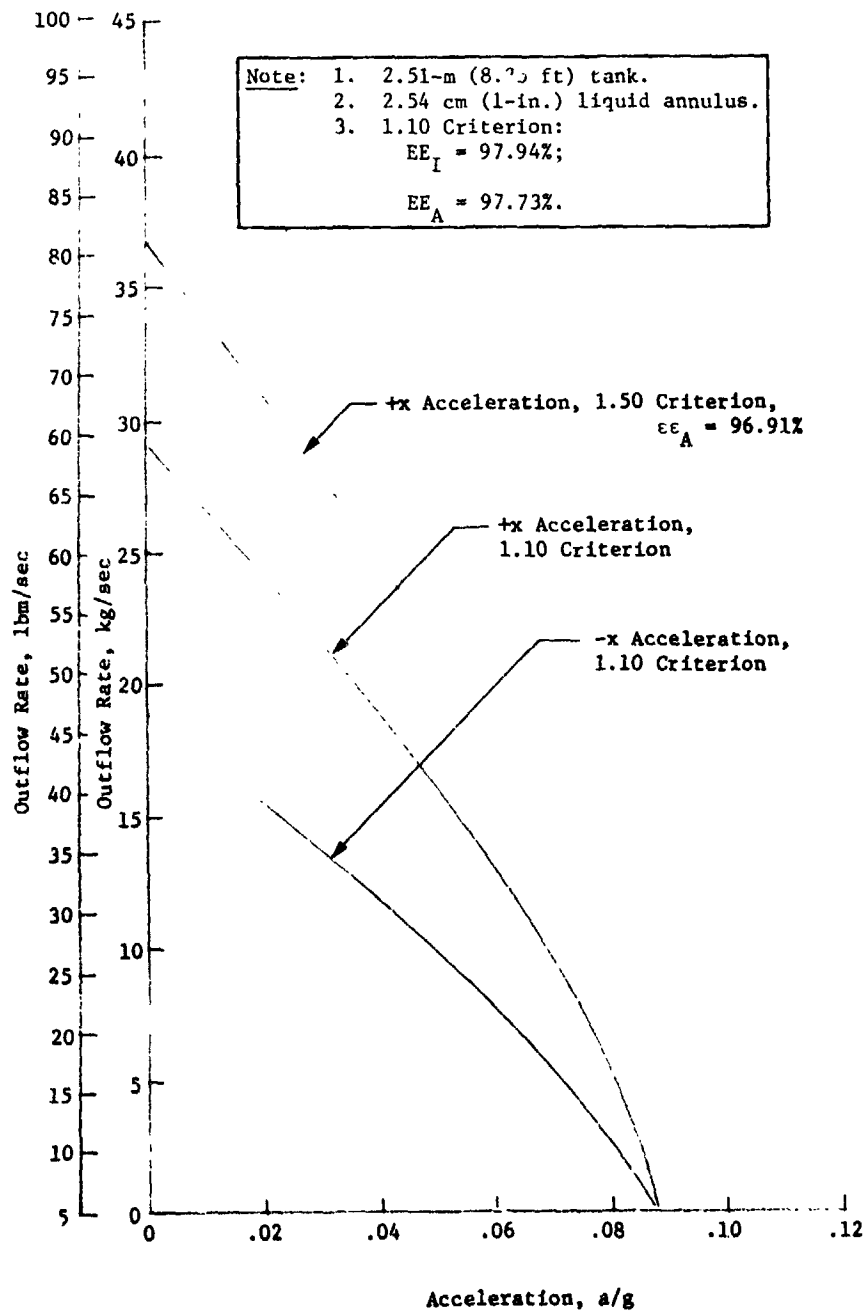


Fig. III-16  $LO_2$  Outflow Rate Capability Comparison for Positive and Negative Accelerations

A further attempt to reduce the weight of the retention devices involved a detailed analysis of the mission duty cycles with regard to the propellant demand timeline. Within a limited range of variations, all of the missions called for use of some propellant from the OMS/RCS tanks within the first 1.0 to 1.5 hours after launch. These demands were not constant for each mission, but were of the same order of magnitude. These usage schedules are shown in Table III-9, representing the total use from the tanks before the first extended coast period in the mission. The coast period begins at the end of the event occurring at the mission time denoted in the table.

Table III-9 Shuttle Mission Initial Propellant Usage

	LH <sub>2</sub> kg (lbm)	LO <sub>2</sub> kg (lbm)
<u>7-Day Polar Mission</u>		
OMS requirements	452.2 (996)	2262 (4982)
RCS requirements	30 (66)	150.3(331)
Total Used to Time 1:35:30	482.1(1062)	2412 (5313)
<u>Space Station Mission</u>		
OMS requirements	172.5 (380)	862.6(1900)
RCS requirements	14.1 (31)	68.1 (150)
Total Used to Time 0:51:08	186.6 (411)	930.7(2050)
<u>Due East Mission</u>		
OMS requirements	315.0 (694)	1576 (3472)
RCS requirements	30 (66)	150.2 (331)
Total Used to Time 1:35:00	345 (760)	1726 (3803)

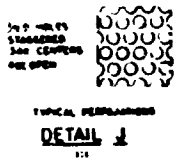
The operational philosophy of the proposed designs during extended low-g periods is that the initial ullage requirements for each propellant load must be contained strictly within the vapor annulus. The 5% ullage load does not represent the entire volume of

the vapor annuli of the designs, particularly in the hydrogen tank, where a large annulus gap is necessary to ensure reasonable venting characteristics. The approach adapted for the integrated OMS/RCS requirements, therefore, was to load some of the mission propellant in the vapor annulus. The propellant masses listed in Table III-9 represent the volume of propellant that will be outflowed almost immediately after launch. Since this propellant mass is not stored in orbit for any period of time, it does not need to be enclosed by the liner.

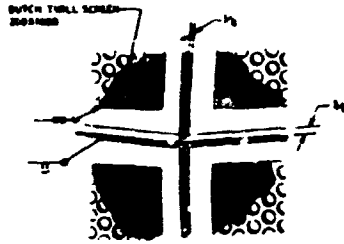
The diameter of the liners for both the LH<sub>2</sub> and LO<sub>2</sub> systems were reduced so that the volume contained in them represented the volume of the initial ullage plus the volume of the propellant to be used during the mission time specified in Table III-9. To make a special design for each mission unnecessary, the propellant volume specified to be used during the first 51 min 8 sec of the space station mission was used to size the liner diameters. This propellant mass represents the least amount required of the three missions before the first coast period. Based on these considerations, the 3.8-m (12.5-ft) diameter LH<sub>2</sub> tank was designed with a 3.58-m (11.75-ft) diameter liner, and the 2.51-m (8.25-ft) diameter LO<sub>2</sub> tank was designed to include a 2.42-m (7.94-ft) diameter liner.

The detailed design drawing for the LH<sub>2</sub> acquisition/expulsion system is shown in Fig. III-16. The LO<sub>2</sub> system is not pictured because, except for the dimensions, it would essentially be identical in appearance. The system is an all-aluminum welded design fabricated of 200x1400 aluminum Dutch twill screen and 0.076-cm (0.030-in.) (50% open area) aluminum perforated plate. The channels are tapered from a rectangular cross-section at the liner equator to an essentially square cross-section at the point where they enter the manifold near the pole of the device or in the start tank manifold. The tapered design was adopted so that the material required to make the manifold would be minimized, thus saving weight.

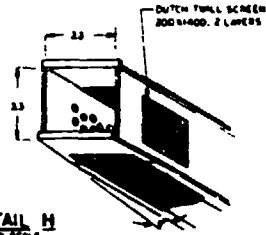
The design consists of 20 gore panels in each hemisphere. The gore sections are perforated plate covered with a layer of 200x1400 screen. An outflow channel is located in the center of each panel. The channels are fabricated of both plate and perforated plate and are covered with two layers of 200x1400 screen where required. All the screen attachments are made by continuous resistance seam welds. Under an IRAD program, this design approach



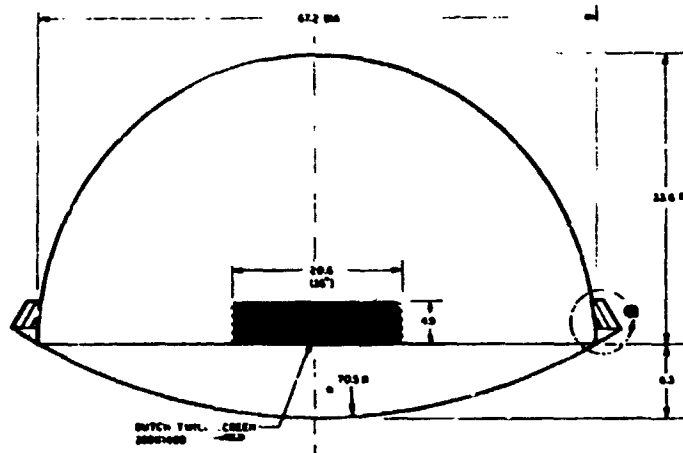
**DETAIL J**  
NO SCALE



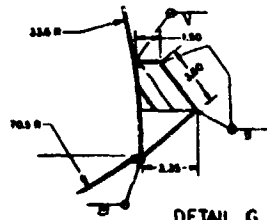
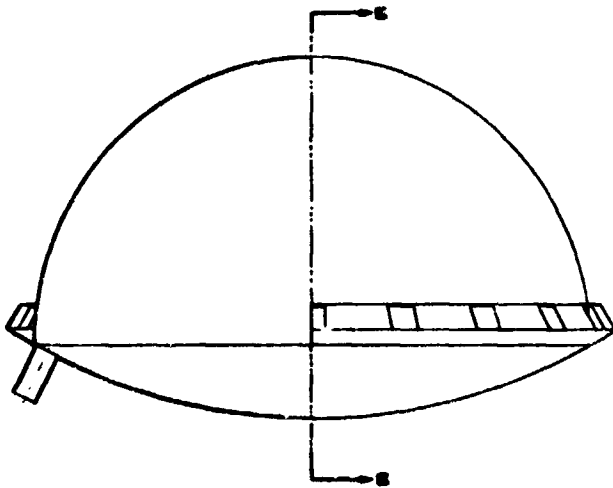
**DETAIL K**  
NO SCALE



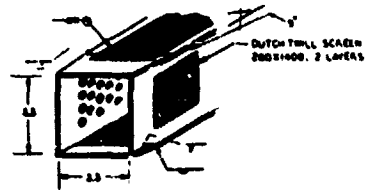
**DETAIL H**  
NO SCALE



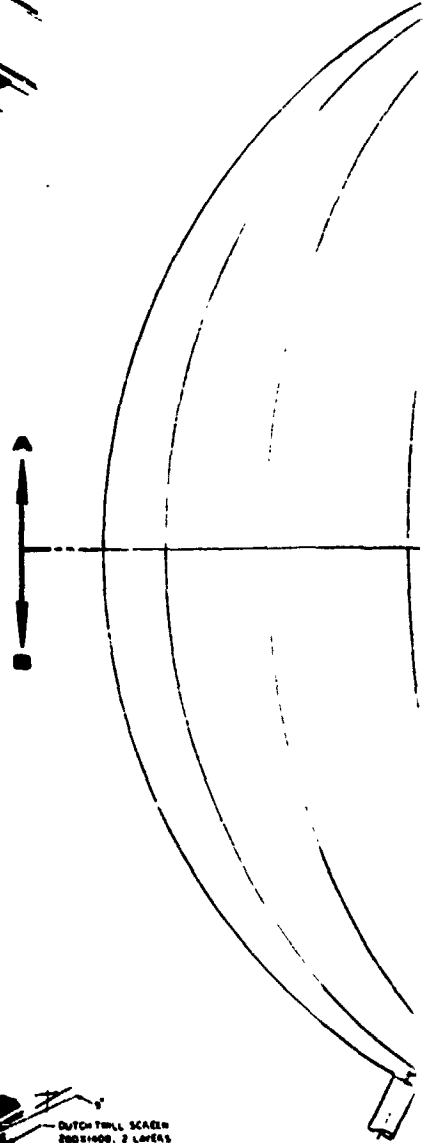
**SECTION E-E**



**DETAIL G**  
1:3



**DETAIL E**  
NO SCALE



**FOLDOUT FRAME**

FC

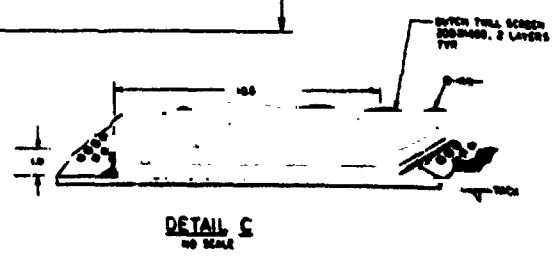
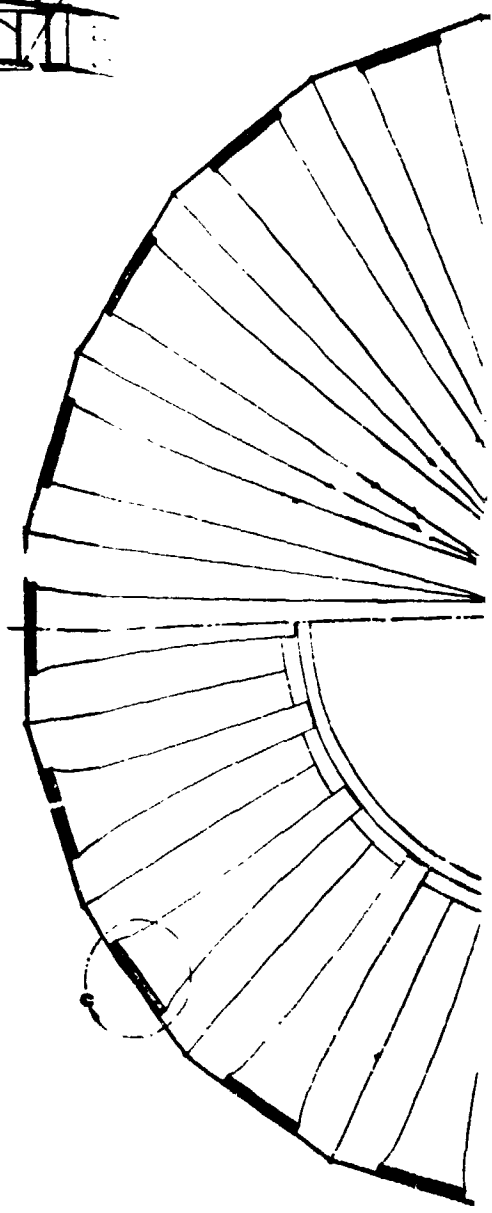
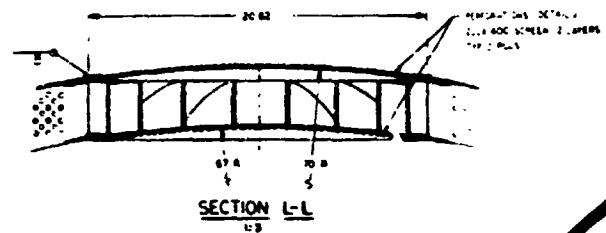
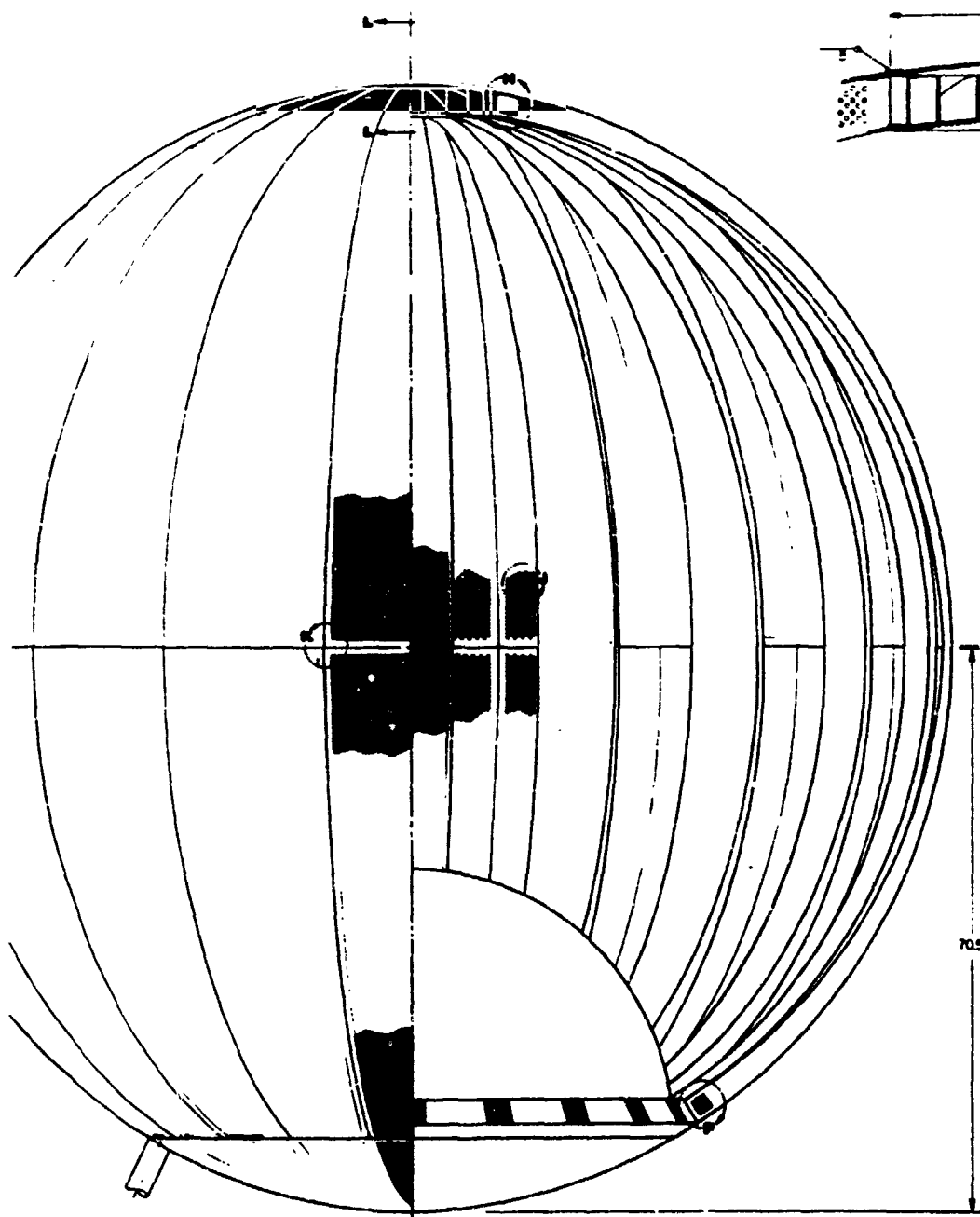
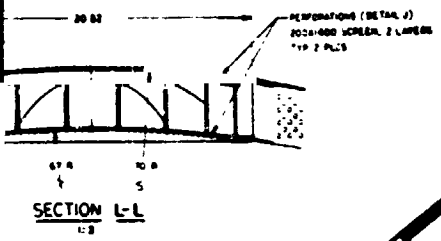


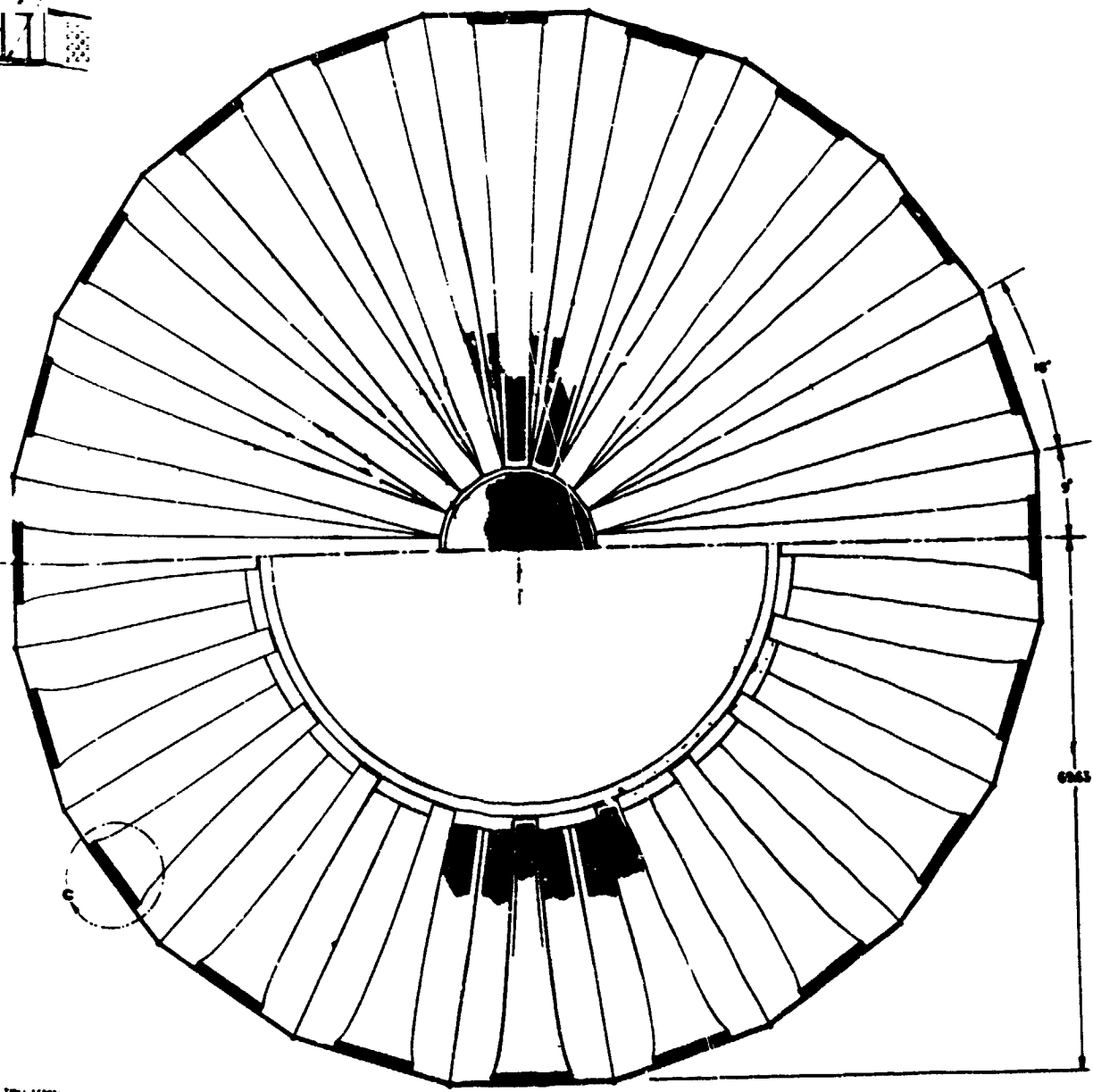
Fig. III-1

FOLDOUT FRAME  
2

REINFORCING DETAILS  
3



HALF SECTION A-A



HALF SECTION B-B

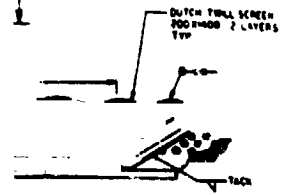


Fig. III-16 Detail Design for LH<sub>2</sub> Acquisition/Expulsion System

III-41 and III-42

WOLFOOT DRAWING  
3

was verified through the fabrication and assembly of a 1.77-in (70-in.) liner. (See Chap. IV, Vol III.)

A reentry tank is included in one tank for each propellant. The channels drain into a manifold around the reentry tank and the manifold discharges into the reentry tank through a single entry port. All propellant expelled from the systems is flowed through the single outflow line of the reentry tank. The outflow line is positioned so that during the reentry phase of the Shuttle mission the acceleration will settle the propellant over the exit port and complete tank draining will be possible. The entry port into the reentry tank is directly opposite the outflow line so that during 2.3-g reentry, propellant will be unable to drain out of the tank through this opening.

The inlet port of the reentry tank is covered with screen backed by perforated plate so that propellant will be held in the tank by capillary action, if required, during the terminal portion of the low-g part of the mission. Placing this screen in the system flow path created an additional pressure loss in the fluid. The inlet port was sized so the loss experienced by the flowing propellant was not of such a magnitude as to require the start tank dome weights to become excessive. The inlet port for the hydrogen system was sized so that a  $0.31\text{-N/cm}^2$  (0.45-psi) pressure drop was experienced by the  $\text{LH}_2$  flowing through it. The domes for the  $\text{LH}_2$  start tank were then designed for a  $0.52\text{-N/cm}^2$  (0.75-psi) collapsing pressure; the dome material thicknesses are 0.076 cm (0.030 in.) and 0.177 cm (0.070 in.), respectively.

Similarly, the 56.9-cm (22.4-in.) radius dome of the  $\text{LO}_2$  reentry tank is 0.089cm (0.035 in.) thick and the 120-cm (47.2-in.) radius dome is 0.1828 cm (0.072 in.) thick, based on a  $1.38\text{-N/cm}^2$  (2.0-psi) collapsing pressure. The radii of the tank domes represent a tank volume sufficient for all propellant requirements during the reentry maneuver so that once the reentry is initiated, the capillary channels no longer have a function in the propellant delivery system.

A summary of the design geometry details is presented in Table III-10 for both the  $\text{LH}_2$  and  $\text{LO}_2$  systems. The figures listed for the channel dimensions represent the cross-sectional dimensions at the equator followed by the cross-sectional dimensions at the manifolds.

Table III-10 Acquisition/Expulsion System - Dimension Summary

	LH <sub>2</sub>	LO <sub>2</sub>
<b>Outer Liner and Feeder Channels</b>		
Diameter, m (ft)	3.58 (11.75)	2.42 (7.94)
Gas Annulus, cm (in.)	11.4 (4.50)	4.73 (1.865)
Communication Screen Mesh	200x1400	200x1400
Channel Screen Mesh, 2 layers	200x1400	200x1400
Perforated Plate, Percent Open Area	50	50
Liquid Annulus at Equator, cm (in.)	2.54 (1.0)	2.54 (1.0)
Channel Width at Equator, cm (in.)	26.9 (10.6)	8.23 (3.24)
Channel Width at Manifold, cm (in.)	8.4 (3.3)	4.57 (1.8)
Channel Depth at Equator, cm (in.)	2.54 (1.0)	2.54 (1.0)
Channel Depth at Manifold, cm (in.)	8.4 (3.3)	4.57 (1.8)
Communication Screen Width at Equator, cm (in.)	28	29.5
Number of Feeder Channels	20	20
<b>Reentry Tank, in Tank 2 Only,</b>		
Volume, m <sup>3</sup> (ft <sup>3</sup> )	1.54 (54.6)	0.453 (16.0)

The final system weights are shown in Table III-11. It should be noted that in the secondary tank (tank 2) for each propellant, the weight of the channels is less than in the other tank for that propellant. This is because the length of the channels is reduced in one of the hemispheres by the presence of the reentry tank. These weights were established before the results of the analysis of structural characteristics for fine mesh screens became available. The results of that analysis indicate that the removal of the supporting perforated plate from the communication screen in the LH<sub>2</sub> design is feasible. The capillary retention pressure of 200x1400 screen in LO<sub>2</sub> makes the removal of the perforated plate support from the screen unfeasible because unsupported screen spans must be small.

Table III-11 Propellant Storage System Dry Mass for Integrated OMS

Component	LO <sub>2</sub> Storage System Mass, kg (lbm)		LO <sub>2</sub> Storage System Mass, with perforated plate, kg (lbm)		LH <sub>2</sub> Storage System Mass without perforated plate, kg (lbm)	
	Tank 1	Tank 2	Tank 1	Tank 2	Tank 1	Tank 2
Vacuum Jacket, including Girth Ring	347.7 (766)	347.7 (766)	1206 (2657)	1206 (2657)	1206 (2657)	1206 (2657)
Inner Tank, including Girth Ring, P = 34.45 N/cm <sup>2</sup> (50 psia)	123.0 (271)	123.0 (271)	280 (616)	280 (616)	280 (616)	280 (616)
Acquisition/Expulsion System						
Screen Liner	23.8 (52.5)	23.8 (52.5)	52.2 (115.1)	52.2 (115.1)	36.3 (80.0)	36.3 (80.0)
Feeder Channels	15.8 (34.8)	13.2 (29.2)	37.2 (81.9)	31.3 (69.0)	37.2 (81.9)	31.3 (69.0)
Reentry Tank and Manifold		11.4 (25.2)		22.7 (50.1)		22.7 (50.1)
Manifold, Supports, Weld, etc	1.13 (2.5)	1.13 (2.5)	3.04 (6.7)	2.67 (5.9)	3.04 (6.7)	2.67 (5.9)
Subtotal	40.7 (89.8)	49.6 (109.4)	52.5 (115.7)	109 (240.1)	76.5 (168.6)	93.1 (205.0)
Total System Mass	466.2 (1026.8)	475 (1046.2)	1578 (3476.7)	1595 (3513.1)	1562 (3441.6)	1580 (3478.0)

Note: Estimate does not include mass of insulation or other thermal protection system components.

The screen, unsupported by perforated plate, requires support members spaced at approximately 30.4-cm (12-in.) intervals along the communication screen length. This technique could result in a potential saving of approximately 15.9 kg (35 lbm) for each tank of the hydrogen system. On that basis, each of the screen liners could weigh approximately 36.3 kg (80 lbm). These weights are also included in Table III-11.

A summary of the final performance capabilities is shown in Table III-12. The designs are capable of meeting all the mission requirements outlined in Section A.

Table III-12 Acquisition/Expulsion System - Performance Characteristics

HYDROSTATIC STABILITY*	LH <sub>2</sub> , 3.58-m (11.75-ft) Dia Tank, a/g	LO <sub>2</sub> 2.42-m (7.94-ft) Dia Tank, a/g	
Channel Screen, 2 Layers 200x1400	0.154	0.094	
Communication, 200x1400	0.077	0.047	
OUTFLOW CAPABILITY	EE <sub>I</sub> /EE <sub>A</sub>	Flow Rate kg/sec (lb/sec)	a/g (Maximum)
Lox Tank 1	98.1/97.9	8.17 (18)	0.057(-X), 0.072(+X)
Lox Tank 2	98.1/97.9	8.17 (18)	0.057(-X), 0.072(+X)
Lox Tank 2 with Reentry Tank		8.17 (18)	0.057(-X), 0.072(+X)
LH <sub>2</sub> Tank 1	97.3/97.0	2.72 (6)	0.087(-X), 0.114(+X)
LH <sub>2</sub> Tank 2	97.3/97.0	2.72 (6)	0.087(-X), 0.114(+X)
LH <sub>2</sub> Tank 2 with Reentry Tank		2.72 (6)	0.087(-X), 0.114(+X)
* Safety Factor = 2.0 EE <sub>I</sub> = Ideal Expulsion Efficiency EE <sub>A</sub> = Actual Expulsion Efficiency (1.10 Criterion)			

The final assembly configuration and assembly details are shown in Fig. III-17 for the LH<sub>2</sub> system and Fig. III-18 for the LO<sub>2</sub> system. The tanks containing the liner and channel acquisition/expulsion devices are suspended from a series of cables inside the vacuum jacket. The vacuum jacket also contains an aluminized Mylar multilayer insulation blanket. The combination of the vacuum and the multilayer insulation ensures that the 1.57 W/m<sup>2</sup> (0.5 Btu/hr-ft<sup>2</sup>) environmental heating rate incident on the propellant tank will not be exceeded.

The liner itself is also suspended within the propellant tank by a series of cables. The liners in both the LH<sub>2</sub> and LO<sub>2</sub> systems are positioned eccentrically in the tanks so the largest vapor annulus gap is located at the pressurization and vent port, and the smallest vapor annulus gap is located at the fill and drain line. This technique was used to take advantage of the minimum

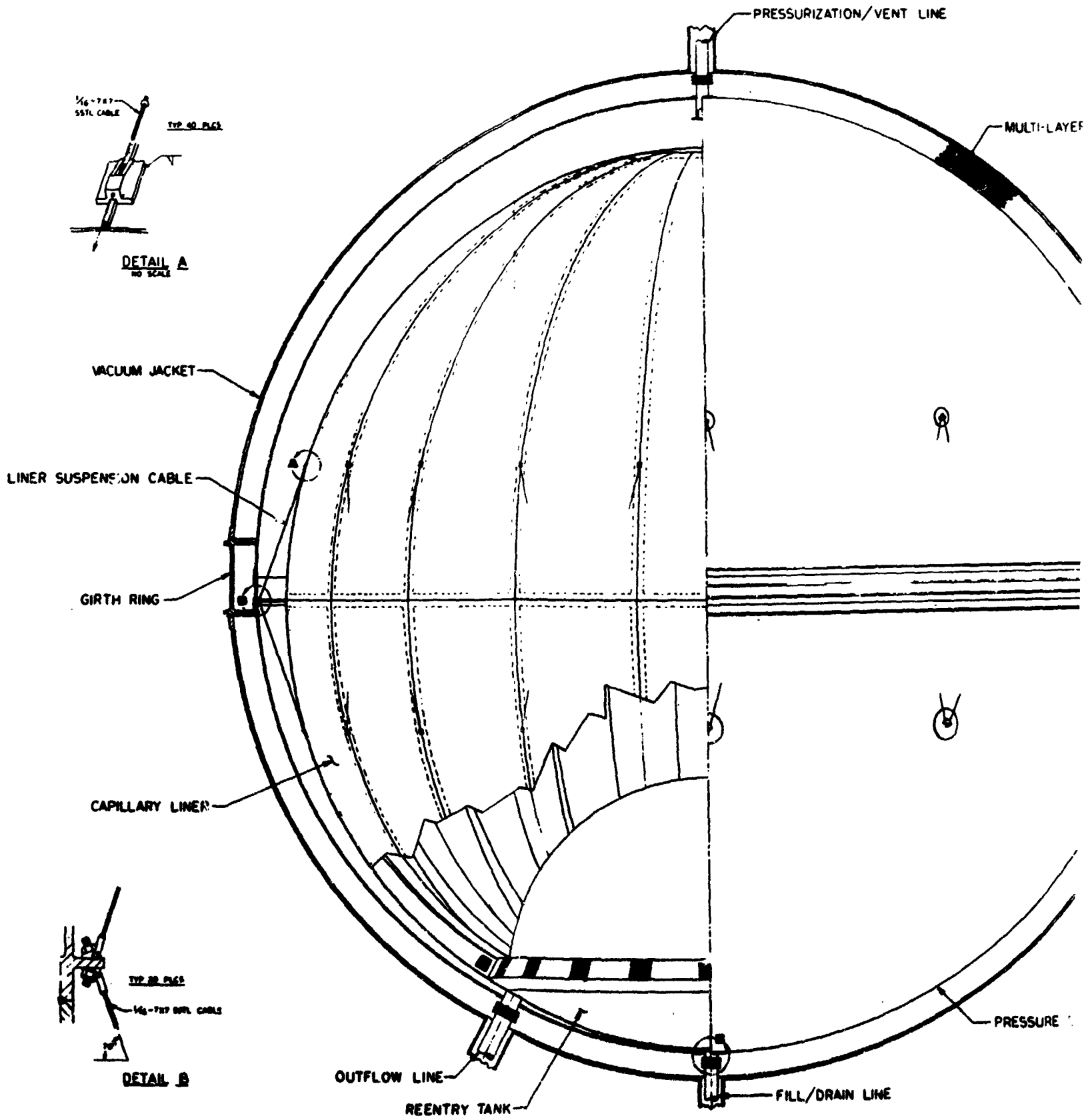
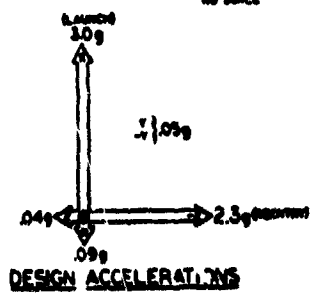
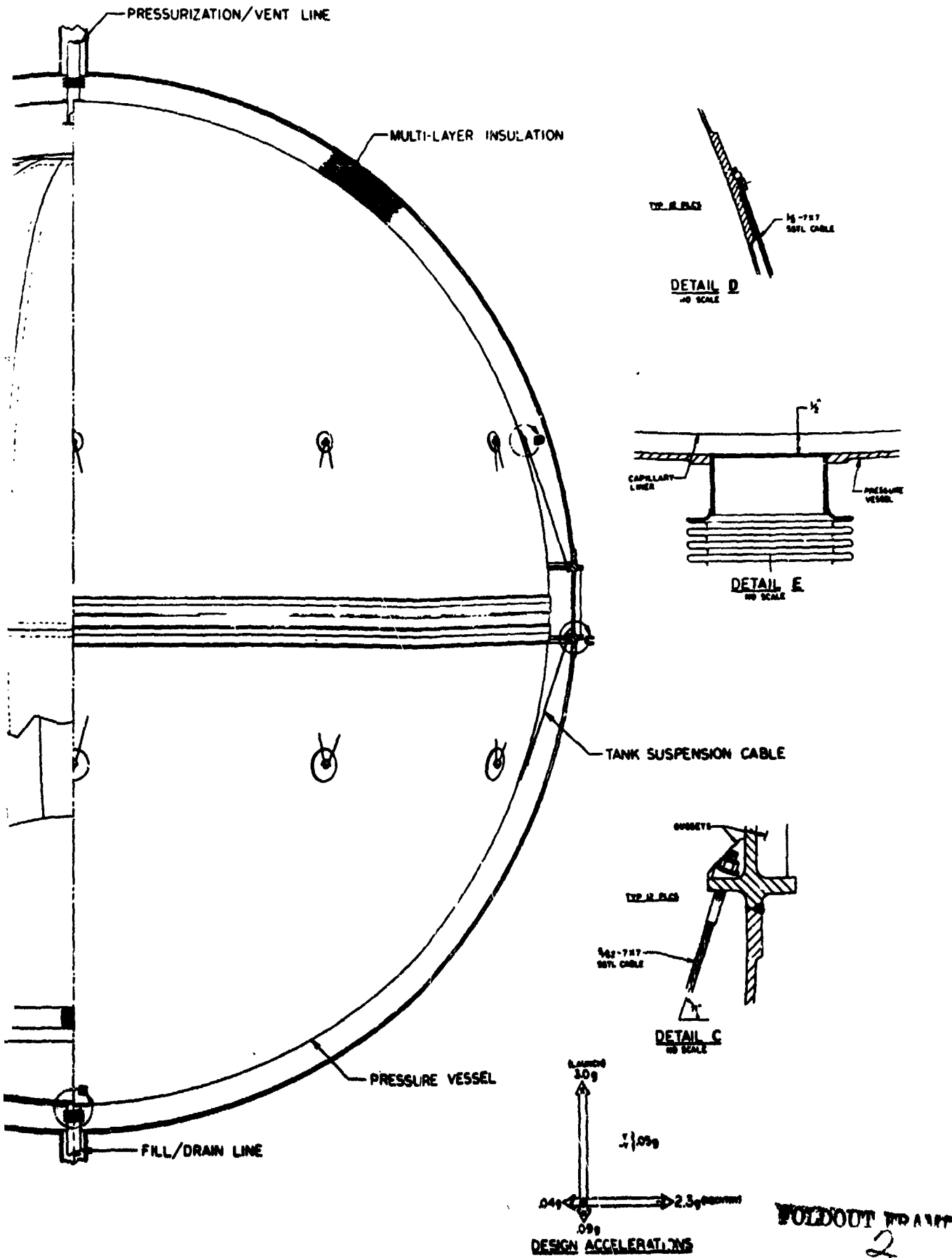


Fig. III-17 LH<sub>2</sub> Acquisition

FOLDOUT FRAME



FOLDOUT FROM FIG. 2

Fig. III-17 LH<sub>2</sub> Acquisition/Expulsion System and Tank Assembly Details

III-47 and III-48

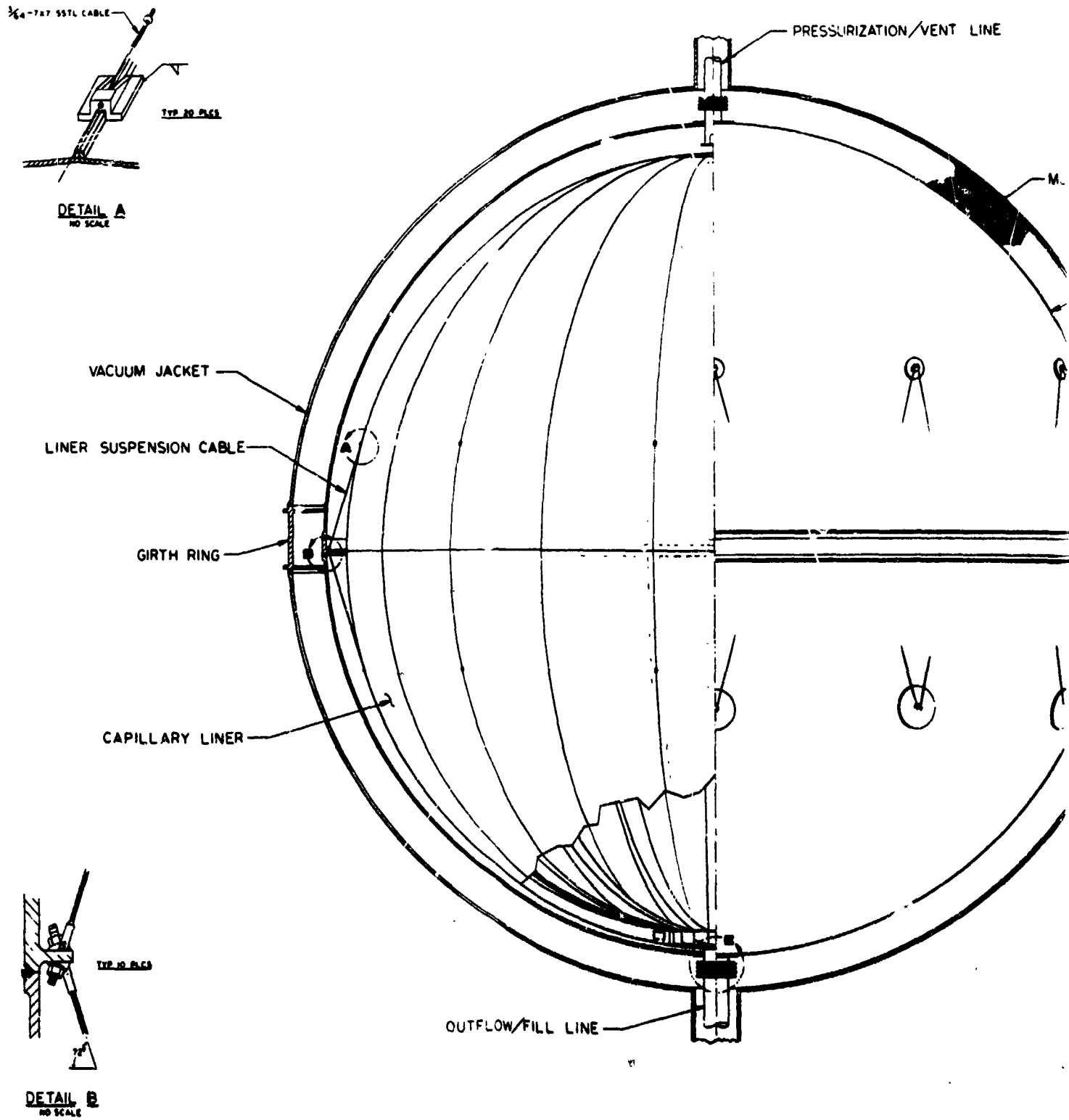


Fig. III-18 LO<sub>2</sub> Acquist

**FOLDBOUT FRAME**

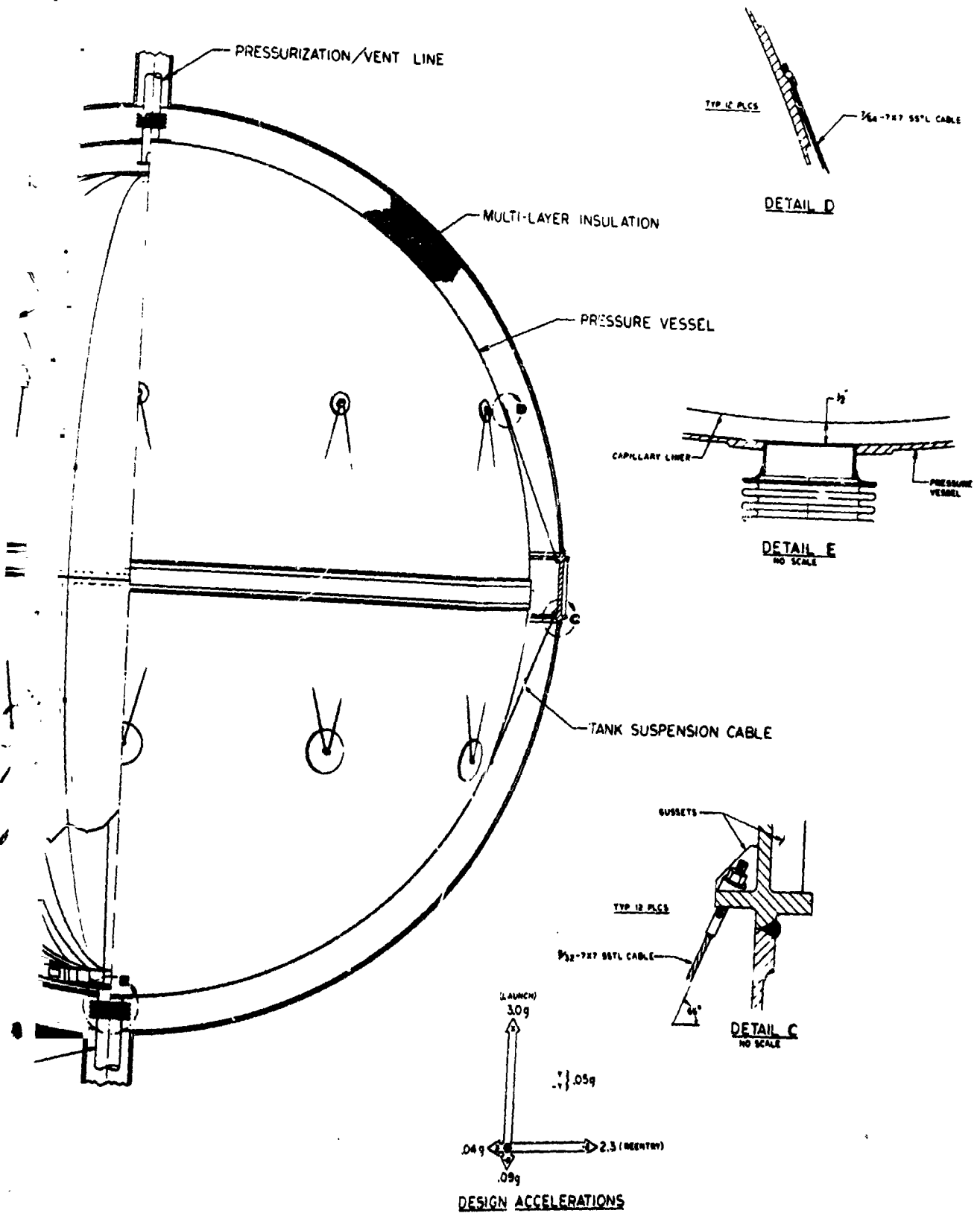


Fig. III-18 LO<sub>2</sub> Acquisition/Expulsion System and Tank Assembly Details

III-49 and III-50

FOLDOUT FRAME

free surface energy of any propellant present in the outer annulus. With this eccentric annulus configuration in a zero-g condition, the minimum free surface energy phenomenon will cause the propellant to be positioned away from the vent port, thus allowing venting even though all the liquid may not be contained within the acquisition/expulsion device.

After completing the detail design effort, the designs were reviewed by the Beech Aircraft Corporation (BAC) of Boulder, Colorado, and were found to be completely adequate. The results of the BAC review are summarized below with the detailed discussion presented in Ref. III-6. BAC evaluated the cable suspension method for the pressure vessel and screen assembly and considered it to be conservative. Screen assembly cleaning could be achieved by using proper techniques and sequences. Also, BAC felt that proper inspection techniques could be established to verify cleanliness after repeated use. In handling large screen assemblies, BAC indicated that standard procedures for handling man-rated flight components could also be used during manufacturing, storage, and transportation. It was also concluded that the maintenance problems should be minimal and would consist primarily of checking and maintaining cleanliness. In evaluating the proposed filling procedure, BAC stated that with proper care no significant problems should occur.

## 2. Feedline

Capillary feedline design incorporates cylindrical screen devices to hold the cryogenic liquid away from the feedline wall and assure gas-free liquid. The pressure gradient on these devices is ideally always from the outer gaseous region to the inner liquid core and has a maximum value equal to the bubble point of the screen configuration. For a single 325x2300 stainless steel Dutch-twill screen, this maximum is  $0.05 \text{ N/cm}^2$  (0.72 psi) for  $\text{LH}_2$  and  $0.36 \text{ N/cm}^2$  (0.512 psi) for  $\text{LO}_2$ . This pressure gradient must be sustained without degrading the system's performance.

As discussed previously, there are two ways of fabricating screen retention devices. For feedline application the screen must be supported by a backup plate (at least for larger diameters) to prevent screen buckling or distortion due to pressure gradients. No amount of screen deflection or distortion can be tolerated, because of the reduction in flow area and possible degradation in the system pressure retention capability.

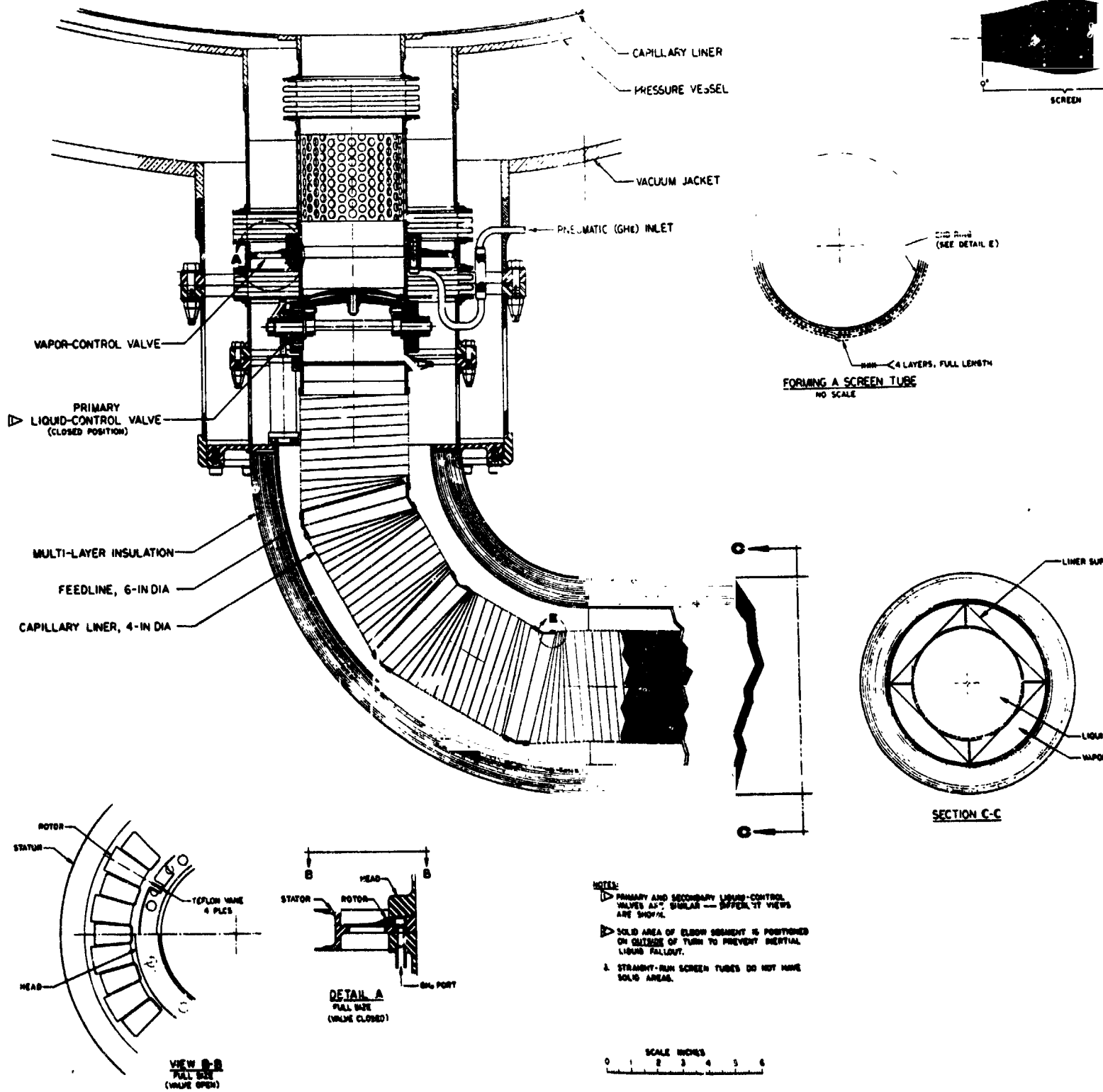
Feedline design is based on additive pressure retention capability caused by layering the screens. To ensure this capability, adjoining screen layers must be separated by spacer material, which also provides structural support. Any lightweight stainless steel material such as perforated plate or perforated shim stock will serve this purpose.

A representative feedline design is shown in Fig. III-19. A 15.2-cm (6-in.) feedline is shown with a 10.2-cm (4-in.) diameter screen liner. The screen liner has two screen layers with perforated plate or suitable spacer material between the layers. The drawing shows the feedline coupled to a storage tank. The feedline shown is not vacuum-jacketed but is covered with multilayer insulation. However, the basic design is not affected by the presence of a vacuum jacket.

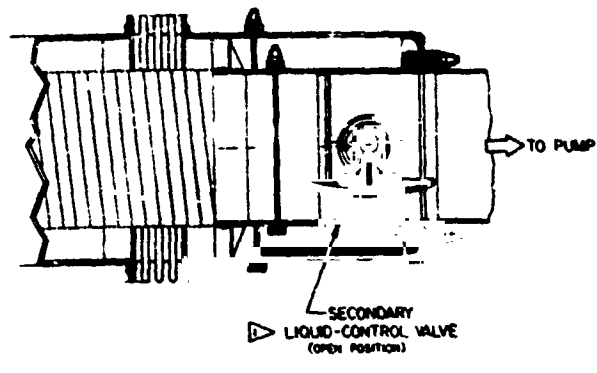
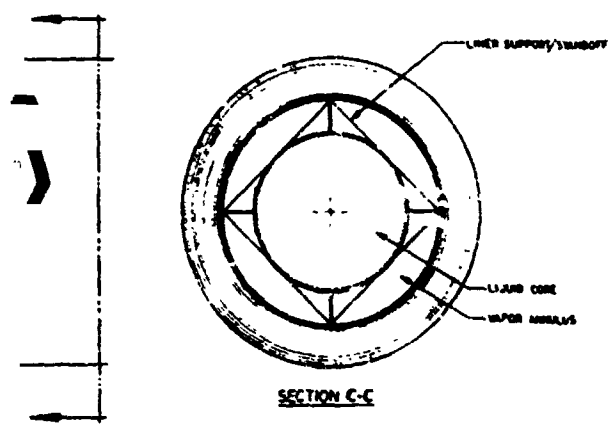
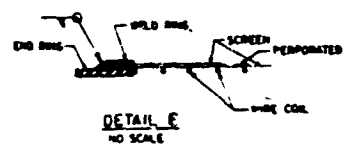
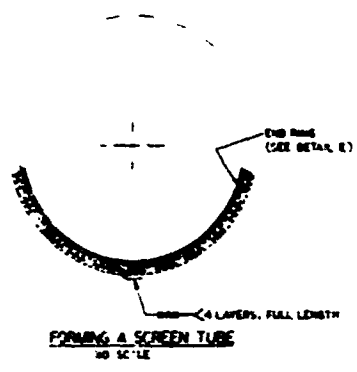
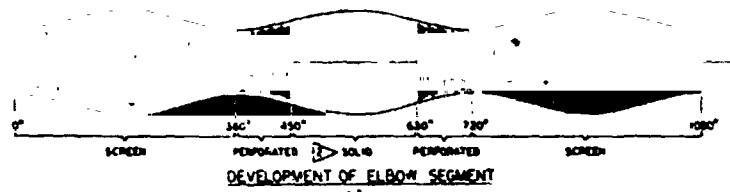
A pre valve is shown at the feedline-tank interface which may or may not be incorporated into the system without affecting performance. The basic function of a pre valve would be to prevent liquid from entering the feedline before orbital altitude is obtained. This gives added flexibility to the propellant feed system capability. Should a pre valve be desirable it must incorporate a valve in the vapor annulus as well as prevent liquid from entering this region when the tank is filled. The vapor control valve shown has this feature and is pneumatically actuated. Valve desirability depends on a tradeoff between valve weight and the added flexibility and weight savings caused by reduced feedline boiloff during orbit injection. A secondary liquid-control valve is also shown at the feedline/pump interface.

Expansion joints are shown at tank and turbopump interfaces and may be necessary at other locations depending on feedline geometry. Because of the small temperature gradient expected between the feedline and screen liner, thermal expansion in this area is not considered a problem.

Line fabrication and support details in the feedline are also shown. A multiple screen liner is formed by first joining alternate segments of screen and spacer material. The width of these segments is equal to the circumference of the layer. The resulting screen-spacer-plate sheet is formed into a cylindrical liner by rolling it into the proper diameter and joining it to end rings at each end of the liner section. The outside screen layer seam must be joined and sealed by resistance welding.



FOLDOUT FRAME



CENTRAL VIEWS  
IS POSITIONED IN HORIZONTAL  
UP SIDE

Fig. III-19 Capillary Feedline Configuration

III-53 and III-54

FOLDOUT FRAME

Feedline bends are fabricated from a series of screen liner segments as shown in the tank feedline main view. Fabricating an elbow segment is also shown in detail. The procedure is basically the same as for straight liner sections except that curved screen and spacer segments are used. Also a solid section is incorporated into the spacer material and located on the outside of the bend to prevent inertial liquid dropout.

The liner is supported inside the feedline by a series of standoffs. Standoff geometry may vary according to the size of the liner relative to the feedline. A triangular support would minimize heat leak without sacrificing structural stability. The square support shown is a thin metal sheet with a hole the diameter of the liner cut in it. Four gussets are shown to give the support added structural capability. The support may be made of any suitable material, preferably having a low conductivity, such as fiberglass to minimize heat shorts. As mentioned in the design analysis, stainless-steel Dutch-twill 325x2300 mesh screen was selected because of its superior pressure retention capability and compatibility with the stainless steel feedline. Perforated 0.012-cm (0.005-in.) stainless steel shim stock was chosen as the spacer and support material.

The OMS and RCS feedline diameters for the capillary system are the sum of the baseline diameters plus twice the vapor annulus gap, plus twice the liner thickness. The liner thickness is calculated from the required layers of screen and spacer material. Determinations of the vapor annulus gap size must consider screen liner thickness, vapor annulus volume requirements, and ease of fabrication, as well as the weight penalty associated with increased feedline diameter. This weight is in addition to the liner and support structure weight. The resulting annulus gap associated with feedline diameters of 12.7 cm (5 in.) and 11.4 cm (4.5 in.) for the LH<sub>2</sub> and LO<sub>2</sub> system were consistent with these considerations.

A summary of detailed design data for the integrated OMS/RCS capillary feedline is shown in Table III-13. Geometry and weight considerations for both propellant systems are included. Total weight, as well as that for individual components, is shown for all systems. It is interesting to note the larger percentage of total system weight represented by the screen liner for the LH<sub>2</sub> systems compared to LO<sub>2</sub> systems. The LH<sub>2</sub> OMS and RCS screen liner accounts for approximately 26% and 15%, respectively, of the total weight. For both LO<sub>2</sub> systems (OMS and RCS), only 5% of the total system weight is attributable to the capillary screen liner. This is due to the significantly larger number of screen layers required for the LH<sub>2</sub> systems and shows the importance of minimizing the number of screen layers.

Table III-13 Integrated CMS/RCS Capillary Feedline Detailed Design Data

GEOMETRY	LH <sub>2</sub>				LO <sub>2</sub>			
	OMS		RCS		OMS		RCS	
Screen Liner:								
ID, cm (in.)	10.2	(4)	10.2	(4)	10.2	(4)	10.2	(4)
OD, cm (in.)	10.56	(4.16)	10.36	(4.08)	10.3	4.01	10.3	4.01
Vapor Annulus Gap, cm (in.)	1.06	(.42)	1.17	(.46)	0.64	(0.25)	0.64	(0.25)
Feedline ID, cm (in.)	12.7	(5)	12.7	(5)	11.4	(4.5)	11.4	(4.5)
Weight, kg (lbm)								
Vacuum Jacket	139	(306)	23.8	(52.5)	34	(75)	22.7	(50)
Insulation	17.5	(38.4)	2.9	(6.4)	8.3	(18.3)	5.5	(12.2)
Feedline	34.9	(76.8)	5.8	(12.8)	11.1	(24.5)	7.5	(16.4)
Screen Liner	68.6	(151)	5.7	(12.6)	2.9	(6.3)	1.9	(4.2)
Supporting Structure	5.9	(13)	0.9	(2)	1.4	(3)	0.9	(2)
Total	265.9	(585.2)	39.1	(86.3)	57.7	(127.1)	38.5	(84.8)

As discussed previously, maintaining the integrity of capillary retention capability is important in the fabrication of any capillary device. The same care and procedure should be followed during fabrication of the feedline system as is used in construction of the storage tank system. This includes thorough bubble point testing of the device as well as assuring the structural integrity of all welds and attachments.

D. RESULTS AND CONCLUSIONS

Designs for the acquisition/expulsion system of the integrated OMS/RCS LH<sub>2</sub> and LO<sub>2</sub> systems were prepared. Designs for both the storage tanks and feedlines of the LO<sub>2</sub> and LH<sub>2</sub> systems are included. The acquisition/expulsion systems were designed to satisfy all of the expected propellant expulsion and storage requirements of a typical integrated OMS/RCS duty cycle. This includes gas-free liquid expulsions during the random accelerations of several orbit-to-orbit maneuvers and during the high reentry accelerations.

The designs presented are passive, lightweight, reliable, and flexible. An experimental program was conducted using a representative subscale LH<sub>2</sub> model, which verified some of the operational characteristics of the designs in a 1-g environment. Also the ability to fabricate, assemble, and inspect these designs was demonstrated by building and checking out a 1.78-m (70-in.) diameter screen liner and channel assembly under an IR & D program. In addition, the Beech Aircraft Corporation (BAC) reviewed the designs and found them to be completely adequate structurally and found no significant problems associated with the cleaning, inspection, handling, and maintenance of these systems.

It can be concluded that the designs presented in this chapter are capable of satisfying all of the varied mission duty cycles and design criteria of the integrated OMS/RCS LO<sub>2</sub> and LH<sub>2</sub> systems. Furthermore, confidence in the adequacy of the designs has been gained through the experimental programs conducted under this study. Additional design credibility was gained from a thorough design review conducted by the Beech Aircraft Corporation. A complete development plan for these designs is outlined in Chapter VI of this volume.

#### IV. DEDICATED OMS (LO<sub>2</sub>) POINT DESIGN

The analysis and design of a Space Shuttle dedicated LO<sub>2</sub> OMS propellant management system makes use of much of the basic information and the analytical tools presented in Chapter II. These include screen wicking data, screen structural data, modeling of system flow dynamics, and modeling of system thermodynamics. Both a high-pressure and a low-pressure system were considered for the system design. The low pressure system was, in many ways, similar to those designs established for the integrated OMS/RCS acquisition/expulsion systems presented in Chapter III and much of the analysis developed for the integrated OMS/RCS was also applicable to the low pressure system discussed here.

##### A. DESIGN REQUIREMENTS AND CRITERIA

This section describes the Space Shuttle orbital configuration and related vehicle/mission requirements, which were used to design the acquisition/expulsion device for the LO<sub>2</sub> tanks of the Earth orbital maneuvering system (OMS). The requirements reflect the most recent orbiter concepts available at the time of the study.

##### 1. General Requirements

A general consideration of earth storable propellants is presented in detail in Volume V of this report. This study concerns only the LO<sub>2</sub> acquisition/expulsion design for a dedicated OMS system. However, the general performance and design requirements for Space Shuttle fueled with earth-storable propellant were considered applicable. These are summarized briefly below.

The systems were designed for ease of inspection, checkout, and maintenance, including removal and replacement of parts. The acquisition/expulsion devices were designed to operate satisfactorily throughout the range of acceleration and thermal environments anticipated during the Shuttle operation. The OMS propellant management device was designed to function for a minimum service life of 100 to 500 missions over a 10-year period. At least seven days of self-sustaining lifetime was provided, with extended mission

life capability of up to 30 days. The storage capacity of the tanks was designed for 152 to 427 m/sec (500 to 1400 fps) delta velocity propellants. The capability of receiving propellants while on orbit was provided for. Table IV-1 shows the entire OMS candidate propellant list, although only LO<sub>2</sub> was considered in this study.

*Table IV-1 Earth Storable OMS Candidate Propellant Performance*

Oxidizer/Fuel	Mixture Ratio	Specific Impulse $\bar{I}_{sp}$ , N-sec/kg (lbf-sec/lbm)
N <sub>2</sub> O <sub>4</sub> /A-50	1.60	3070 (314)
N <sub>2</sub> O <sub>4</sub> /MMH	..60	3051 (312)
N <sub>2</sub> O <sub>4</sub> /N <sub>2</sub> H <sub>4</sub>	1.11	3090 (316)
LO <sub>2</sub> /A-50	1.33	3286 (336)
LO <sub>2</sub> /MMH	1.43	3266 (334)
LO <sub>2</sub> /N <sub>2</sub> H <sub>4</sub>	0.95	3296 (337)
LO <sub>2</sub> /UDMH	1.68	3256 (333)
LO <sub>2</sub> /RP-1	2.63	3139 (321)
LO <sub>2</sub> /C <sub>3</sub> H <sub>8</sub>	2.80	3217 (329)

2. Design Missions

Three specific missions were used as baseline for the dedicated OMS system: (1) an easterly launch; (2) a polar launch; and (3) a space station resupply. Table IV-2 shows the delta velocity requirements for each of the three missions. Figures IV-1 through IV-3 show the timelines for each of the missions.

3. Tankage Geometry

Table IV-3 lists the tank dimensions considered for the study and shows the sizes of cylindrical tanks considered for the high pressure systems, 172.5 N/cm<sup>2</sup> (250 psia). Low pressure systems, with storage pressures near ambient, were designed for spherical tanks of the same volume. Minimum ullage volumes of up to 5% were allowed to prevent overpressurization due to propellant expansion.

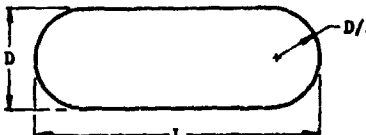
Table IV-2 OMS Mission Requirements

Design--Easterly Launch 29,510 kg (65,000 lb) Payload (Required), 185 km (100 n mi), 7 days		Reference--South Polar Launch 18,160 kg (40,000 lb) Payload (Minimum), 185 km (100 n mi), 7 days		Reference--Resupply Mission, 11,350 kg (25,000 lb) Payload (Minimum), 500 km (270 n mi), 7 days	
Function	$\Delta V$ m/sec (ft/sec)	Function	$\Delta V$ m/sec (ft/sec)	Function	$\Delta V$ m/sec (ft/sec)
Circularization	27.4 (90)	Circularization	27.4 (90)	Phasing Burn	40.5 (133)
Terminal Phase Initiation	9.75 (32)	On Orbit	9.75 (32)	Orbit Correction	12.2 (40)
Deorbit Burn	76.2 (250)	Deorbit Burn	76.2 (250)	Orbit Correction	7.6 (25)
Excess	191 (628)	Excess	39.0 (128)	Phasing Burn	85.9 (282)
				Phasing Burn	72.5 (238)
				Orbit Correction	6.7 (22)
				Terminal Phase	10.9 (36)
				Deorbit	134. (440)
				Excess	56 (184)
<b>Total</b>	<b>304.8 (1000)</b>	<b>Total</b>	<b>152.4 (500)</b>	<b>Total</b>	<b>426.3 (1400)</b>

Table IV-3 Propellant Tankage Requirements for OMS Propellant Acquisition System

Propellants	Propellant Temperature Range		Tank Length, L		Tank Diameter, D		Volume/Tank <sup>a</sup>	
	°K	°R	m	ft	m	ft	m <sup>3</sup>	ft <sup>3</sup>
1. N <sub>2</sub> O <sub>4</sub> /ASG	275-322/272-322	495-580/490-580	3.87/3.84	12.7/12.6	0.97/0.97	3.2/3.2	2.60/2.55	92.0/90.2
2. N <sub>2</sub> O <sub>4</sub> /MMH	275-322/255-322	495-580/460-580	3.87/3.87	12.7/12.7	0.97/0.97	3.2/3.2	2.61/2.60	92.5/91.9
3. N <sub>2</sub> O <sub>4</sub> /N <sub>2</sub> H <sub>4</sub>	275-322/278-322	495-580/500-580	3.65/3.93	12.0/12.9	0.91/0.97	3.0/3.2	2.20/2.81	77.9/99.4
4. LOX/H <sub>2</sub>	90-97/19-22	162-175/35-40	4.14/6.12	13.6/20.1	1.03/1.52	3.4/5.0	3.24/10.32	114.7/365.0
5. LOX/C <sub>2</sub> H <sub>6</sub>	90-97/225-233	162-175/405-420	4.39/3.84	14.4/12.6	1.09/0.94	3.6/3.1	3.77/2.52	133.4/89.3
6. LOX/MP-1	90-97/255-322	162-175/460-580	4.39/3.56	14.4/11.7	1.09/0.88	3.6/2.9	3.77/2.03	133.1/72
7. LOX/MPH	90-97/255-322	162-175/450-580	4.02/3.90	13.2/12.8	1.00/0.97	3.3/3.2	2.94/2.67	104.1/94.5
8. LOX/N <sub>2</sub> H <sub>4</sub>	90-97/278-322	162-175/500-580	3.78/4.00	12.4/13.1	0.94/1.00	3.1/3.3	2.41/2.85	85.2/100.7
9. LOX/A-50	90-97/272-322	162-175/490-580	3.96/3.90	13.0/12.8	1.00/0.97	3.3/3.2	2.82/2.66	99.7/94.2
10. LOX/UDPH	90-97/255-322	162-175/460-580	4.11/3.93	13.5/12.9	1.03/0.97	3.4/3.2	3.13/2.72	110.9/96.3

<sup>a</sup>OMS configuration has one fuel tank and one oxidizer tank in each of two modules.



#### 4. Acceleration Criteria

Acceleration criteria developed for this study, based on the best available information, were as follows:

Translational Accelerations (OMS)--Minimum, 0.0216 g  
Max  $r_{max}$ , 0.0706 g

RCS Accelerations (in any direction)-- 2 thrusters, 0.0129 g  
4 thrusters, 0.0258 g  
6 thrusters, 0.0388 g  
8 thrusters, 0.0517 g

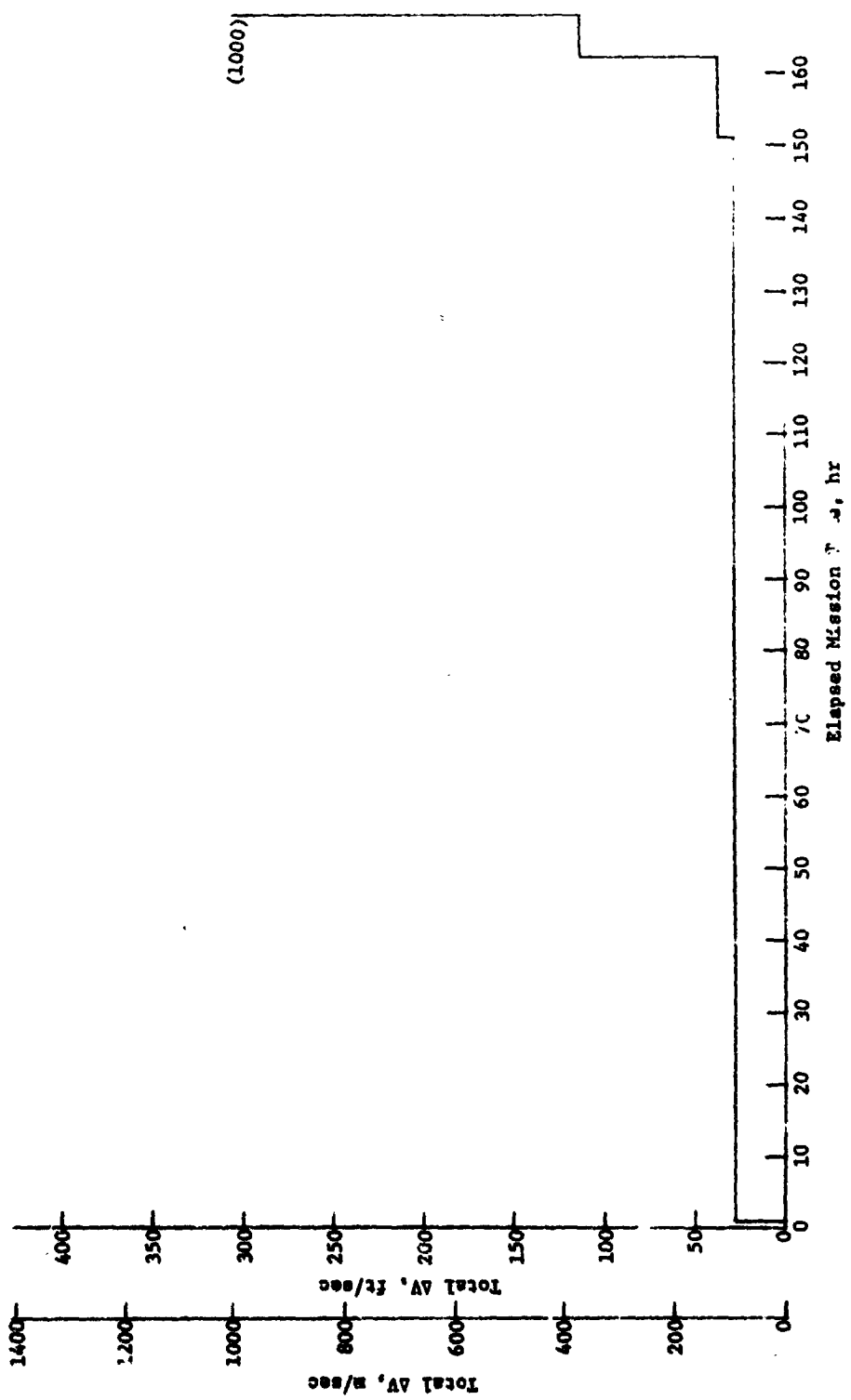


Fig. IV-1 OMS Maneuver Requirements for Easterly Launch

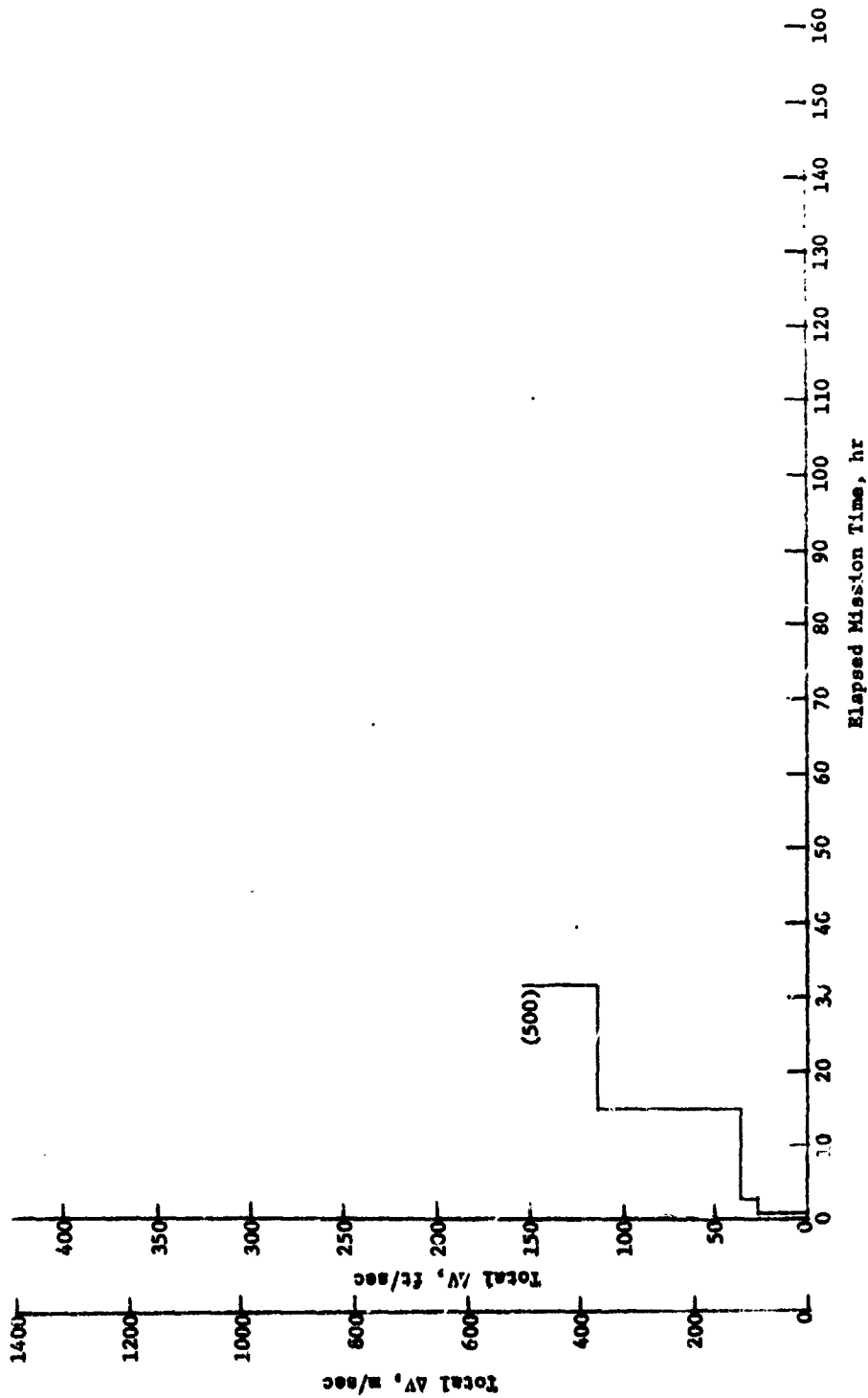


Fig. IV-2 OMS Maneuver Requirements for Polar Mission

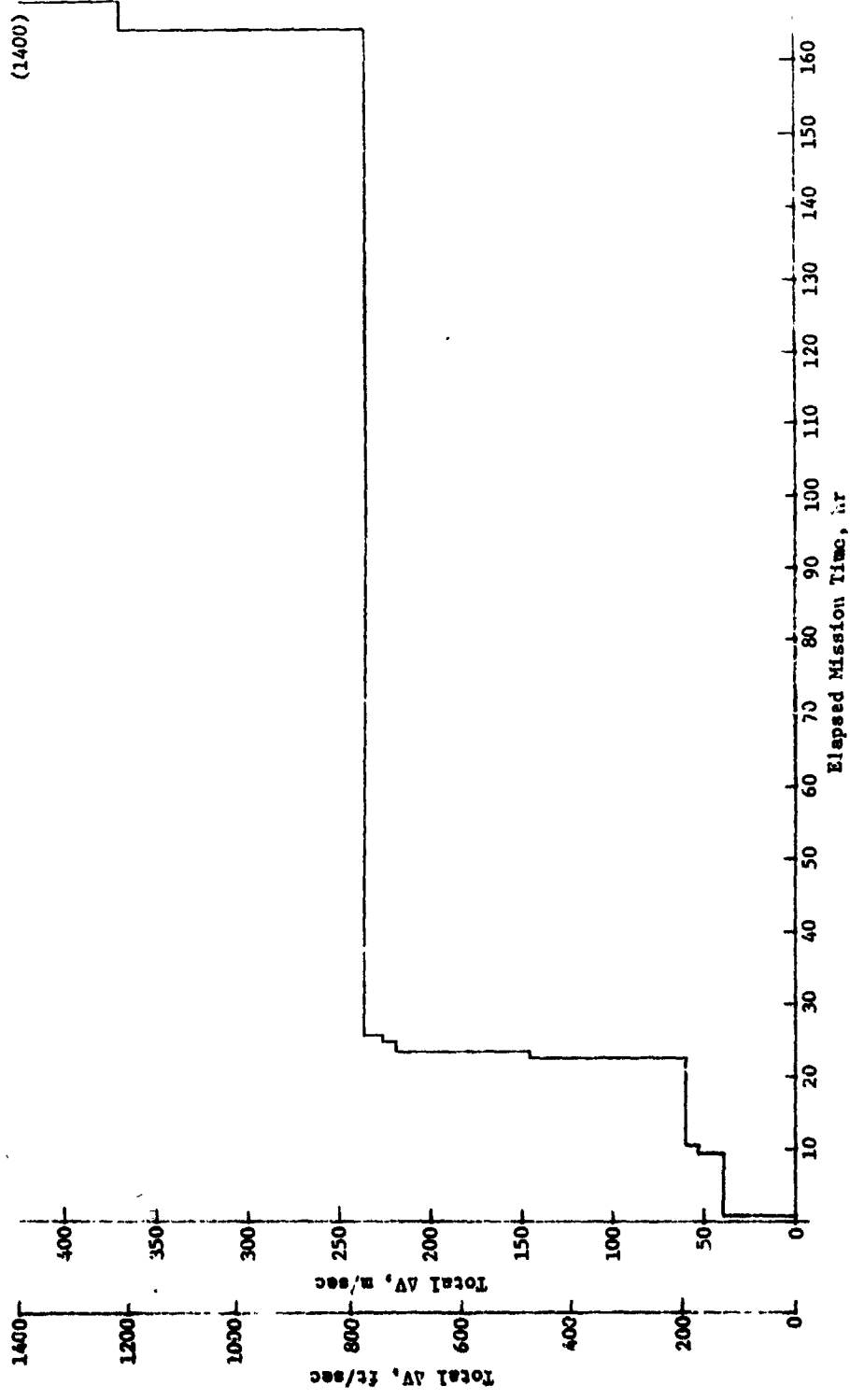


Fig. IV-3 OMS Maneuver Requirements for Resupply Mission

For purposes of the study, no more than four thrusters in any one direction would be operated at any time. Directional acceleration criteria were as follows:

Pitch-Yaw, 0.0241 g

Roll, 0.00938 g

5. Thermal Criteria

The thermal criteria used for the dedicated OMS LO<sub>2</sub> system were those criteria established for the integrated OMS/RCS system of Chapter III. The steady-state environmental heating rate for the tank was considered to be 1.58 W/m<sup>2</sup> (0.5 Btu/hr-ft<sup>2</sup>) and the transient soakback heat from the engine was considered to be 239 W/m<sup>2</sup> (76 Btu/hr-ft<sup>2</sup>).

6. Propellant Utilization Criteria

The following propellant utilization requirements were considered in designing the acquisition/expulsion system to provide gas-free liquid on demand. It was designed to provide liquid expulsion instantaneously without allowing time for propellant settling before expulsion. The liquid expulsion periods were assumed to vary from the minimum impulse bit of 6 sec to a single continuous outflow duration of 1000 sec or more. The system was designed to provide any number of liquid expulsions for these durations until propellant depletion and to assure the highest expulsion efficiency. The design flowrates are shown in Table IV-4.

Table IV-4 Propellant Flow Rate Ranges for an OMS Propulsion Module

Propellants	$\dot{W}_O$ , kg/sec (lbm/sec)		$\dot{W}_F$ , kg/sec (lbm/sec)	
	Minimum	Maximum	Minimum	Maximum
H <sub>2</sub> O <sub>4</sub> /A-50	3.11 (6.86)	8.90 (19.6)	1.94 (4.27)	5.54 (12.2)
H <sub>2</sub> O <sub>4</sub> /MMH	3.13 (6.90)	8.94 (19.7)	1.95 (4.31)	5.58 (12.3)
H <sub>2</sub> O <sub>4</sub> /N <sub>2</sub> H <sub>4</sub>	2.71 (5.81)	7.54 (16.6)	2.38 (5.25)	6.81 (15.0)
LO <sub>2</sub> /A-50	3.5 (7.85)	1.02 (22.4)	2.03 (4.48)	5.81 (12.8)
LO <sub>2</sub> /MMH	3.6 (7.92)	1.03 (22.6)	1.95 (4.31)	5.58 (12.3)
LO <sub>2</sub> /N <sub>2</sub> H <sub>4</sub>	2.8 (6.16)	8.0 (17.6)	2.41 (5.32)	6.90 (15.2)
LO <sub>2</sub> /UDMH	2.3 (5.08)	6.6 (14.5)	1.78 (3.92)	5.08 (11.2)
LO <sub>2</sub> /RP-1	2.7 (5.98)	7.8 (17.1)	1.36 (3.01)	3.90 (8.6)
LO <sub>2</sub> /C <sub>3</sub> H <sub>8</sub>	3.0 (6.59)	8.5 (18.8)	1.27 (2.80)	3.53 (8.0)

Note:  $15,540 \text{ N (3500 lbf)} < F_R < 44,480 \text{ N (10,000 lbf)}$ .

## B. DESIGN ANALYSIS

Both the low- and high-pressure LO<sub>2</sub> dedicated OMS designs are analyzed. Emphasis in the low pressure design was placed on optimizing the system weight, whereas the major part of the high-pressure analysis involved correct sizing of the trap system for stability and refilling.

### 1. Low-Pressure System

The low-pressure LO<sub>2</sub> dedicated OMS propellant tanks were to be designed in spherical configurations. The approach was to design one tank for the largest LO<sub>2</sub> volume requirement shown in Table IV-3. For LO<sub>2</sub> with methane, this volume is 3.77m<sup>3</sup> (133.4 ft<sup>3</sup>). The equivalent volume is contained in a spherical tank with a 96.62-cm (38.04-in.) radius. However, a tank with a 96.62-cm (38.09 in.) radius of exactly 3.79 m<sup>3</sup> (134 ft<sup>3</sup>) volume was used for the design comparisons. A true spherical liner inside this tank, which would contain 95% of the tank volume (thereby leaving a vapor annulus for the 5% ullage load), would have a radius of 95.09 cm (37.44 in.).

The LO<sub>2</sub> tank for this dedicated OMS application is considerably smaller than either the LH<sub>2</sub> or the LO<sub>2</sub> tanks of the integrated OMS/RCS systems discussed in the preceding chapter. It was not clear that the conclusions reached in Chapter III were completely applicable to the smaller systems. Therefore, further analysis of configuration impacts on system design were conducted to more clearly define optimum systems.

The first analysis was directed at determining the possible limitations on system geometry imposed by the 5% vapor annulus criterion. Figure IV-4 compares the radius of a polysphere to the radius of a sphere of equal volume. A polysphere containing 95% of the tank volume cannot have a radius that exceeds the radius of the tank containing it. A sphere with a radius of 95.09 cm (37.44 in.) represents the smallest geometric solid that can contain the 95% volume. Thus, any geometric figure such as a polysphere with a finite number of sides will have a larger radius. The ratio of the two limiting radii, 97.75:95.09 cm (38.09:37.44 in.), is 1.017. This ratio represents the largest ratio of radii which the system could accommodate. Figure IV-4 indicates that the 95% volume polyspherical liner contained in the tank must have more than eleven sides. This restriction establishes the lower limit for further investigation.

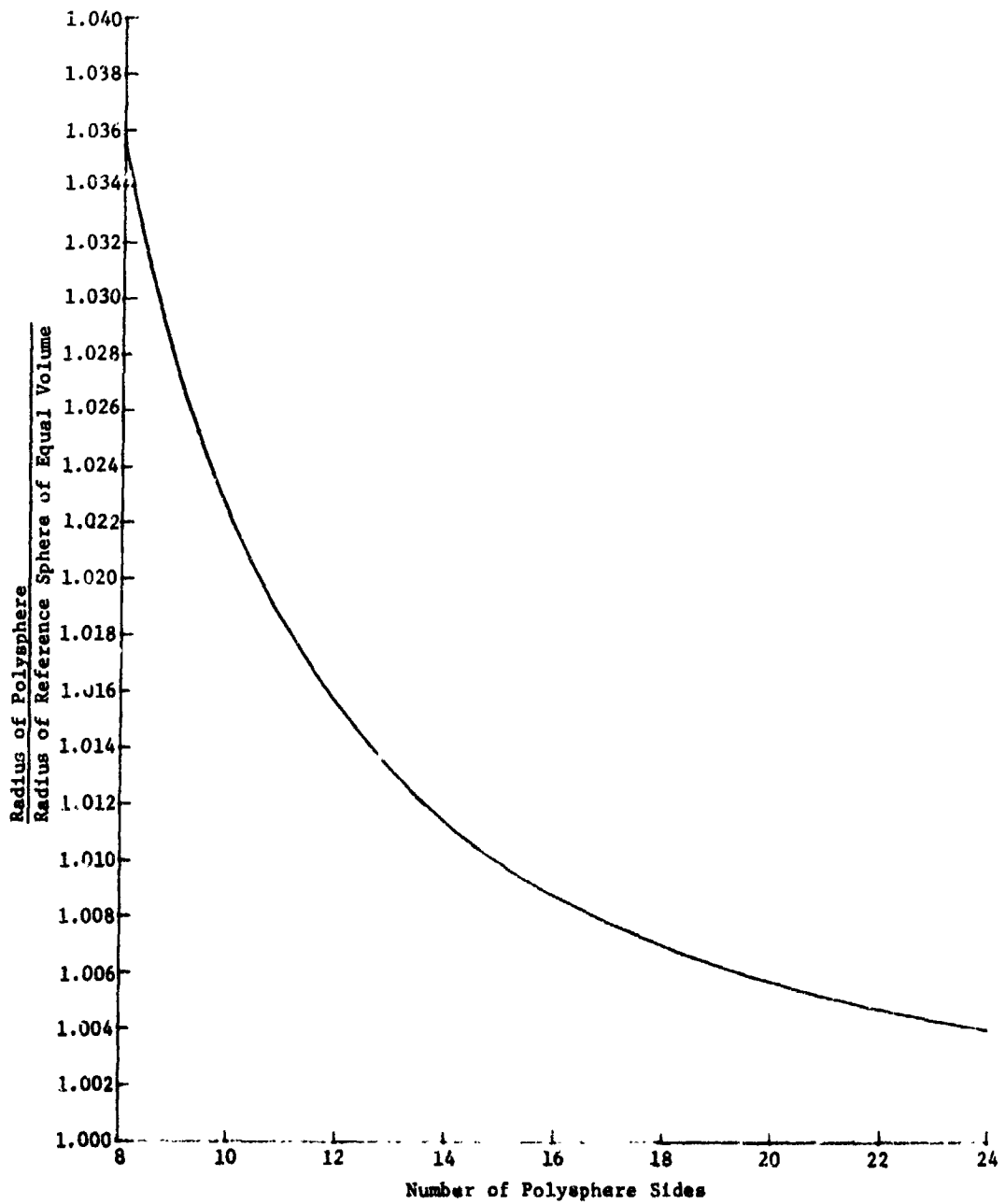


Fig. IV-4 Radius of Polysphere with Volume Equal to Reference Sphere Having a Radius Equal to 1.000

Figure IV-5 shows the largest polysphere that could be contained within a specific sphere. The figure indicates that the largest octosphere that could be placed in the sphere would contain only 90.0% of the loaded propellant. This percentage increases with an increase in the number of sides. For example, a 20-sided polysphere would hold 98.25% of the circumscribed tank volume. Figure IV-5 again demonstrates that for 95% containment within the device, the polysphere must have more than eleven sides.

The surface area of a screen device provides a good estimate of system weight, because weight is generally directly proportional to surface area. Figure IV-6 shows the effect the number of sides of a polysphere has on the surface area of the device when compared with the spherical case of either the same volume or the same radius. The figure shows that a polysphere of eight sides with a volume equal to a sphere will have 4.5% more surface area than the sphere. The percentage is still greater than 1% with a 16-sided polysphere.

These curves demonstrate the expected result that as the number of sides of a polysphere increase, the physical characteristics of a sphere are more closely approximated. However, the curves are useful for quickly eliminating impractical design configurations and estimating weights of proposed concepts.

From this point, the design analysis proceeded to an evaluation of two related design features: (1) wicking distance between the channels, and (2) the aspect ratio of the channels. These two design features are functionally related because the combined cross-sectional flow area of the channels was held constant for each configuration studied. The total flow area of the channels was held constant so that the flow characteristics in the channels would be approximately the same for a wide range of system configurations.

The aspect ratio of the channels is defined, for purposes of this study, as the ratio of the channel dimension in the circumferential direction to the channel dimension in the radial direction. This ratio is illustrated in Fig. IV-7.

For a specific number of channels and a fixed total cross-sectional area, as the channel aspect ratio decreases the wicking distance or the distance between the channels must increase. Accordingly, a set of conditions could exist in which a low number aspect ratio (normally  $< 1$ ) would require a wicking distance in excess of the

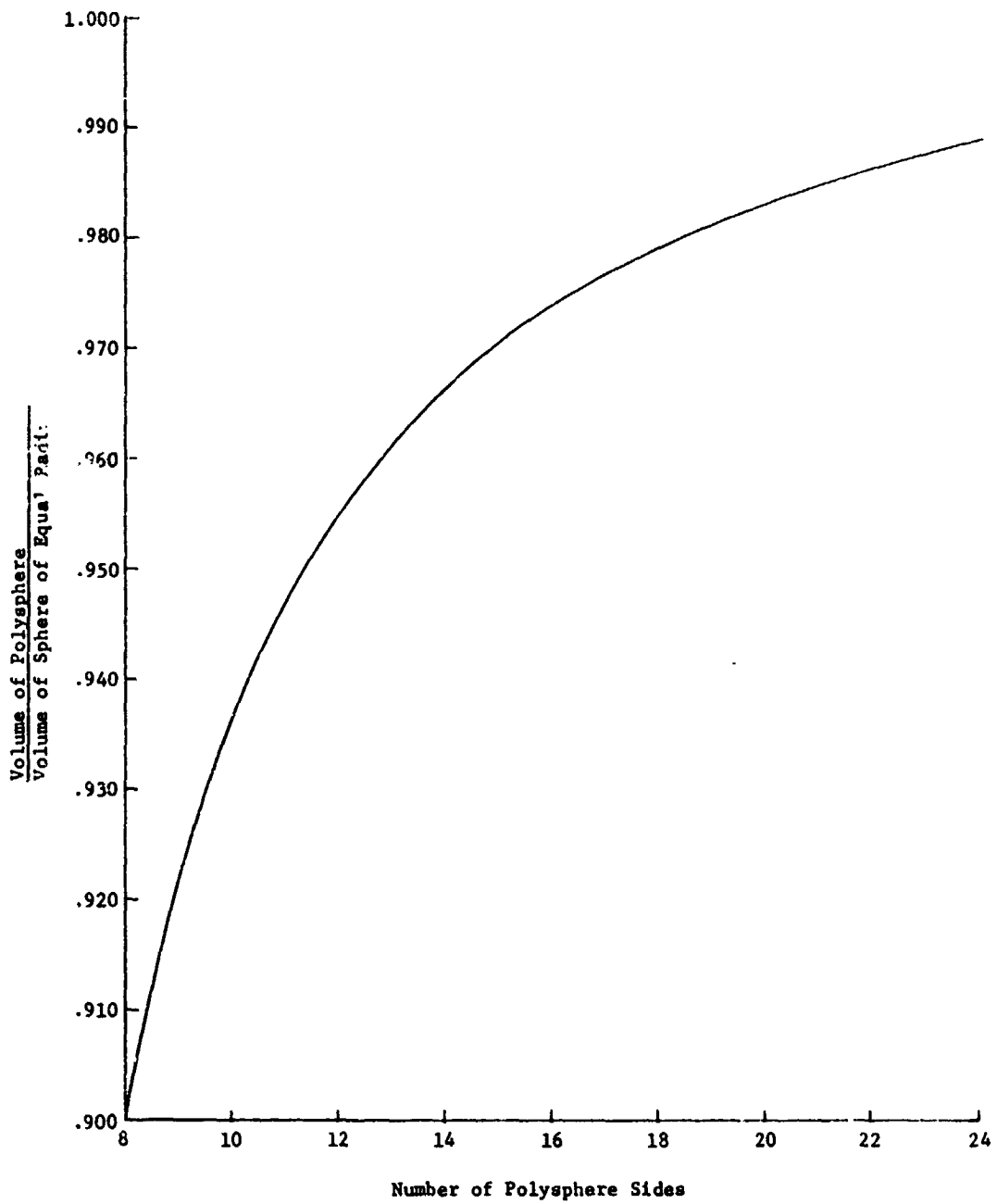


Fig. IV-5 Volume of Polyisphere with Radius Equal to Reference Sphere Radius

C<sup>13</sup>

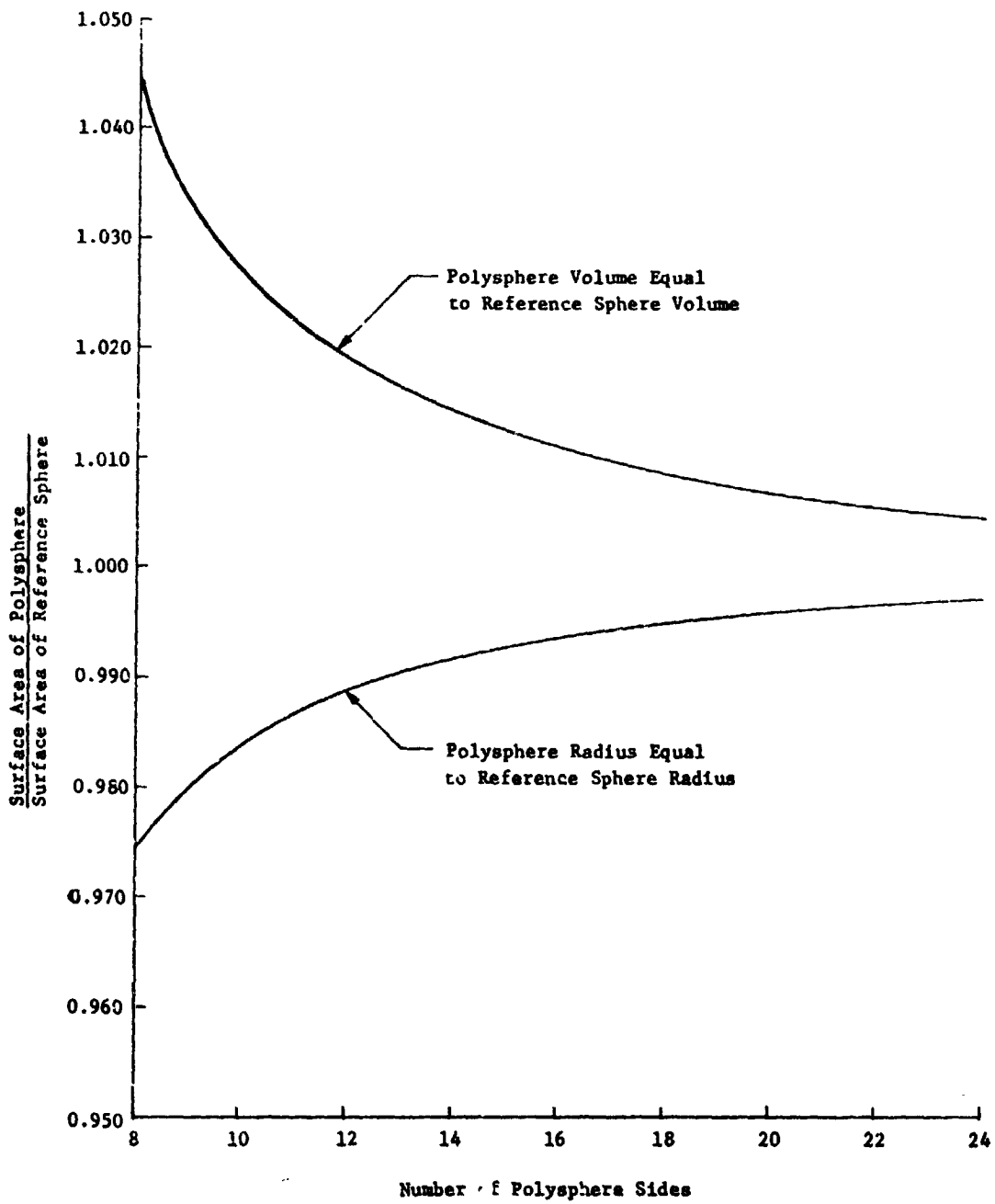


Fig. IV-6 Surface Area of Polysphere Compared to Reference Sphere with Surface Area Equal to 1.000

wicking capability of the screen. Therefore, because there is an upper limit on the distance a propellant can wick in a particular screen, there is a concomitant lower limit on the aspect ratio of the channels for any configuration.

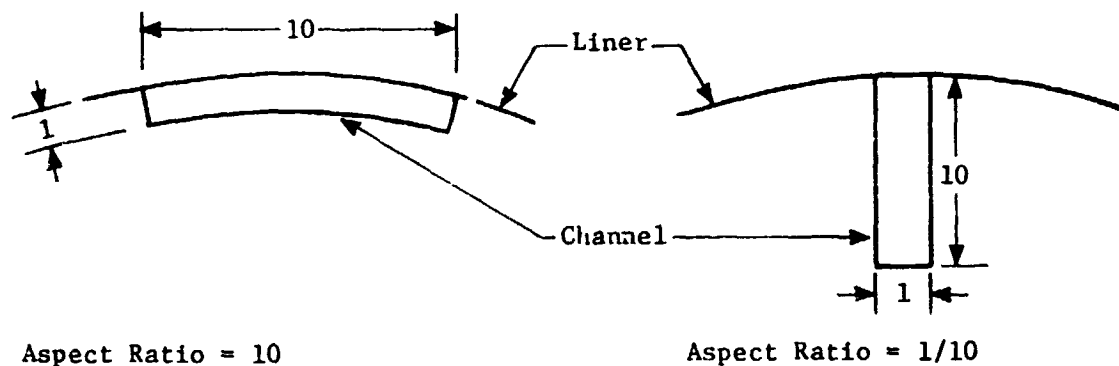


Figure IV-7 Illustration of Aspect Ratio

The consideration of a wide range of channel aspect ratios required a basic assumption regarding system fabrication. With channels having very large aspect ratios (on the order of 10), a channel that included screen only on the inner and outer spherical surfaces would have ample screen surface to assure small pressure losses due to propellant flow into the device. Conversely, for designs with low aspect ratios (aspect ratio  $<1$ ), the screen on the inner spherical surface adds little to the total surface area of the device. For this design, the sides of the channels must be fabricated of screen to assure adequate screen area. Therefore, it was assumed that all three interior surfaces of the channels were composed of screen backed by perforated plate.

The designs were also assumed to be of all aluminum welded construction, which is consistent with the design approach established under the integrated OMS/RCS design effort. Communication screens were considered to be a single layer of 200x1400 aluminum perforated plate. The channels were considered to be two layers of 200x1400 aluminum Dutch-twill screen separated by the aluminum perforated plate structural member. Weights of various systems were determined based on these assumptions.

Several different channel configurations were investigated through a range of wicking lengths. The wicking lengths represent the spacing between the channels. The maximum spacing considered was 38.1 cm (15 in.) because the analysis described in Chapter II of this volume indicated 38.1 cm (15 in.) to be a maximum distance

for  $LO_2$  wicking with the specified environmental heat leak of  $1.58 \text{ W/m}^2$  ( $0.5 \text{ Btu/hr-ft}^2$ ). It should be noted that this wicking distance was selected as a result of a preliminary wicking analysis. Further wicking analyses (presented in Chapter II), performed subsequent to the design of the integrated OMS system, have shown  $LO_2$  to have additional wicking capability in 200x1400 Dutch-twill screen. Therefore, the designs are somewhat conservative.

As a result of previous findings, no configurations were considered that were less than 12-sided polyspheres; i.e., no fewer than 12 channels were considered. Figure IV-8 shows the results of weight comparisons for the different configurations. The figure illustrates two noteworthy trends for channel designs. The first is that the fewer channels in the system, the lighter the optimized design will tend to be. The second observation is that each channel system, consisting of a fixed number of channels, has a well-defined minimum weight value. These minima occur at different wicking lengths for different numbers of channels, but these different wicking lengths correspond to essentially the same aspect ratio for all configurations. For this particular tank geometry, that minimum weight aspect ratio is approximately equal to 2.

Investigations were made to determine whether an aspect ratio of 2 was universally optimum. These investigations showed that each tank system and each fabrication material has a unique optimum aspect ratio. Moreover, as the total cross-sectional area of the devices changes, the optimum channel aspect ratio changes also. For example, for the hydrogen tank considered for the integrated OMS/RCS system defined in Chap. III, the optimum aspect ratio for a stainless steel system was approximately 2.5. For the same system fabricated of aluminum, the optimum aspect ratio was approximately 6. However, the weight deviated only about 0.908 kg (2 lbm) (less than 1%) between aspect ratios of 4 and 10. Figure IV-8 also shows that for the  $3.8 \text{ m}^3$  ( $134 \text{ ft}^3$ )  $LO_2$  tank studied, the optimum system weight increases approximately 0.18 kg (0.4 lbm) per channel and a representative system weight would lie in the 17.25 to 18.6 kg (38 to 41 lbm) range.

The volume of propellant contained in the acquisition/expulsion device is an important concern because the smaller that volume, the higher the expulsion efficiency. In terms of residual weight, the volume contained by the device assumes added significance for this design because of the high density of  $LO_2$ . Each of the configurations considered in this study was analyzed to determine this residual weight.

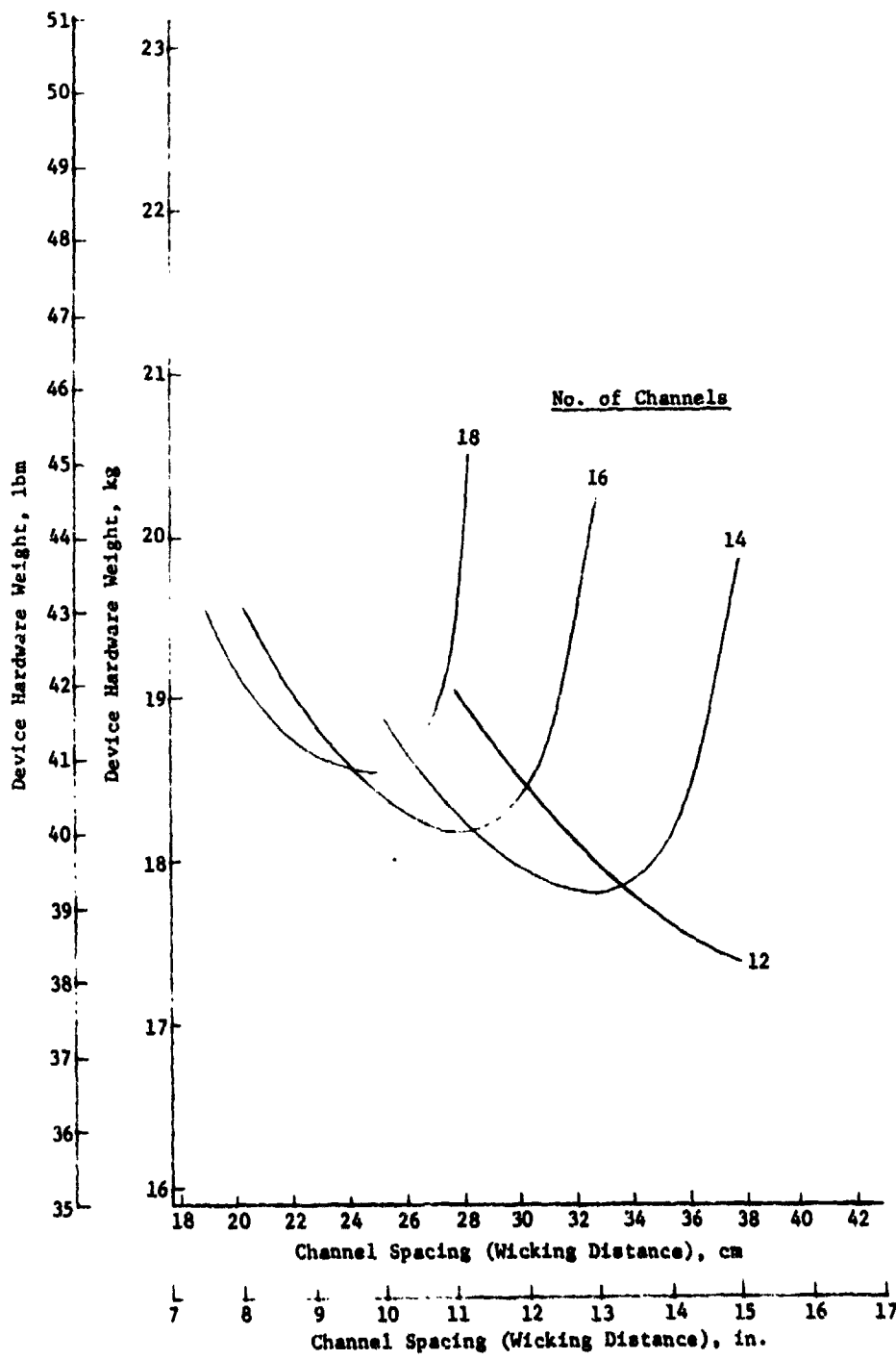


Fig. IV-8 Device Hardware Weight Comparisons

The impact of various combinations of channel number and spacing was determined and results are shown in Fig. IV-9. The figure shows that for each channel configuration there exists a maximum residual weight that tends to increase as the number of channels in the system is reduced. The individual maxima occur at aspect ratios approximately equal to unity, although these maxima occur at different channel spacings. Thus, the system hardware weight minima and the system propellant residual weight maxima do not occur at the same aspect ratio.

The curves in Fig. IV-9 tend to drop rapidly on the right-hand side of the maximum values. This right-hand side is the area where aspect ratios are less than unity. This would seem to imply that some significant weight savings, in terms of reduced residuals, could be realized by selecting designs from this side of the curve. However, the majority of the weights represented by this portion of the curve are for configurations that would be impractical to fabricate. As the aspect ratios become much less than unity, for this design application, the circumferential dimension of the channels becomes too small to make fabrication practical.

The effect of the various channel configurations on outflow capability was also assessed. It was determined that as the aspect ratio decreased the flow rate capability increased. Figures IV-10 and IV-11 show how this phenomenon relates to the system hardware/residual weight and channel spacing relationships. When the aspect ratios of the channels are large ( $\gg 1$ ) or small ( $\ll 1$ ), the viscous pressure losses due to flow of fluid in the channels comprise a proportionally larger portion of the total available pressure differential (determined by the bubble point of the screen) than do the viscous pressure losses in channels of the same cross-sectional area whose aspect ratios are closer to unity. However, the total pressure losses are smaller for a given flow rate at a smaller aspect ratio than they are at a larger one because of the unique geometry of the channels as they form a manifold near the tank outlet. Generally, the smaller the aspect ratio, the larger the screen area available for flow into the device. Since flow area through the screens comprises a large portion of the total pressure drop in a system, the outflow rate capability is increased as the aspect ratio decreases (Fig. IV-10 and IV-11).

Figure IV-12 illustrates the total weight of the systems investigated. This weight is the sum of the hardware weight and the residual weight of the system. Also shown are lines approximating the constant channel depths for the systems. These lines of constant channel depth indicate that the variation in weight for

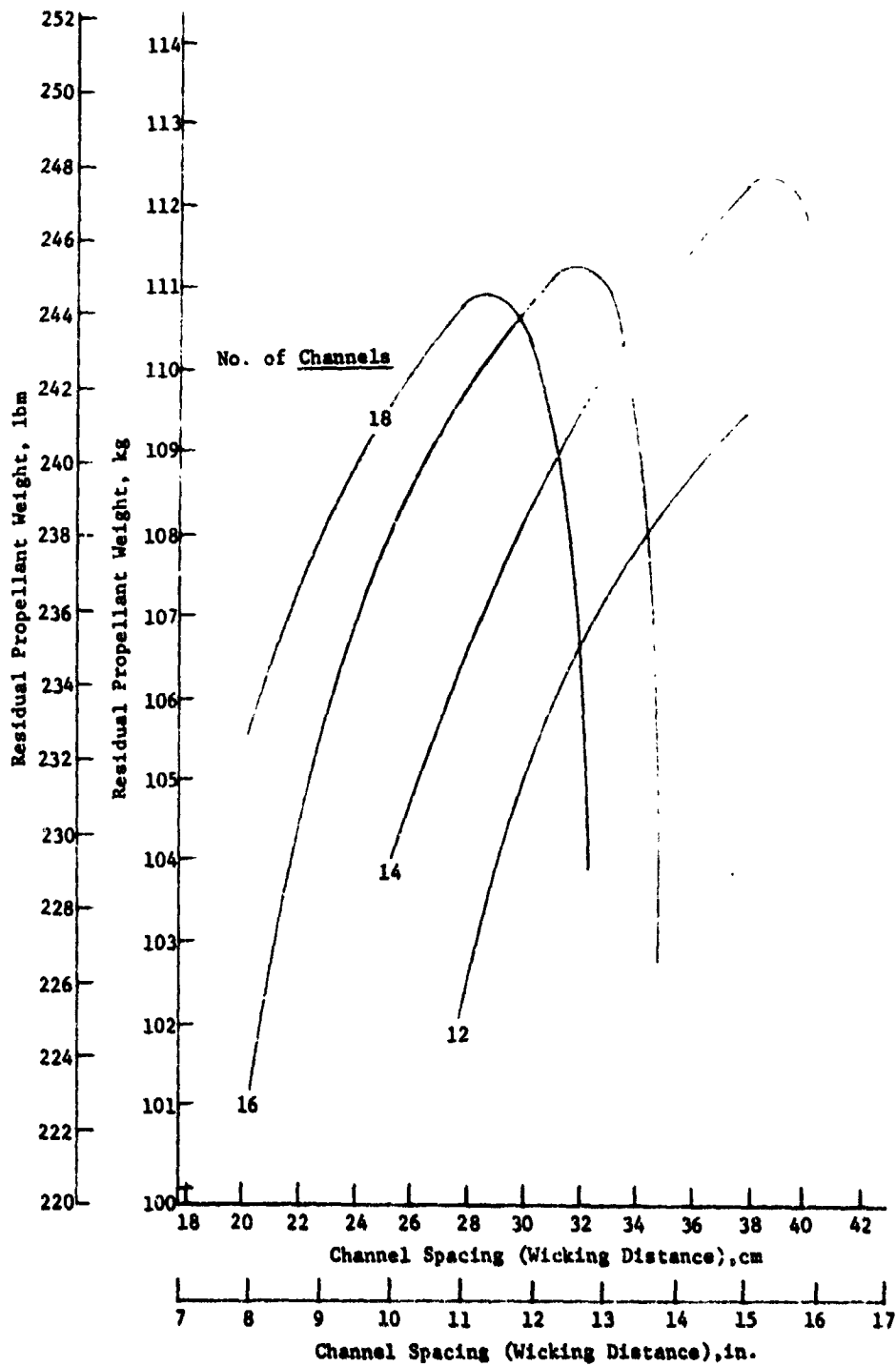


Fig. IV-9 Residual Propellant Weight Comparisons

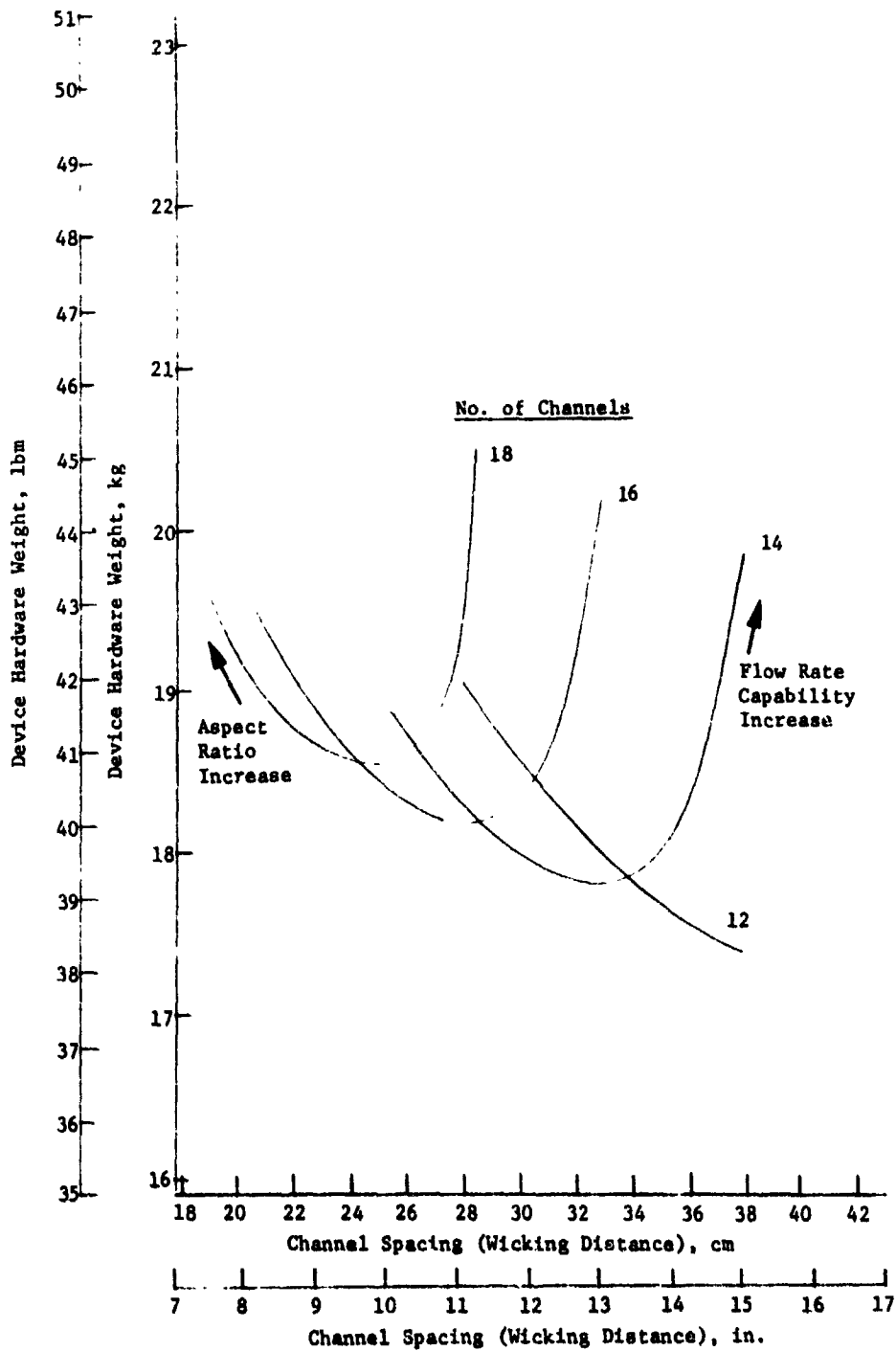


Fig. IV-10 Relationship of Flow Rate Capability to Device Hardware Weight

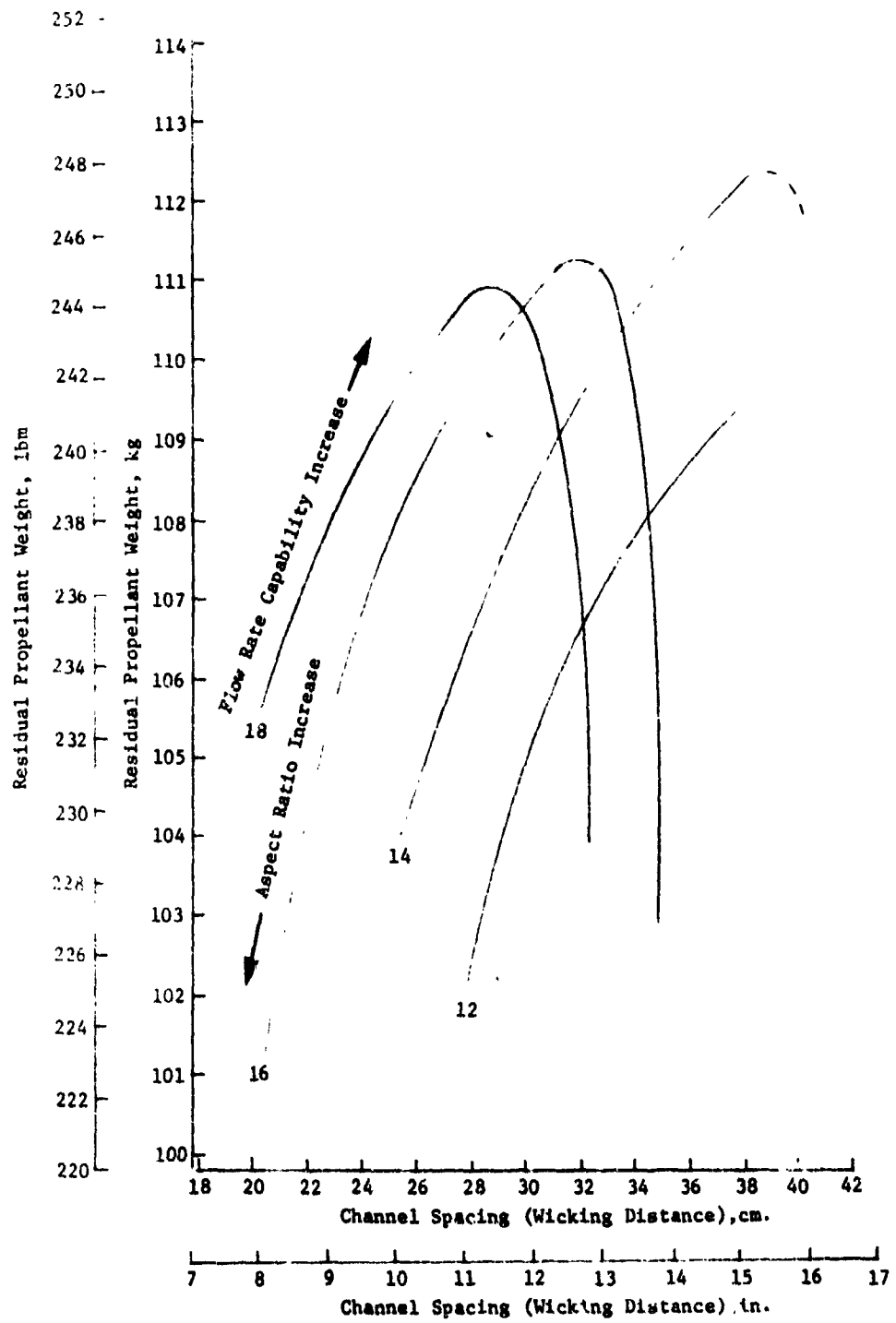


Fig. IV-11 Relationship of Flow Rate Capability to Residual Weight

systems of varying numbers of channels with a 2.54-cm (1-in.) depth is only approximately 1.36 kg (3 lbm). This difference represents approximately 1% of the total weight of hardware and residuals.

Because the weight difference between systems was not large, arbitrary criteria became more important in the ultimate selection of the system. Experience gained from fabricating various test articles for the experimental phases of this program indicates that some minimum channel depth exists below which fabrication difficulties begin to offset other potential benefits. Therefore, a minimum channel depth of 1.9 cm (3/4 in.) was selected.

Figure IV-12 shows that for a 1.9-cm (3/4-in.) channel depth the weights range from 125 kg (276 lbm) for 12 channels to 127 kg (279 lbm) for 18 channels. Although the 12-channel design is not significantly lighter than any of the others shown, it is more attractive from a fabrication standpoint. With fewer channels and sides of the polysphere liner, fewer welds must be made to fabricate the device. From a fabrication cost standpoint, this represents a potentially significant manufacturing cost saving.

Therefore, the selected system for the low pressure dedicated OMS application consists of a dodecasphere (12-sided polysphere) screen liner with a radius of 96.6 cm (38.02 in.). The device incorporates 12 channels, each 1.9 cm (0.75 in.) in depth, spaced approximately 34.3 cm (13.5 in.) apart at the equator of the liner. The liner is fabricated of 50% open, 0.76-mm (0.030-in.) aluminum perforated plate with one layer of 200x1400 aluminum Dutch-twill screen. The channels are fabricated of 50% open, 0.76-mm (0.030-in.) aluminum perforated plate covered with two layers of aluminum 200x1400 Dutch-twill screen.

The flow rate capability of the selected design is shown in Fig. IV-13 for accelerations in both the plus and minus x direction. From Table IV-4, the maximum flow rate for LO<sub>2</sub> of 102.6 kg/sec (226 lbm/sec) occurs when it is combined with RP-1. The minimum rate is with hydrazine and is 6.6 kg/sec (14.5 lbm/sec). The maximum flow rate can be accommodated at an acceleration rate of 0.044 g in the -x direction and 0.072 g in the +x direction. The minimum outflow rate can be maintained at 0.078 g in -x and 0.096 g in the +x direction. The OMS-produced acceleration is always in the +x direction and the capability of the system to function in an acceleration environment exceeds the 0.0706-g (+x) OMS acceleration criteria. Therefore, the design is sufficient for all proposed missions for which LO<sub>2</sub> is the oxidizer.

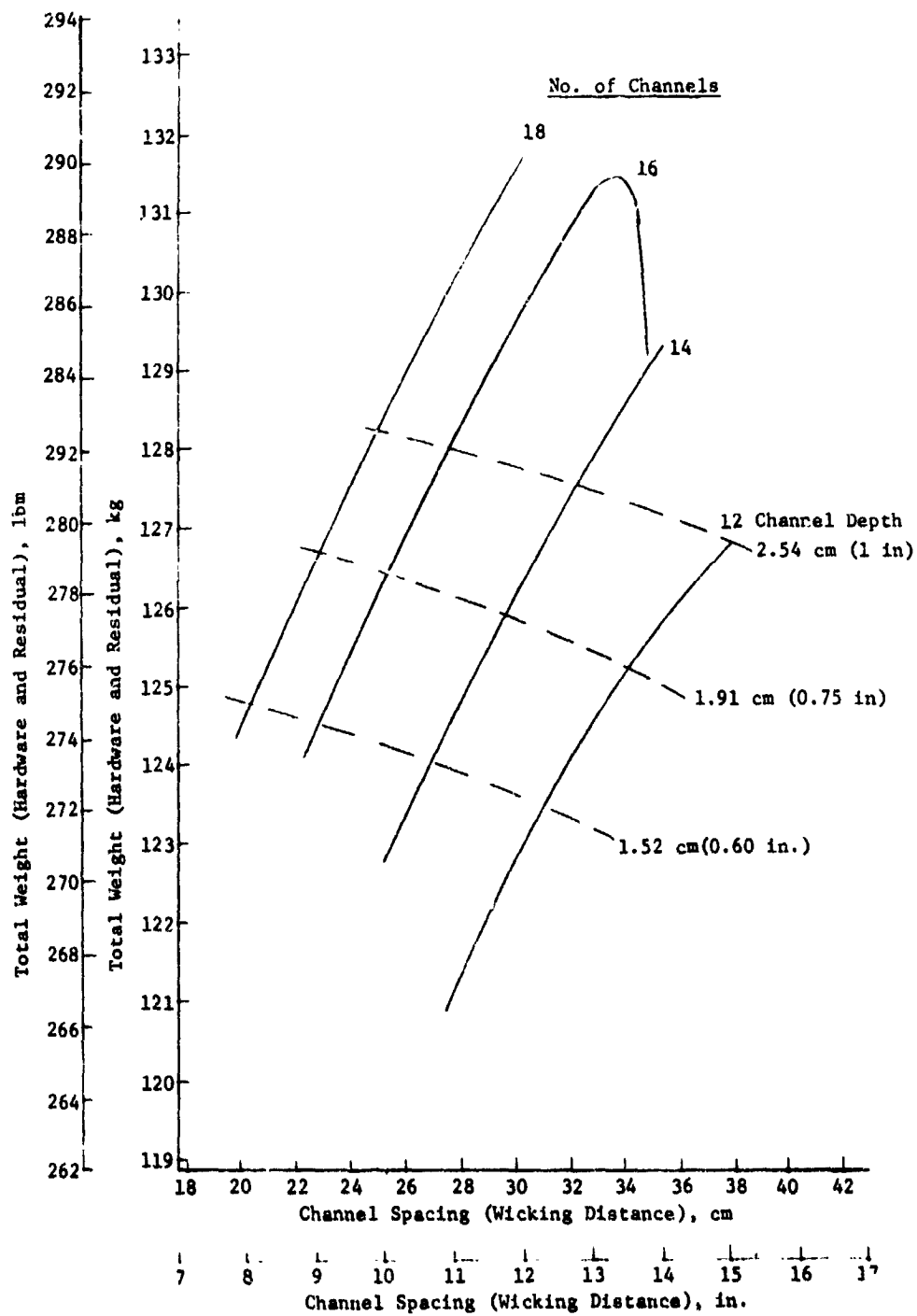


Fig. IV-12 Total System Weight Comparisons

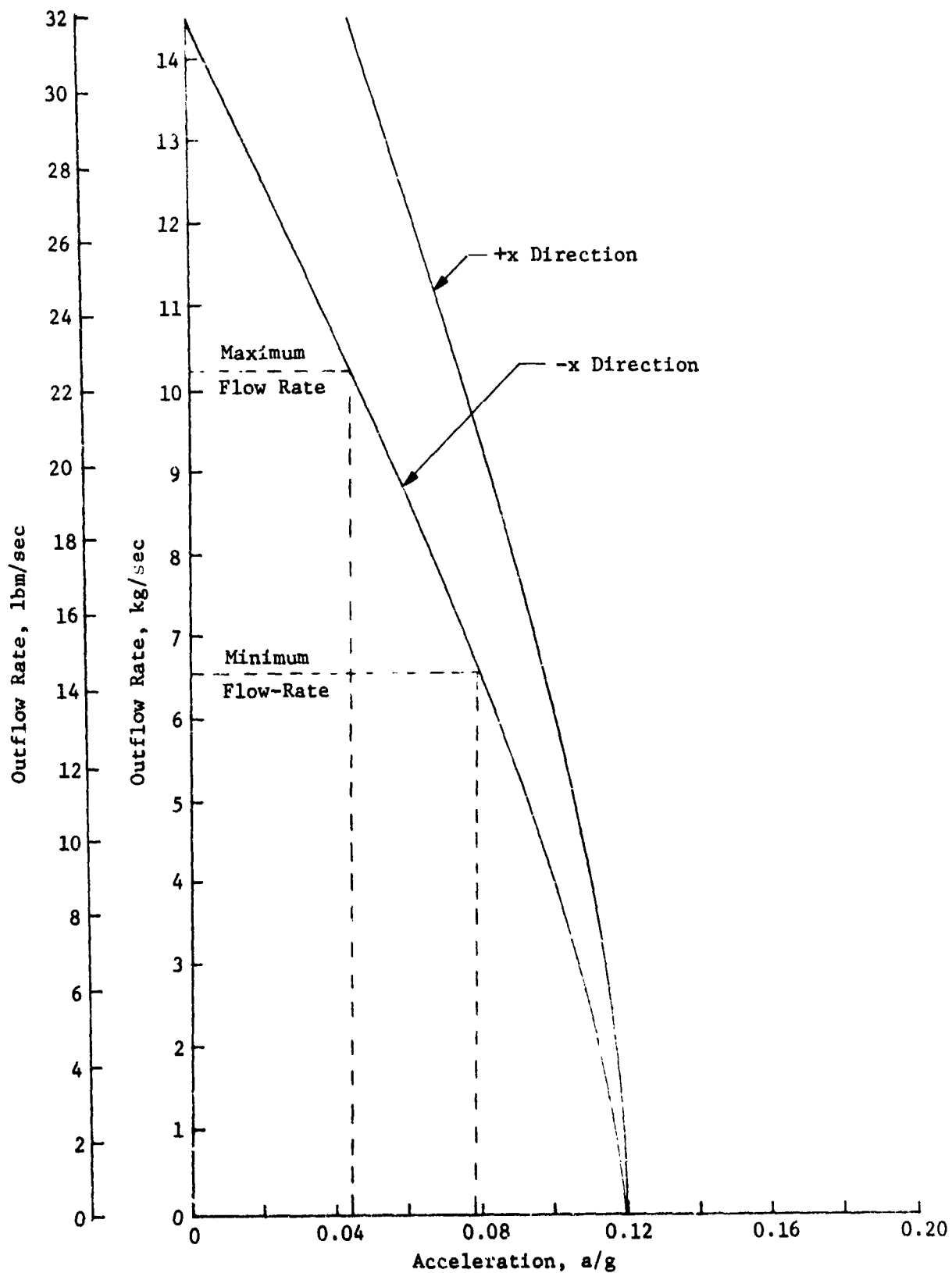


Fig. IV-13 Outflow Rate Capability for Selected Design

## 2. High-Pressure System

The high-pressure LO<sub>2</sub> dedicated OMS system delivers propellant to the using system at a tank pressure of 151.6 N/cm<sup>2</sup> (220 psia). Between outflow events, the tank pressure decays to the value representing a saturated condition of the propellant. The propellant tanks were analyzed using the computer models detailed in Chapter II of this volume.

A pressure history for the dedicated OMS LO<sub>2</sub> system using helium pressurization on a representative Shuttle mission is shown in Fig. IV-14. The figure shows that after the first pressurization event, the pressure in the tank decays to a value of approximately 79.2 N/cm<sup>2</sup> (115 psia). During the ensuing coast period of more than five days, the environmental heat load causes the saturation pressure to increase to 96.5 N/cm<sup>2</sup> (140 psia). This coast period is followed by other pressurization and outflow events at the termination of the mission. Between each pressurization event, the pressure again decays to a value only slightly higher than the previous saturation pressure. The significant point to be noted from Fig. IV-14 is that the tank pressure never reaches 151.6 N/cm<sup>2</sup> (220 psia). If that pressure were reached, venting of the tank would be necessary to maintain that pressure. Therefore, for mission durations of seven days, it is not necessary to vent the propellant tanks.

A full tank screen liner is included in acquisition/expulsion designs to provide the capability of venting when necessary. But, because venting is not needed in the high-pressure dedicated OMS LO<sub>2</sub> tank, the need for a full tank screen liner is obviated. Moreover, a tank without a full liner need not be spherical, so the dedicated OMS LO<sub>2</sub> tanks for the high-pressure system were considered to be of cylindrical configuration with hemispherical end domes.

With the exclusion of a full liner from the tank designs and the requirement of the dedicated OMS tanks to outflow only during the settling acceleration produced by the OMS engine, refillable traps become attractive propellant management candidates. The accelerations produced by the OMS engine tend to settle the propellant over the tank outlet. Thus, by positioning a screen trap over the tank outlet, the device can be refilled during an OMS maneuver.

The trap must be of a size sufficient to contain the volume of propellant required to start the OMS engines and settle the bulk propellant over the trap again. At that time, propellant from the

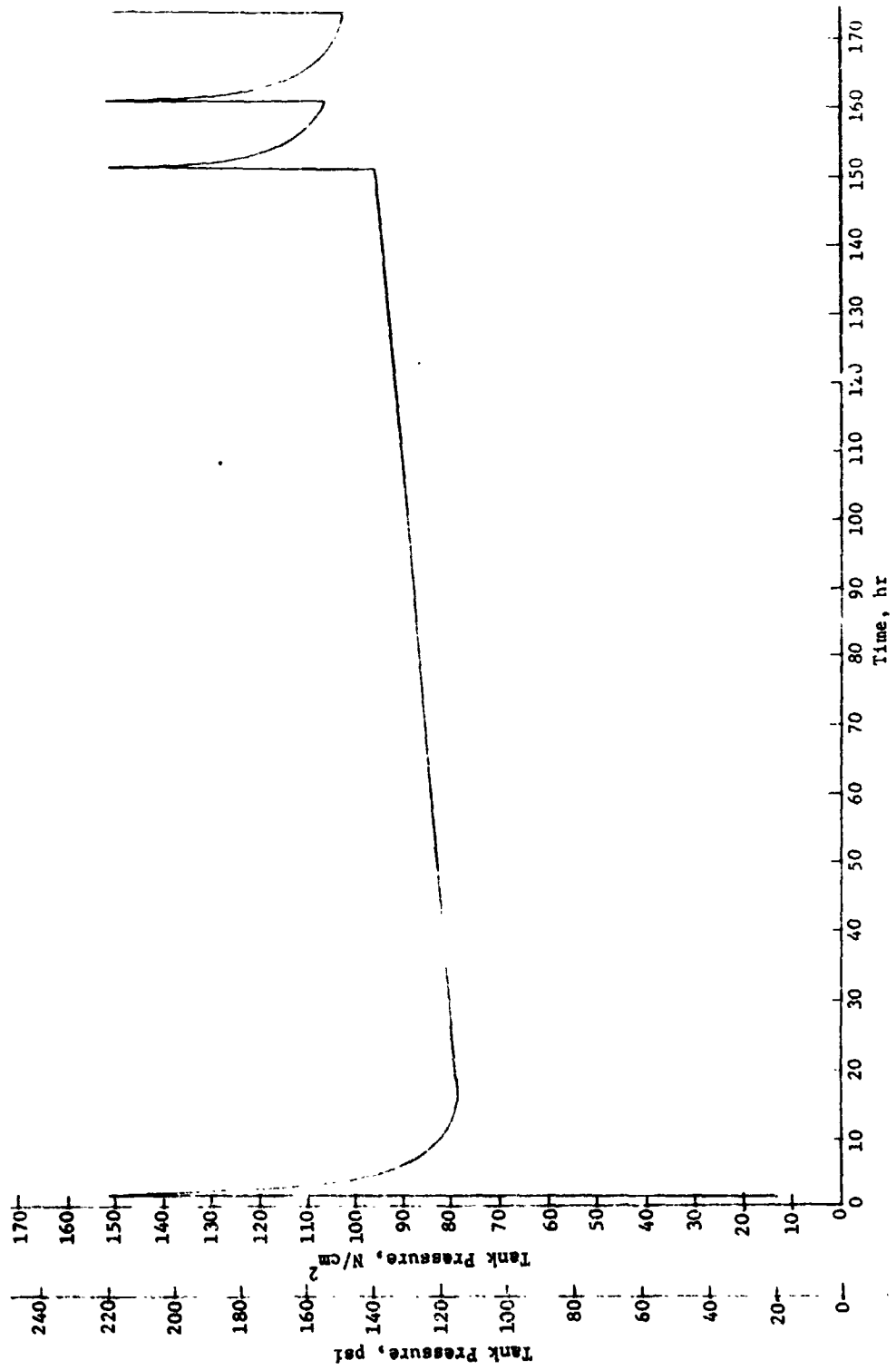


Fig. IV-14 Dedicated OMS LO<sub>2</sub> Tank Pressure History

bulk region can refill the trap and feed the OMS engine directly. For the dedicated OMS system this trap size is determined by the amount of time required to settle the remaining propellant for the final OMS engine firing of the mission.

Of the three missions outlined in the design criteria, the easterly launch mission presents the worst case for resettling because only 31% of the original propellant remains onboard at the initiation of the terminal OMS maneuver. The cylindrical OMS tank dimensions are 1.1 m (3.6 ft) in diameter and 4.4 m (14.4 ft) in length including spherical end domes. Based on an initial 5% ullage load and 31% propellant remaining immediately prior to final OMS engine firing, the worst-case propellant orientation would leave the liquid 302.5 cm (119.1 in.) from the tank outlet. This distance assumes that the liquid has been settled at the tank end opposite the outlet and has a flat interface.

For an orbiter having a weight of 85,000 kg (170,000 lbm) returning to Earth with a 20,430 kg (45,000 lbm) payload and the remainder of the OMS fuel load, the acceleration at the initiation of the final deorbit OMS burn would be 0.0272 g. The settling time can be determined using the following equation:

$$t = \tau \sqrt{\frac{2h}{a}} \quad \text{[IV-1]}$$

where  $t$  = settling time, sec

$\tau$  = dimensionless safety factor

$h$  = settling distance, m (ft)

$a$  = vehicle's acceleration, m/sec<sup>2</sup> (ft/sec<sup>2</sup>)

For this mission, the settling time is 4.76 sec. For a  $\tau$  value of 2.0, the total settling time becomes 9.52 sec. At a flow rate of 10.3 kg/sec (22.6 lbm/sec), the mass of propellant the trap must contain is 97.6 kg (215 lbm). This mass requirement assumes a trap configuration that is completely stable at all times except during refilling. Because there may be acceleration anomalies that could cause momentary screen instabilities and loss of liquid from the trap, the device volume was arbitrarily increased by one-third to contain 130.3 kg (287 lbm).

One advantage of trap systems is the possibility of modular installation. This type of fabrication allows easy removal and inspection. Modular installation can be accomplished by making the

trap an integral part of a tank access cover which bolts onto a flange in the tank dome. From a design standpoint it is desirable to limit the size of the tank port covered by the tank access cover to a diameter half that of the tank diameter. Therefore, the trap diameter was also limited to a diameter of half that of the tank diameter. For the dedicated LO<sub>2</sub> OMS tank the trap diameter was fixed at 54.8 cm (21.6 in.). To contain the required 130.3 kg (287 lbm) of LO<sub>2</sub> the trap must have a height of 44.7 cm (17.6 in.). The basic dimensions of the trap installed in the tank are shown in Fig. IV-15.

The trap is fabricated of aluminum screen and perforated plate. A liquid outflow annulus is included in the trap and liquid flows from the trap bulk region into the annulus. The liquid annulus is connected directly to the OMS feedline to provide the outflow path. The screen forming the liquid annulus is a single layer of 200x1400 Dutch-twill aluminum backed by 50% open area aluminum perforated plate. The trap cover is fabricated in a similar manner of 165x800 Dutch-twill screen. This coarser mesh screen on the trap cover has a lower bubble point and provides a preferential path for vapor ingestion into the trap bulk region rather than into the liquid annulus. This phenomenon would be possible only during the short time when liquid is being expelled from the trap before the tank bulk propellant has settled over the trap. The trap screens are stable during all maneuvers of the RCS system and will refill only during an OMS maneuver.

The tube extending above the trap cover is the trap vent tube. The holes in the top of the vent tube have been sized to be stable under lateral (RCS) accelerations, but unstable during an OMS-produced acceleration. During an OMS engine firing, the holes in the vent tube first allow pressurant to enter the trap, forcing liquid out of the device. When the trap is covered with liquid after settling is complete, the holes in the vent tube allow vapor to be vented from the trap as propellant flows into the trap through the trap cover. The vent tube can be fabricated of solid material because a screen vent tube would offer little, if any, additional benefit or capability to the design. The length of the vent tube is determined by the hydrostatic head required to cause the holes in the top of the tube to be unstable when propellant is settled over it during an OMS maneuver.

One advantage of refillable trap systems is their relatively light weight. Moreover, the trap design proposed here may be removed from the tank. The trap shown in Fig. IV-15 would weigh approximately 3.17 kg (7 lbm). This represents less than 0.1% of the total LO<sub>2</sub> loaded into the tank.



### 3. Offloading Considerations

As noted in the integrated OMS/RCS discussion in Chapter III, offloading requirements present some special problems for capillary acquisition/expulsion systems. In particular, designs incorporating nonrefillable channel designs (such as the low-pressure system design) cannot be offloaded more than a few percent and still remain full during the relatively high-g launch.

To accommodate the offload requirement in the low-pressure system if it should be necessary, a truncated channel system in a cylindrical tank configuration would be a feasible option. A schematic of this design is shown in Fig. IV-16.

As seen in the figure, this concept is a basic dual screen liner variation which encloses a volume equivalent to the smallest anticipated total propellant load for the tank. For maximum offloading, all of the propellant can be contained within this device at launch. For a lesser degree of offloading, some of the propellant will not be initially contained in the device.

The device incorporates a partial liner and channels into a system that can be both vented and refilled. The top of the device includes a coverplate, which serves as the coverplate on the refillable trap and allows liquid to refill the bulk region of the device during an OMS-produced acceleration. The channels also extend across the coverplate so that communication is possible between the settled bulk propellant not included in the device and the outlet. This feature allows outflowing of propellant even though it may momentarily not be included inside the truncated liner volume.

For the high pressure system, the trap design can accommodate any anticipated offload.

### C. DETAILED DESIGN

Detailed design drawings of the proposed dedicated OMS LO<sub>2</sub> systems have been omitted from this chapter because we included detailed designs for the integrated OMS/RCS in Chapter III. These are somewhat larger than the system considered here, but are very representative of the design and fabrication techniques necessary to produce the smaller liner/channel system for the dedicated OMS. It should be

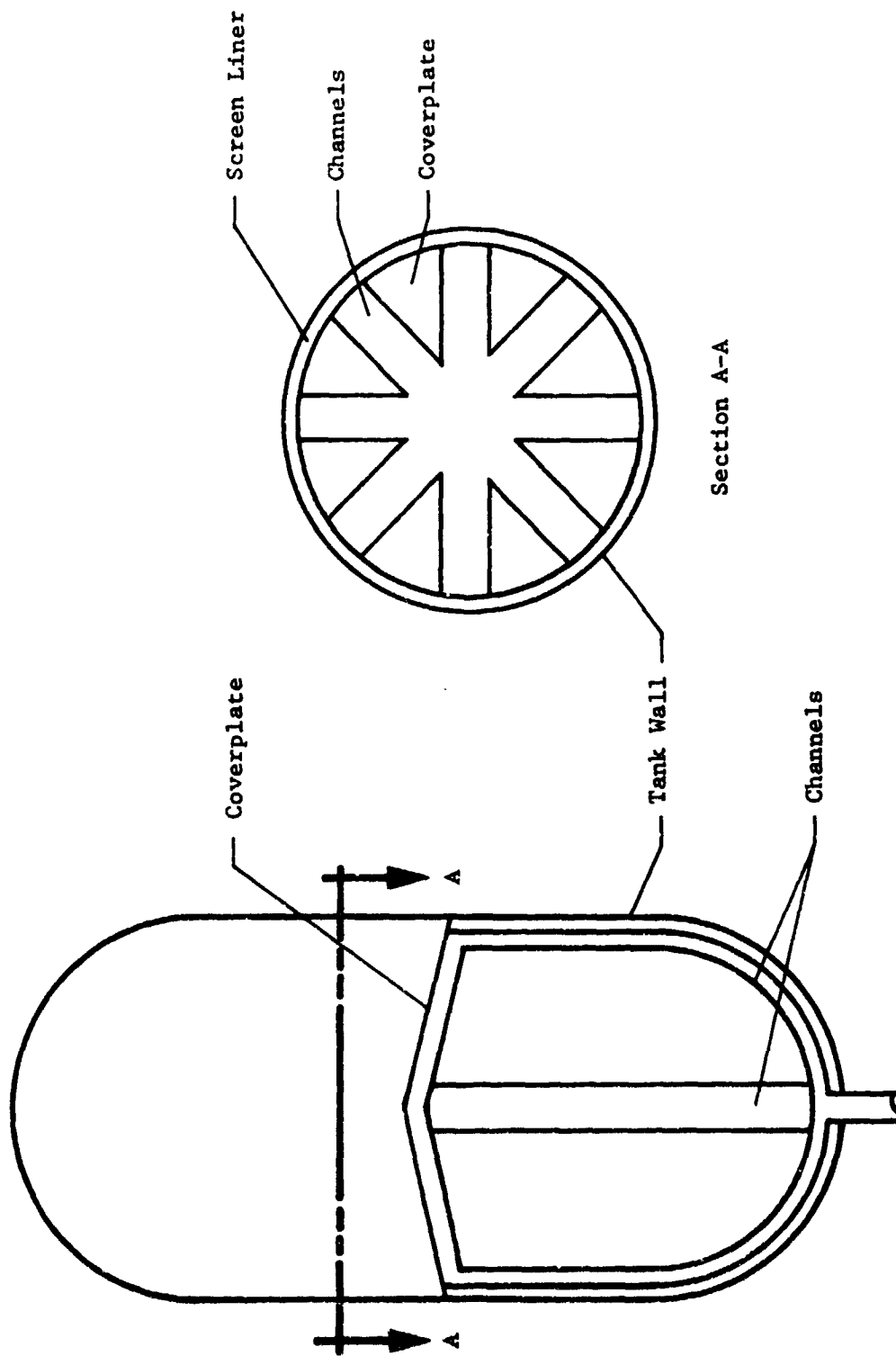


Fig. IV-16 Truncated Channel System for a Cylindrical Tank

noted that the channel system selected here is nearly identical to the 177.8 cm (70-in.) channel system fabricated under an IR&D program. Fabrication and design details of this system are discussed in considerable detail in Volume III. All the information necessary for a detailed design of a channel system is available from these sources.

A trap detail design is presented in Chapter V and includes the detailed design drawings. Additionally, the refillable trap design, presented here, was largely based on the significant effort devoted to the Earth-storable propellant system studies of Volume V. This effort has also developed more details for the design of refillable traps in addition to other systems. These efforts make the presentation of detailed designs here redundant.

#### RESULTS AND CONCLUSIONS

Designs for the acquisition/expulsion system of the dedicated OMS/RCS LO<sub>2</sub> system were prepared. The designs include configurations for both high-pressure and low-pressure systems. The acquisition/expulsion systems were designed to satisfy all of the anticipated propellant expulsion and storage requirements of a typical dedicated OMS LO<sub>2</sub> system duty cycle. This includes gas-free liquid expulsion during the acceleration of several orbit-to-orbit maneuvers. The designs are passive, lightweight, reliable, and flexible. The ability to fabricate, assemble, and inspect these designs was demonstrated by building and checking out a 177.8 cm (70-in.) diameter screen liner and channel assembly, nearly identical in design to the system proposed here, under an IR&D program.

It can be concluded that these designs are capable of satisfying all the varied mission duty cycles and design criteria of the dedicated OMS LO<sub>2</sub> system. Furthermore, confidence in the adequacy of the designs was gained through the experimental programs described in Volume III. Additional credibility in the designs was gained from a thorough design review conducted by the Beech Aircraft Corporation.

## V. SPACE TUG POINT DESIGN

---

The Space Tug is a proposed unmanned, reusable vehicle to be carried into a low Earth orbit within the cargo bay of the Space Shuttle Orbiter. It is expected to be operational at approximately the same time as the Orbiter. The configuration, which uses a liquid hydrogen/liquid oxygen propellant combination, is being considered as an operational version of the Tug. Because of the strong candidacy of the Space Tug as an operational vehicle, the evaluation of its cryogenic propellant storage and feed system was considered appropriate to complement the two Shuttle orbiter designs presented in Chapters III and IV.

The method of approach for this point design was consistent with those just mentioned. First, the Tug design requirements and mission duty cycles were identified. This was followed by reviewing the NASA Space Tug baseline designs (Ref V-1) and also the Tug point design studies (Ref V-2 and V-3). A preliminary study selected the Martin Marietta cryogenic acquisition/expulsion systems for further evaluation from the candidate systems presented in Chapter II. After applying the Tug design criteria and mission requirements, a detail design analysis was conducted, which yielded a detailed design. The Martin Marietta designs were compared with the NASA baseline design.

### A. MISSION AND SPACECRAFT CRITERIA

The Space Tug is carried into a low earth orbit within the cargo bay of the Space Shuttle Orbiter. It separates from the Orbiter and continues to a higher orbit to deploy and/or retrieve a payload. After deployment and retrieval, the Tug returns to the Shuttle Orbiter for the return flight to earth. It is a reusable, unmanned, and remotely controlled spacecraft. Some of the criteria used to design the Tug are presented. All of this information was derived from NASA's baseline Tug document (Ref V-1).

#### 1. General Design Guidelines

The following general guidelines and operational ground rules are considered important for the design of the propellant storage and feed system.

a. *General Guidelines:*

- 1) Advanced materials and concepts are used, assuming a 1976 technology.
- 2) The Tug is designed for a successful mission completion probability of 0.97. This reliability figure does not account for any degradation that might be caused by Shuttle or payload failures and does not consider the possibility of completing a mission in a degraded mode or using additional support from the ground or from Shuttle.
- 3) The Tug is designed as an integral vehicle with none of the subsystems designed to be removable as a kit or single unit.
- 4) In a mission-abort mode (Shuttle once-around abort only) while the Tug is still in the Shuttle payload bay, the Tug is capable of dumping its propellants and safing the subsystems for safe reentry and landing.

b. *Operational Ground Rules*

- 1) The Tug is designed for ground-based operation with all propellant loading, payload/Tug assembly, maintenance repair, and refurbishment to be done on the ground. The only orbital operations are Tug undocking and redocking with Shuttle and payload, and minimum functional testing of the Tug before separating from the Shuttle.
- 2) The Tug is designed for an on-orbit staytime of six days unattached from the Shuttle. It is designed to stay one additional day in the Shuttle cargo bay in a standby condition during earth-to-orbit ascent and orbit-to-earth descent for a total of seven days.
- 3) The Tug is designed for the following operational requirements:
  - a) To separate from the Shuttle at 296.3 km (160 n mi), 28.5-deg with a 1362 kg (3000 lbm), 4.57x7.62-m (15x25-ft) payload attached; ascend to a geosynchronous orbit; deploy the payload; retrieve a 1362 kg (3000 lbm), 4.57x7.62-m (15x25-ft) payload within 7408 km (4,000 n mi) of the deployed payload; return to the Shuttle with the retrieved payload; redock with the Shuttle and return to earth.

- b) To separate from the Shuttle at 296.6 km (160 n mi), 28.5-deg with a 3623 kg (7980 lbm), 4.57x7.62-m (15x25-ft) payload attached; ascend to geosynchronous orbit; deploy the payload; dock and return.
- c) To separate from the Shuttle at 296.3 km (160 n mi) without a payload; ascend to geosynchronous orbit; rendezvous and dock with a 1911 kg (4120 lbm) payload; return with that payload to the Shuttle.
- 4) The Tug (without propellant) and its payload will be installed in the Shuttle cargo bay. The Tug is designed to be installed with the Shuttle either horizontally or vertically. Detailed checks on the Tug and payload are to be performed to installation.
- 5) The Tug is designed to remain in the Shuttle cargo bay in a safe condition for a maximum of 24 hr after landing, at which time it will be removed and returned to a maintenance refurbishment area.

## 2. Performance Requirements and Mission Duty Cycle

The vehicle performance requirements and mission duty cycle that were used to design the Tug propellant storage and feed systems are discussed here.

a. *Delta V Budget* - The delta V budget shown in Table V-1 was used for the baseline Tug mission. The baseline Tug mission assumes that a payload is deployed and retrieved at geosynchronous altitude  $3.58 \times 10^4$  km (19,364 n mi) and that the deployed and retrieved payloads are separated by some angular distance. For this mission, a retro delta V of 15.2 m/sec (50 ft/sec) is imparted to the Tug after deployment in order to accomplish retrieval.

The gravity losses incurred during a thrusting maneuver are a function of the vehicle weight, payload weight, and engine thrust. For the point design, the initial Tug weight is assumed to be  $1.20 \times 10^5$  kg (65,000 lbm) and the engine thrust is 44,400 N (10,000 lbf).

Table V-1  $\Delta V$  Budget Equatorial Synchronous Orbit

Event	$\Delta V$ m/sec (ft/sec)		
	Main Engine	Orbit Maneuver	APS
Separate from Shuttle at 296 km (160 n mi)			3.04 (10)
Perigee Burn	2447 (8,030)		
Gravity and Turning Losses	94.4 (310)		
Midcourse Correction			15.2 (50)
Apogee Burn	1785 (5,858)		
Gravity and Turning Losses	3.048 (10)		
Stationkeeping			9.14 (30)
Deploy Payload			3.04 (10)
Inject into Phasing Orbit for Retrieve Payload		30.48 (100)	
Retrieve Payload		30.48 (100)	4.57 (15)
Deorbit	1784 (5,854)		
Gravity and Turning Losses	2.13 (7)		
Midcourse Correction			15.2 (50)
First 314.8-km (170-n mi) Perigee Burn	2331 (7,649)		
Gravity and Turning Losses	7.62 (25)		
Circularization at 314.8-km (170-n mi) Burn	112 (368)		
Terminal Rendezvous		30.48 (100)	4.57 (15)
Dock with Shuttle at 314.9-km (170-n mi)			3.04 (10)
Contingency (2%)	171 (562)		
<b>Total</b>	<b>8739 (28,673)</b>	<b>91.4 (300)</b>	<b>57.9 (190)</b>

b. *Mission Profile and Timeline* - The orbital operations timeline that satisfies the delta V budget is presented in Table V-2. The Tug is used to deploy a payload, retrieve a different payload from the mission orbit, and return and dock with the Shuttle Orbiter in a 314.8 km (170 n mi) orbit. The payload to be retrieved could not exceed a 7408 km (4000 n mi) distance from the Tug at the start of retrieval.

The timeline describes the events, time duration and delta V required to perform the events. Also, the propulsion system used to perform each event and the propellants consumed and remaining are identified. The propellant consumption schedule is consistent with the delta V budget, propulsion system performance requirements, and the baseline Tug weight requirements. The maximum mission of the Tug from liftoff to return to the launch site is seven days.

### 3. Propulsion System Characteristics and Requirements

The Tug has two propulsion systems--the main propulsion system (MPS) performs the large delta V maneuvers and the auxiliary propulsion system (APS) performs the required attitude control maneuvers. The general requirements and limitations of the MPS and APS are described in the following sections. Operating characteristics and performance requirements for each propulsion system are also discussed.

a. *General* - The Tug MPS and APS are designed to satisfy the following requirements and limitations.

- 1) No direct physical interface exists between the Tug propulsion system and the payload.
- 2) While in orbit after separation from the Shuttle, the Tug propulsion system will provide attitude control for the Tug with or without payload. The Tug will not provide attitude control for experiment pointing.
- 3) No propellant sharing will exist between Tug and the payload.
- 4) The Tug can be loaded with propellants, pressurants, and other fluid reagents while in the Shuttle cargo bay on the launch pad. This is accomplished through fill and drain systems that are separate from those of the Shuttle, but accessible with Shuttle on the pad in the vertical position and with the payload doors closed.

- 5) Propellant loading will be accomplished in such a manner that no contaminants are introduced into the Shuttle cargo bay.
- 6) The Tug engine compartment can be purged by conditioned gas while in the Shuttle cargo bay on the launch pad.
- 7) The Tug will be capable of safely venting propellant boiloff gases while on the launch pad, during launch and flight, in orbit, and during reentry while still in the Shuttle cargo bay.
- 8) In the event of abort, the Tug can safely dump propellants before Shuttle Orbiter landing. Propellant dump provisions are provided only during the orbital coast phase of an abort-to-orbit mode. Acceleration for Tug propellant settling is provided by Shuttle.
- 9) The propulsion system of the Tug will be remotely checked out while in the cargo bay before launch and while in orbit before separation from the Shuttle.
- 10) No propellant sharing will exist between Tug and Shuttle.
- 11) Tug propulsion system prestart functions will be accomplished after deployment, but before Tug and payload/Shuttle separation.
- 12) All Tug propulsion systems will be required to be in a safe condition before reentry from orbit in the Shuttle.
- 13) After retrieval from orbit, the Tug propellant vent and purge interface will be reestablished.
- 14) Before reentry, the Tug propellant tanks will be purged of residuals. Purge gases will be stored in the Shuttle cargo bay.
- 15) Contaminants from the APS thrusters do not impinge harmfully on the payload.
- 16) The MPS and APS will be designed to meet fail operational/fail-safe criteria.

Table V-2. Space Tug Timeline

Event No.	Event	Time, hr	Duration	Propellant Used		LO <sub>2</sub> Used		LO <sub>2</sub> Remaining		LH <sub>2</sub> Used		LH <sub>2</sub> Remaining		ΔV	
				kg	lbm	kg	lbm	kg	lbm	kg	lbm	kg	lbm	kg	lbm
1	Check out Tug and payload	5.06	2.00 hr	--	--	--	--	21,741	47,889	--	--	3038	8013	--	--
2	Deploy Space Tug	5.06	28 sec	24.1	53	19	42	21,722	47,847	5.0	11	3633	8002	3.048	10
3	Phase into orbit for longitude correction	17.06	12 hr	--	--	--	--	--	--	--	--	--	--	--	--
4	Burn and inject into 160x19,300 n mi transfer orbit; change phase 2 deg	17.06	21.1 min	12,226	26,930	10,805	23,800	11,242	24,764	1746	3847	1886	4155	2542	8340
5	Coast to 19,300 n mi apogee	19.06	2.00 min	--	--	--	--	--	--	--	--	--	--	--	--
6	Midcourse correction	19.06	81 sec	69.4	153	55.4	122	11,187	24,642	14.0	31	1872	4124	15.2	50
7	Coast to 19,300 n mi apogee	22.35	3.29 sec	--	--	--	--	--	--	--	--	--	--	--	--
8	Change plane to 26.5° and circularize to 0°, synchronous orbit	22.39	9.18 min	5,321	11,721	4,560	10,046	6,626	14,596	760.4	1675	1112	2450	1794	5888
9	Coast and orbit trim maneuvers	46.35	3.4 sec	28.1	62	22.7	50	6,603	14,546	5.45	12	1106	2438	9.14	30
10	Deploy payload	47.35	10.7 sec	9.5	21	7.26	16	6,596	14,530	2.27	5	1104	2433	3.048	10
11	Phase to retrieve returning payload	95.35	7.4 sec	68.1	150	58.11	128	6,538	14,402	9.98	22	1094	2411	30.48	100
12	Rendezvous with returning payload	97.35	7.4 sec	68.1	150	58.11	128	6,571	14,474	9.98	22	1084	2389	30.48	100
13	Dock Tug with payload	98.35	21 sec	15.89	35	11.35	25	6,469	14,249	2.72	6	1081	2383	4.57	15
14	Safe payload	98.85	0.5 hr	--	--	--	--	--	--	--	--	--	--	--	--
15	Phase in orbit for nodal crossing	104.45	5.6 hr	--	--	--	--	--	--	--	--	--	--	--	--
16	Burn and inject into 170-n-mi perigee transfer orbit, change plane 26.5°	104.45	6.11 min	3,543	7,805	3,037	6,690	3,431	7,559	506.2	115	576.6	1268	1786	5861
17	Coast to 170-n mi perigee	106.74	2.31 hr	--	--	--	--	--	--	--	--	--	--	--	--
18	Midcourse correction	106.74	46 sec	31.3	69	24.9	55	3,406	7,504	6.35	14	569.3	1254	15.2	50
19	Coast to 170-n mi perigee	109.74	3.00 hr	--	--	--	--	--	--	--	--	--	--	--	--
20	Inject into 170x388 n mi phasing ellipse, change plane 2°	109.74	5.12 min	2,884	6,354	1,542	5,600	864.4	1,904	424.0	934	145.3	320	209	7674
21	Coast one revolution in phasing ellipse	111.32	1.58 hr	--	--	--	--	--	--	--	--	--	--	--	--
22	Burn and inject into 170x170 n mi delta V orbit	111.32	0.01 sec	108.0	238	92.61	20	771.8	1,700	15.43	34	129.8	286	112	368
23	Coast one revolution in 170x170 n mi orbit	112.84	1.52 hr	--	--	--	--	--	--	--	--	--	--	--	--
24	Shuttle execute terminal phase rendezvous and docking	113.59	0.75 hr	--	--	--	--	--	--	--	--	--	--	--	--
25	Tug and Shuttle rendezvous	115.59	76 sec	29.96	66	25.87	57	745.9	1,643	4.08	9	125.7	277	30.48	100
			7 sec	5.44	12	4.54	10	741.4	1,633	0.908	2	124.8	275	15.2	50
			4 sec	3.63	8	2.72	6	738.6	1,627	0.908	2	123.9	273	3.048	10
26	Dock with Shuttle	116.59	4 sec	3.63	8	2.72	6	738.6	1,627	0.908	2	123.9	273	3.048	10

\* FPS = throttled (20%) main propulsion system.

3. *MPS Operating Characteristics and Requirements* - For the Space Tug point design study, a single advanced state-of-the-art high-performance LO<sub>2</sub>/LH<sub>2</sub> engine was baselined. The engine characteristics are presented in Table V-3. The engine has a variable thrust and an idle mode capability. For the large delta V maneuvers, the full engine thrust level is used. For intermediate delta V maneuvers, the engine is throttled down to 20% of full thrust. The reduced thrust operation eliminates extremely short burns that would occur if the full thrust mode was used. A pressure-fed idle mode is utilized for turbopump and thrust chamber chilldown before start. For this operational mode, a low chamber pressure [less than 6.89 N/cm<sup>2</sup> (10 psia)] produces a thrust of 63 lbf.

Table V-3 *MPS Operating Characteristics and Requirements*

Propellants	Liquid Oxygen/Liquid Hydrogen
Engine Thrust 100%/20%	44,480/8,896 (10,000/2,000 lbf)
Pressure Fed Idle Mode Thrust	280.2 N (63 lbf)
Nominal Engine Mixture Ratio	60:1
Engine Chamber Pressure	1268 N/cm <sup>2</sup> (1840 psia)
Specific Impulse at 100% Thrust	470 sec
Specific impulse at 20% Thrust	460 sec
Liquid Hydrogen NPSH	4.57 m (15 ft) of LH <sub>2</sub>
Liquid Oxygen NPSH	0.609 m (2 ft) of LO <sub>2</sub>
LH <sub>2</sub> Tank Operating Pressure	15.16 ± 1 N/cm <sup>2</sup> (22 ± 1.5 psia)
LO <sub>2</sub> Tank Operating Pressure	13.8 ± 1 N/cm <sup>2</sup> (20 ± 1.5 psia)
LH <sub>2</sub> Tank Venting Pressure	15.5 N/cm <sup>2</sup> (22.5 psia)
LO <sub>2</sub> Tank Venting Pressure	14.1 N/cm <sup>2</sup> (20.5 psia)
LH <sub>2</sub> Flow Rate	1.61 kg/sec (3.55 lbfm/sec)
LO <sub>2</sub> Flow Rate	8.06 kg/sec (17.75 lbfm/sec)

The engine is equipped with boost pumps for both propellants to allow NPSH of 4.57 m (15 ft) for LH<sub>2</sub> and 0.61 m (2 ft) for LO<sub>2</sub>. The tank operating pressures are 15.2 (22 + 1.5 psia) for the LH<sub>2</sub> tank and 13.8 + 1 N/cm<sup>2</sup> (20 + 1.5 psia) for the LO<sub>2</sub> tank. The vent relief settings for the vent valves are 15.5 N/cm<sup>2</sup> (22.5 psia) and 14.1 N/cm<sup>2</sup> (20.5 psia) for the LH<sub>2</sub> and LO<sub>2</sub> tanks, respectively.

c. *APS Operating Characteristics and Requirements* - The APS operating characteristics and requirements are summarized in Table V-4. This system provides the required thrust and total impulse to (1) maintain vehicle attitude control, (2) perform stage delta V maneuvers for mid-course corrections, (3) perform translational maneuvers during rendezvous and docking, and (4) perform vehicle and sensor pointing as required.

The APS has 16 thrusters with 132 N (30 lbf) thrust each, mounted in clusters of four at 90 deg intervals around the stage circumference. The thrusters operate on gaseous hydrogen and oxygen at a mixture ratio of 4:1. Pitch, yaw, and roll control is provided by firing appropriate pairs of thrusters. Translation is obtained by firing pairs or quadruplets. The total maximum impulse available from the APS is 780,624 N/sec (175,500 lbf/sec).

Table V-4 *APS Operating Characteristics and Requirements*

Propellants	Gaseous Oxygen/Gaseous Hydrogen
Number of Thrusters	16 (4 clusters of 4 each)
Thrust Level	132 N (30 lbf per thruster)
Specific Impulse	380 sec
Total Impulse Size	780,624 N/sec (175,500 lb/sec)
Mixture Ratio	4:1
GO <sub>2</sub> Flow Rate, maximum*	0.113 kg/sec (0.25 lbm/sec)
GH <sub>2</sub> Flow Rate, maximum*	0.036 kg/sec (0.08 lbm/sec)
*The maximum flow rates occur (Ref V-2) when four thrusters are fired simultaneously. The flow rates also consider mass requirements for the propellant conditioning gas generators.	

d. *Acceleration and Thermal Characteristics and Requirements* - The mission acceleration and thermal environments affect the design of the propellant storage and feed system. The acceleration levels and thermal characteristics that were used in evaluating and designing the Tug propellant storage and feed systems are presented in the following paragraphs.

1) *Acceleration Environment* - The Tug acceleration environment is determined by the propulsion system thrust levels and vehicle weight. In order to define the acceleration environment as a function of the mission timeline, it is necessary to know the variation of the vehicle weight during the mission. In addition to the propellant consumption schedule given in Table V-2 a summary of the Tug weights used to calculate the acceleration environment is presented in Table V-5.

Table V-5 *Space Tug Weight Summary*

Total Tug Weight with 1362 kg (3000 lbm) Payload	29,510 kg (65,000 lbm)
Tug Burnout Weight, Including Residuals, But Not Payload	2814.8 kg (6200 lbm)
Payload Weight	
Deploy and Retrieve Payload	1362 kg (3000 lbm)
Deploy Only	3623 kg (7980 lbm)
Retrieve Only	1911 kg (4210 lbm)

A summary of the acceleration environment is presented in Table V-6. The maximum acceleration during a MPS event is 1.51 g, which occurs at the end of the burn to circularize into 314.8x 314.8-km (170 by 170-n mi) orbit without a payload. The minimum acceleration during a MPS event is 0.092 g, occurring at the start of the first throttled (20% thrust) burn. All of the MPS thrusting maneuvers produce accelerations in the axial direction, which settle propellants in the aft end of the tanks. The APS thrusting maneuvers produce accelerations in any direction. A maximum APS acceleration of 0.02 g occurs during a translational maneuver with four thrusters firing and also during rotational maneuvers.

Table V-6 Summary of Space Tug Accelerations

<u>Main Propulsion System</u>	
Maximum Acceleration in Forward Direction	1.51 g
Minimum Acceleration in Forward Direction	0.092 g
<u>Auxiliary Propulsion System</u>	
Maximum Acceleration in Any Direction	0.02 g

2) *Thermal Environment* - The Tug thermal environment is determined by the baseline design of the thermal protection system outlined in Ref V-1. Using the information presented in Refs V-1 and V-2, the important heating rates and thermal protection parameters were identified and used to establish an overall heat flux for each storage tank. The overall heat flux is used to evaluate and design the propellant storage system, specifically, the pressurization and venting analyses.

The baseline Tug thermal protection system for the main LO<sub>2</sub> and LH<sub>2</sub> tanks is a multilayer insulation (MLI) concept using two blankets with 10 layers each of perforated goldized Kapton and Dacron net spaces. A Nomex mesh tension membrane is used as the purge bag over the insulation. Each strut of the fiberglass tank support system is covered with one blanket of MLI to minimize the heat leak. In addition to the MLI on the main tanks, the dedicated APS tanks (located inside the LO<sub>2</sub> and LH<sub>2</sub> tanks) are insulated with foam to isolate them from the main tanks. The LH<sub>2</sub> MPS feedline has a 6.09 cm (2.4 in.) inside diameter. From the tank to the engine inlet, the feedline is wrapped with an additional blanket of MLI and purged with helium. The LO<sub>2</sub> MPS feedline has a 7.36 cm (2.9 in.) inside diameter and is wrapped with teflon tape. The APS feedlines are vacuum-jacketed stainless steel with 1.27 cm (1/2 in.) inside diameter. Both the APS feedlines and the LH<sub>2</sub> MPS feedline have heat exchanger tubes through which a continuous flow 1.081 kg/hr (0.18 lbm/hr) of hydrogen is maintained to keep the lines chilled. A summary of the Tug thermal characteristics is presented in Table V-7.

Table V-7 Space Tug Thermal Characteristics

Main Propellant Storage Tanks

Insulation: Multilayer Double Goldized Kapton with Dacron Net Spacers

Configuration: 2 Blankets, 10 layers each

Insulation Performance:  $k_{\text{eff}} = 1.90 \times 10^{-5} \text{ W/m}^2\text{-}^\circ\text{K}$  ( $1.1 \times 10^{-5} \text{ Btu/hr-ft-}^\circ\text{R}$ )

$\rho k_{\text{eff}} = 4.35 \times 10^{-7} \text{ W-kg/hr-m}^2\text{-}^\circ\text{K}$   
( $3.4 \times 10^{-5} \text{ Btu-lbm/hr-ft}^2\text{-}^\circ\text{R}$ )

$\epsilon = 0.05$

Insulation Weight: LH<sub>2</sub> Tank = 80.35 kg (177 lbm)

LO<sub>2</sub> Tank = 38.6 kg (85 lbm)

Tank Supports Heating Rate: LH<sub>2</sub> Tank, 1.43 W (5.0 Btu/hr)

LO<sub>2</sub> Tank, 2.93 W (10.0 Btu/hr)

MPS Feedline Heating Rate: LH<sub>2</sub> Tank, 1.43 W (5.0 Btu/hr)

LO<sub>2</sub> Tank, 0.586 W (2.0 Btu/hr)

Overall Heat Flux,

Estimated in Chapter IV: LH<sub>2</sub> and LO<sub>2</sub> tanks,  
 $0.315 \text{ W/m}^2$   
( $0.1 \text{ Btu/ft}^2\text{-hr}$ )

APS Storage Tanks

Insulation: Spray Foam on Tanks

Insulation Weight: LH<sub>2</sub> APS Tank = 5.0 kg (11 lbm)

LO<sub>2</sub> APS Tank = 2.72 kg (6 lbm)

## B. NASA BASELINE PROPELLANT STORAGE AND FEED SYSTEMS DESCRIPTION

The propellant storage and feed systems include all of the sub-assemblies required to store and deliver liquid propellants to the MPS engine and the APS propellant conditioning units. This section describes the propellant storage and feed systems for the Space Tug MPS and APS that were baselined in Ref V-1. Additional information on the propellant storage and feed systems was obtained from Ref V-2 and V-3.

### 1. MPS Propellant Storage and Feed System

The general schematic of the MPS LO<sub>2</sub> and LH<sub>2</sub> storage and feed systems is shown in Fig. V-1. The MPS storage tanks and the feedline systems are described in the following paragraphs.

a. *Storage Tank* - The storage tank includes all the pressure vessels and associated hardware required to maintain and deliver liquid propellants at the required temperatures and pressures to the MPS engine. Included as part of the storage tank are subsystems such as the tankage, thermal protection systems, pressurization, acquisition/expulsion, venting and propellant utilization. The thermal protection was described previously.

1) *Tankage* - The LH<sub>2</sub> tank is a cylindrical, 2014-T651 aluminum alloy tank, 416 cm (164 in.) in diameter with hemispherical bulkheads. The LO<sub>2</sub> tank is an ellipsoidal structure consisting of welded 2015-T651 aluminum alloy bulkheads. The tank volumes are 53.8 m<sup>3</sup> (1904 ft<sup>3</sup>) and 20.0 m<sup>3</sup> (707 ft<sup>3</sup>) for the LH<sub>2</sub> and LO<sub>2</sub> tanks, respectively. The tanks are sized to store a capacity of 3639 kg of (8,013 lbm) of LH<sub>2</sub> and 21,741 kg (47,889 lbm) of LO<sub>2</sub> with 5% initial ullage in each tank. The weight of two tanks is 161 kg (355 lbm) and 140 kg (310 lbm) for the LH<sub>2</sub> and LO<sub>2</sub> tanks, respectively.

2) *Propellant Acquisition/Expulsion and Venting* - Reference V-1 states that in-orbit venting is not anticipated during the low-g coast periods. However, before some of the engine burn periods, venting will be required to cool the main tank propellants and maintain the proper NPSH at the pump inlets. This in-orbit venting will be accomplished after main tank propellants are settled by an idle mode operation of the main engine.

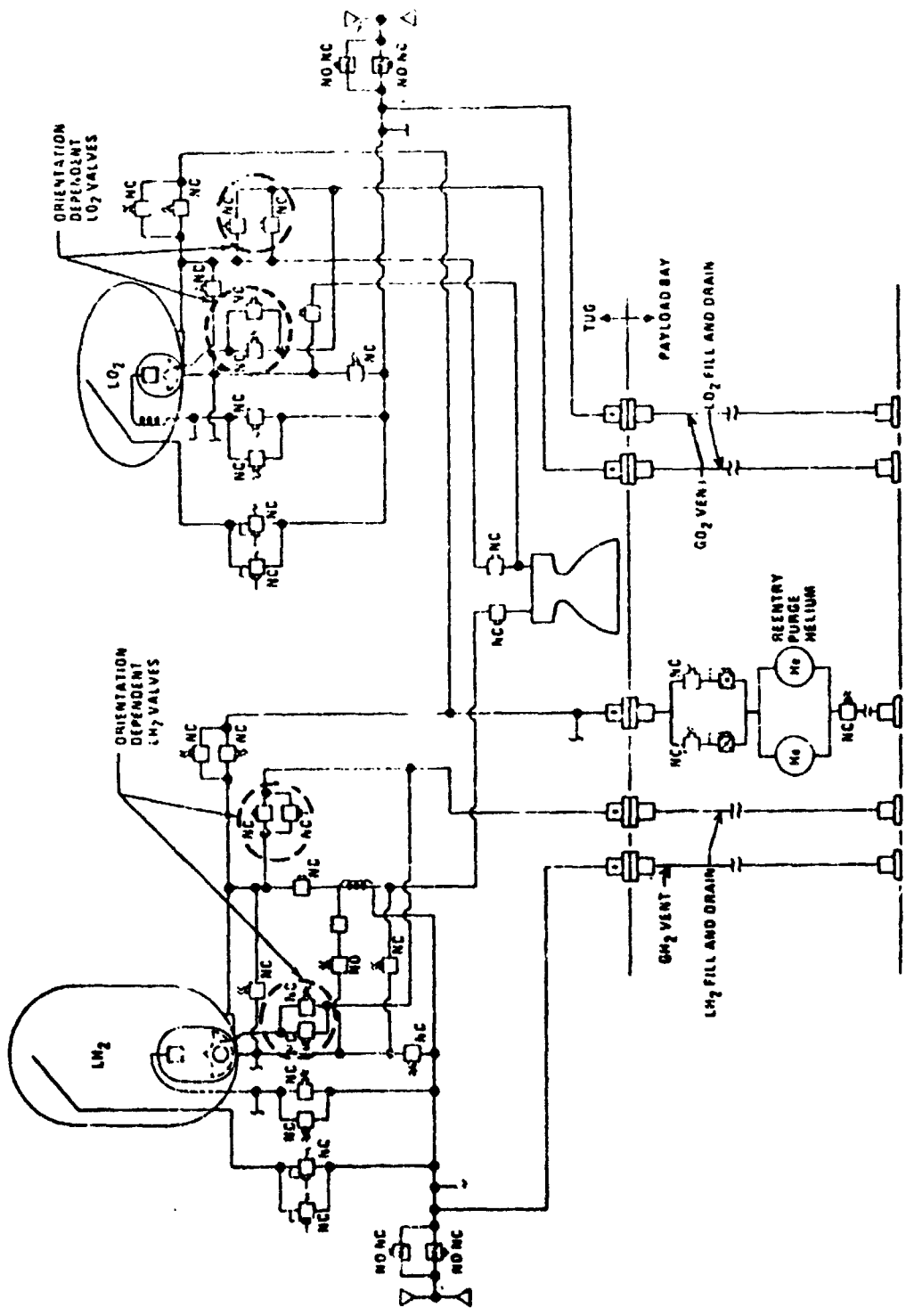


Fig. V-1 NASA Baseline MPS Schematic

The idle mode operation uses propellants from the APS tanks to cool the MPS turbopumps and main engine thrust chamber. The propellants are then ignited to produce 280.2 N (63 lbf) thrust. The total time available for this operation is 145 sec. A total time of 45 sec is allocated for clearing the propellants from the vent ports and 45 sec is allocated for tank repressurization. The remaining 65 seconds are available for the venting operation. The gas-free liquid expulsion is accomplished following the settling of the main tank propellants over the outlet. The total mass of propellants required for the idle mode operation during the Tug mission is 56.8 kg (125 lbm).

3) *Pressurization System* - The pressurization system is autogenous and obtains pressurants from the APS gas accumulators. Pressurant temperatures are 166.8°K (300°R) and 278.0°K (500°R) for GH<sub>2</sub> and GO<sub>2</sub> respectively. The tank operating pressures are 15.17 ± 1.0 N/cm<sup>2</sup> (22 ± 1.5 psia) for the LO<sub>2</sub> tank and 13.8 ± 1.0 N/cm<sup>2</sup> (20 ± 1.5 psia) for the LH<sub>2</sub> tank.

4) *Propellant Utilization System* - A closed-loop propellant utilization system minimizes the propellant residuals. The system uses capacitance probes located inside the main propellant tanks to continuously monitor liquid levels during burn periods.

b. *MPS Feedlines* - The feed system consists of the ducting and valving required to route propellants from the tanks to the engine. The LH<sub>2</sub> feedline has an inside diameter of 6.1 cm (2.4 in.) and is wrapped with multilayer insulation. A hydrogen heat exchanger is used to remove heat from the feedline to maintain liquid at the engine interface. The heat exchanger consists of 6.35 mm (1/4-in.) of tubing brazed to the feedline wall. The LO<sub>2</sub> feedline has an inside diameter of 7.36 cm (2.9 in.) and is wrapped with Teflon tape. Because of its short length, no propellant conditioning is required for the LO<sub>2</sub> feedline. The LO<sub>2</sub> feedline length is estimated to be 0.457 m (1.5 ft) and LH<sub>2</sub> feedline length is approximately 6.70 m (22 ft).

## 2. APS Propellant Storage and Feed System

The APS propellant storage and feed system is completely independent of the MPS storage and feed system. The APS propellant storage and feed system maintains and delivers liquid propellants to the inlet of the APS propellant conditioning units, which condition the propellants for recharging the GH<sub>2</sub> and GO<sub>2</sub> accumulators. The accumulators provide gaseous propellants to the APS thrusters and pressurize the main propellant tanks before and during a main engine burn. In addition, the APS storage and

feed system supplies liquid propellants to the main engine during the idle mode operation and liquid hydrogen for LH<sub>2</sub> feedline, APS feedline, and turbopump cooling. The general schematic for the APS storage and feed system is shown in Fig. V-2.

a. *Storage Tank Design* - The APS propellants are stored in insulated tanks mounted on the inside bottom of the MPS tanks. The cylindrical LH<sub>2</sub> APS tank is approximately 183 cm (72 in.) long with a diameter of 122.1 cm (48 in.). The LO<sub>2</sub> APS tank is also cylindrical, and has a diameter of 76 cm (30 in.) and a length of 92.2 cm (36.3 in.). Both tanks are insulated with foam that weighs 5.0 kg (11 lbm) and 2.7 kg (6 lbm) for the LH<sub>2</sub> and LO<sub>2</sub> APS tanks, respectively. The weights of the APS propellant tanks are 24.9 kg (55 lbm) and 13.6 kg (30 lbm) for the LH<sub>2</sub> and LO<sub>2</sub> tanks, respectively.

Propellant acquisition/expulsion devices are mounted inside the APS tanks to provide the gas-free liquid expulsion during low-g. The devices use capillary screens that are configured in a basket or trap arrangement at the bottom of each tank. The trap can be refilled with APS propellants under the main engine acceleration environment. The trap volume is sized for worst-case propellant usage between refills. The weights of the screen devices are 10.8 kg (24 lbm) and 4.08 kg (9 lbm) for the APS LH<sub>2</sub> and LO<sub>2</sub> tanks, respectively.

The APS tanks are pressurized using gaseous helium. A 0.05 m<sup>3</sup> (1.75 ft<sup>3</sup>) spherical tank is used to store the helium at 2068 N/cm<sup>2</sup> (3,000 psia) within the APS LH<sub>2</sub> tank. The helium pressurant for the LO<sub>2</sub> APS tank is routed through a heat exchanger in the LO<sub>2</sub> MPS tank to raise its temperature to that of liquid oxygen before it enters the tank. The helium pressurant for the LH<sub>2</sub> APS tanks enters the tank at the normal helium storage temperature. The helium storage container is titanium and weighs 13.16 kg (29 lbm). The total mass of stored helium is approximately 9.62 kg (21.2 lbm). The weight of the associated helium pressurization plumbing and valving is estimated to be 13.6 kg (30 lbm).

APS tank venting is provided by routing vent lines to the MPS vent system. The APS tankage is protected from negative pressures by appropriate valving.

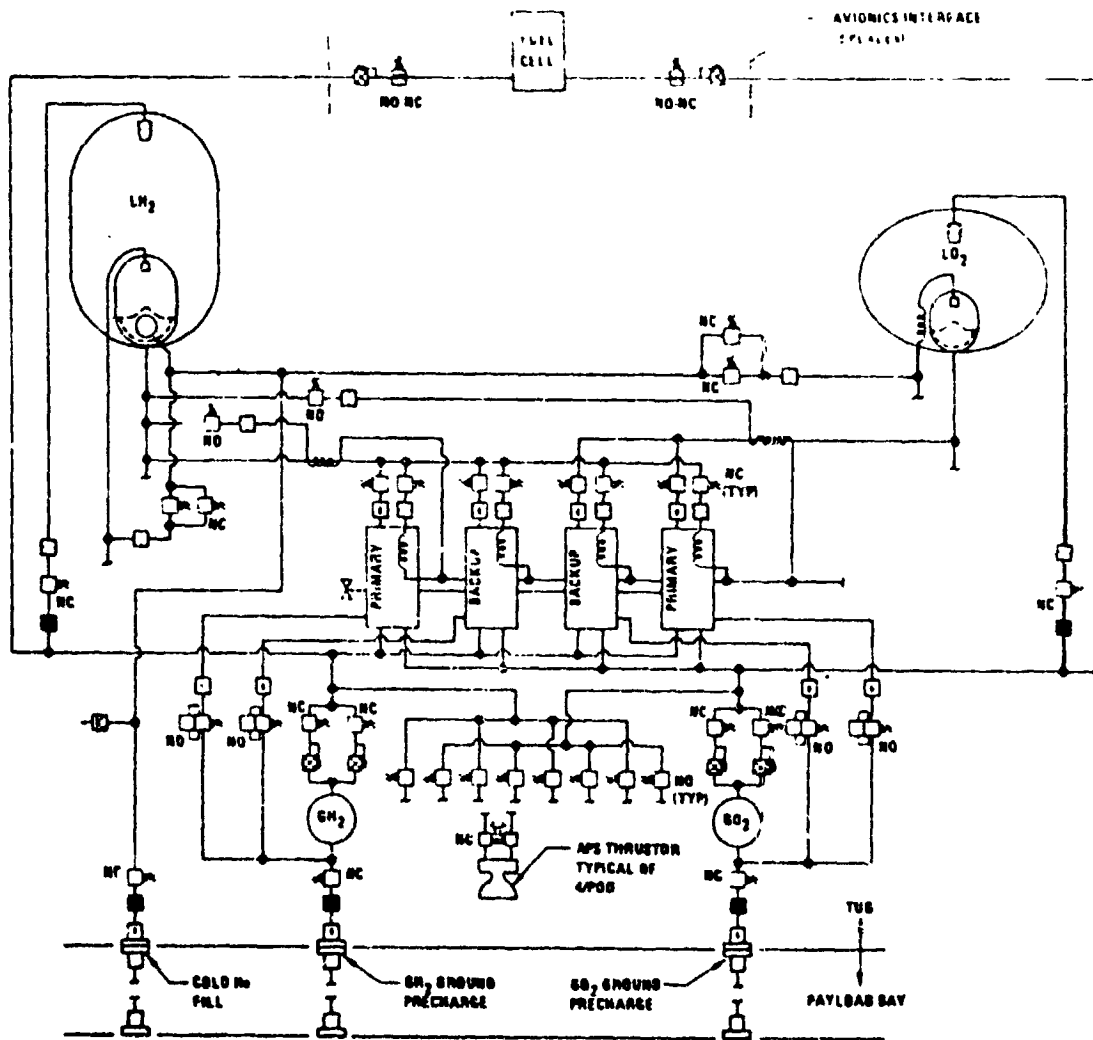


Fig. V-2 NASA Baseline APS Schematic

b. *APS Feedline* - The APS feed system consist of the necessary lines, valves, and regulators to route propellants from the APS tanks to the APS propellant conditioning units, the MPS engine, and the liquid hydrogen heat exchangers. The feedlines are 1.27 cm (1/2 in.) inside diameter vacuum jacketed stainless steel lines. To maintain the APS turbopumps and feedlines in a chilled condition, liquid hydrogen is continuously flowed 0.081 kg/hr (0.18 lbm/hr) through the heat exchangers, mounted on the outside of the feedlines and on the pumps, and then is dumped overboard.

C. MARTIN MARIETTA PROPELLANT STORAGE AND FEED SYSTEM

This section presents Martin Marietta's designs for the Space Tug LH<sub>2</sub> and LO<sub>2</sub> propellant storage and feed systems. The design effort was concentrated on the subsystems that affect the acquisition and expulsion of gas-free liquid propellants for both MPS and APS. Attention was also given to methods for accomplishing liquid-free venting to achieve tank pressure control during low-g coast periods. There was no evaluation or investigation of the thermal protection system for the propellant utilization system. The baseline thermal protection system and propellant utilization system described in the previous section are compatible with the Martin Marietta designs presented.

The following paragraphs discuss the preliminary design and design analyses conducted to define the propellant storage and feed systems for the Tug. The design effort was separated into storage tank designs and feedline designs. However, the two designs use the same concept and are functionally inseparable.

1. Preliminary Design

a. *Storage Tanks* - Martin Marietta proposes three alternative designs to the NASA baseline Space Tug. Each of the designs can satisfy the baseline Space Tug mission as a minimum requirement. However, all the Martin Marietta designs, except the basic design, offer the advantages of increased flexibility and reduced complexity while remaining competitive from a weight standpoint. The basic Martin Marietta design is a refillable trap, the second alternative is a system of channels, and the third is either a trap or channel system with the addition of a full screen-liner.

All three designs are variations of the Martin Marietta Dual-Screen-Liner (DSL) concept. The operational characteristics of these systems were discussed in Chapter II.

Using the Martin Marietta concepts, the propellant storage and feed system requirements for both the MPS and APS can be satisfied with a single storage tank for each propellant. The Martin Marietta designs are integrated MPS and APS storage systems rather than dedicated systems as baselined by NASA.

In addition to selecting the storage tank designs, the preliminary design analysis identified the capillary retention requirements resulting from the Tug acceleration environment. The design approach followed was consistent with that of the two previous designs. The chief consideration when designing a system to prevent gas ingestion into the controlled liquid region is the hydrostatic head to which the system will be exposed. If the differential pressure expressed by

$$P = \rho gh$$

[V-1]

exceeds the pressure retention capability of the screen, the screen will become unstable and vapor will enter the controlled liquid region. The larger the hydrostatic head (expressed by  $h$  in the equation) exposed under the same conditions of acceleration, the finer must be the weave of the screen employed. There is a practical limit to the fineness of screen meshes, but, because the capillary retention capability of multiple layer screens is additive, the problem of capillary retention requirements exceeding the capability of a single screen layer of even the finest meshes can be circumvented. Figures V-3 and V-4 illustrate how multiple layered screens must be employed for various conditions of acceleration and hydrostatic head.

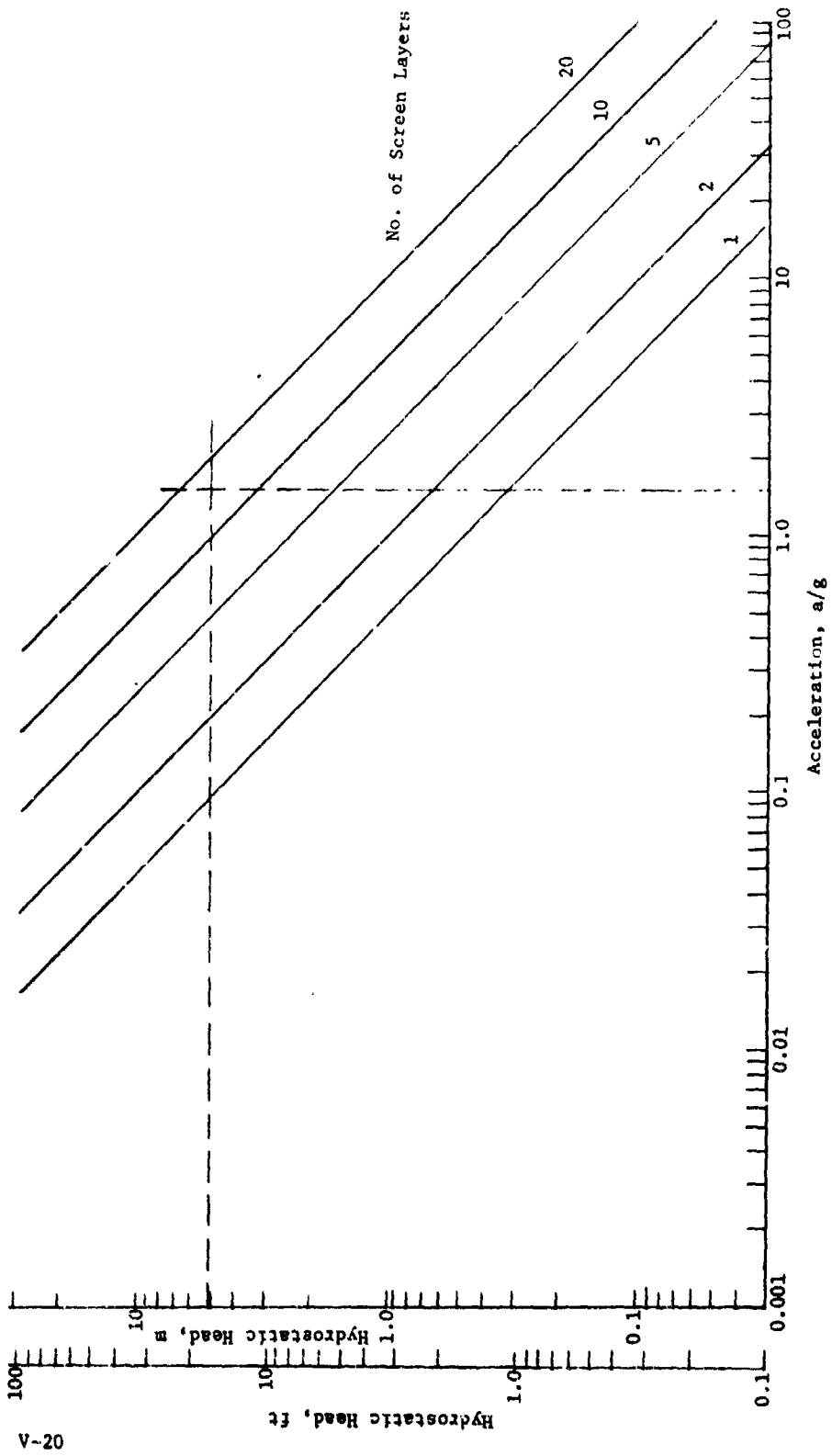


Fig. V-3 Hydrostatic Head Retention Capability of Multiple Layers of 200x1400 Dutch Twill Screen in Liquid Hydrogen

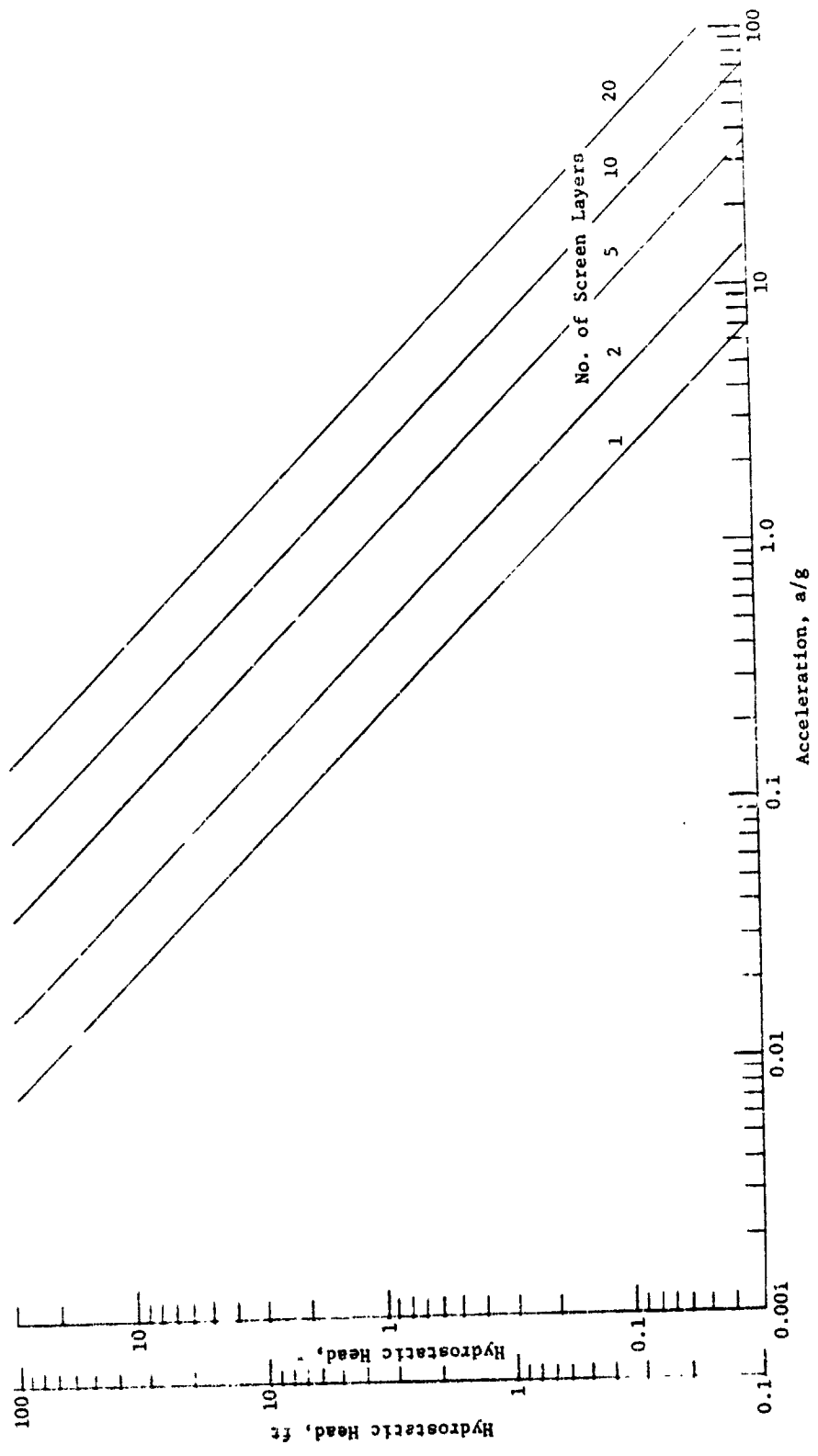


Fig. V-4 Hydrostatic Head Retention Capability of Multiple Layers of 200x1400 Dutch Twill Screen in Liquid Oxygen

In the feeder channel design, the hydrostatic head, against which the capillary device must maintain a stable condition, is essentially the length of the tank liner, or 5.2 m (17 ft), in the Tug LH<sub>2</sub> tank. The maximum acceleration produced by the MPS engine thrust is approximately 1.5 g. Because an operational requirement of the system is that the channels always remain stable, Fig. V-3 shows that an aluminum system using the finest commercially available aluminum Dutch twill screen (200x1400) would require 16 layers of screen to support 5.18 m (17 ft) of LP<sub>2</sub> at 1.5 g. This is illustrated by the horizontal and vertical dashed lines on the figure. The figure shows that a trapped liquid annulus, 0.304-m (1.0-ft) high, would require only one layer of screen. Similarly, on Fig. V-4, the LO<sub>2</sub> system trap could be designed for 1.5 g with a liquid annulus, 14.2 cm (0.47 ft or 5.6 in.) high.

The liquid annulus of the trap is designed so it will not break down and ingest vapor. However, the trap cover plate must be designed so that, under certain conditions of acceleration, i.e., an MPS burn, it will become unstable and allow liquid to enter the trap while the vapor is purged out of the trap. This is necessary because the trap is sized so it contains only enough propellant to satisfy propellant requirements between MPS burns. The refillable characteristics are similar to those of the NASA baseline APS low-g expulsion/acquisition devices.

Absolute stability is not a requirement of the fully lined tank of the trap design. The function of the liner is twofold. It will (1) keep liquid from contacting the tank wall and (2) provide a space from which the system can be vented. Continuous venting is not a system requirement. The liner can be allowed to break down during a full MPS burn. Under these circumstances, liquid will enter the vapor annulus between the screen liner and the tank wall. This liquid can be forced back into the central region by the increasing pressure in the vapor annulus caused by the normal ambient heat leak into the tank after the screen has become fully rewetted during a zero-g coast period. These processes are detailed and analyzed in Subsection 2, Design Analysis.

With the basic designs for the propellant storage tank established by this preliminary design analysis, a more detailed analysis of the various aspects of the concept was undertaken. A summary of that analysis, along with schematic diagrams of the candidate systems for both the oxygen and hydrogen tanks and a more specific discussion of some of the design features follows in Subsection 2.

b. *Feedlines* - For the feedline design, the DSL concept was also considered as an alternative to the NASA baseline thermodynamic vent system (TVS). By expanding LH<sub>2</sub> and passing it through heat exchangers, the TVS maintains liquid propellant in the LH<sub>2</sub> MPS feedline and the LO<sub>2</sub> and LH<sub>2</sub> APS feedlines. Because of the low LH<sub>2</sub> tank pressure, a thermodynamic advantage is realized only in the LO<sub>2</sub> APS feedline. The amount of superheat obtainable in LH<sub>2</sub> heat exchanger systems is negligible. Some system complexity is added because of the TVS control system.

Technical considerations important to the design and operation of a capillary feedline system were presented in Chapter II. The discussion presented was general in nature and established the preliminary design for the screen liner feedline concept. After establishing operational ground rules and design criteria, a more detailed analysis of the various aspects of the concept was undertaken. The Tug design criteria, operational requirements, and feedline geometries were applied to the screen liner feedline concept. A detailed design of the feedline and a discussion of specific design features follows.

## 2. Design Analysis

Detail design analyses of several critical operational requirements and system geometries were applied to the preliminary designs presented previously to yield critical sizing parameters. The results of the design analyses were used in the detailed designs of the propellant storage and feed systems.

Schematic diagrams of the Martin Marietta design alternatives were presented in Chapter II. The various analyses unique to each of these designs are discussed here.

a. *Refillable Trap System* - The first alternative to the NASA baseline system is a screen trap positioned over the tank outlet. The traps are designed to maintain stable conditions under all accelerations imposed by the mission except under the acceleration produced by the full-thrust firing of the MPS engine. The trap cover is designed so that the settling bulk propellant will refill the trap during MPS operation.

The trap dimensions were established as the result of analyses discussed later. The volume of the LH<sub>2</sub> trap is 0.82 m<sup>3</sup> (28.9 ft<sup>3</sup>) and the volume of the LO<sub>2</sub> trap is 0.27 m<sup>3</sup> (9.41 ft<sup>3</sup>). In addition to the screen trap system, the design includes a screen feedline to eliminate the need for an active thermodynamic feedline

cooling system. The dimensions of the feedline screens are 7.37 cm (2.9 in.) in diameter for LO<sub>2</sub> and 6.1 cm (2.4 in.) in diameter for LH<sub>2</sub>. A 5.1-mm (0.2 in.) vapor annulus is provided in both feedlines.

1) *Propellant Utilization Analysis* - The trap for the acquisition system must be sized so it contains sufficient propellant to satisfy all the requirements occurring between MPS burns. The propellant requirements include:

- a) The maximum APS requirement between any two MPS burns, including requirements for systems that tap the APS, such as the autogenous pressurization system and the fuel cells;
- b) Sufficient propellant to start the MPS engine and settle the bulk propellant;
- c) Liquid for engine chilldown prior to start;
- d) Provisions for liquid lost from the trap because of vaporization at the screen surfaces due to environmental heat load and engine soakback heat.

Table V-2 shows that the most severe requirement for propellant occurs between Events 8 and 16. During this 72-hr period, 165.7 kg (365 lbm) of LO<sub>2</sub> and 30.4 kg (67 lbm) of LH<sub>2</sub> are used by the APS system.

The propellant required to start the MPS engine and settle the bulk propellant is variable, depending on the time in the mission. A worst-case analysis would use the lowest acceleration level experienced during the mission. However, the propellant utilization schedule is such that there is no possibility for the trap to be uncovered until after the perigee burn, Event 4. The next firing of the MPS engine produces an acceleration of approximately 0.45 g which was used to determine the settling time in the following equation.

$$t = \tau \sqrt{2h/a} \quad [V-2]$$

The distance, *h*, across which the propellant must be settled was assumed to be the entire length of the longest tank (LH<sub>2</sub> tank), i.e., 5.33 m (17.5 ft). The  $\tau$  term is essentially a safety factor and was assumed to be 3 for this analysis. Using these assumptions, the resulting settling time is 4.5 seconds, and at 1.61 kg/sec (3.55 lbm/sec) and 8.05 kg/sec (17.75 lbm/sec) for LH<sub>2</sub> and LO<sub>2</sub>, respectively, the requirements are 7.26 kg (16 lbm) of LH<sub>2</sub> and 36.3 kg (80 lbm) of LO<sub>2</sub>.

The vaporization that could occur at the trap screen surfaces would be the result of two separate sources of heat. The environmental heat leak into both the hydrogen and oxygen tanks is approximately  $0.315 \text{ W/m}^2$  ( $0.1 \text{ Btu/hr-ft}^2$ ). The steady-state heat soakback from the engine feedline into the trap was assumed to be  $5,270 \text{ W}$  ( $5 \text{ Btu/hr}$ ) in the hydrogen tank and  $2,108 \text{ W}$  ( $2 \text{ Btu/hr}$ ) in the oxygen tank. Therefore, the total heat input to the traps was assumed to be  $9,633 \text{ W}$  ( $9.14 \text{ Btu/hr}$ ) in the  $\text{LH}_2$  trap and  $3,425 \text{ W}$  ( $3.25 \text{ Btu/hr}$ ) in the  $\text{LO}_2$  trap. Over a 72-hour period the resulting vaporization was found to be  $1.55 \text{ kg}$  ( $3.43 \text{ lbm}$ ) of  $\text{LH}_2$  and  $1.151$  ( $2.54 \text{ lbm}$ ) of  $\text{LO}_2$ .

A summary of the propellant requirements for the traps is shown in Table V-8.

Table V-8  $\text{LO}_2$  and  $\text{LH}_2$  Requirements for Trap Design

	Mass, kg (lbm)		Volume, $\text{m}^3$ ( $\text{ft}^3$ )	
	$\text{LH}_2$	$\text{LO}_2$	$\text{LH}_2$	$\text{LO}_2$
APS	30.4 (67)	165.7 (365)	0.425 (15)	0.145 (5.13)
Resettle	7.2 (16)	36.3 (80)	0.101 (3.6)	0.0316 (1.12)
Vaporization	1.5 (3.4)	1.14 (2.5)	0.02 (0.7)	$8.5 \times 10^{-4}$ (0.03)
Total	39.23 (86.4)	203.2 (447.5)	0.546 (19.3)	0.177 (6.28)

The traps were sized to accommodate  $0.817 \text{ m}^3$  ( $28.9 \text{ ft}^3$ ) in the  $\text{LH}_2$  trap and  $0.2663 \text{ m}^3$  ( $9.41 \text{ ft}^3$ ) in the  $\text{LO}_2$  trap, which includes a 1.5 safety factor on the total volumes in Table V-8.

Table V-9 shows the actual safety factor for the settling requirements

Table V-9 Propellant Trap Settling Safety Factors

	LH <sub>2</sub>	LO <sub>2</sub>
Volume in Trap at Beginning of Coast Period, m <sup>3</sup> (ft <sup>3</sup> )	2.7 (28.9)	0.87 (9.41)
Used by APS or Lost Due to Vaporization during Coast, m <sup>3</sup> (ft <sup>3</sup> )	1.45 (15.7)	0.48 (5.16)
Remaining Prior to MPS Burn, m <sup>3</sup> (ft <sup>3</sup> )	1.22 (13.2)	0.39 (4.25)
Required for Resettling, m <sup>3</sup> (ft <sup>3</sup> )	0.33 (3.6)	0.10 (1.12)
Safety Factor	13.2/3.6 = 3.67	4.25/1.12 = 3.8

2) *Hydrostatic Analysis* - The ultimate size and shape of any capillary screen retention device is largely determined by hydrostatic considerations. This is especially true of traps and, particularly, refillable traps. A refillable trap must, by its very nature, be unstable under certain conditions of acceleration, while remaining stable at other times. Satisfying these criteria involves the careful selection of differing screen meshes for use on the various parts of the trap device.

Figure V-5 illustrates the critical dimensions considered in the stability analysis. The dimension,  $h_1$ , represents the height of the controlled liquid region or the trap liquid annulus. This dimension must be such that the screens containing the liquid in the liquid annulus do not become unstable and allow vapor to enter the liquid region. The entry of vapor into the liquid annulus is a serious occurrence because (1) liquid propellant rocket engines and their associated pumps are, generally, not capable of accepting liquid-vapor mixtures and (2) a sufficient amount of vapor could exist in the trap annulus that would cause the trap to cease functioning properly. The liquid annulus must, therefore, be designed so the screen selection is stable under the highest accelerations in the +x and -x (axial) direction and also under all accelerations in the +y or +z (lateral) directions over the distance, w, denoted in Fig. V-5.

Designing the cover plate for a refillable trap requires careful attention to the dimensions denoted as  $h_2$ , and  $h_3$ . The cover plate must function properly under four discrete sets of conditions.

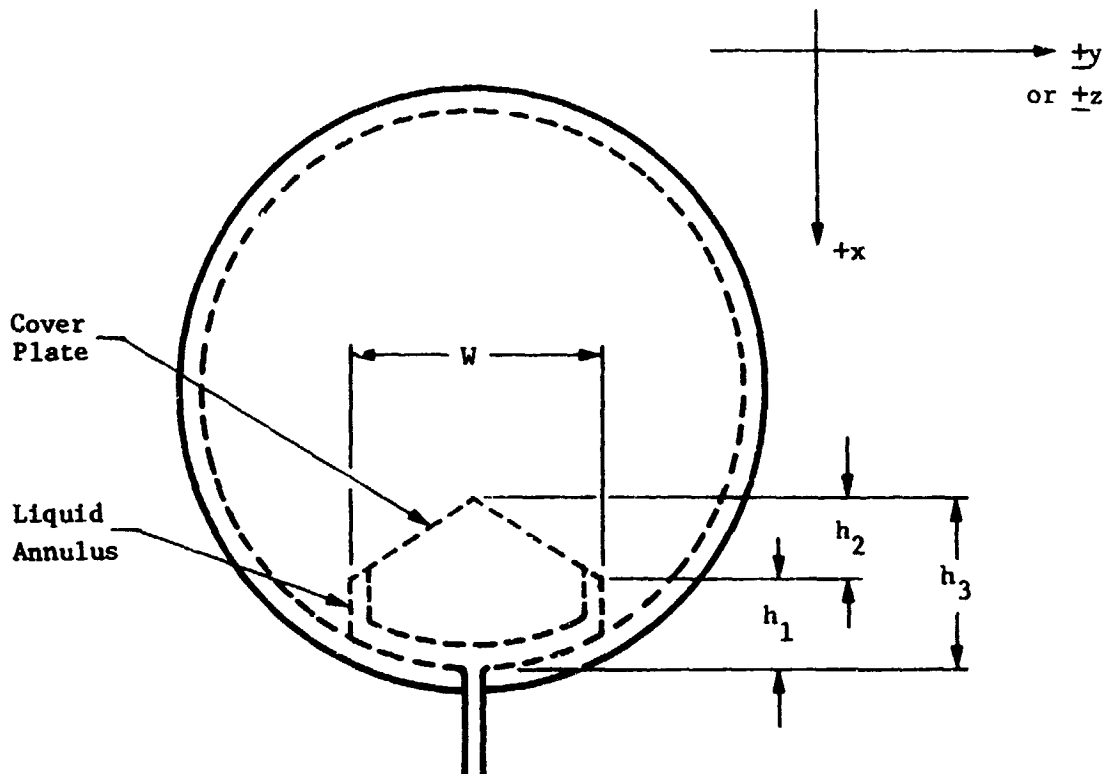


Figure V-5 Refillable Trap Schematic

*Condition 1* - The trap is completely uncovered and the acceleration is in the  $-x$  direction in Fig. V-5. This is essentially a settling mode condition. Under this condition, the total exposed hydrostatic head is the dimension,  $h_3$ . While it is desirable to maintain stability during this kind of maneuver, it is not absolutely essential during an MPS burn because any propellants will be settled over the trap within approximately 1.5 sec.

*Condition 2* - The trap is uncovered and acceleration is in the  $+x$  direction. This condition tends to move propellant to the opposite end of the tank, away from the trap. The hydrostatic head for the trap is still,  $h_3$ , but in this case the cover plate must remain stable for the hydrostatic head denoted by,  $h_2$ .

*Condition 3* - The trap is uncovered and the acceleration is in the  $+y$  or  $+z$  direction. This condition results from a translational or rotational APS maneuver. If the tank is on the centerline of the vehicle, the translational maneuver causes larger hydrostatic heads and the trap cover plate must be stable across the dimension,  $W$ .

*Condition 4* - The trap is covered by settled propellant and the acceleration is in the  $-x$  direction. This is a refill mode. The cover plate must be unstable over the distance,  $h_2$ , for the acceleration conditions imposed so the liquid will enter the trap and purge the trapped vapor. This condition will occur during an MPS burn.

These conditions must be satisfied while considering the additional constraint that the trap must contain a predetermined volume of propellant.

Designing a refillable trap that will satisfy all the conditions discussed while containing a specified amount of propellant may not always be possible. This is particularly true if the critical accelerations are generally of the same magnitude. However, the acceleration environment produced by the Space Tug makes it a vehicle that is particularly adaptable to the refillable trap concept.

Figures V-6 and V-7 were used as an aid to the proper selection of screen meshes for the trap cover plates for  $LH_2$  and  $LO_2$  tanks. The curves represent the capillary retention capability of individual screen types with the two cryogenics of interest. Superimposed on the graphs are shaded areas representing the area through which a curve must pass to satisfy the condition indicated. The conditions are those set forth on the previous page with regard to refillable trap design. Only those curves that pass through all three of the shaded areas represent a screen, which would satisfy all the requirements and be acceptable for the trap cover plate design. Condition 4 was determined by using the lowest acceleration for which the trap cover plate must be unstable. This condition occurs at the end of the apogee burn and at the beginning of the deorbit burn. The coordinates for Condition 4 are  $h_2$  and 0.46 g. The coordinates for Condition 2 are  $h_2$  and 0.02 g and for Condition 3 they are  $W$  and 0.02 g. In the coordinate system the lower left-hand quadrant represents unstable conditions while the upper right-hand quadrant represents stable conditions. Figure V-8 illustrates these quadrants.

Figure V-6 shows that only two screen options are available for the hydrogen system, 24x110 and 30x150. The oxygen system (Fig. V-7) has four options; however, two screen options are marginal leaving 30x150 and 80x700.

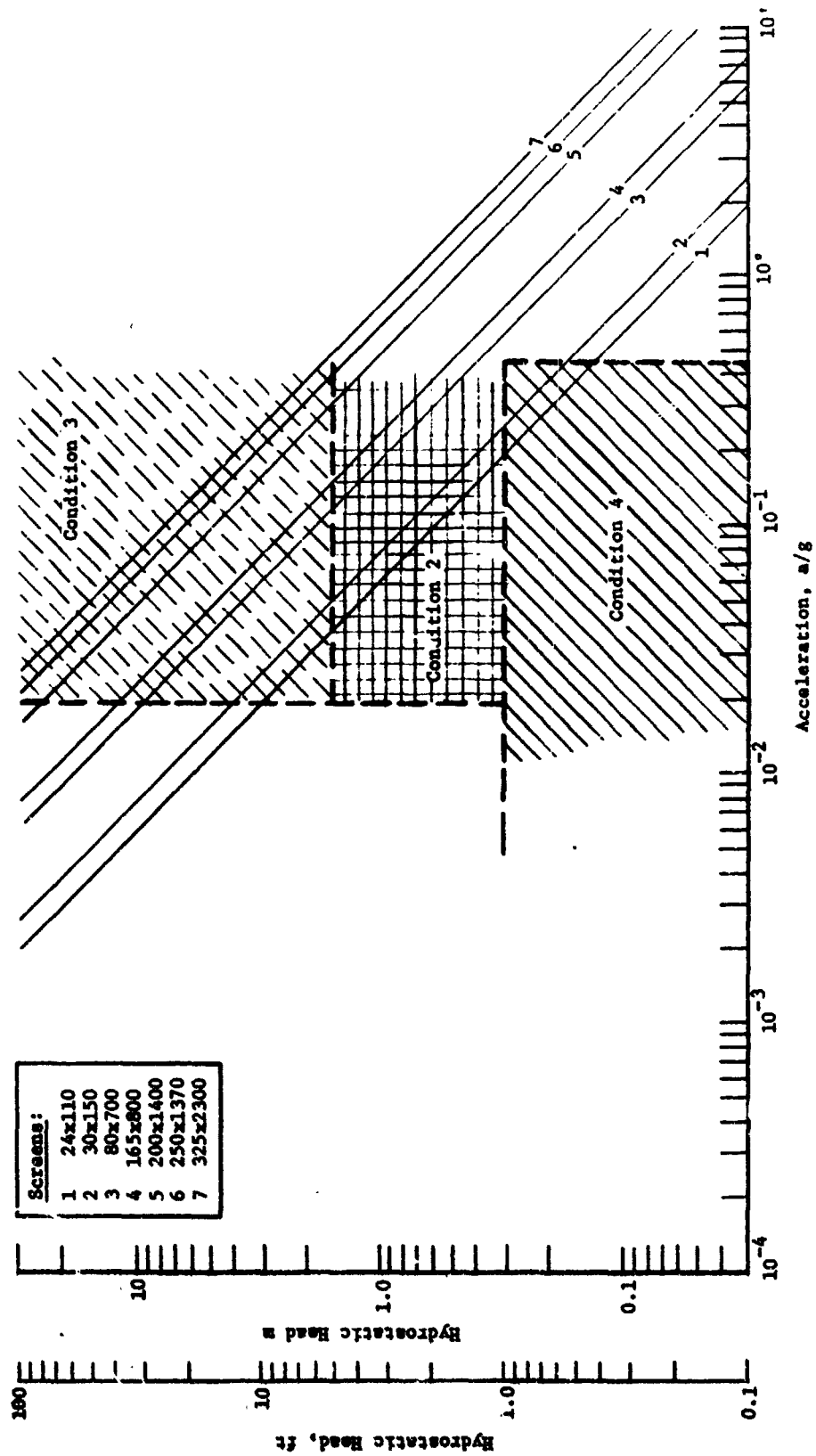


Fig. V-6 Hydrostatic Head Retention Capability of Selected Screens in Liquid Hydrogen

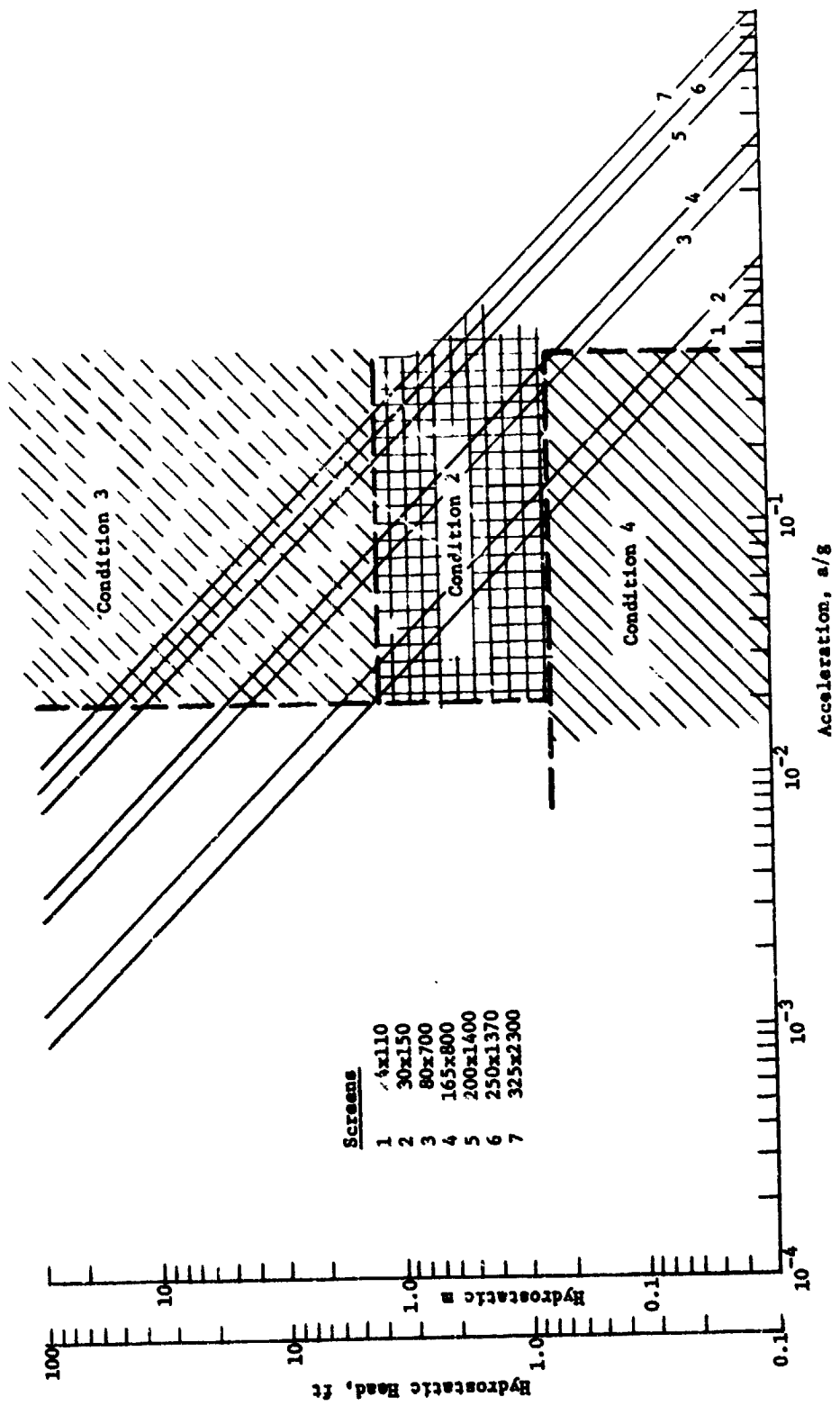


Fig. V-7 Hydrostatic Head Retention Capability of Selected Screens in Liquid Oxygen

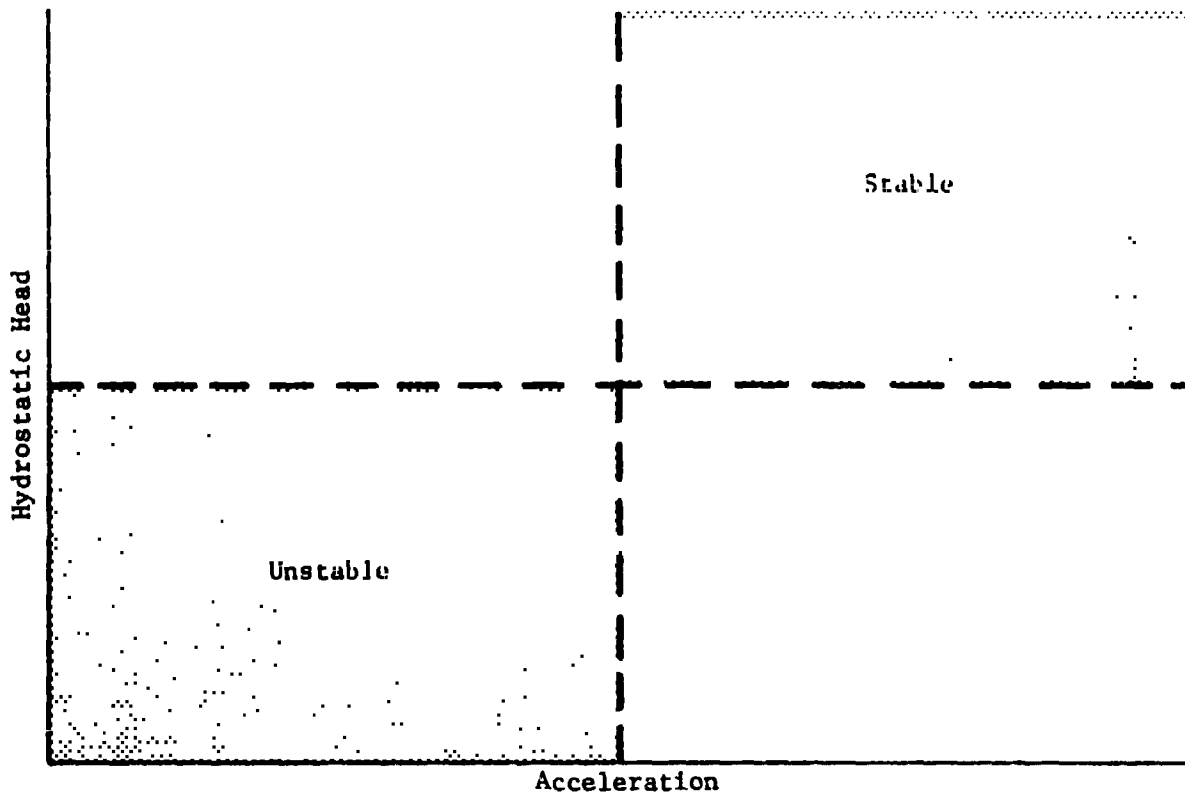


Figure V-8 Illustration of Stable and Unstable Region

Normal design practice calls for the application of a safety factor when designing screen systems. This philosophy is usually adopted to assure that the system will function properly despite degradations in the bubble point of the screens which may occur during the forming and fabrication process. Using the selected screens the estimated safety factors for the systems are shown in Table V-10.

Table V-10 Propellant Trap Design Safety Factors

Condition	LH <sub>2</sub>	LO <sub>2</sub>
1	2	2
2	13	17.5
3	2.6	3.5
4	1.79	1.32

It should be noted that the safety factor listed for Condition 4 is in favor of breakdown. A safety factor of 1 would normally assure the occurrence of breakdown.

The addition of a screen feedline to the system introduces a special condition to the problem of hydrostatic stability. The feedline effectively increases the values of  $h_1$  and  $h_3$  to include to include the feedline length. This can add considerably to the hydrostatic head. In the case of the hydrogen system, the inclusion of a feedline means an addition on the order of 3.65 m (12 ft).

With the screen feedline, the system may be allowed a functional anomaly. When the MPS engine is fired, the feedline is allowed to break down and drop liquid out into the feedline liquid annulus. This liquid is replaced from the trap reservoir so that vapor is not ingested into the system. The liquid level rises in the feedline vapor annulus until the distance between the rising liquid level and the top of the liquid annulus of the trap represents head retention capability of the screen. At that point the liquid level in the feedline vapor annulus will cease rising and the system will function normally as described previously. This loss of liquid represents a very small amount and may only occur in the LO<sub>2</sub> MPS feedline.

This operational mode does depend somewhat on the transient characteristics of the engine, pumps, and valve system. The fluid flowing down the feedline will experience some pressure loss due to viscous effects; conversely, the acceleration produced by the engine will cause the pressure to increase and always be highest at the engine valve inlet. If the fluid demanded by the pump spinup and engine start transient causes a pressure drop that exceeds the pressure built up by the acceleration start transient exceeding the bubble point of the feedline screen, then vapor will momentarily be ingested into the feedline flow. The type of information necessary to evaluate this possibility was not available; therefore, no attempt was made to carry out the analysis.

b. *Channel System* - The channel system proposed as the second alternative to the NASA baseline design is functionally similar to the trap system previously described. The channel system uses a screen-enclosed, controlled-liquid region in direct communication with the tank outlet. The design consists of a number of screen feeder channels spaced around the tank perimeter and extending the full length of the tank. These channels supply liquid on demand from the bulk liquid region through a manifold to the tank outlet. The channels are positioned so that one or

more channels will always be in contact with the propellant and outflow will be possible. Because of the large hydrostatic head and acceleration environment, the screen surfaces of the feeder channels are fabricated of multiple screen layers to take advantage of the additive nature of individual screen capillary retention capabilities. This is necessary because the screens have the capability of wicking liquid, and any vapor that is ingested into a channel through the screen may be trapped when the screen wicks over again. A significant amount of trapped vapor in the channels could, in certain situations, render the channels inoperative. Therefore, the system must be designed to prevent vapor ingestion into the controlled liquid region, i.e., the channels.

1) *Hydrostatic Head Requirements* - Figures V-3 and V-4 illustrate the multilayered screen requirements for the LH<sub>2</sub> and LO<sub>2</sub> tanks, respectively. When a screen device extends the full length of a tank and is exposed to a high acceleration environment, the number of screens required to maintain the device in a stable condition increases notably. As illustrated, the LH<sub>2</sub> tank requires 16 layers of 200x1400 Dutch-twill screen.

Any screen device with large surface areas requiring many layers of screen suffers a weight penalty. Weight can be reduced by limiting the screen surface areas to the minimum required by other than hydrostatic considerations. These considerations are discussed in the following sections.

2) *Hydrodynamic Requirements* - The screen surface area of a screen device may be reduced by reducing the size of the device. The approach taken with the channel design was to reduce the size by limiting the number of channels to the fewest number possible consistent with hydrodynamic considerations and propellant demand requirements.

With a minimum number of channels in the design, it is highly probable that, for a large part of the time, only one channel will be in contact with the bulk fluid. Therefore, the channels were sized so that one channel could handle the propellant flow rate requirements of the MPS engine. The cross-sectional area of the channels was selected so that the viscous losses in the channel and the velocity head were acceptable when compared to the available capillary retention capability. The channel design also considered configurations that, although they minimized the total amount of screen in the systems, still exposed large screen areas to the propellant in cases where the bulk propellant was nearly exhausted. This consideration reduces the effects of viscous losses due to flow of propellant into the system from the bulk region.

3) *Configuration Tradeoffs* - In order to determine which of several candidate design and configuration combinations was the most attractive from a weight standpoint, a comparison matrix was constructed. The matrix for the LH<sub>2</sub> tank appears in Fig. V-9.

The four most reasonable channel configurations and four representative channel designs were combined to compare system hardware weight, residual propellant weight, potentially unavailable propellant weight, and the combined weight of these three.

The first configuration selected was a conventional four-channel design. Four channels were considered to be the minimum number necessary to function properly. The second configuration added two intersecting channel rings to the four-channel configuration. Each ring was positioned at the intersection of the tank-hemispherical end dome and the barrel section. The third configuration was a six-channel design. The fourth configuration was identical to the second, except that all but one of the channels in the barrel section had been removed.

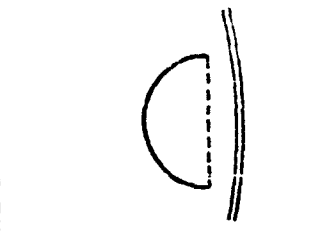
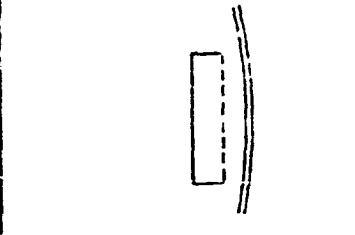
These channel designs were selected, primarily, because they reduced the total screen area. The first design was fastened directly to the tank wall, thereby, eliminating one channel side. The second design represented those designs adopted for applications where high acceleration loads were not present. The third and fourth designs reduced the necessary screen to a single channel side only. Both the channel configurations and designs are depicted in the matrix headings.

The weights entered in the matrix represent the four weight considerations previously mentioned. Hardware weight is entered in the upper left quadrant of each matrix square. The three figures represent weights using three different screens. The top number represents the weight of a 200x1400 aluminum Dutch-twill screen system. The other two numbers represent system weights for aluminum screen systems of 325x2300 and 450x2750 Dutch-twill. These meshes are not currently commercially available at the present time and serve only to illustrate the potential weight savings to be realized by developing these aluminum screens.

The number in the upper right quadrant represents the weight of the propellant contained within the device. The number in the lower right quadrant represents the weight of propellant that could remain in the tank under the most adverse conditions

Channel Cross Sectional Configuration							
Channel Arrangement							
 4 Channels	78.49 (158.5)	54.44 (110.0)	131.96 (266.61)	53.71 (108.5)	54.57 (110.26)	53.71 (108.5)	32.3
	40.20 (81.22)		62.38 (126.04)		40.40 (81.63)		27.0
	33.57 (67.83)		53.77 (108.64)		37.95 (76.07)		11.5
 4 Channels	403.17 (814.58)	270.2 (546)	455.89 (921.11)	270.2 (546)	378.51 (764.76)	270.2 (546)	111.1
	364.88 (737.22)	6.44	386.32 (780.54)	6.44	361.33 (736.13)	6.44	55.0
	358.25 (723.83)		377.71 (763.14)		361.88 (731.17)		77.1
 4 Channels w/rings	146.48 (295.96)	97.28 (196.5)	91.34 (186.49)	95.92 (191.0)	120.54 (243.55)	95.51 (195.0)	143.1
	75.03 (151.54)		62.92 (126.11)		84.07 (169.86)		100.1
	62.66 (126.60)		57.74 (116.17)		77.76 (157.11)		92.1
 4 Channels w/rings	255.57 (516.36)	11.8 (23.9)	238.79 (478.29)	11.8 (23.9)	228.88 (462.45)	11.8 (23.9)	253.1
	184.11 (371.94)	0.28%	176.26 (353.61)	0.28%	192.41 (388.76)	0.28%	208.1
	171.74 (347.00)		163.54 (327.08)		186.10 (376.01)		200.1
 6 Channels	173.45 (346.9)	81.17 (164.0)	163.11 (326.22)	80.18 (162.0)	99.57 (201.18)	79.93 (161.5)	121.1
	59.14 (119.48)		52.31 (105.91)		69.65 (140.72)		83.1
	49.39 (99.79)		49.27 (99.14)		64.42 (130.16)		77.1
 6 Channels	249.43 (503.97)	52.8 (106.7)	298.13 (602.35)	52.8 (106.7)	229.34 (463.28)	52.8 (106.7)	254.1
	193.11 (390.18)	1.25%	225.00 (454.61)	1.25%	202.39 (408.92)	1.25%	216.1
	183.37 (370.49)		212.26 (428.87)		197.66 (399.36)		210.1
 4 Channels w/rings 1 Channel in barrel	136.25 (275.28)	90.33 (182.5)	185.51 (374.82)	91.07 (184.0)	112.84 (227.99)	90.08 (182.0)	136.1
	69.79 (141.00)		103.01 (208.13)		78.76 (159.14)		94.1
	58.28 (117.76)		88.24 (178.28)		72.87 (147.23)		86.1
 4 Channels w/rings 1 Channel in barrel	238.40 (481.68)	11.8 (23.9)	288.41 (582.72)	11.8 (23.9)	214.75 (433.89)	11.8 (23.9)	238.1
	171.94 (347.40)	0.28%	105.90 (213.8)	0.28%	180.67 (365.04)	0.28%	197.1
	160.44 (324.16)		191.12 (386.16)		174.28 (353.13)		181.1

FOLDOUT FRAME

				
53.71 (108.5)	54.57 (110.26) 40.40 (81.63) 37.95 (76.67)	53.71 (108.5)	82.37 (166.32) 57.02 (115.21) 52.65 (106.37)	53.71 (108.5)
270.2 (546) 6.4%	378.51 (764.76) 364.33 (736.13) 361.88 (711.17)	270.2 (546) 6.4%	406.25 (820.82) 380.96 (769.71) 376.58 (760.87)	270.2 (546) 6.4%
95.92 (193.0)	120.54 (243.55) 84.07 (169.86) 77.76 (157.11)	96.51 (195.0)	143.78 (294.50) 130.70 (263.46) 92.90 (187.70)	95.52 (193.0)
11.8 (23.9) 0.28%	228.88 (462.45) 192.41 (388.76) 186.10 (376.01)	11.8 (23.9) 0.28%	253.11 (511.40) 208.05 (420.36) 200.25 (404.60)	11.8 (23.9) 0.23%
80.18 (167.0)	99.57 (201.18) 69.65 (140.72) 64.42 (130.16)	79.93 (161.5)	121.36 (245.20) 85.99 (169.70) 77.52 (156.63)	80.18 (162.0)
52.8 (106.7) 1.25%	229.34 (463.38) 202.39 (408.92) 197.66 (399.36)	52.8 (106.7) 1.25%	254.35 (513.90) 216.98 (438.40) 210.52 (425.33)	52.8 (106.7) 1.25%
91.07 (184.0)	112.84 (227.99) 78.76 (159.14) 72.87 (147.23)	90.08 (182.0)	136.22 (275.23) 94.15 (190.23) 86.87 (175.51)	91.07 (184.0)
11.8 (23.9) 0.28%	214.75 (432.89) 180.67 (365.04) 174.28 (353.13)	11.8 (23.9) 0.28%	239.12 (483.13) 197.05 (398.13) 189.76 (383.41)	11.8 (23.9) 0.28%

Legend

Hardware Weight 200x1400 A <sup>2</sup> 375x2300 A <sup>2</sup> 450x2750 A <sup>2</sup>	Weight of Hydrogen Trapped in Device
Total Weight of Hardware, & Trapped & Unrecoverable Propellant	Weight & Percentage of Unrecoverable Propellant

Weight, kg (lbm)

Fig. V-9 Weight Tradeoff Matrix for LH<sub>2</sub> Channel Designs

V-35 and V-36

FOLDOUT FRAME

without being in contact with the device and, therefore, unavailable for expulsion. Also indicated is the equivalent percentage of the total propellant load that this weight represents.

The results of the matrix study show that the four-channel configuration is not attractive because the potentially unavailable propellant weight is comparatively high. The other three configurations are closely grouped. The six-channel design has the smallest hardware weight, but, potentially, can trap five times as much liquid as the other two. The weight advantages realized by removing the channels in the barrel section are small in the four-channel and ring design and the modes of anomalous failure are increased. Therefore, the configuration consisting of four channels with intersecting circumferential rings was adopted. Of the channel designs, the semicircular design was consistently lighter and was, therefore, chosen as the preferred design.

This combination was also adopted for the LO<sub>2</sub> tank with the difference that only one intersecting ring was added to the basic four-channel configuration. That ring is at the equator of the LO<sub>2</sub> tank. The hardware weight for the system is approximated at 43.3 kg (95.4 lbm).

A way of further reducing the weight of the system hardware is to design the channels with screen "windows" instead of continuous screen surfaces. These windows could be large enough to handle the required flow rates without imposing large pressure loss penalties on the system. They could be strategically placed so that perhaps only a few could cover all possible propellant orientations. These considerations require more detailed mission duty cycle and timeline information that is not available. Therefore, no attempt to assess the potential weight savings was undertaken.

The weights for hardware indicated for the channel systems do not include estimates of the weight additions necessitated by various fabrication and joining processes. These weights are not considered significant and do not alter the relative attractiveness of the proposed systems. A reasonable figure for estimating these weights would probably be 10% of the listed hardware weight.

*c. Full Liner System* - The full liner system proposed as the third Martin Marietta alternative to the NASA baseline system is a variation of the two designs previously discussed. A full tank screen liner is added to the trap or the channel design (as shown in Fig. II-2 and II-3). The channels and trap are constructed as an integral part of the liner and are located on the inner side of

the liner in the bulk propellant region. The liner provides the added capability of venting the system at any time during the mission. This capability is realized, however, by adding some weight to the system.

1) *Trap and Channel Systems* - The specific details of the re-fillable trap are unaltered by the addition of the liner to the system. However, the channel system requires some design modification in the positioning of the screen surfaces. Adding the liner makes it impossible for the propellant to enter the channel through the side nearest the tank wall because the propellant is kept off the tank wall by the liner. Therefore, the screen surface must be changed. The difficulty in designing a curved multiple layer screen surface to withstand the buckling pressure load experienced by the channel required the use of a cross-sectional shape other than the semicircular design proposed previously. The design selected appears in Fig. V-10.

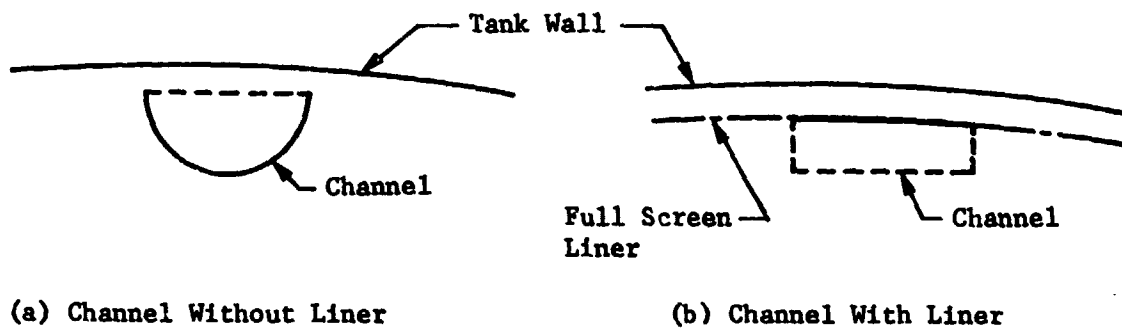


Figure V-10 Channel Configurations for Application With and Without a Full Tank Screen Liner

The screen surfaces are on the inside of the liner and the outer surface is made of plate. That latter surface serves no function in the design, other than to withstand the hydrostatic head, and there is no need for screen.

The purpose of the liner is to provide the capability of non-mission-dependent venting, and, as such, must be able to support some pressure differential to function properly. To do this the screen must be fully wetted. Special provisions required to assure that the screen is wet are discussed next.

2) *Wicking Analysis* - After a MPS burn the screen and liquid will have entered the vapor annulus. The screen liner may have dried out. This is especially true near the pressurization port, because the pressurant must enter through the screen liner to cause the propellant to be expelled. In order for the tank to be vented again following a MPS burn, the liquid in the vapor annulus must be forced back into the bulk propellant region inside the screen liner. This can be done only after the screen liner is rewetted.

The average environmental heat load in the tank is not large. Even so, as discussed in Chapter II, a single layer of unsupported screen will not wick liquid in a zero-g condition more than a few inches. It will eventually reach an equilibrium state at which the liquid front will cease to advance along the screen because the mass flow into the screen is balanced by the vaporization rate along the wetted screen length. Moreover, the mass flow rate in the screen is a function of the viscous losses encountered by flowing liquid through the screen. Therefore, since the screen cannot rewick along its whole length from a source in a fixed position, an additional method of rewetting must be provided.

A number of channels were included in the design to pump liquid along the screen liner from the pool of liquid that will have settled at one end of the tank after a MPS burn. The channels are designed to take advantage of the pressure difference that exists across a curved liquid-vapor interface as expressed in the basic relationship

$$\Delta P = \sigma \left( \frac{1}{R_1} + \frac{1}{R_2} \right) \quad [V-3]$$

where  $\sigma$  is the fluid surface tension and  $R_1$  and  $R_2$  are the principle radii of curvature of the interface at the point of interest.

The channels have a V-shaped cross-section, which provides the flow area for transferring fluid.

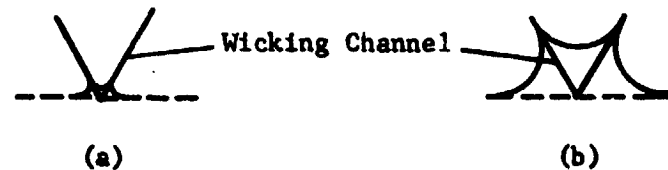


Figure V-11 Cross-Section of Wicking Channel

As shown in Fig. V-11(a), at the point where the channel enters the pool of settled propellant, the surface tension of the fluid will cause a very small radius of curvature to be formed in the channel. When the MPS burn is terminated, the stable zero-g interface assumed by the settled propellant will have a large radius when compared to the radius in the channel at the point where the channel enters the pool. These differences in curvature will result in a lower fluid pressure in the channel than in the bulk propellant. This pressure gradient will tend to flow propellant from the bulk volume into the channels. The advancing interface in the channel will continue to have a small radius, while the channel upstream of the advancing interface will gradually fill with fluid, as in Fig. V-11(b). In a low-g ( $10^{-5}$  g) situation, the channels will eventually be filled.

The channels are designed so that when filled to a certain minimum level, the liquid will come into contact with the adjacent screen and begin to wick into the screen perpendicularly away from the channels. The channels are spaced so that the distance between them does not exceed twice the distance that can be wicked by the screen alone under a steady heat leak of  $0.315 \text{ W/m}^2$  ( $0.1 \text{ Btu/hr-ft}^2$ ).

As the liquid flows into the channels it is affected by both the gravitational environment and the viscous drag associated with the flow. Under the worst conditions these two forces can act in an additive manner to retard the flow and even limit the length of the channel that can be filled. This problem was studied extensively under work performed for the Viking Orbiter. Zero-g drop tower experiments were performed with subscale models and the results of these tests were correlated to analytical models (Ref V-4). These results indicate that wicking times of several minutes are reasonable. Using the model described in Chapter II, wicking in the screens to half the distance between the channels is estimated at 2.5 minutes for  $\text{LH}_2$  across 11.4 cm (4.5 in.) and 4 minutes for  $\text{LO}_2$  across 30.4 cm (12 in.).

3) *Pressurization Analysis* - Adding the full liner with the additional system capability of venting at any time requires knowledge of the functional characteristics of the pressurization and venting system.

a) *System Operating Characteristics* - For all the Martin Marietta designs, the system operation was simplified over that of the NASA baseline. The Martin Marietta system uses only autogeneous pressurization for both the MPS and APS expulsion requirements. Also,

because the Martin Marietta design does not use separate tanks for APS propellant storage, a single vent system for each of the MPS tanks is used. Pressurization takes place in the same manner as the NASA baseline for the nonliner Martin Marietta designs; therefore, this discussion is devoted to the liner case.

During a pressurization event, the autogenous gas enters the outer annulus so that it does not impinge on the outer liner. After exceeding the bubble point of the screen liner, the pressurant enters the bulk region and the tank pressure increases to the pressure regulator setting. During outflow, pressurization continues in the same manner with the outer annulus gas temperatures being higher than the bulk ullage temperature.

After completing an outflow period, the tank pressure drops, rapidly and the gas temperatures cool down to approximately liquid temperature. During a high acceleration burn period, liquid from the bulk region will enter the usually liquid-free outer annulus because of the high hydrostatic heads and also because of some localized dryout of the outer liner. However, following the expulsion event, the outer liner will rewet as mentioned in the previous section and capillary stability will be established. During the following coast period, the pressure rise in the outer annulus will force the liquid back into the bulk region. As mentioned in the wicking analysis discussion, this will take only a few minutes and then venting of the outer annulus can be accomplished without venting any liquid. Venting using the preferred system discussed in Chapter II, is initiated following the pressure collapse which usually takes several hours.

*b. Mission Simulation* - The pressurization and venting processes for the Martin Marietta propellant storage and feed system were simulated using the mission timeline given in Table V-2. Because of the unique propellant control and management devices employed, simulation of these processes cannot be accomplished using typical tank thermodynamic computer programs. A typical computer program predicts tank pressures and fluid temperature histories for flat gas/liquid interfaces, bulk liquid in contact with the tank wall, etc. The pressurization and venting analyses and simulations were conducted using the DSL computer program discussed in Chapter II.

For the mission simulation, the external heat leak is assumed to be constant over the entire tank wall. Heat leak into the tank was computed using the thermal protection criteria presented in Section A. The calculations, using an effective thermal conductivity for the MLI of  $1.9 \times 10^{-7}$  W/cm-°K ( $1.1 \times 10^{-5}$  Btu/hr-ft-°F) and an ambient temperature of 294.6°K (530°R), yield a heat leak of  $0.315$  W/m<sup>2</sup> (0.1 Btu/hr-ft<sup>2</sup>) for both tanks.

For pressurization and outflow, the MPS operating characteristics and requirements presented in Table V-3 were used. The total pressurant used for all of the pressurization and expulsion events (both MPS and A'S) was calculated. The total vented mass for each tank was calculated over the 117-hour mission. The pressure and fluid temperature histories for each tank were predicted with the liquid temperature histories considered to be one of the more critical of the parameters. In order to satisfy the NPSH requirements the vapor pressure of the bulk liquid could not exceed 13.1 N/cm<sup>2</sup> (19 psia) and 12.41 N/cm<sup>2</sup> (18 psia) in the LH<sub>2</sub> and LO<sub>2</sub> tanks, respectively.

The results of the mission simulations are presented in Table V-11 and in Fig. V-12 and V-13. Table V-11 gives a summary of such important pressurization and venting parameters as pressurant usage, vented mass, vent frequency, and final conditions for each propellant tank. Figures V-12 and V-13 show that the vapor pressure in each tank never got above the vapor pressure required to satisfy NPSH. The peaks indicate a pressurization and outflow event followed by a pressure collapse during coast. For the long coast periods, the tank pressure decreased and approached the vapor pressure corresponding to bulk liquid temperature. The DSL venting technique was capable of maintaining the required tank pressure and liquid vapor pressure in each tank.

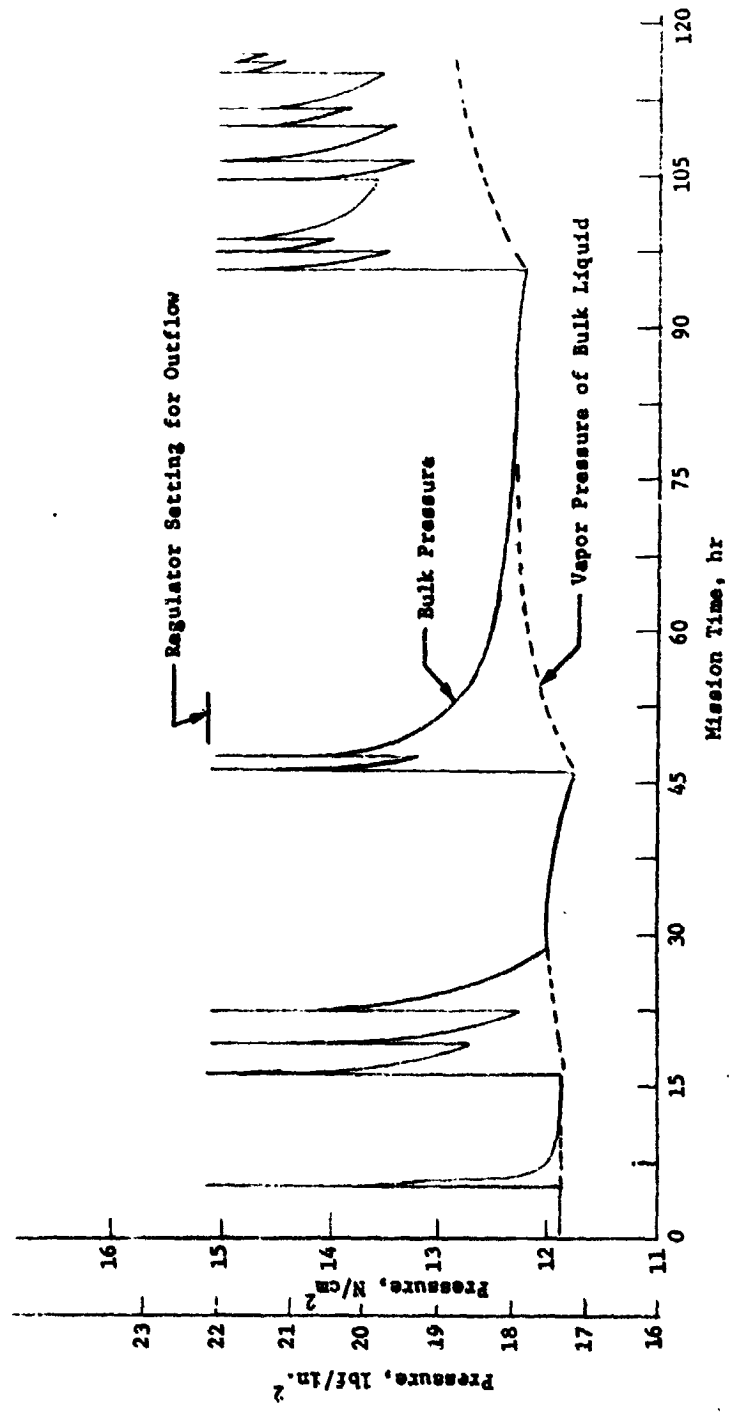


Fig. V-12 Space Tug LH<sub>2</sub> Tank Pressure History for Martin Marietta Design

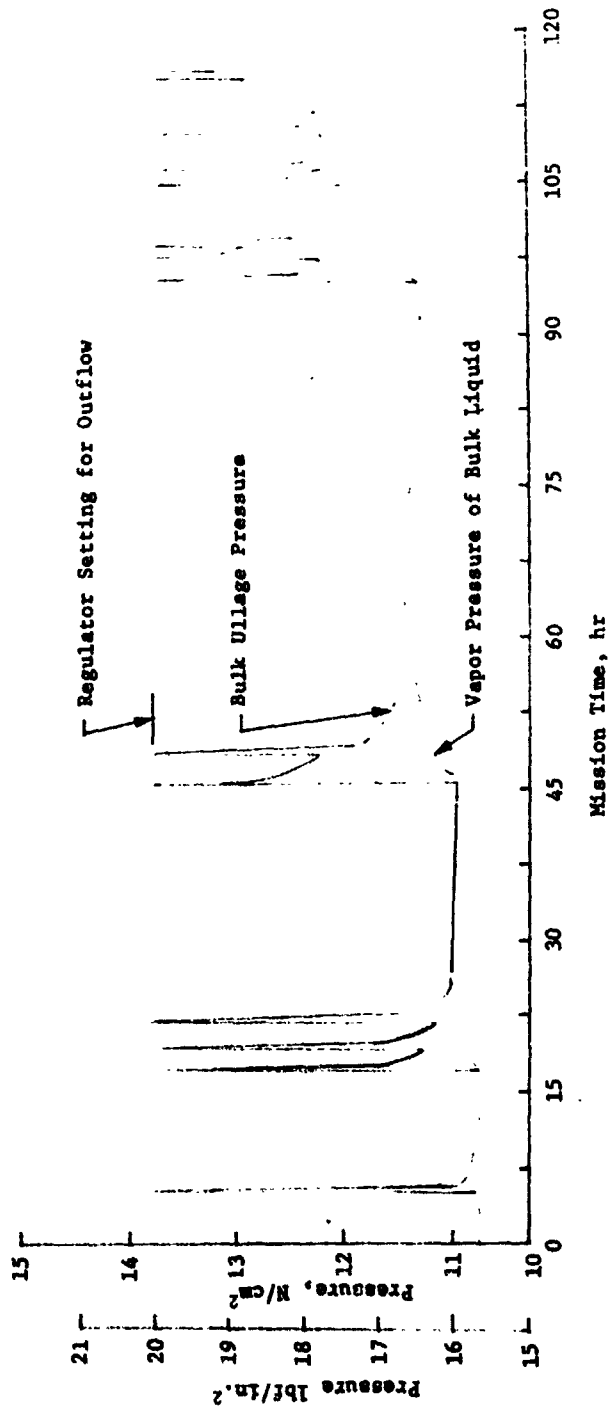


Fig. V-13 Space Tug LO<sub>2</sub> Tank Pressure History for Martin Marietta Design

Table V-11 Results of Pressurization and Venting Simulation

Parameters	LO <sub>2</sub> Tank	LH <sub>2</sub> Tank
Initial Liquid Temperature, °K (°R)	91.2 (164)	20.8 (37.5)
Initial Pressure, N/m <sup>2</sup> (psia)	10.75 (15.6)	11.5 (17.3)
Vent Band, N/m <sup>2</sup> (psi)	0.207 (0.3)	0.028 (0.04)
Vent Frequency, cycles/hour	3.3	12
Total Mass Vented, kg (lbm)	16.1 (35.5)	27.2 (60)
Pressurant Temperature, °K (°R)	278 (500)	166.8 (300)
Total Pressurant Required, kg (lbm °K)	96.7 (213)	19.06 (42)
Final Bulk Liquid Temperature, °K (°R)	92.1 (165.6)	21.2 (38.1)
Final Vapor Pressure, N/m <sup>2</sup> (psia)	12.3 (17.8)	12.9 (18.8)
Mission Time = 116.6 hours.		

d. *Feedline Analysis* - A screen liner weight comparison similar to that performed for the integrated OMS/RCS was conducted for the Space Tug propulsion system to determine weight penalties associated with stainless steel and aluminum fine mesh screens. A similar result was obtained, in that, although a weight savings may be realized (MPS feedlines 20% and APS only 10%) with aluminum screen, it is not significant enough to outweigh the other important design criteria in screen selection. Because Space Tug feedlines are also stainless steel, compatibility was a major concern.

An approach consistent with the integrated OMS/RCS feedline study was applied to the Space Tug propulsion systems. Analyses were conducted to identify screen liner feedline design as applied to the MPS and APS LH<sub>2</sub> and LO<sub>2</sub> systems for each acquisition/expulsion device previously presented. The number of layers of 325x 2300 Dutch twill screen required to maintain a gas-free liquid core were established and the propellant boiloff from each line estimated. The design approach considered storage tanks with and

without screen liners separately because there is a basic change in design ground rules for the two concepts. This is discussed in detail in the following subsections.

1) *MPS Feedline Design Analysis* - The imposed acceleration of the MPS is always positive, i.e., a vector in the opposite direction of feedline flow and tending to settle propellants in the aft end of the tanks. As previously discussed, this is an optimum design condition because the term  $\rho g L$  becomes negative in Eq [II-10], helping to decrease the pressure drop along the feedline. The worst design condition for the MPS feedline would, therefore, be for the minimum acceleration during system operation. This approach is valid for all of the acquisition/expulsion devices analyzed for the Space Tug MPS.

Based on MPS full thrust flow rates of 1.61 kg/sec (3.55 lbfm/sec) and 8.05 kg/sec (17.15 lbfm/sec) for the LH<sub>2</sub> and LO<sub>2</sub> systems, respectively, corresponding feedline velocities are 7.92 and 1.64 m/sec (26 and 5.38 ft/sec). These values were used throughout the MPS capillary feedline analysis.

*Storage Tanks without Screen Liners* - The proposed nonlinear storage tank concepts do not provide a low-g venting capability. Therefore the engine idle mode must be used for propellant conditioning and venting capability as discussed in Section B. Under these conditions, propellant settling is possible in the MPS feedlines as well as in the propellant tanks.

Based on engine idle mode thrust and duration of 267 N (60 lbf) and 145 sec, respectively, calculations were made to determine settling distances. These distances are consistently greater than those required for the propellant to travel to the feedline outlet. Therefore, liquid will displace the gas, resulting in a feedline vapor annulus filled with liquid during normal engine operation. Under these conditions, gas ingestion into the feedline liquid core becomes impossible. Should some gas remain, however, gas ingestion is still precluded as long as liquid is present, because screen resistance to liquid penetration is much less than for a gas.

For an acquisition/expulsion device without a screen liner, the main design requirement for the MPS feedlines is that the bubble point of the feedline screen be greater than the bubble point of the communication screen. A single layer of 325x2300 mesh stainless steel Dutch-twill screen meets this criterion. Therefore, a single screen layer is sufficient to assure that gas-free liquid

is provided to the MPS turbopumps for both the LH<sub>2</sub> and LO<sub>2</sub> feedlines for the nonlinear storage tank systems. It should be noted that the primary function of the screen liner in this feedline design is to maintain gas-free liquid within the liquid core during coast when incident heating of the feedline is vaporizing propellant at the screen surface.

*Storage tanks with screen liners* - The propellant acquisition/expulsion devices with full tank liners provide low-g venting capability independent of the system duty cycle. Therefore, propellant settling and engine idle mode operation is not required. The screen liner in the designs presented is unstable throughout most of the baseline mission, which assures propellant settling in the feedline at steady-state conditions. However, during engine start, this condition may not exist and propellant settling during the MPS start transient is of major interest.

Based on MPS thrust buildup data (Ref V-2), propellant settling distances during the MPS engine start transient were calculated at various full thrust acceleration levels using Eq [V-2]. These data are shown in Table V-12 with the required distance for propellant settling at the feedline outlet shown for both propellants. It is clear from these data that propellants will not be settled in the feedline before full thrust is reached. The system must, therefore, operate with a gas-filled vapor annulus to satisfy Eq [II-10].

Table V-12 Propellant Settling Distance during MPS Start Transient

Full Thrust Acceleration, g	Propellant Settling Distance, m (ft)	Approximate Required Settling Distance, m (ft)	
		LH <sub>2</sub>	LO <sub>2</sub>
0.16	0.045 (0.147)	6.70 (22)	0.914 (3)
1.3	0.363 (1.19)	10.36 (34)	3.05 (10)
1.51	0.421 (1.38)	11.28 (37)	3.35 (11)

Solutions of Eq [II-10] at various acceleration values for the LH<sub>2</sub> system are shown in Fig. V-14. Curves for the feedline outlet and inlet are shown for both storage tank concepts. These numbers conservatively represent the required layers of screen necessary to assure gas-free liquid in the feedline core. Maximum and minimum MPS accelerations are also shown.

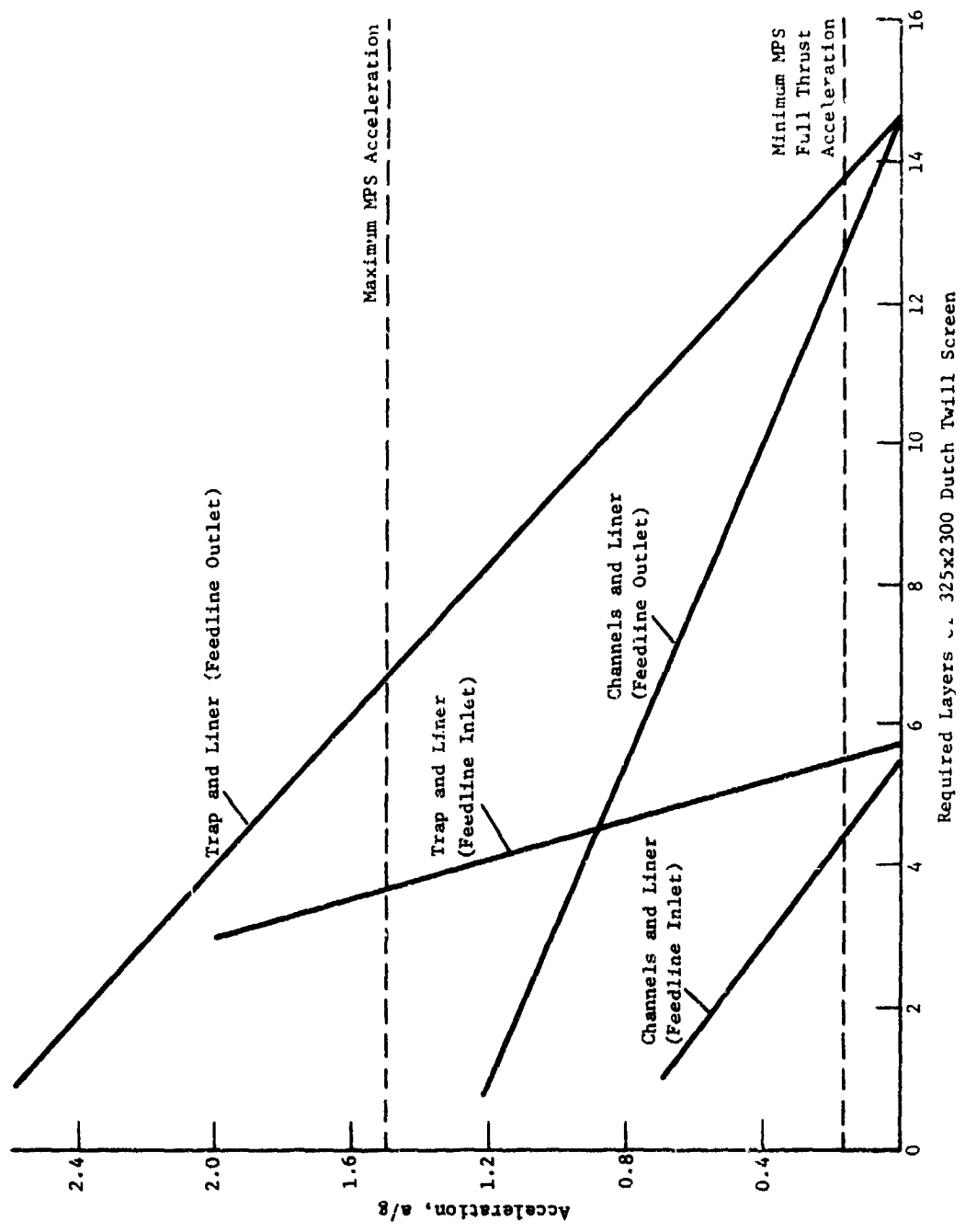


Fig. V-14 LH<sub>2</sub> MPS Capillary Feedline Design Requirements for Space Tug MPS

At low-g levels the number of screen layers required at the feedline outlet is significantly greater than at the inlet because the  $\rho g L$  term is small compared to the viscous loss term. Designing for worst-case conditions (0.10 g acceleration) requires 6 layers of screen at the feedline inlet and 14 layers of screen at the outlet for the trap system. The channel system requires 5 and 13 layers of screen for the feedline inlet and outlet, respectively.

Using these numbers the required layers of screen as a function of feedline length is plotted in Fig. V-15 for the  $LH_2$  MPS. The average number of screen layers, as determined at the feedline midpoint are 10 and 9 for the trap and channel systems, respectively. These numbers result in liner weight savings, compared to a design where the layers of screen are constant for the entire feedline length.

As mentioned in Reference V-1 and V-2, the  $LO_2$  MPS feedline does not require active thermal conditioning because of its short length. However, should propellant conditioning become desirable, the necessary design data are shown in Fig. V-16. Two layers of screen are required to preclude gas ingestion with a trap device and only one layer is required for a channel system. The added acceleration head, due to the increased  $L$ , of the channel system accounts for the reduction in the required screen layers.

Table V-13 summarizes the design requirements for a Space Tug MPS capillary feedline system.

Table V-13 Space Tug MPS Capillary Feedline Design Requirements

Acquisition/Expulsion System	Required Layers of 325x2300 Mech Screen	
	$LH_2$	$LO_2$
Trap without Liner	1	1
Channel without Liner	1	1
Trap with Liner	*14, 6	2
Channel with Liner	*13, 5	1

\*At feedline outlet and inlet, respectively.

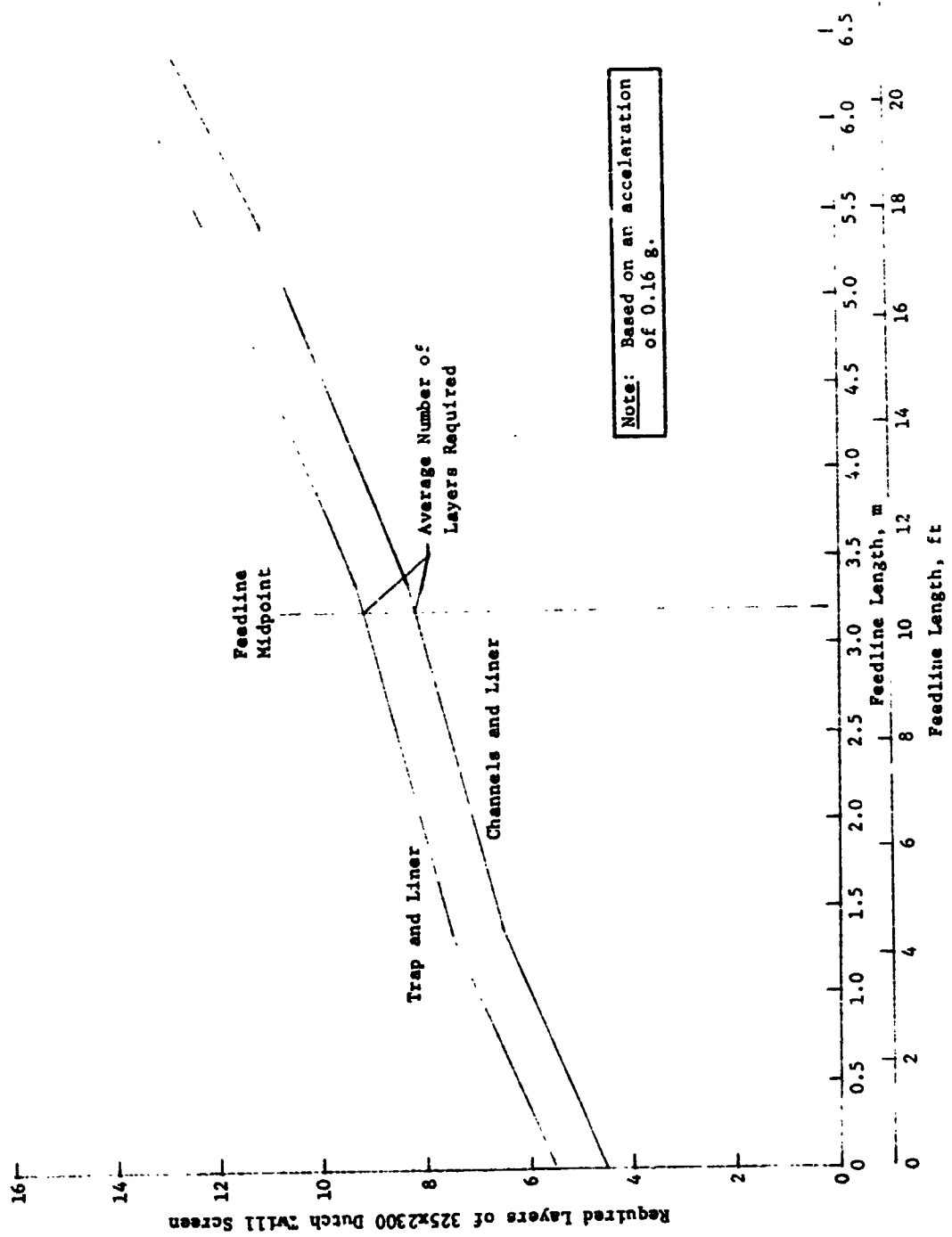


Fig. V-15 Required Layers of Screen vs Feedline Length for LH<sub>2</sub> MPS Feedline

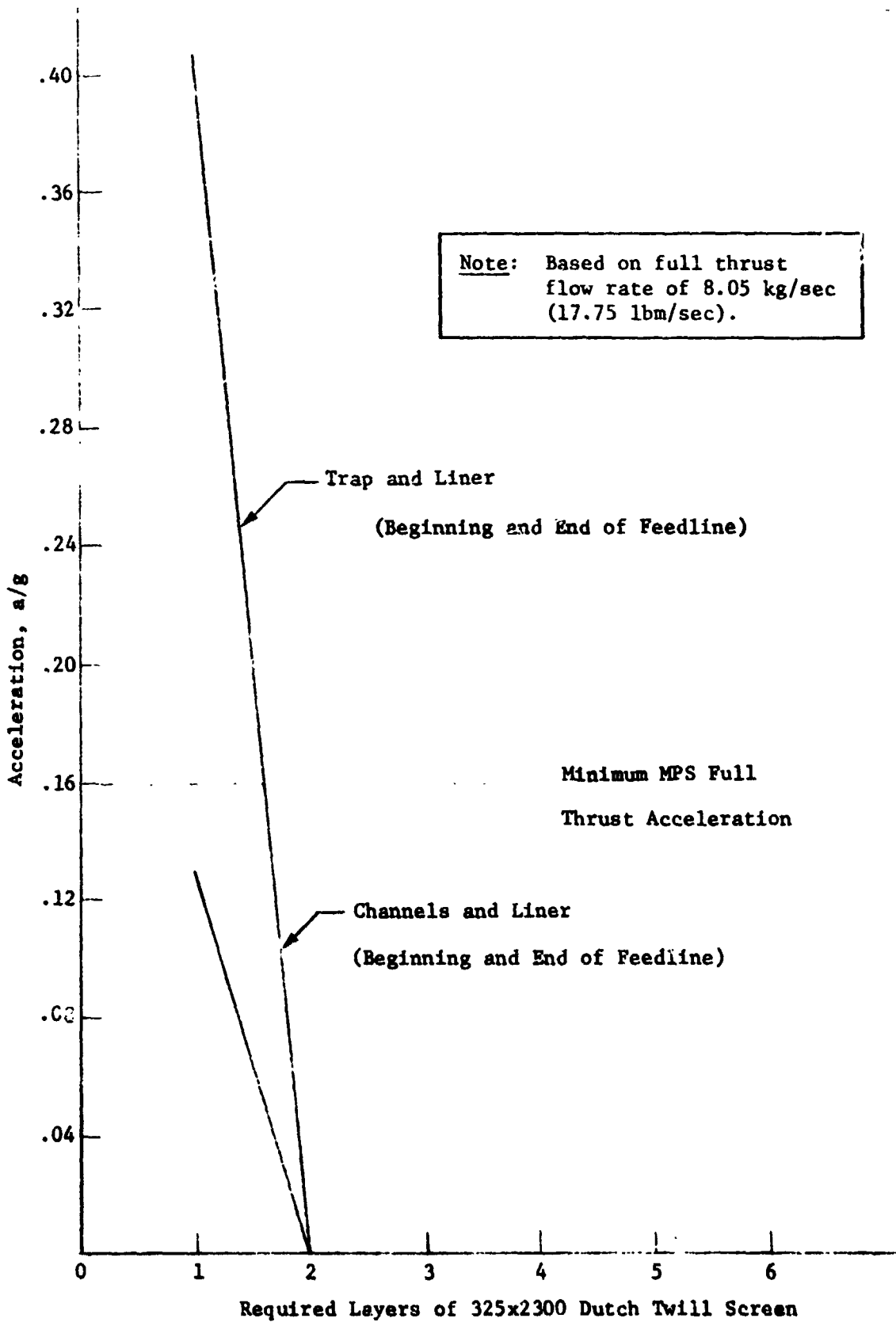


Fig. V-16  $LO_2$  Capillary Feedline Design Requirements for Space Trug MPS

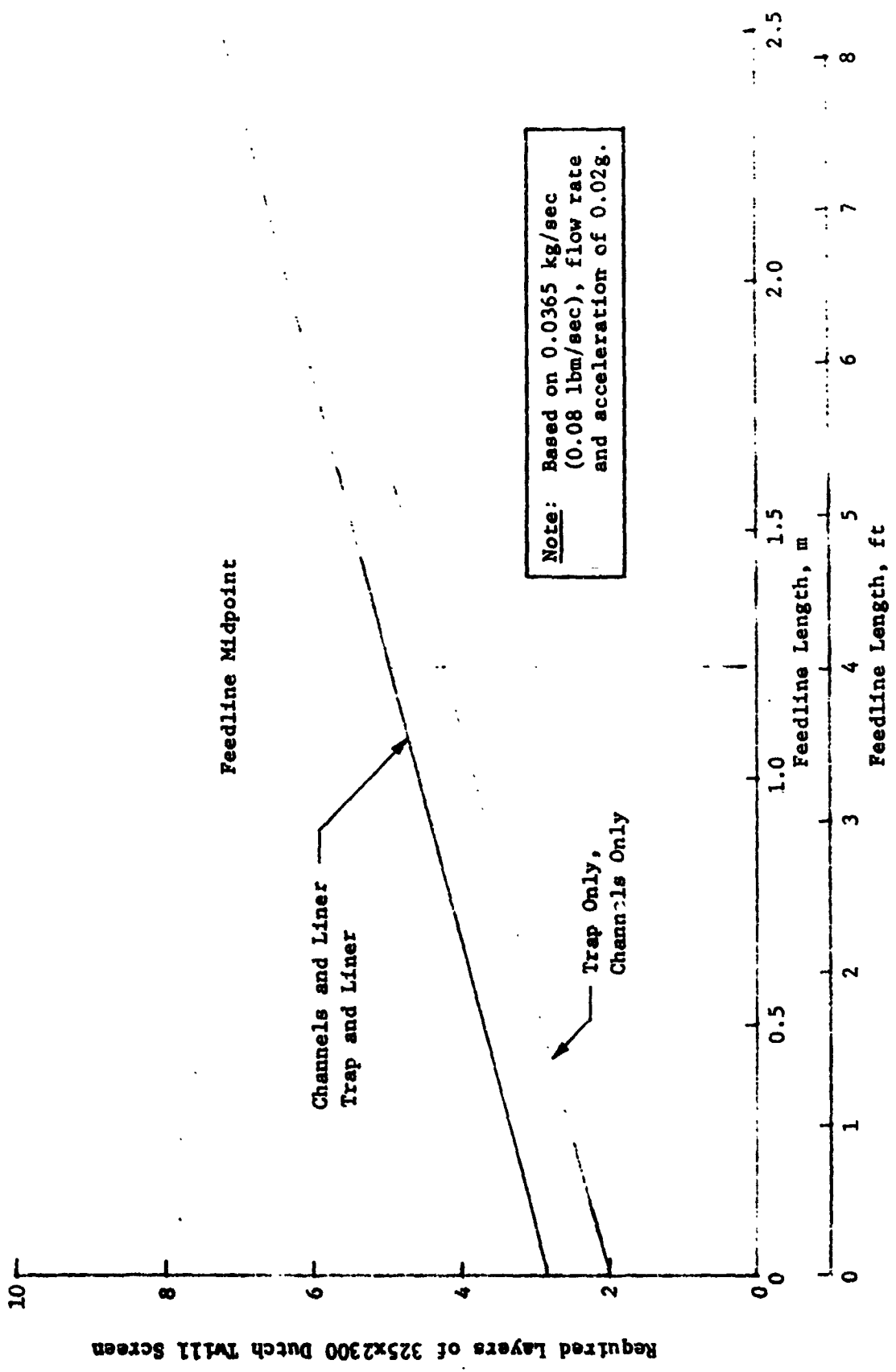
2) *APS Feedline Analysis* - The acceleration environment for the APS is significantly different from the MPS just discussed. Acceleration in any direction may be encountered during system operation with magnitudes as high as 0.02 g. This results in a worst-case design condition for capillary feedlines; i.e., an acceleration vector in the direction of flow. The term  $\rho g L$  in Eq [II-10] is now additive with the rest of the pressure losses. Also, under these conditions, liquid cannot be forced into the feedline vapor annulus region regardless of the acquisition/expulsion device used.

APS flow rates are 0.036 kg/sec (0.08 lbm/sec) for LH<sub>2</sub> and 0.11 k/sec (0.25 lbm/sec) for LO<sub>2</sub>. Resulting feedline velocities are 4.11 and 0.79 m/sec (13.5 and 2.61 ft/sec) for LH<sub>2</sub> and LO<sub>2</sub>, respectively. Based on these data, an acceleration of 0.020 g, and a feedline length of 2.44 m (8 ft) for both systems, the required layers of screen were determined for each acquisition/expulsion device concept.

*Storage Tanks without Screen Liners* - APS operation is basically unaffected by the presence or absence of a storage tank liner. The capillary feedline system must supply gas-free liquid with a gas-filled vapor annulus whether or not a liner is present in the acquisition/expulsion system. Proper design requires that Eq [II-10] be satisfied. The layers of screen required to satisfy this relationship are shown in Fig. V-17 as a function of feedline length for the LH<sub>2</sub> system. An average of 4.2 layers of 325x2300 Dutch-twill screen are required for both the trap and channel systems without a storage tank liner. A maximum of seven screen layers are required at the feedline outlet.

Requirements are less demanding for the LO<sub>2</sub> system. Due to the small feedline velocity and increased screen pressure retention capability with LO<sub>2</sub>, a maximum of two layers of screen are required at the feedline outlet for the trap system. At the inlet only one layer of screen is required. For a channel acquisition/expulsion system, we presume that a single layer of screen throughout the feedline length will assure a gas-free liquid core.

*Storage Tanks with Screen Liners* - The addition of a tank liner to the storage tank acquisition/expulsion device does not affect the basic operational environment of the APS capillary feedline. However, the pressure drop in the system is increased by an amount equal to the bubble point of the liner. This added loss must be accounted for in the design of the feedline system. The effect on feedline design is to require an additional screen layer compared with the nonliner systems.



CS-A

Fig. V-17 LH<sub>2</sub> Capillary Feedline Required Layers of Screen

The required screen layers for the LH<sub>2</sub> system are shown in Fig. V-17 as a function of feedline length for the subject acquisition/expulsion devices with a tank liner. A maximum of eight screen layers are required at the feedline outlet while only three layers are required at the inlet for both the trap and channel systems. For the LO<sub>2</sub> system, two layers of screen are required throughout the length of the feedline for both the trap and channel systems when a full tank liner is incorporated into the acquisition/expulsion device.

The APS capillary feedline design requirements are summarized in Table V-14.

Table V-14 Space Tug APS Capillary Feedline Design Requirements

Acquisition/Expulsion System	Required Layers of 325x2300 Mesh Screen	
	LH <sub>2</sub>	LO <sub>2</sub>
Trap without Liner	7, 2*	2, 1*
Channel without Liner	7, 2	1
Trap with Liner	8, 3	2
Channel with Liner	8, 3	2

\*Requirements at feedline outlet and inlet, respectively.

3) *Boiloff Analysis* - As mentioned earlier, the effective cooling capacity of a capillary feedline at low pressures is due mainly to the heat of vaporization of the liquid used. During equilibrium conditions and for a simplified analysis, the amount of propellant boiled off can be estimated by the heat of vaporization of the fluid divided by the heating rate,  $q$ .

Liquid hydrogen APS feedline heating fluxes are assumed to be the same as those for the MPS feedline, which are based on an environment temperature of 238.7°K (-30°F) and feedline temperature of 20°K (-423°F). A single 10-layer blanket of MLI results in a heating rate of 1.43 W (5 Btu/hr). Liquid oxygen boiloff was calculated using the same heat flux associated with LH<sub>2</sub> heating rates. This should be a conservative approach due to the lower temperature differentials with LO<sub>2</sub> as compared to LH<sub>2</sub>.

Table V-15 summarizes the propellant losses due to feedline boil-off for both the MPS and APS. Total propellant boiloff is 1.87 kg (4.13 lbm) of LH<sub>2</sub> and 0.91 kg (2.0 lbm) of LO<sub>2</sub> based on a Space Tug six day mission. These values do not include losses due to feedline or engine chardown but are for liquid filled lines at thermal equilibrium. Chardown times and boiloff should not vary significantly from those specified in the baseline document.

Table V-15 Estimated Boiloff for a Martin Marietta Screen Liner Feedline

	LH <sub>2</sub>		LO <sub>2</sub>	
	MPS	APS	MPS	APS
Boiloff Rate, kg/hr (lbm/hr)	0.012(0.026)	0.0013(0.0028)	0.0041(0.009)	0.0024(0.0054)
Total (MPS +APS) kg/hr (lbm/hr)	0.013(0.029)		0.0065(0.014)	
Propellant Boiloff,* kg (lbm)	1.87(4.13)		0.91(2.00)	
*Based on a Space Tug 6-day mission ..				

#### D. DETAILED DESIGN

This section presents the Martin Marietta detailed designs for the Space Tug LH<sub>2</sub> and LO<sub>2</sub> storage and feed systems. Engineering drawings illustrate the storage tank designs. The results of selected detail weight evaluations are presented, as well as a discussion of the fabrication and structural considerations for the designs.

##### 1. Storage Tank Designs

There are essentially two methods of fabricating screen propellant acquisition system: (1) with screen supported by perforated plate and (2) with screen attached to a framework but unsupported by any backup material between attachment points. A wetted screen can

support a pressure differential that depends on the bubble point of the wetting fluid. Therefore, the screen and any supporting structure must be able to withstand the tensile stress of that internal differential pressure or the compressive buckling stress of the external differential pressure. The capillary retention capability of 200x1400 Dutch-twill in LH<sub>2</sub> is approximately 0.034 N/cm<sup>2</sup> (0.050 psi) and, in LO<sub>2</sub>, it is approximately 0.26 N/cm<sup>2</sup> (0.375 psi). Capillary systems are normally designed for the buckling failure mode; this is also the case of the Space Tug design.

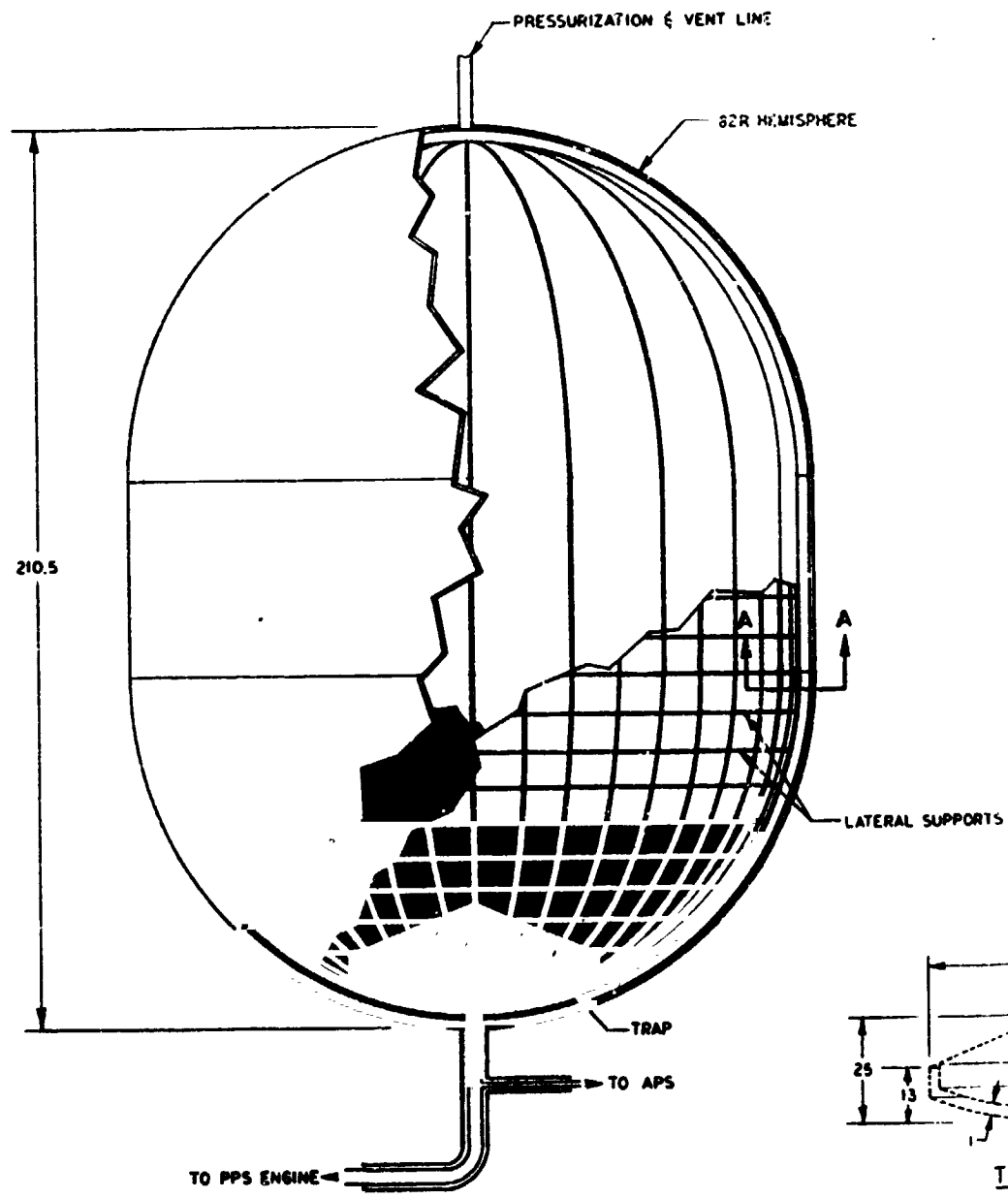
In the case where the design incorporates screen backed by perforated plate, the perforated plate carries the load and little additional structural support is needed. Where unsupported screen is used, the framework carries the compressive load while the screen attached to the framework experiences tensile stress. Where possible, the various designs for both the LH<sub>2</sub> and LO<sub>2</sub> propellant acquisition/expulsion systems were analyzed for minimum weight using both construction techniques.

The designs for the LH<sub>2</sub> and LO<sub>2</sub> refillable trap systems are shown in Fig. V-18 and V-19, respectively. The figures also include a screen liner; however, the design of the trap is unchanged by the addition of the liner. The trap is fabricated of perforated plate and screen. The annular section of the trap has two layers of 200x1400 screen and the structure is formed by fabricating a sandwich of two screen layers separated by the perforated plate. The trap is positioned away from the wall so that communication exists between the vapor annulus of the feedline and the tank volume, which is not occupied by the trap. The trap weights for aluminum and stainless steel were compared to assess the merits of the two structural material possibilities. Those weights appear in Table V-16.

Table V-16 Weight Comparison of LO<sub>2</sub> and LH<sub>2</sub> Trap Designs

	Aluminum Design	Stainless Steel Design
LO <sub>2</sub> Trap, kg (lbm)	4.63 (10.21)	15.7 (34.58)
LH <sub>2</sub> Trap, kg (lbm)	16.16 (35.6)	42.76 (94.2)

Clearly, the aluminum system holds the advantage in weight even though thicker gage materials are required in the design. Therefore, aluminum was selected for the Martin Marietta trap designs as the first alternative to the NASA baseline system.



**ASSEMBLY**  
1:20

**FOLDOUT FRAME**

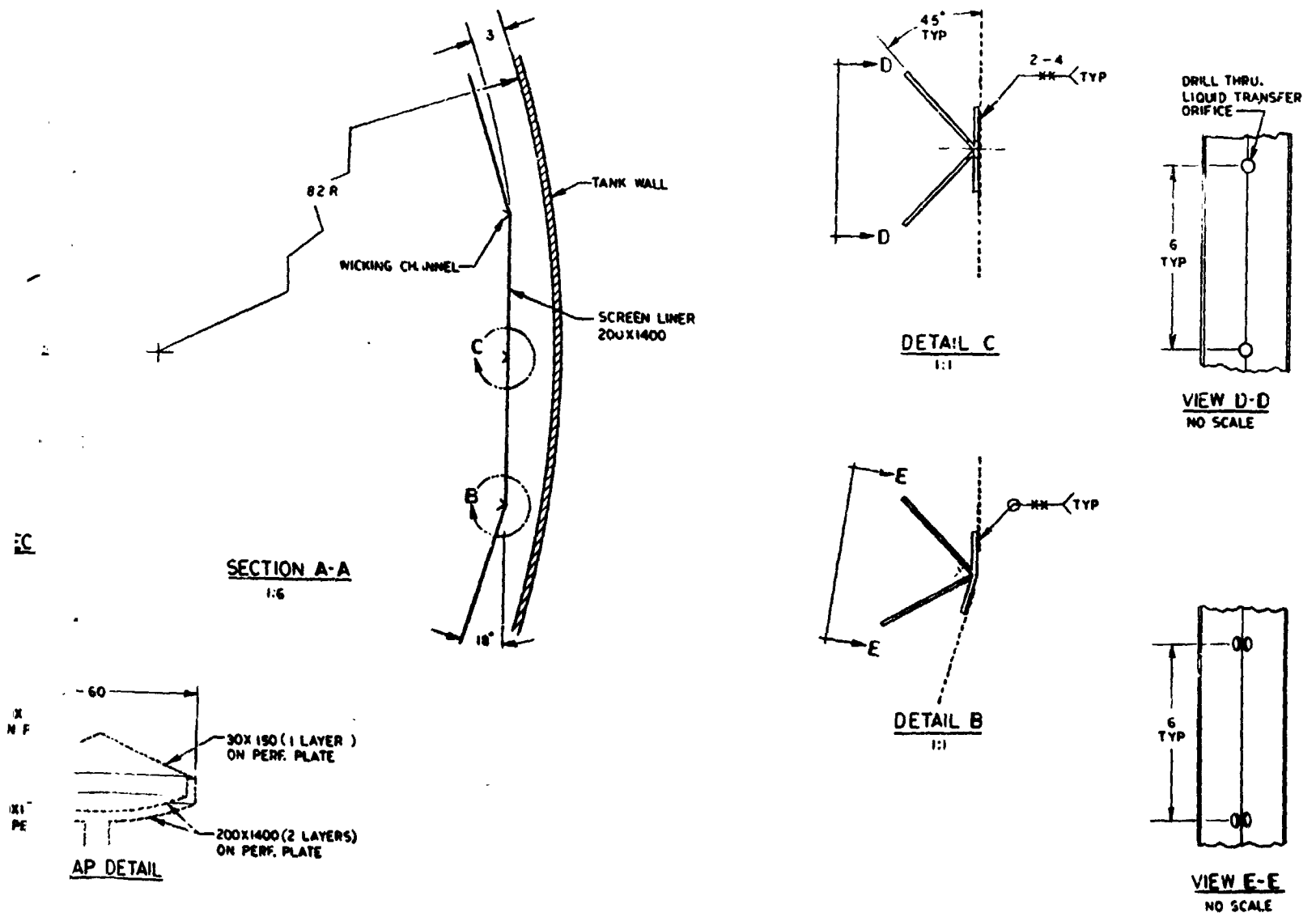
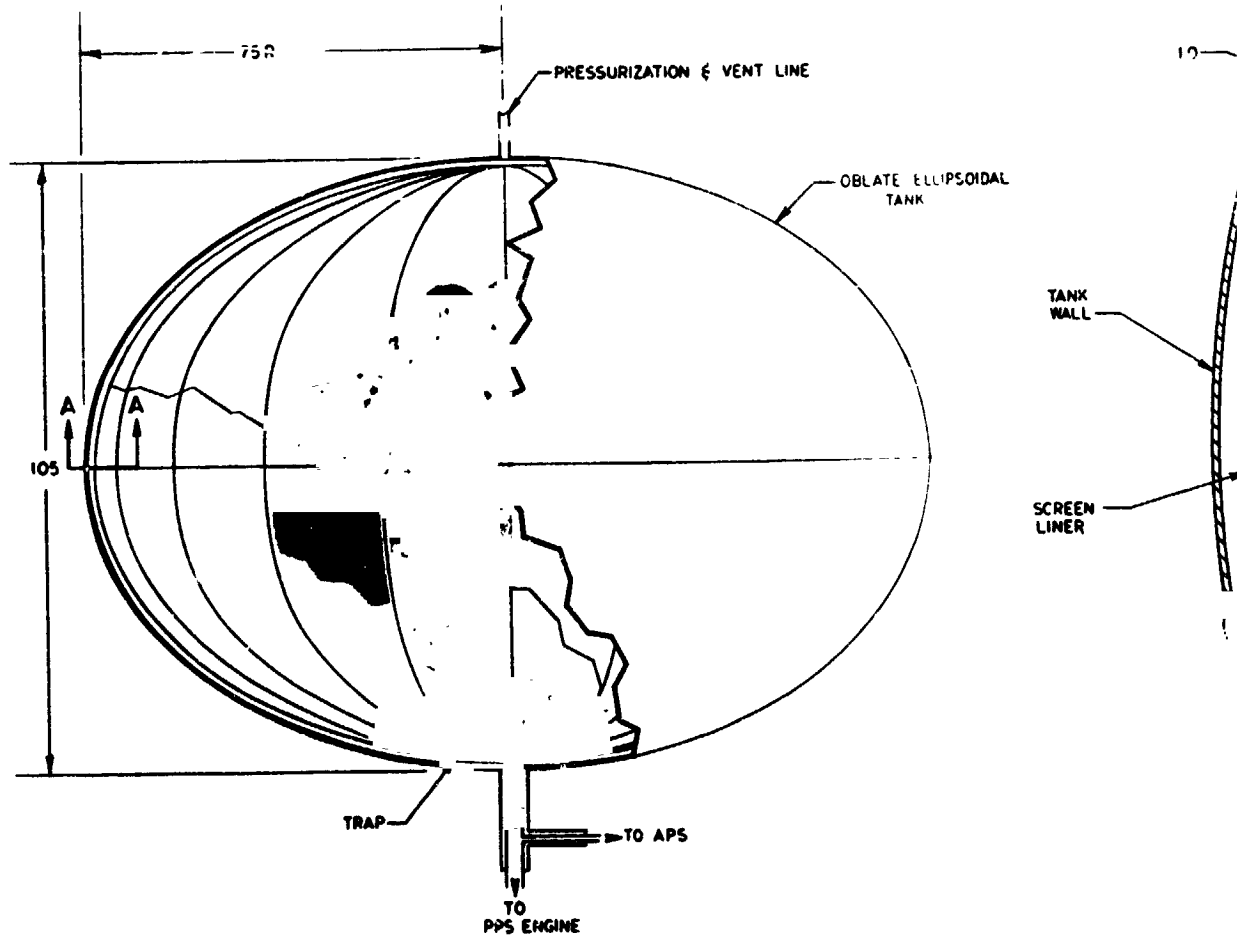


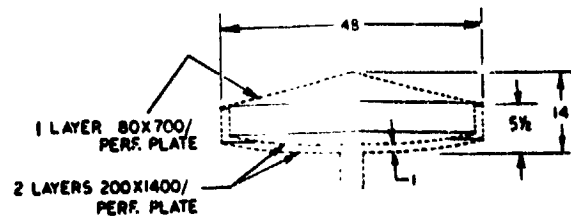
Fig. V-18 LH<sub>2</sub> Trap System for Space Tug

V-57 and V-58

**FOLDOUT FRAME**  
2



**ASSEMBLY**  
1:15



**TRAP DETAIL**

**FOLDOUT FRAME**

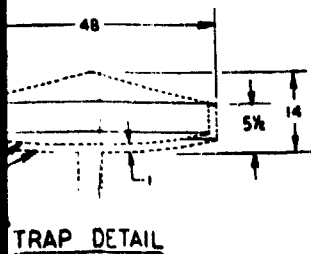
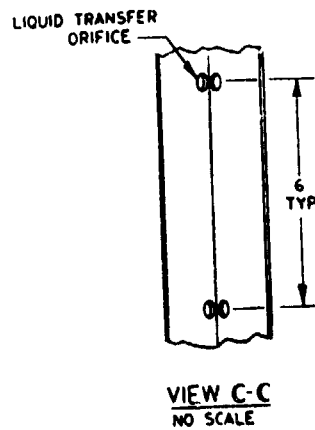
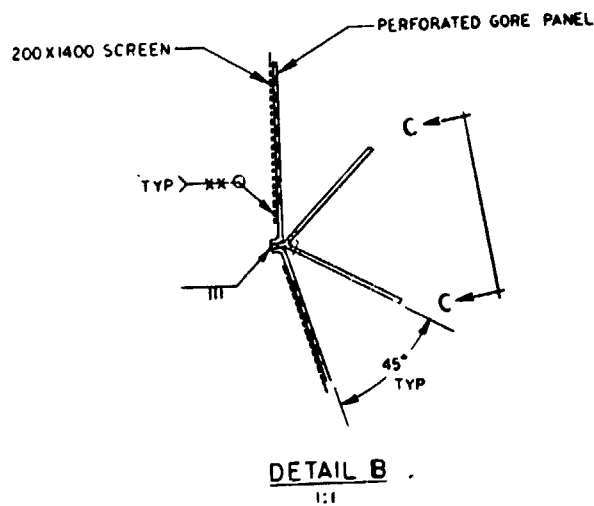
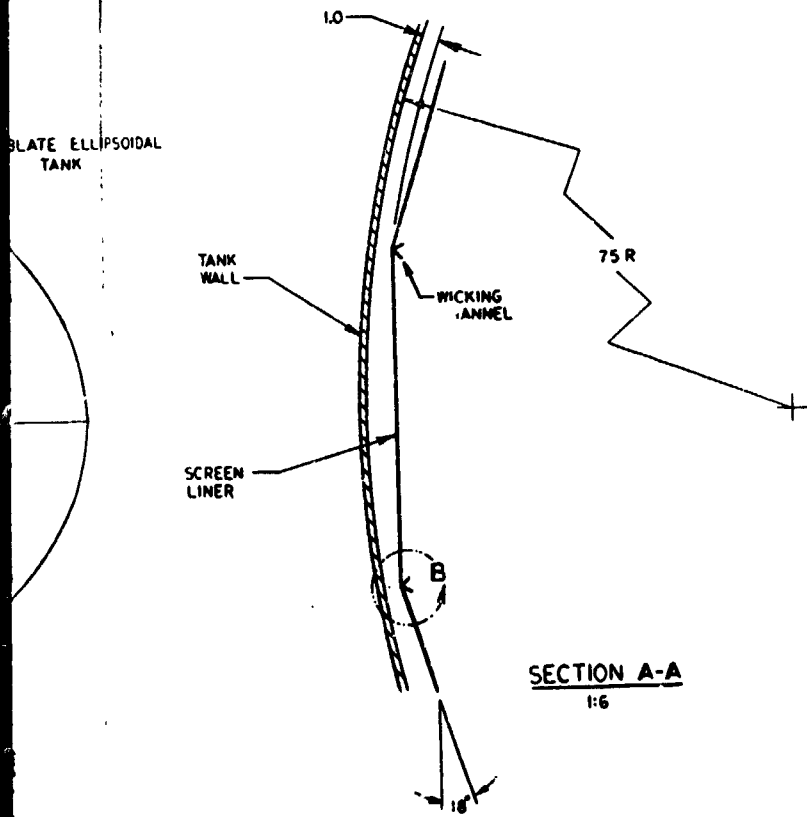


Fig. V-19 LO<sub>2</sub> Trap System for Space Tug

V-59 and V-60

FOLDOUT FRAME

2

The channel system proposed as the second alternative to the NASA baseline design is also an aluminum system. The plate used to form the semicircular section of the channels is 0.76 mm (0.030 in.) gage. The system designs are shown in Fig. V-20. The screens placed diametrically across the channel are supported only at their points of attachment to the channel edges. As determined previously, the system hardware weights are 110.5 kg (243.5 lbm) and 43.3 kg (95.4 lbm) for the LH<sub>2</sub> and LO<sub>2</sub> tanks, respectively, when aluminum is used.

The third Martin Marietta alternative to the NASA baseline design incorporates a full tank screen liner into either of the other two designs. The trap and channel designs were relatively simple in design and fabrication. Adding the liner to the system requires some additional considerations. The liner must be wetted so that it can support the pressure differential necessary for proper venting. The liner screen distances across which wicking must occur are too large to depend on wicking from any one liquid source such as the channels, the trap, or the settle bulk propellant. The wicking channels described previously were incorporated into the design to provide the capability to wick liquid to the screen liner. These channels also serve as structural members to support the screen liner.

The LH<sub>2</sub> and LO<sub>2</sub> trap and liner designs are shown in Fig. V-18 and V-19. The designs for the LH<sub>2</sub> and LO<sub>2</sub> propellant acquisition/expulsion system were analyzed for minimum weight, considering both construction techniques (1) screen backed by perforated plate and (2) unsupported screen attached to a wicking channel framework. Both aluminum and stainless steel were considered in the comparison.

The weight comparison study also considered the maximum wicking length of a given screen and fluid combination to determine which was more critical--the maximum wicking length or the maximum distance between support points across which a screen can maintain structural integrity. Structural integrity in the case of screens is a severe definition. Not only can screen rupture not be tolerated, but even a degradation of the screen bubble point, caused by slight enlargement of the screen pores, is unacceptable.

For a LH<sub>2</sub> screen liner, the maximum distance between the supporting channels for the 200x1400 mesh aluminum screen is 22.8 cm (9 in.) and is determined by the structural criteria presented in Chapter II. The maximum distance for the same kind of structure for stainless steel is approximately 45.7 cm (18 in.) also determined by structural criteria. For oxygen the maximum distance between wicking channels for aluminum screen backed by perforated plate is 83.8 cm (33 in.) and is determined by wicking criteria presented in Chapter II, while for stainless steel unsupported screen is 22.8 cm (9 in.), determined by structural considerations. The four fabrication options listed here were the lightest of eight options originally available. A summary of this information is presented in Table V-17.

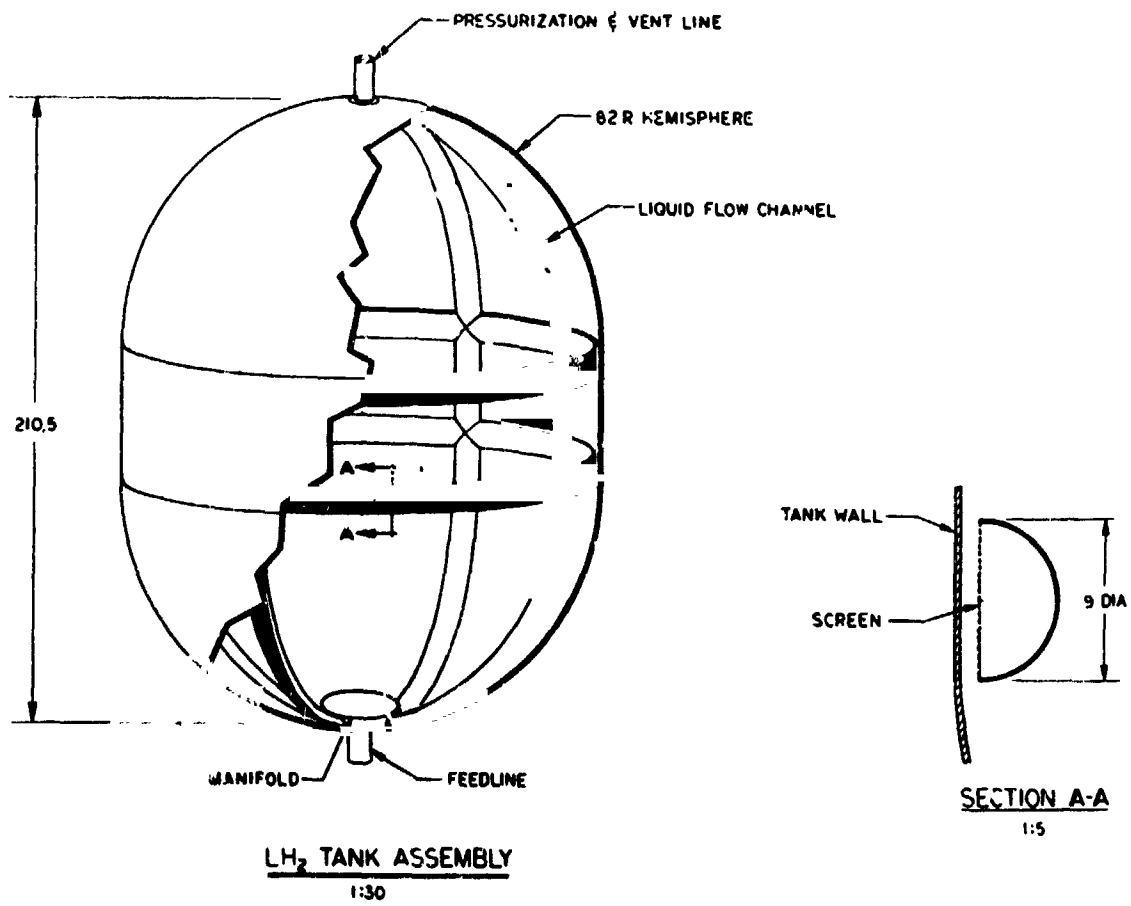
Table V-17 Channel Spacing Design Options and Criteria

Type of Screen	Design Criteria	Channel Spacing, cm (in.)	
		LO <sub>2</sub> Liner	LH <sub>2</sub> Liner
Aluminum	Structural	Perforated Plate*	22.8 (9.0)*
200x1400 Mesh	Wicking	83.8 (33.0)	76.2 (20.0)
Stainless Steel	Structural	22.8 (9.0)*	45.7 (18.0)*
200x1400 Mesh	Wicking	83.8 (33.0)	76.2 (20.0)

\*Designates the controlling criterion.

A weight comparison study of the two LO<sub>2</sub> candidate construction materials (stainless steel and aluminum) was performed using the trap and liner design. The stainless steel design consisted of an unsupported stainless steel screen liner attached to a framework of stainless steel wicking channels similar to those shown in the system drawings, and a trap of stainless steel screen supported by perforated plate.

The channels were spaced 32.8 cm (9 in.) apart. The aluminum design had a liner of perforated-plate-backed screen attached to a framework of flow channels and an aluminum trap identical in design to the stainless steel system trap. The channels for the aluminum liner were spaced 60.9 cm (24 in.) apart. This spacing imposed a slight weight penalty on the aluminum system, but was more realistic in terms of volumetric efficiency because a poly-sphere with 60.9 cm (24 in.) sides more closely approximates the volume of the vehicle tank than does one of 8.3 cm (33 in.) sides. The comparison is summarized in Table V-18.



FOLDOUT FRAME

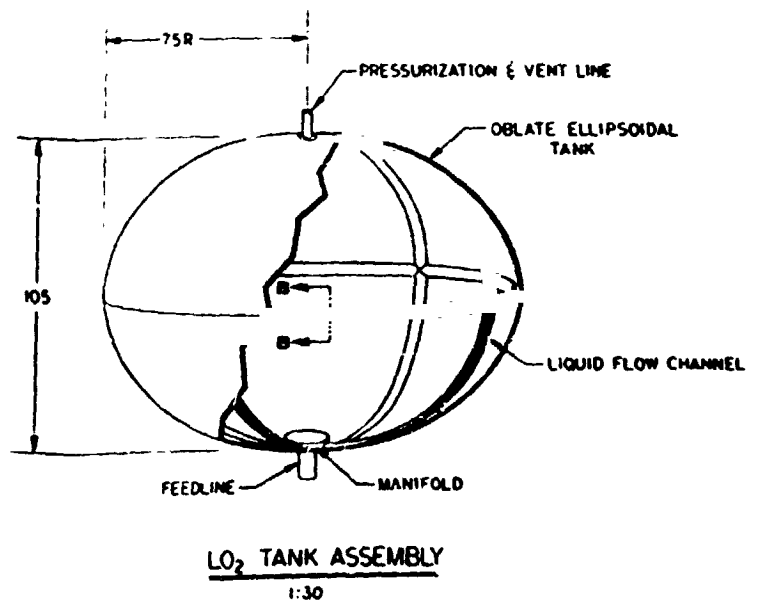
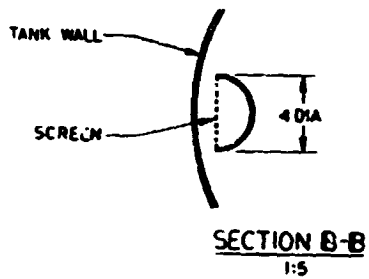


Fig. V-20 LH<sub>2</sub> and LO<sub>2</sub> Channel Systems for Space Tug

V-63 and V-64

FOLDOUT FRAME

2

Table V-18 Weight Comparison of LO<sub>2</sub> Trap and Liner Designs

Component	Aluminum	Stainless Steel
Liner Plate, kg (lbm)	37.81 (83.3)	0 (0)
Liner Screen, kg (lbm)	8.71 (19.2)	17.45 (38.45)
Channels, kg (lbm)	10.62 (23.4)	41.08 (90.5)
Trap (Plate and Screen) kg (lbm)	4.64 (10.21)	15.69 (34.58)
Total	61.79 (136.11)	74.24 (163.53)

The comparison shows quite clearly that the aluminum design of screen backed with perforated plate is lighter than the stainless steel design with unsupported screen. The aluminum design was selected for the LO<sub>2</sub> tank, with a trap and liner.

A similar study was conducted to compare the weights of the LH<sub>2</sub> aluminum and stainless steel designs for the trap and liner. In this study, as in the previous one, all perforated plate was assumed to be minimum gage: 0.76 mm (0.030 in.). The gage for the aluminum channels was also considered to be 0.76 mm (0.030 in.) while the thickness of the stainless steel channels was assumed to be 0.51 mm (0.020 in.). For the aluminum design in the LH<sub>2</sub> tank, the channels or stringers were spaced 22.86 cm (9 in.) apart. In addition to the stringers, additional supporting ribs were also added with 22.86 cm (9 in.) spacing for additional required support of the aluminum screen. The rib gage was also assumed to be 0.76 mm (0.030 in.) and the assumed cross-section appears in Fig. V-21.

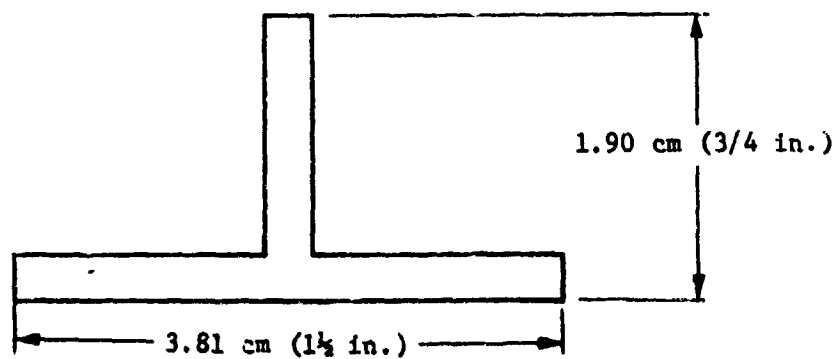


Fig. V-2 Supporting Rib Design for LH<sub>2</sub> Screen Liner

The stainless steel design was similar, but the ribs and stringers were spaced 45.72-cm 18-in. centers. The stainless steel ribs were 0.51-mm (0.020-in.) thick. In all cases the perforated plate was assumed to have an open to closed area ratio of 0.50.

The weight comparison of the two candidate designs is shown in Table V-19.

*Table V-19 Weight Comparison of LH<sub>2</sub> Trap and Liner Designs*

Component	Aluminum	Stainless Steel
Wicking Channels (Stringers), kg (lbm)	48.12 (106.0)	48.12 (106.0)
Ribs, kg (lbm)	28.16 (61.8)	23.6 (52.0)
Screen Liner, kg (lbm)	15.9 (35.2)	31.96 (70.4)
Trap, kg (lbm)	16.1 (35.6)	42.76 (94.2)
<b>Total</b>	<b>108.3 (238.6)</b>	<b>146.5 (322.6)</b>

The table shows that for the LH<sub>2</sub> tank propellant acquisition system application, the aluminum design is also substantially lighter than the stainless steel design and, accordingly, the aluminum design was selected for the Space Tug LH<sub>2</sub> tank with a trap and liner.

Aluminum was also the choice for the channels and liner systems. The breakdown of weights for the LH<sub>2</sub> and LO<sub>2</sub> systems is presented in Table V-20.

*Table V-20 Weights of LH<sub>2</sub> and LO<sub>2</sub> Channel/Liner Designs*

LH <sub>2</sub> , kg (lbm)	LO <sub>2</sub> , kg (lbm)
Wicking Channels 41.45 (91.3)	Wicking Channels 10.6 (23.4)
Ribs 23.33 (51.4)	Liner Screen 7.58 (16.7)
Screen Liner 13.25 (29.2)	Liner Perforated Plate 32.77 (72.2)
Flow Channels 150.27 (331.0)	Flow Channels 58.56 (129.0)
<b>Total 228.31 (502.9)</b>	<b>109.5 (241.3)</b>

The volumes enclosed in the controlled liquid regions of the four designs are  $0.118 \text{ m}^3$  ( $4.18 \text{ ft}^3$ ) for the  $\text{LH}_2$  and  $\text{LO}_2$  trap designs and  $1.23 \text{ m}^3$  ( $43.5 \text{ ft}^3$ ) and  $0.65 \text{ m}^3$  ( $9.38 \text{ ft}^3$ ) for the channel designs.

The cable method used in the integrated OMS/RCS design is also used here for attaching the screen liner assembly to the propellant tank wall. As previously mentioned, this approach was reviewed by Beech Aircraft Corporation. In their judgment, the attachment design is conservative.

An important consideration in the fabrication of the screen device is maintaining the retention capability during any forming and assembly processes. To ensure that the capillary retention capability is within the specifications, the various components of the  $\text{LH}_2$  and  $\text{LO}_2$  systems must be bubble-point tested. The bubble point tests should be conducted after every assembly process in the fabrication sequence. The screen should be checked in the as-received condition before any fabrication is attempted. Each subassembly (for example the trap coverplate) should be checked as it is completed. In the instance where the subassembly employs multiple screen layers, such as the trap liquid annulus or the flow channels, the subassembly should be bubble point tested after each screen layer is added. The large screen liner for the  $\text{LO}_2$  tank can be fabricated in individual gore sections. The  $\text{LO}_2$  tank liner is formed to 20 gore sections of perforated plate and screen in each hemisphere, and the hemispheres are welded together at the equator. Each of these gore sections can be tested for bubble point individually before they are assembled to form the liner.

The  $\text{LH}_2$  liner has no perforated plate. The as-received screen can be bubble point checked and then welded into place on the wicking channel framework. The T-section of the ribs is eliminated at points where they are joined to the wicking channels so that the flow in the channel will not be impeded by obstructions.

## 2. Feedline Design

Important design details in a capillary feedline system were disclosed in the previous analysis of the integrated OMS/RCS feedlines. Except for the dimensions, the discussion presented, as well as Fig. V-19, apply to the Space Tug propulsion system. Fabrication, support structure design, system operation, and integration were considered and will not be discussed here.

Vapor-annulus gap selection was based on the same criteria as those previously discussed. For the Space Tug, baseline diameters are significantly different for the MPS and APS systems. Baseline diameters (screen liner inside diameter) of 6.1 cm (2.4 in.) and 7.4 cm (2.9 in.) for the LH<sub>2</sub> and LO<sub>2</sub> MPS, respectively, and 1.27 cm (0.5 in.) for both APSs are noted. The primary concern in small lines, such as the APS, is fabrication problems arising from system design (close tolerances, etc). For the MPS, the weight penalty associated with increased feedline diameter and the annulus volume required for the boiloff rate are dominating factors. Annulus gaps of 0.95 cm (3/8 in.) and 0.32 cm (1/8 in.) were selected for the MPS and APS feedlines on the basis of these considerations. The resulting feedline geometry was used in estimating capillary feedline weights for the Space Tug systems analyzed.

A breakdown of system weights is shown in Table V-21. The weights shown are for screen liner acquisition/expulsion devices. They are also representative of nonlinear devices as well, with the exception of the LH<sub>2</sub> MPS. A reduction in assembly weight from 33.9 to 22.8 kg (74.8 to 50.2 lbm) is realized for the LH<sub>2</sub> MPS feedline with a nonlinear tank configuration.

Table V-21 Space Tug Capillary Feedline Weights

Weight	LH <sub>2</sub> Feedlines		LO <sub>2</sub> Feedlines	
	MPS	APS	MPS	APS
Screen Liner, kg/m, (lbm/ft)	1.94 (1.3)	0.21 (0.14)	0.34 (0.23)	0.08 (0.05)
Piping, kg/m (lbm/ft)	1.37 (2.26)	0.46 (0.31)	0.87 (2.6)	0.45 (0.30)
Total Feedline, kg/m (lbm/ft)	5.30 (3.56)	0.67 (0.45)	4.22 (2.83)	0.53 (0.36)
Assembly, kg (lbm)	33.9 (74.8)	1.6 (3.6)	3.9 (8.5)	1.3 (2.8)

The capillary liner weight includes the screen and spacer material and excludes support standoffs. Additional weight for standoffs should be small, however. Total capillary feedline weight is simply the sum of liner and piping components. This is given in weight per unit lengths and absolute weight of the system, based

on the estimated lengths of 6.4 m (21 ft) and 0.91 m (3 ft) for the LH<sub>2</sub> and LO<sub>2</sub> MPS lines, respectively, and 2.44 m (8 ft) for both APS lines. The screen liner accounts for only 34% of the total system weight for the LH<sub>2</sub> lines and 11% for the LO<sub>2</sub> lines. The data presented here should be competitive with the baseline design on a weight basis.

E. COMPARISON OF NASA BASELINE AND MARTIN MARIETTA STORAGE AND FEED SYSTEM

1. Operational Considerations

Both the baseline and the Martin Marietta designs use surface tension devices as the basic means for providing gas-free liquid. However, functionally, the two systems differ greatly.

The first Martin Marietta alternative to the baseline design is the refillable trap. This system has capabilities identical to those of the baseline design and at the same time eliminates the requirement for two APS tanks and the APS pressurant supply tank. Thus, the requirement for four pressurization, four vent, and four sets of fill and drain lines (shown in Fig. V-1) has been reduced by 50%. Therefore, the attendant lines and valves are not required. The screen feedline also eliminates the need for the LH<sub>2</sub> feedline heat exchanger on the MPS LH<sub>2</sub> feedline and the APS feedlines. The elimination of these components and subsystems reduces the weight of the system, and, as is discussed in the next section, the refillable trap system is considerably lighter than the baseline design. This condition alone makes it an attractive option.

Of equal importance is the significant increase in the simplicity of all the systems. As many as 12 valves can be eliminated from the baseline feed, fill, drain, and vent system (Fig. V-1), together with the feedline heat exchanger by adopting the Martin Marietta system design. An additional six valves and two feedline heat exchanger can be eliminated from the pressurization system. Because a specific failure rate is intrinsic to each component, a reduction in the number of components implies an increase in the reliability of the overall system. The elimination of the two start tanks in the Martin Marietta designs also reduces the number of pressurization and vent systems by two.

The baseline Space Tug design uses two different pressurization systems. In addition to the autogenous pressurization systems for the main tank, a cold gas helium pressurization system is used in the APS start tank. This high-pressure cold-gas system is heavy when compared to other pressurization schemes. It is also sensitive to changes in the APS or MPS start up requirements. If the requirements for APS propellants were to increase, if the idle mode settling time were increased, or if a different engine requiring more chilldown propellants were substituted in the system, the start tank and related pressurization components would experience significant weight increases. By contrast, the Martin Marietta systems pressurize only with autogenous gas from the accumulators. Any additional pressurant requirements would be met by loading only the additional liquid propellant needed for conversion to the gaseous pressurant.

The Martin Marietta trap design is operationally much more flexible. The size of the APS tanks in the baseline system limits the total usage of the system. A fixed amount of APS usage and/or a fixed number of MPS starts are determined by the tank size. Therefore, a change in the mission requiring more APS usage or more MPS burns would not be possible without major system modifications. The alternative trap design is not nearly so mission limited because the traps are refillable. The only restriction is that the total liquid usage between any two MPS burns must not exceed the capacity of the trap and the MPS thrust duration must be sufficient to settle the propellant and refill the traps. Therefore, changes in the mission can be more readily accommodated by the Martin Marietta refillable trap system design.

In summary, the basic Martin Marietta alternative design offers several advantages over the NASA baseline. The Martin Marietta system offers all the capabilities claimed by the baseline system and both require an idle mode engine operation to settle propellants before venting. However, the Martin Marietta design is lighter, significantly less complex, and hence, more reliable and somewhat less mission-dependent.

Nearly total mission independence is achieved with the second Martin Marietta alternative design, the channel system. Mission independence is achieved at the cost of some weight increase over the trap system. The discussion of the Martin Marietta trap system advantages is applicable to the channel system as well. The important difference between the channel system and the trap or the NASA baseline systems is the freedom from mission constraints that it offers. The channels are positioned so they will always be in contact with the unrestrained bulk liquid somewhere in the

tank. Therefore, as long as there is propellant in the tank, and regardless of when or how the previous mission event occurred, APS activation is possible. Since venting can only occur immediately prior to an MPS burn, the propellant will always be settled when the MPS engine is fired. However, the idle mode engine startup requirement is not constrained in any way by the channel design, and the MPS engine can be restarted as many times as a mission may require.

The Space Tug baseline document indicates that venting during a coast period may not be required. Even though this claim has not been substantiated, the NASA baseline design does not provide for venting capability except during a MPS idle mode. For the purpose of strict comparison, the first two Martin Marietta alternative systems were designed for the same limited venting capability featured by the NASA baseline system. With any system which cannot be vented as conditions may require, an anomalous condition requiring venting during a coast period could jeopardize the mission. There may also be advantages realized from the removal of the requirement for a MPS engine with an idle mode capability. Since the idle mode requirement is dictated strictly by the nature of the acquisition system and its venting capability, the third alternative design proposed by Martin Marietta (which can be vented at any time) offers an attractive option. The third Martin Marietta alternative involves the addition of a full tank screen liner to either of the other two systems--the trap or the channels. The discussion of operational characteristics of those two systems remains valid with the one exception that the third system can be vented as conditions require. The design also removes the propellant from the tank wall, thereby substantially reducing the possibility of localized hot spots and nucleation points in the propellant. Such points can cause rapid increases in pressure rise rates in the tanks. Thus, the trap-liner system is independent of mission constraints to the extent allowable by the trap volume, and the channel liner system has complete functional independence of any mission that might be required of the Tug.

## 2. Weight Considerations

a. *Hardware Weights* - Comparisons between the NASA baseline Space Tug propellant storage and feed system and the weights of the alternative Martin Marietta designs appear in Tables V-22 and V-23. Table V-22 shows the comparison between the NASA baseline and the first two alternatives--the refillable trap system and the channel system. The weights of the MPS feed, fill, drain, and vent system

Table V-22 Comparison of the NASA Baseline and Martin Marietta System Weights (without Liners)

NASA BASELINE DESIGN, kg (lbm)			Martin Marietta Designs, kg (lbm)		
Storage Tanks	LH <sub>2</sub>	LO <sub>2</sub>	Storage Tanks	LH <sub>2</sub>	LO <sub>2</sub>
APS Tank	24.9 (55)	13.6 (30)	Acquisition/Expulsion Devices		
APS Tank Insulation	5.0 (11)	2.7 (6)	1) Refillable Traps	16.16 (35.6)	4.63 (10.2)
Acquisition/Expulsion Device	10.8 (24)	4.08 (9)	2) Channels, without tank liner	110.5 (243.5)	43.3 (95.4)
GHe Storage Tank	13.1 (29)		MPS Feed, Fill, Drain and Vent		
GHe	9.62 (21.2)		Valving	16.3 (36.0)	13.4 (29.6)
GHe Valving and Plumbing	9.08 (20)		Plumbing and Liner	33.5 (73.9)	17.47 (38.5)
	72.7 (160.2)	20.4 (45.0)	Miscellaneous	10.9 (24.1)	5.17 (11.4)
MPS Feed, Fill, Drain and Vent				60.83 (134.0)	36.1 (79.5)
Valving	19.3 (43.9)	17.7 (39.0)	APS Feedline		
Plumbing	36.6 (80.7)	21.8 (48.1)	Plumbing	0.953 (2.1)	0.681 (1.4)
Miscellaneous	11.1 (24.5)	5.8 (12.8)	Screen Liner	0.59 (1.3)	0.681 (1.4)
	67.69 (149.1)	45.35 (99.9)		1.54 (3.4)	1.271 (2.8)
APS Feed line			Total System, Excluding Propellant Tanks		
Plumbing	0.726(1.6)	0.726 (1.6)	Refillable Traps	78.5 (173.0)	42.0 (92.5)
Heat Exchanger	0.635(1.4)	0.635 (1.4)	Channels	172.9 (380.9)	80.6 (177.7)
	1.36 (3.0)	1.36 (3.0)			
Total System, Excluding Propellant Tanks	141.8 (312.3)	67.14 (147.9)			

Table V-23 Comparison of the NASA Baseline and Martin Marietta System Weights (with Liners)

NASA Baseline Design, kg (lbm)			Martin Marietta Designs, kg (lbm)		
Storage Tanks	LH <sub>2</sub>	LO <sub>2</sub>	Storage Tanks	LH <sub>2</sub>	LO <sub>2</sub>
APS Tank	24.9 (55)	13.6 (30)	Acquisition/Expulsion Device		
APS Tank Insulation	5.0 (11)	2.7 (6)	1) Refillable Traps with Liner	108.3 (238.6)	61.78 (136.1)
Acquisition/Expulsion Devices	10.8 (24)	4.08 (9)	2) Channels with Liner	228.3 (502.9)	109.5 (241.3)
GHe Storage Tank	13.1 (29)		MPS Feed, Fill, Drain and Vent		
GHe	9.62 (21.2)		Valving	16.34 (36.0)	13.4 (29.6)
GHe Valving and Plumbing	9.08 (20)		Plumbing	44.7 (98.5)	17.6 (38.8)
	72.7 (160.2)	20.4 (45.0)	Miscellaneous	10.9 (24.1)	5.17 (11.4)
MPS Feed, Fill, Drain and Vent				72.00 (158.6)	36.23 (79.8)
Valving	19.93 (43.9)	17.7 (39.0)	APS Feedline		
Plumbing	36.6 (80.7)	21.8 (48.1)	Plumbing	0.953 (2.1)	0.635 (1.4)
Miscellaneous	11.1 (24.5)	5.8 (12.8)	Screen Liner	0.681 (1.5)	0.635 (1.4)
	67.69 (149.1)	45.35 (99.9)		1.634 (3.6)	1.27 (2.8)
APS Feedline			Total System, Excluding Propellant Tanks		
Plumbing	0.726(1.6)	0.726 (1.6)	Refillable Traps with Liner	181.9 (400.8)	99.28 (218.7)
Heat Exchangers	0.635(1.4)	0.635 (1.4)	Channel with Liner	302.0 (665.1)	147.1 (323.9)
	1.36 (3.0)	1.36 (3.0)			
Total System, Excluding Propellant Tanks	141.8 (312.3)	67.14 (147.9)			

for the Martin Marietta design reflect the savings realized from eliminating a number of unnecessary components from the baseline system.

The basic storage tank weight category indicates that the refillable traps are considerably lighter and the channel system is somewhat heavier than the baseline design. The refillable trap system compares exactly with the capability of the baseline system and is, therefore, an attractive option because of its reduced weight and increased reliability. At some weight increase over the baseline system, the channel design offers complete functional independence of mission duty cycle because it can deliver propellant at any time regardless of the propellant orientation in the tank.

*b. Residual Weights* - Normal design practice involves assessing a weight penalty against a system for the amount of propellant contained within the controlled liquid region of the screen device. For the systems described here, those weights are:

LH<sub>2</sub> trap, 8.53 kg (18.8 lbm)

LO<sub>2</sub> trap, 55.38 kg (122 lbm)

LH<sub>2</sub> channels, 88.5 kg (195 lbm)

LO<sub>2</sub> channels, 302.8 kg (667 lbm)

#### F. CONCLUSIONS

Based on the analytical and comparative evaluations conducted under this study, the Martin Marietta capillary concept offers the best approach for satisfying the cryogenic propellant storage and feed requirements of a typical Earth-orbiting vehicle planned for the late 1970's and early 1980's. The capillary concept can satisfy a wide range of operating conditions and cryogenic storage applications. The basic concept can be easily modified to meet specific design criteria and mission requirements.

In this study the DSL concept was evaluated and modified to satisfy the propellant storage and feed requirements of the Space Tug. A comparison between the preferred Martin Marietta design and the NASA baseline Tug design showed that the Martin Marietta design was much simpler and more passive. The Martin Marietta design requires fewer propellant tanks and associated hardware such as disconnects, lines, valves, etc than the baseline design. In addition the Martin Marietta design eliminates the requirements for propellant settling and venting using the idle mode engine operation. This places the requirement for the idle mode operation entirely on the necessity for turbopump assembly and engine thrust chamber chilldown. Since the Tug requirements emphasize system reusability, long life, high reliability, etc the Martin Marietta propellant storage and feed system cryogenic design is considered to be more attractive than the NASA baseline design, and, therefore, the Martin Marietta design is the preferred system for the Space Tug application. The weight comparison showed that there was some weight saving advantage over the NASA baseline by the Martin Marietta system having equivalent capability; however, systems having increased capability and mission independence incur some additional weight penalties.

## VI. DEVELOPMENT PLAN

The DSL tank/feedline storage system and specific designs were presented in earlier chapters. It is a promising system for incorporation into Earth orbiting vehicles for the subcritical storage of cryogenics. The plan, including cost and schedule, to develop and qualify the DSL design for a specific application and mission will, of course, be different depending on the system/mission criteria and guidelines. For example, qualification costs for the system are drastically different for the manned and unmanned missions. The specific cryogen, system capacity, type of liquid demand (i.e., number of expulsions and desired fluid quality), tank and feedline geometries, packaging, mission duration, adverse acceleration criteria, allowable vent periods and desired fluid quality, cost and schedule implications, number of systems, and design margins will be different from one application to the next.

As discussed in this volume and in Volume III, considerable effort has been expended with regard to analysis, design, fabrication and ground testing to verify the design and operational characteristics of the DSL system. The stratification phenomena (discussed in Volume III) and the limited low-g test durations (provided in drop towers and aircraft flying Keplerian trajectories) justify Martin Marietta's position that an orbital test to verify liquid-free vapor venting performance for the DSL is the key requirement for the development program, regardless of the specific design and application. Two different orbital experiment approaches are presented in Volume IV.

The plan presented in this chapter deals with the development of the DSL tank/feedline design for use in the integrated SS/RCS system (LH<sub>2</sub> and LO<sub>2</sub> storage). The integrated storage application is discussed in Chapter III.

This plan emphasizes the events, costs, and schedule for developing the system to be incorporated into the orbiter. Costs are budgetary and 1973 dollars.

A. OBJECTIVES, GUIDELINES AND APPROACH

1. Objectives

The objectives of this plan are to outline the steps and estimate costs associated with the development of the DSL cryogenic propellant storage and feed system.

2. Guidelines

The DSL system considered is the integrated OMS/RCS design developed under this phase of the program and shown schematically in Fig. II-59. The propellants are liquid oxygen and liquid hydrogen. Because the primary problems associated with the storage and use of cryogenics are created by their low temperatures, the development efforts for liquid hydrogen and liquid oxygen are considered to be similar with respect to cost and complexity. Our experience over the past few years has involved the development of spherical and cylindrical screen configurations in sizes ranging from less than 0.3-m (1-ft) dia to a spherical DSL tank 1.78-m (70-in.) dia. While building this latter device, screen fabrication techniques were developed that allow realistic assessment of the development requirements for full-scale cryogenic systems.

The system components were shown in Fig. II-59 and include the following.

- 1) The propellant tank assemblies are spherical and are 3.81-m (12.5-ft) in diameter for the LH<sub>2</sub> system and 2.51-m (8.25-ft) in diameter for the LO<sub>2</sub> system.
- 2) The propellant management device in each storage tank is a complete screen liner with 20 liquid feed channels. One tank for each propellant contains a reentry tank as part of the liquid outlet manifold.
- 3) The OMS and RCS feedlines are vacuum jacketed with capillary screen liners. The tank-to-tank transfer lines are vacuum jacketed, but not screen lined. The OMS and RCS liquid hydrogen feedlines are 18.3-m (60-ft) and 3.05-m (10-ft) long, respectively, with an inside diameter of 10.2-cm (4-in.). The OMS and RCS liquid oxygen feedlines are 4.58-m (15-ft) and 3.5-m (10-ft) long, respectively, and also have an inside diameter of 10.2 cm (4 in.).

For this plan, only one tank and feedline for each propellant will be developed. Other propellant system components such as valves and disconnects are not covered by the plan and will be simulated for development testing using existing ground type components.

3. Approach

Although testing of the DSL tank concept under 1 g (as described in Volume III) has verified predicted liquid expulsion performance and other critical operational characteristics, stratification effects prevented liquid-free venting. The latter must be successfully demonstrated during an extended low-g test. A program to design, build, and fly such an orbital experiment is described in Volume IV. The orbital module includes a 0.76-m (30-in.) diameter  $LO_2$  tank with a complete liner and 12 flow channels, similar in design to the OMS/RCS tank configurations. A screen liner feedline was also included as part of this module to provide low-g demonstrations of single phase  $LO_2$  expulsions and intermittent and near-continuous vapor venting. This type of orbital experiment provides final verification of the DSL propellant management design for cryogen storage. A number of flight options were investigated as reported in Volume IV. One of the two preferred options, a dedicated payload on the Atlas F, or Atlas F/Burner II, launch vehicle would cost between \$5 and \$7 million. The second option, to fly the test module on the Titan III/Centaur proof flight as a tertiary payload, indicated a cost of only \$1.6 million. This lower cost was due to the shared payload approach and because the experiment was allowed essentially unlimited weight and space within the payload shroud. The flight was also one-of-a-kind with a relatively short time schedule.

In summary, the cost for the orbital demonstration can range from the \$1.6 million (tertiary payload) to \$7 million (dedicated payload). The reader should refer to Volume IV for details of the orbital program plan.

In addition to the orbital demonstration program, a second 18-month program is also required to develop the specific prototype DSL system design. The basic elements of this program (shown in Fig. VI-1) are detailed in this chapter. The second program is initiated following completion of the orbital program.

After program go-ahead, the design requirements and criteria are identified and a design specification document is published. This document establishes the guidelines and ground rules for the 6-month detail design effort that terminates with the completion of detail fabrication drawings for the prototype DSL tank and feedline system.

Some subscale model tests will be conducted to support the design effort. In addition to these tests, the engineering laboratory will fabricate and assemble the test fixtures required for the prototype DSL tank and feedline performance tests. The 10-month fabrication and assembly effort will start at the end of the fourth month after program go-ahead. All of the fabrication and assembly will be done at Martin Marietta's fabrication facility.

The detail schedule and costs for this development program are presented in the final section of this chapter.

## B. DSL TANK AND FEEDLINE DEVELOPMENT REQUIREMENTS

### 1. General

The work items and costs associated with the development of the complete airborne cryogenic propellant storage and feed system are not covered by this plan. The detailed development steps and costs for the DSL tank and feedline are treated because this type of system has not yet been used in a spacecraft. The following paragraphs describe the required development effort for the DSL tank and feedline to be brought to the flight qualified status.

### 2. DSL Tank and Feedline

The DSL tank and feedline designs used for this development study were shown in Chapter III (Fig. III-16 through III-18). The capillary screen assemblies for both the tanks and the feedlines consist of stainless steel (300 series) Dutch twill screen sections resistance-welded to perforated stainless steel sheet metal subassemblies. The assembled liners are suspended within the aluminum alloy propellant tanks by braided stainless steel cables. The tank vent lines are of aluminum alloy and the tank liquid outlet lines are stainless steel. The propellant tanks are covered by multilayer insulation consisting of alternate layers of aluminumized Mylar and glass paper. The tank assemblies are suspended within titanium spherical vacuum jackets using braided stainless steel cables.



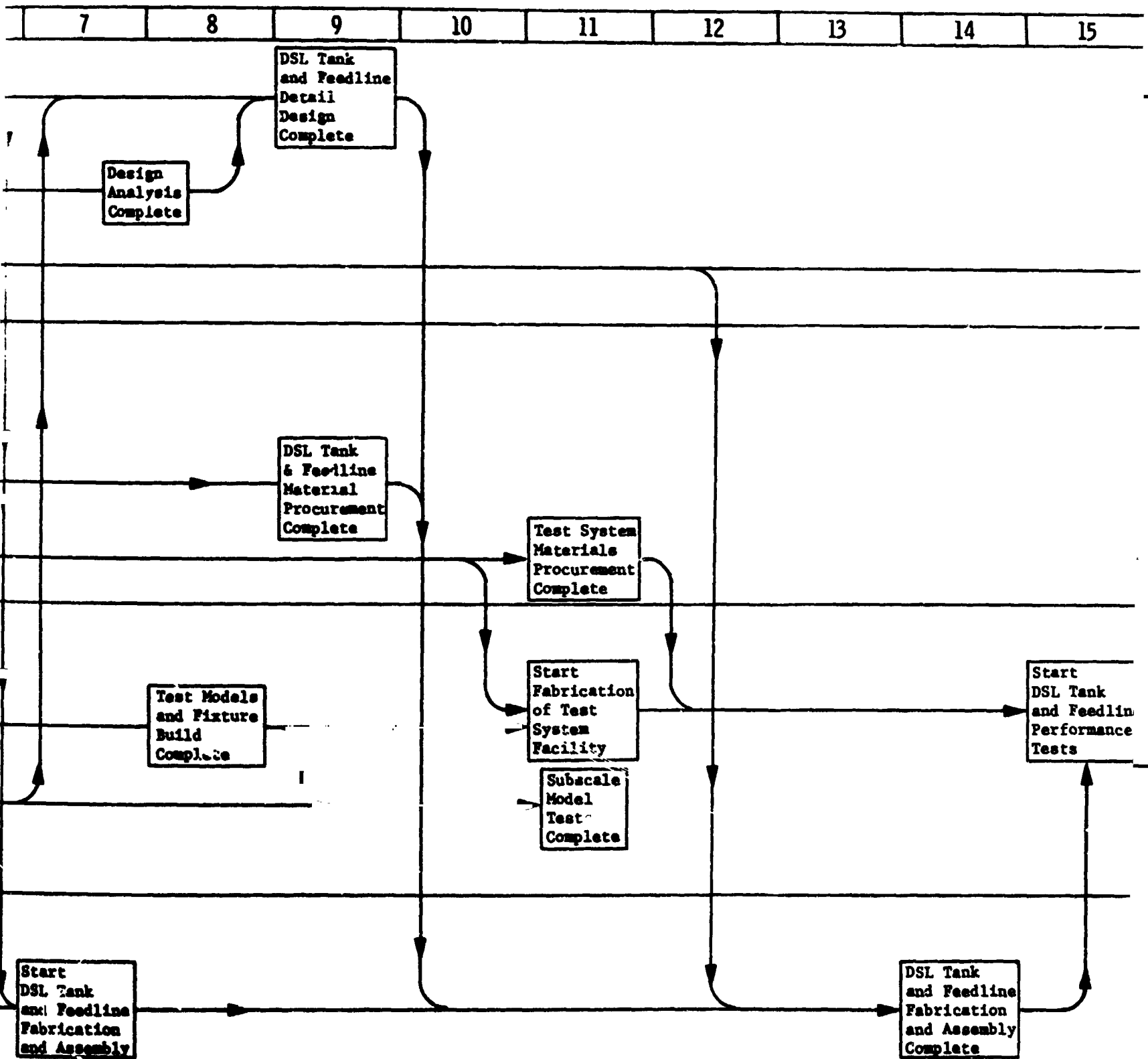


Fig. VI-1 Development Program for Full-

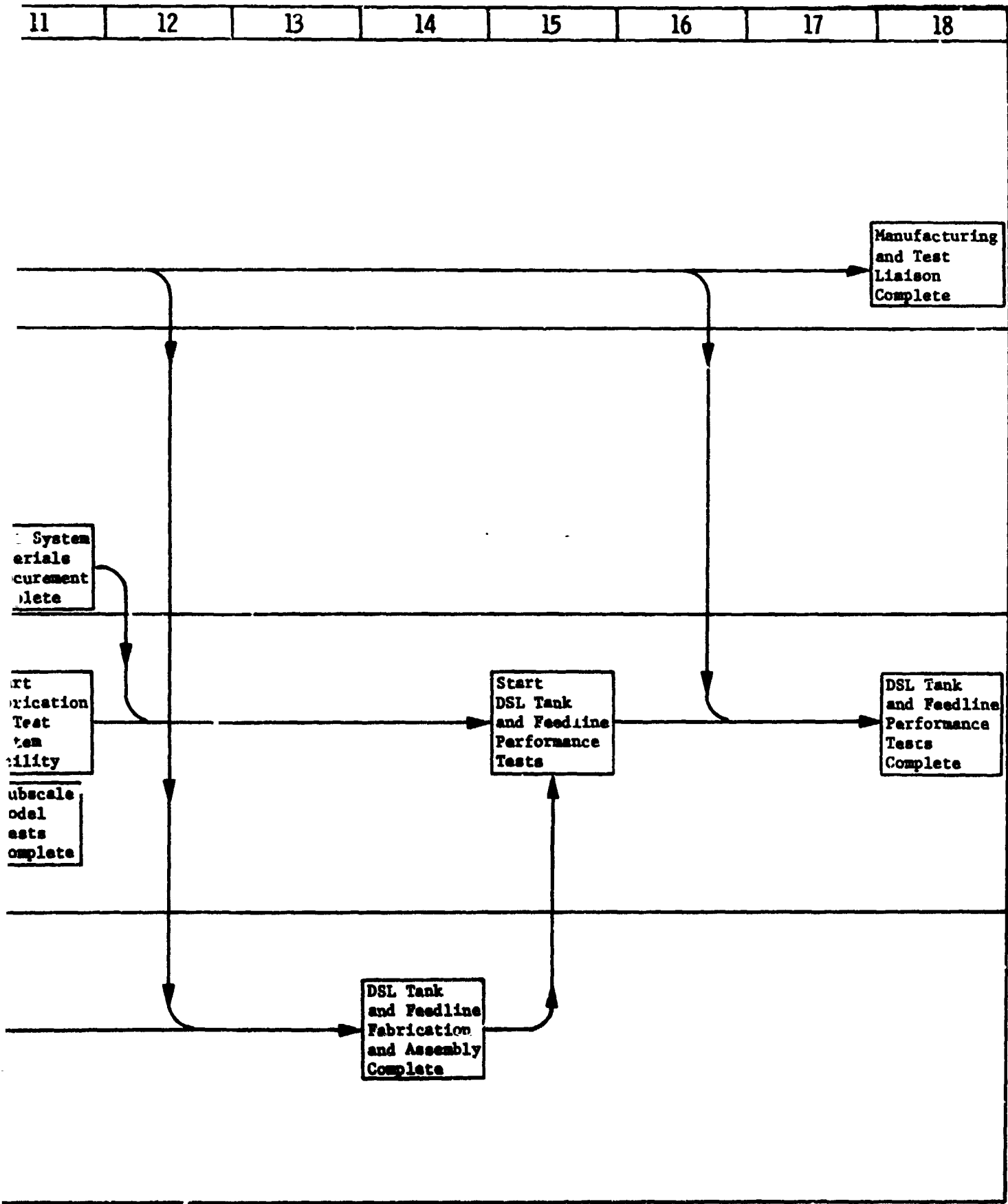


Fig. VI-1 Development Program for Full-Scale Cryogenic Acquisition/Expulsion System  
VI-5 and VI-6

FOLDED PAGE

The engine feedline assemblies are similar to those for the tanks with regard to construction and materials. Screen liner assemblies are of fine mesh stainless steel screen and perforated stainless steel sheet.

3. Development Status Summary

Tables VI-1 and VI-2 present summaries of the key design items for the DSL tank and feedline system, along with an assessment of the development status of each. Fabrication development status is presented in Table VI-3. Although such a system has not been flown, the considerable analysis, design, and testing conducted under this phase of the program during Contract NAS9-10480 and under Martin Marietta in-house programs, have produced a high level of development. However, a number of the design, fabrication, assembly, and inspection details require additional investigation.

The long-term low-g data obtained from the orbital experiment will complete the information needed to verify the DSL design and full-scale system performance. The thermodynamic data obtained, for example, will substantiate the analytical model used to size the tank and feedline annuli and tank line sizes, as well as establish the insulation requirements. The experiment, in addition to providing a demonstration of vapor venting and single-phase liquid expulsion, will also allow evaluation of the prototype vent control system.

C. PROTOTYPE SYSTEM DEVELOPMENT

The second phase of the development program will be initiated following the completion of the orbital test program. The objectives of this phase are to complete the development of the flight prototype LH<sub>2</sub> and LO<sub>2</sub> acquisition/expulsion systems. During this phase, the results of the orbital test program will be used to evaluate the integrated OMS/RCS designs (presented in Chapter III) and make design changes as required. Detailed fabrication drawings will be made and two prototype (LH<sub>2</sub> and LO<sub>2</sub>) systems will be fabricated and tested. The design analysis, fabrication and testing tasks are detailed in the following paragraphs.

Table VI-1 DSL Tank Development Summary

Design Feature	Development Status	Additional Development
<b>Performance</b>		
Vapor Venting	Stratification phenomena prevented 1-g venting tests under Phase A.	Need orbital test to verify performance. (See Vol IV)
Liquid Expulsion	Minus 1 g LH <sub>2</sub> successfully expelled using 63.5-cm (25-in.) dia model . . . Subscale DSL models in KC-135 using methanol as test liquid during low-g tests in November 1971	No more ground tests . . . orbital test data are desirable.
Transient Phenomena	Startup and shutdown (expulsion) effects on interface stability analyzed under Phase A; MDAC also analyzed under present MSFC contract.	None. MDAC is studying these effects further under APB Breadboard Program with MSFC. (Contract NAS8-2757)
Pressure Drop	Considerable data available for viscous flow and entrance (flow through perforated material) losses to design DSL system.	None.
Bulk Propellant Control	Bulk propellant support demonstrated in KC-135 tests with noncryogenics. Phase A LH <sub>2</sub> ground tests, as well.	Data from extended low-g orbital tests are desirable.
Interface Stability	Considerable data for perforated material are available from previous programs, NAS9-8y39, NAS8-21259, and NAS8-20837, for example. Ground test data, including drop tower and KC-135, are available for screen and perforated plate under normal and parallel (with regard to foraminous material surface) accelerations. Vibrational effects experimentally evaluated under Phase A.	None.
Liquid Damping	Damping of liquid using foraminous material experimentally evaluated and categorized under drop tower study, Contracts NAS8-21259 and NAS8-20837.	None. Orbital data are desirable.
Bubble Point	Measured for single and multilayer screen under Phase A using methanol, LN <sub>2</sub> , and LO <sub>2</sub> ; Lockheed has also measured bubble point using LO <sub>2</sub> under AF contract.	None. MDAC is measuring bubble point using LH <sub>2</sub> under on-going LERC contract.
Passive Communication Liner	Performance demonstrated in KC-135 tests using noncryogenics; Phase A LH <sub>2</sub> tests also.	Data from orbital test desired . . . not required.
Screen Wicking	Satisfactorily demonstrated under pressurization and expulsion tests during Phase A tests.	Orbital data would be beneficial.

Table VI-1 (cont.)

Design Feature	Development Status	Additional Development
<u>Performance</u>		
Incipient Boiling	The LH <sub>2</sub> tests under Phase A showed that liquid expulsion could be achieved without generating vapor within the liquid flow channels. Superheat required for localized boiling has been studied by University of Michigan under MSFC funding for several, consecutive years. Marangoni effect was also studied by MMC under Project GLEO, Contract NAS8-11328. Numerous other studies reported in the literature.	Orbital experiment desired.
Pressurization	GH <sub>2</sub> and GHe pressurization successfully demonstrated for continuous and intermittent LH <sub>2</sub> -1 g expulsions under Phase A.	None . . . orbital data would further verify performance.
Vapor Collapse	Studied analytically and experimentally (KC-135 tests) under Phase A.	Orbital experiment desired.
Tank Loading	Successfully demonstrated using LN <sub>2</sub> and LH <sub>2</sub> under Phase A test using 63 5-cm (25-in.) diameter model.	None.
<u>System Controls</u>		
Vapor Venting	System developed for Phase A tests appears adequate for LH <sub>2</sub> and LO <sub>2</sub> orbital storage.	Orbital test would be beneficial.
Fluid Quality	Liquid/vapor sensors and flowmeters used in Phase A LH <sub>2</sub> tests appear adequate for LH <sub>2</sub> and LO <sub>2</sub> storage.	Orbital test data appear desirable.
Mass Gaging	No such device has been used; however, nucleonics system under development by AF and RF gaging being developed by NASA appear to be suitable to DSL.	Orbital test data are desirable.
<u>Inspection</u>		
Spray Technique	Concept to spray liquid over screen device to bubble check has been experimentally verified using small tank models and for the 1.78-m (70-in.) diameter	Additional 1-g testing would provide additional verification.
Bubble Point	See earlier item.	None.

Table VI-2 DSL Feedline Development Summary

Design Feature	Development Status	Additional Development
<u>Performance</u>		
Vapor Venting	Successfully demonstrated for 1.01-m (40-in.) long model using Freon under 1-g tests, Phase A. MMA IR&D Program in progress to demonstrate venting for 6.1-m (20-ft) long model using LN <sub>2</sub> as test liquid.	IR&D Program in progress. Orbital test is required.
Liquid Expulsion	Successfully demonstrated for 1.01-m (40-in.) long model using Freon under 1-g tests, Phase A. MMA IR&D Program in progress.	IR&D Program in progress. Orbital test is desired.
Transient Phenomena	Freon system (above) was successfully demonstrated under startup and shutdown sequences; on-going LN <sub>2</sub> IR&D Program to provide additional data.	IR&D Program in progress.
Wet and Dry Liner Conditions	The Freon system, mentioned earlier, was successfully demonstrated under initially wet conditions. The LN <sub>2</sub> IR&D Program in progress will provide these 1-g data.	Orbital experiment is required.
Heat Soakback	Analysis has been performed under Phase A and under Contract NAS7-754 and other contracts. Specific point design is required to assess engine heat soakback, turbopump assembly (TPA), effects on DSL design.	Additional 1-g tests and orbital test required.
<u>System Controls</u>		
Vapor Venting	See DSL tank (similar item).	Orbital test data are desirable.
Fluid Quality	See DSL tank (similar item).	Orbital data are desirable.
Valving	Valving to join feedline vapor region with that for tank. Analysis and design done under Phase A and Phase C (Vol IV).	Orbital data are desirable.
<u>Inspection</u>		
Spray Technique	See DSL tank (similar item).	Additional 1-g testing desired.
Bubble Point	See DSL tank (similar item).	None.

Table VI-3 Fabrication Development Summary

Design Feature	Development Status	Additional Development
Fine-Mesh Screen Forming	Techniques are available for single and compound curvature. The latter, however, presently degrades screen bubble point by as much as 50%. The single curvature technique used for the 63.5-cm (25.0-in.) diameter model under Phase A, and for the 1.78-m (70-in.) diameter screen liner under the MMA IR&D Program, is acceptable. The bubble point degradation is nearly zero when compared to the "as received" bubble point.	None required; however, more work is required for the double curvature if it is to become a candidate forming technique.
Screen Joining	Joining of the Dutch twill screen has been successfully demonstrated for stainless, aluminum, and titanium. Stainless systems have successfully been flown. The joining techniques include brazing, welding, and various diffusion bonding techniques. The 63.5-cm (25.0-in.) diameter model used nearly 100% tin solder for cost and schedule reasons.	More work is desired for the aluminum and titanium to reach the stainless status.
Dissimilar Metal Joining	The usual practice is to avoid the use of dissimilar metals; however, techniques are available. For example, under JPL Contract 951709, Martin Marietta joined stainless screen to titanium plate using rivets covered by water glass.	More work is desired.
Multilayer Screen	The Dutch twill screen channels for the 63.5-cm (25.0-in.) diameter model were composed of two layers of screen. The feedline, in particular, for the integrated RCS/QMS system baselined here requires multilayer screen. More of this work is planned under a Martin Marietta IR&D Program during calendar year 1973.	More work is desired with regard to closely spaced fine-mesh screen layers.
Cleaning Techniques	Martin Marietta, under previous IR&D work, has demonstrated chemical cleaning and other techniques acceptable for fine mesh screen. In fact, data are available for immersion of 325x2300 screen in liquid fluorine for up to 35 days. No effect on bubble point was measured.	None.
Inspection	See bubble point technique, as discussed earlier.	None.
Screen Support	Various techniques have been developed to support the fine-mesh screen...porforated plate, coarse screen, and combinations of screen and plate.	None.
Screen-to-Tank	Different support techniques are presented in this volume and in Volume IV to support the screen configuration within the tank and feedline.	None. Orbital experiment is desired.

1. Design Analysis

The design analysis conducted under Phase A (discussed in Chapter III) yielded engineering or conceptual type drawings for the integrated OMS/RCS LH<sub>2</sub> and LO<sub>2</sub> systems. The analytical models and design methods used were verified by ground tests. These designs were also reviewed by Beech Aircraft Corporation of Boulder, Colorado (Ref VI-1), and found to be completely adequate for incorporation into a man-rated, flight qualified cryogenic storage system.

Under this design analysis task, the orbital test results will be reviewed. The test data will be used to modify the analytical models and design methods developed under Phase A as required. The integrated OMS/RCS designs will then be reevaluated and the required design will be built. A design task to develop detailed fabrication drawings for two prototype (LH<sub>2</sub> and LO<sub>2</sub>) systems will be conducted.

Analyses that will be performed to support the detailed design effort include stress and dynamic, thermal and thermodynamic, and fluid mechanics. With the basic system configuration and size established (i.e., tank volume, feedline length and diameters, and valving requirements) a system layout will be made to locate major components and select support and attachment points. The combined stress and dynamic analysis will be conducted using launch and flight accelerations, acoustic loading, propellant tank slosh, pyrotechnic shock, and vibration as input data. This analysis will be subject to several iterations as the component designs are made. It will continue throughout the 6-month design task with the final iteration following the final design changes.

The thermal and thermodynamic and the fluid mechanics analyses under this task will review the results of the orbital test program. Of particular interest in the thermal and thermodynamic area will be the venting performance characteristics, the low-g thermal stratification effects, and end heating on the feedline. Low-g fluid mechanics data, which impact the design, include screen wicking, communication screen performance, and bulk fluid control. Design modifications will be incorporated based on these data.

## 2. Fabrication and Test

Under this task, the manufacturing and inspection techniques required to produce a full-scale flight qualified system will be developed. Forming and joining screen segments and screen and sheet metal sections are basic fabrication tasks. All devices fabricated to date have been accomplished by skilled laboratory technicians on a one-of-a-kind basis. Soft soldering, fusion welding, and resistance seam and spot welding methods have been used to build the test devices. In every case, the test device was used for basic capillary device performance investigation. Methods now must be developed to form and join sections of a full-scale system capable of withstanding flight environments. In addition, the inspection techniques required of a full-scale system must be developed. In particular, an in-tank and in-feedline method of verifying screen liner integrity and cleanliness will be developed. This work will be accomplished as a part of the fabrication of the tanks and feedlines for the scale model test program.

Fabrication and assembly of the subscale test models will be done in Martin Marietta's Engineering Test Laboratory. These test devices do not require the formal engineering drawings or the quality control during fabrication that flight hardware requires. Fabrication and assembly of the prototype tanks and feedlines, on the other hand, will be completed in the manufacturing area. This effort requires the planning and control normally used with deliverable flight hardware. Formal quality control techniques, tooling, and standard manufacturing processes will be used to develop the overall manufacturing plan for fabrication of flight systems. Fabrication and assembly of procured parts such as the vent-control components will occur at vendor plants under controls similar to those used for the tanks and feedlines. These suppliers are regulated by component design specifications and a component acceptance test is used to provide a final check of supplier manufacturing quality.

At least one complete system for each propellant will be fabricated and assembled for the system development test. Major components of the system will be assembled in the manufacturing area. These will then be moved into the laboratory test area for complete system assembly. Because the major features of the system provide for low-g propellant management, which cannot be tested under 1-g conditions, the test program will be relatively conventional. Fill and drain, outflow, pressure cycling, temperature cycling, and thermal performance tests will make up the major portion of the test program.

D. DSL TANK AND FEEDLINE COSTS

Cost estimates for the developing of the DSL tank and feedline systems are presented under two categories: (1) the Orbital Experiment and (2) Prototype DSL Tank and Feedline Development. Table VI-4 lists the cost for each item and total cost for each category of development. Again, it must be emphasized that cost estimates are budgetary.

Table VI-4 DSL Tank and Feedline Development Program Costs

Program Phase	Costs
I. Orbital Test Program	\$1.6 to \$7M
II. Prototype DSL Tank and Feedline Development	
A. Design Analysis	\$460K
B. Fabrication	\$575K
C. Development Tests	\$370K
D. Additional Development Items	
1. Fine-Mesh Screen Forming and Joining	\$ 30K
2. Dissimilar Metal Joints	\$ 30K
3. DSL Inspection and Checkout	\$ 53K
Subtotal	\$1.52M
TOTAL COSTS	\$3.12 to \$8.52M

Costs for the full-scale DSL tank and feedline include the development of two flight hardware quality tanks and feedlines, with the remainder of the development test system made up of unqualified ground components. Also, costs are presented for the development of three items that were not considered under the orbital test program: (1) fine mesh screen forming and joining (2) dissimilar metal joints, and (3) DSL inspection and checkout.

**E. DEVELOPMENT PROGRAM SCHEDULE**

The program schedule with milestones for development of the tank and feedlines for the integrated OMS/RCS propellant storage and feed system is shown in Fig. VI-2. The 20-month span covers all necessary operations from program go-ahead to the end of development test for the prototype systems. All supplier components such as shutoff valves, regulators, check valves and filters are not flight qualified during the program. The propellant tanks, including propellant management devices and the screen liner feedlines, complete development testing at a component and system level and are ready for system flight qualification at the end of 20 months. An area of concern with regard to maintaining the schedule is the development of manufacturing techniques for full-scale DSL tank and feedline fabrication. Work to date has been of a developmental nature with considerable handcrafting by skilled specialized technicians. This type of fabrication now must be scaled up to normal manufacturing operations.

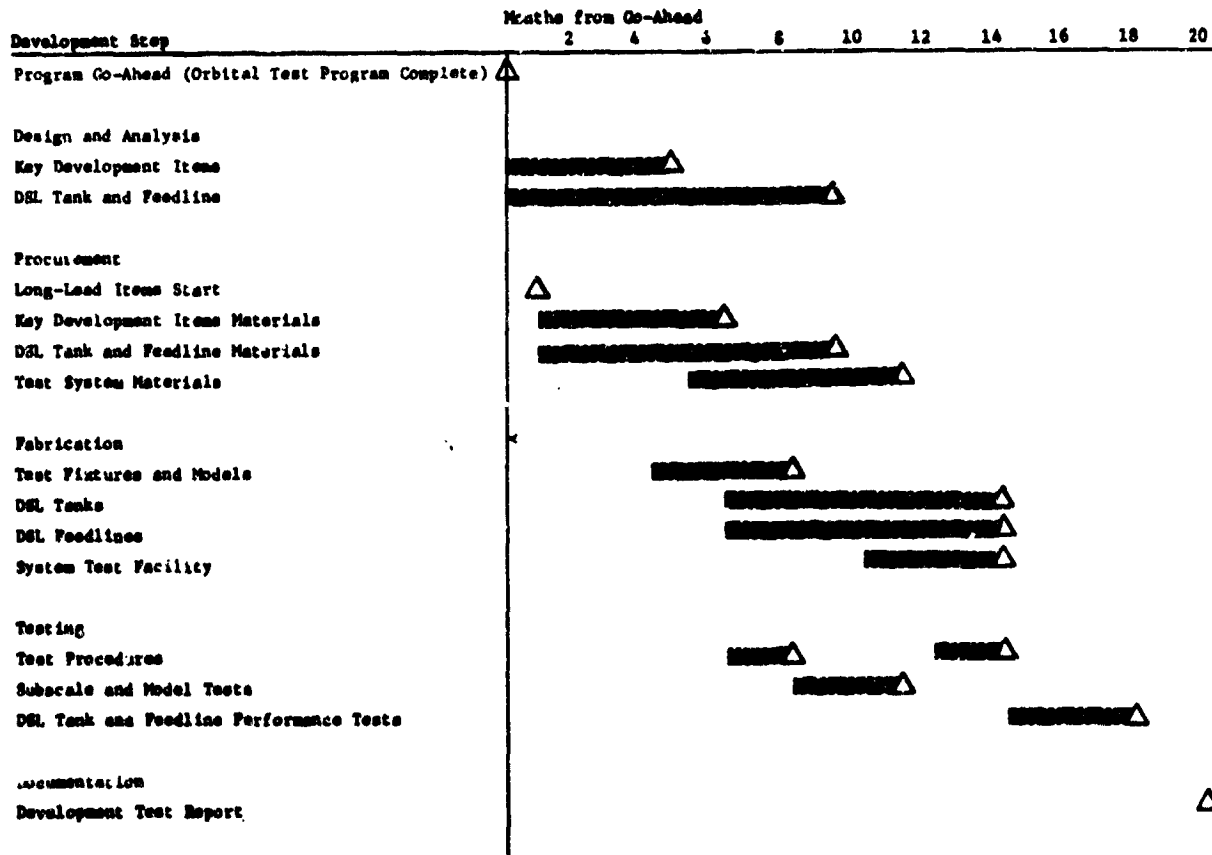


*Fig. VI-2 DSL Tank and Feedline Development Status*

## VII. CONCLUSIONS AND RECOMMENDATIONS

The passive DSL tank/feedline design is extremely attractive for efficient and reliable subcritical storage of cryogenics during extended periods at low-g. The results obtained during this phase of a rather significant analytical and experimental effort tend to verify the predicted DSL performance and operational flexibility. The acquisition/expulsion system designs presented here for the integrated OMS/RCS (LH<sub>2</sub> and LO<sub>2</sub>), the dedicated OMS (LO<sub>2</sub>), and the Space Tug (LH<sub>2</sub> and LO<sub>2</sub>) appear most capable of satisfactorily meeting the spacecraft and mission requirements. The designs were developed using the analytical and design methods verified by the comprehensive ground tests conducted under this phase of the program. Testing of a representative subscale DSL tank model, using LH<sub>2</sub> as the test liquid, successfully demonstrated vapor-free liquid outflow and the performance of the communication (gas annulus-to bulk region) screen liner. However, testing of this 63-cm (25-in.) diameter model, described in Volume III, did not demonstrate liquid-free vapor venting because of the 1-g thermal stratification phenomena.

It is recommended, therefore, that the next step in verifying the DSL concept is to conduct the orbital test program outlined in Volume IV. The orbital test bed provides the long-term, low-g environment needed to demonstrate vapor venting, liquid cryogen outflow, and bulk fluid control. This test is considered to be a vital step in the development plan outlined in Chapter VI.

## VIII. REFERENCES

---

### Chapter I

- I-1 *Passive Retention/Expulsion Methods for Subcritical Storage of Cryogens, Final Report.* MCR-71-58. Martin Marietta Corporation, Denver, Colorado, July 1971.
- I-2 H. L. Paynter: Zero-or Reduced-Gravity Storage System for Two-Phase Fluid. U.S. Patent No. 3,486,302, dated December 30, 1969. [Continuation of Application Serial No. 565,030, June 22, 1966.]
- I-3 *Passive Retention/Expulsion Methods for Subcritical Storage of Cryogens, Summary Report.* MCR-71-37. Martin Marietta Corporation, Denver, Colorado, July 1971.
- I-4 H. L. Paynter: *Design Requirements Document - Cryogenic Acquisition/Expulsion System Program.* MCR-71-252. Martin Marietta Corporation, Denver, Colorado, 27 August 1971.
- I-5 H. L. Paynter: *Experimental Test Plan - Cryogenic Acquisition/Expulsion System Program.* MCR-71-310. Martin Marietta Corporation, Denver, Colorado.

### Chapter II

- II-1 H. L. Paynter et al.: *Experimental Investigation of Capillary Propellant Control Devices for Low-Gravity Environments, Volume I - Summary Report.* MCR-69-585. Martin Marietta Corporation, Denver, Colorado. June 1970. (Contract NAS8-21259).
- II-2 H. L. Paynter et al.: *Experimental Investigation of Capillary Propellant Control Devices for Low-Gravity Environments, Volume II - Final Report.* Martin Marietta Corporation, Denver, Colorado. June 1970. (Contracts NAS8-20837 and NAS8-21259).
- II-3 H. L. Paynter et al.: *Passive Retention/Expulsion Methods for Subcritical Storage of Cryogens - Final Report.* Martin Marietta Corporation, Denver, Colorado. July 1971. (Contract NAS9-10480).
- II-4 R. Eberhardt, et al.: *Propellant Mass Gaging, Venting, and Handling Technology.* S-72-48828-03. Martin Marietta Corporation, Denver, Colorado, December 1972.

- II-5 *Cryogenic and Industrial Gases*, Vol V, No. 3, March 1970, p 60.
- II-6 J. C. Armour and J. N. Cannon: *Fluid Flow Through Woven Screens*, AIChE Journal, Vol 14, No. 3, May 1968, p 415-420.
- II-7 John Parmakian: *Waterhammer Analysis*, Dover Publications Inc., New York, 1963.
- II-8 V. L. Streeter and E. B. Wylie: *Hydraulic Transients*, McGraw-Hill, Inc., New York, 1967.
- II-9 B. D. Neff and E. F. Wollam: *Feedline Trades for Liquid OMS, Space Shuttle Program Propulsion Design Note No. O-MMC-PROP-5010*, Martin Marietta Corporation, Denver, Colorado, February 1971.
- II-10 P. R. Chun: "Some Experiments on Screen Wick Dry-out Limits," *Transactions of ASME Journal of Heat Transfer*, New York, New York, February 1972, p 46-51.
- II-11 R. A. Seban and A. Abhet: *Steady and Maximum Evaporation from Screen Wicks*, ASME Paper No. 71-WA/HT-12, New York, New York, August 1971.
- II-12 *Low Gravity Propellant Control Using Capillary Devices in Large Scale Cryogenic Vehicles, Design Handbook*. Report No. GDC-DDB-70-006. NASA Contract NAS8-21465, General Dynamics/Convair, August 1970.
- II-13 G. M. Dusinberre: *Heat Transfer Calculations by Finite Differences*. International Textbook Co., Scranton, Pennsylvania, 1961.
- II-14 R. P. Warren: *Low-G Fluid Behavior and Control*, Martin Marietta Corporation, Denver, Colorado, R-71-48631-003. Progress Report. 1971.
- II-15 *Passive Retention/Expulsion Methods for Subcritical Storage of Cryogens*, Final Report. MCR-71-58. Martin Marietta Corporation, Denver, Colorado, July 1971.
- II-16 E. Y. Harper et al.: *Analytical and Experimental Study of Stratification in Standard and Reduced Gravity Fields*, Lockheed Missiles and Space Company, Sunnyvale, California. Also published in *Proceedings of the Conferences on Propellant Tank Pressurization and Stratification*, January 20 and 21, 1965.

- II-17 B. D. Neff: *Study of Cryogenic Propellants, Stratification Reduction, Final Report.* MCR-65-33, Contract NAS8-5208. Martin Marietta Corporation, Denver, Colorado, August 1965.
- II-18 L. W. Florschuetz and B. T. Chao: "On the Mechanics of Vapor Bubble Collapse," *Transactions of the ASME, Journal of Heat Transfer*, Vol 87, Series C, May 1965, p 209-220.
- II-19 V. F. Prisnyakov: "Condensation of Vapor Bubbles in Liquid," *International Journal of Heat and Transfer*, Vol 14, 1971, p 353-356.
- II-20 H. C. Hewitt and J. D. Parker: "Bubble Growth and Collapse in Liquid Nitrogen," *Transactions of ASME Journal of Heat Transfer*, Vol 90, Series C, February 1968, p 22-26.
- II-21 S. A. Zwick and M. S. Plesset: "On the Dynamics of Small Vapor Bubbles in Liquids," *Journal of Mathematics and Physics*, Vol 33, 1954, p 308-330.
- II-22 D. A. Fester and P. E. Bingham: *Evaluation of Fine Mesh Screen Devices in Liquid Fluorine.* R-70-48631-010. Martin Marietta Corporation, Denver, Colorado, June 1970.

### Chapter III

- III-1 *Attitude Control Propulsion System (ACPS) Requirements and Duty Cycles, Phase B Final Report,* North American Rockwell Corporation, June 1971. [Contract NAS9-10960]
- III-2 *Space Shuttle Orbiter, Part 1, Orbiter, Attitude Control and Maneuver Propulsion.* Report MDC E0382, Enclosure to Memo SSPI-E450-578. McDonnell Douglas Corporation, June 30, 1971.
- III-3 *Design Requirements Document--Cryogenic Acquisition/Expulsion System Program.* MCR-71-252. Martin Marietta Corporation, Denver, Colorado, August 27, 1971.
- III-4 *Low-Gravity Propellant Control Using Capillary Devices in Large Scale Cryogenic Vehicles, Design Handbook.* Report No. GDC DDB70-006. General Dynamics/Convair, August 1970. [Contract NAS8-21465]

- III-5 *Space Shuttle Program Propulsion Design Note, Feedline Trades for Liquid OMS, Design Note No. O-MMC-PROP-5010. February 1971.*
- III-6 *Review of Martin Conceptual Design for Passive Acquisition/Retention Devices in Cryogenic Tanks. Report BR15535. Beech Aircraft Corporation, Boulder, Colorado, July 28, 1972.*

#### Chapter V

- V-1 *Baseline Tug Definition Document. Rev A. NASA-George C. Marshall Space Flight Center, Huntsville, Alabama, June 26, 1972.*
- V-2 *Final Report, Space Tug Point Design Study, MDAC-G2818. McDonnell Douglas Astronautics Company-West, Huntington Beach, California, February 1972.*
- V-3 *Final Report, Space Tug Point Design Study. NAR SD72-SA-0032. Rocketdyne Division, North American Rockwell Corporation, Canoga Park, California, February 1972.*
- V-4 *Viking Orbiter 1975 - Impact of Contact Angle on PMD Performance. Report No. SE004-47-03 [JPL Contract No. 953261]. Martin Marietta Corporation, Denver, Colorado, June 1972.*
- V-5 *R. P. Warren: Low-g Fluid Behavior and Control Progress Report 1971. R-71-48631-003. Martin Marietta Corporation, Denver, Colorado, 1971.*

#### Chapter VI

- VI-1 *Review of Martin (Marietta) Conceptual Design for Passive Acquisition/Retention Devices in Cryogenic Tanks. Report BR15535. Beech Aircraft Corporation, Boulder, Colorado, July 28, 1972.*